Analysis of DNA Methylation Patterns in Hepatocellular Carcinoma to Identify Novel Therapeutic Targets and Biomarkers that Predict Response to Therapy

A thesis submitted in part requirement for the degree of Doctor of Philosophy

Chalermsin Permtermsin

Supervisors

Dr. Gordon Strathdee
Dr. Ruchi Shukla
Prof. Helen Reeves

Biosciences Institute
Faculty of Medical Sciences
Newcastle University

July 2023

Abstract

Hepatocellular carcinoma (HCC) is the most common type of liver cancer, accounting for over 90% of cases. The treatment outcome for HCC patients is very poor and over 70% of patients present with disease that is incurable by current therapies. Furthermore, current therapies for HCC patients often have low efficacy and significant toxicities. Thus, there is a critical need for the development of novel therapeutic approaches and the optimisation of currently used therapies to improve the outcomes for HCC patients. We developed a novel bioinformatics pipeline, which integrates genome-wide DNA methylation and gene expression data, to identify genes required for the survival of cancer cells but not normal cells. Targeting these genes may induce "synthetic lethality" (SL), specifically killing cancer cells with little or no impact on healthy ones. Based on global DNA methylation patterns, five potential HCC subgroups were identified. Subgroup 2 exhibited the most unique methylation profile and was utilised for SL gene analysis. This identified two candidate SL genes, T-lymphoma invasion and metastasis 1 (*TIAM1*) and lactate dehydrogenase B (*LDHB*). Available HCC cell lines were characterised for their global methylation patterns and expression of *TIAM1* and *LDHB*. Analysis releveled SNU182 and PLC/PRF-5 as potential HCC subgroup 2 representative cell lines (positive expression and hypomethylation of *TIAM1* and *LDHB*) and HepG2 and Huh-7 (negative expression and hypermethylation of *TIAM1* and *LDHB*) as non-subgroup 2 cell lines. TIAM1 belongs to a family of guanine nucleotide exchange factors (GEFs) known to activate RAC1 signalling and plays a role in cancer cell growth, adhesion, and invasion. The HCC cell lines as well as additional non-HCC liver cell lines positive for *TIAM1* and *LDHB* SK-Hep1 (cholangiocarcinoma) and HHL5 (immortalised hepatocytes) were used to investigate the functional relevance of *TIAM1* utilising siRNA silencing and a specific TIAM1/Rac1 signalling inhibitor (NSC23766). siRNA targeting *TIAM1* inhibited cell proliferation in *TIAM1* positive (subgroup 2) HCC cell lines but had no effect on *TIAM1* negative cell lines and cell proliferation was also suppressed at significantly lower NSC23766 concentrations in the *TIAM1* positive compared with the *TIAM1* negative HCC lines. Thus, confirming *TIAM1* as a potential SL gene for HCC subgroup 2. *LDHB* is a metabolic gene that encodes the B subunit of the lactate dehydrogenase enzyme, which catalyses the interconversion of pyruvate and lactate. Since the HCC subgroup 2 representative cell lines exhibit subgroup specific expression of *LDHB*, we tested their sensitivity to metabolic inhibitors (2-DG and metformin) and GNE-140 (LDH inhibitor). The result showed that the sensitivity of 2-DG and metformin was HCC subgroup 2 independent. In addition, the sensitivity to the LDH inhibitor GNE-140 did not correlate with *LDHB* expression status. Radiotherapy is a common treatment choice for cancer patients. The development of radioresistance is common in numerous cancer types including HCC, but metabolic interventions have shown promise as radiosensitisers. Hence, we evaluated radiation synergy with metabolic inhibitors (2-DG and metformin) and its potential correlation with the LDHB status of the cells. No radiosensitisation effect for either of the inhibitor individually or in combination was observed in any of the HCC cell lines tested. However, potential synergy between 2-DG and metformin was observed in some cell lines independent of their LDHB status. Overall, the study provides evidence towards exploiting *TIAM1* as a potential therapeutic target for a subgroup of HCC. In addition, a combination of 2-DG and metformin should be explored further as a potential treatment strategy for HCC. **564 words**

Declaration

I certify that no part of the information in this thesis has previously been submitted for a degree or other qualification at this or any other university. Unless otherwise stated in the thesis text, I declare that this thesis is my own unaided work, completed entirely by myself under the guidance of my supervisors.

Acknowledgments

I would like to extend a special thank you to my family, especially my deceased mother and father, and my beloved friend (who passed away on July 1, 2022, from prostate cancer), who continue to watch over my Ph.D. journey from heaven. In addition, I would like to thank myself for surviving the most challenging conditions for a Ph.D. while studying outside the Kingdom of Thailand. It was extremely difficult for me because I was the oldest student from Thailand to receive a scholarship to study at Newcastle University in the United Kingdom. I started my Ph.D. studies at the age of 44 and completed them at the age of almost 50.

I would like to thank Professors Nicola Curtin and James Allan, who were on my academic panel, for their help and advice in school and for letting me keep going with my Ph.D. studies until I graduated.

I would like to thank my supervisors, Dr. Gordon Strathdee, Dr. Ruchi Shukla, and Professor Helen Reeves, for their support, assistance with problem solving, and hard work with me until graduation.

I would like to thank Misti McCain, who assisted me at the start of my doctoral program, for her assistance. I would like to extend special appreciation to my liver cancer group, including Dr. Praveen Dhondurao Sudhindar and Dr. Bassier Zadran. Also, I would like to thank Dr. Lalchungnunga Nunga, Dr. Nurettin Ayvali, Dr. Devi Nandana Suchitra, Mrs. Hande Atasoy, and the rest of the POG staff for being nice to me while I worked on my project at the POG building.

I would like to thank the graduate school, faculty of medical science, for providing me with a letter of acceptance despite the fact that I did not meet the standard requirements to study. I would like to thank the Doctoral College for giving me the 12-week COVID-19 impact funding scholarship and fee-free extension until graduation.

I would like to thank the Royal Thai Government, the Office of Atoms for Peace, and the Royal Thai Embassy's Office of Educational Affairs for sponsoring this event and helping all Thai students studying in the UK.

Lastly, I would like to extend my deepest gratitude to His Majesty King Bhumibol Adulyadej (King Rama IX), the Greatest King of Thailand. On December 17th, 1998, King Rama IX presented me with a bachelor's degree in pharmaceutical sciences from Khonkaen University, The Kingdom of Thailand. King Rama IX inspired my pursuit of a doctorate. After King Rama IX's passing on October 13th, 2016, I had decided to study at the Strathclyde Institute of Pharmacy and Biomedical Sciences, University of Strathclyde, Glasgow, Scotland, before transferring to study at the Northern Institute for Cancer Research (NICR), medical school at Newcastle University, in 2017. NICR is now known as the Biosciences Institute, Faculty of Medical Sciences.

Table of Contents

List of Figures

Lists of tables

Abbreviations

AASLD	The American Association for the Study of Liver Disease
Acetyl-CoA	Acetyl coenzyme A
ADP	Adenosine diphosphate
AFP	Alpha-fetoprotein
AFTB1	Aflatoxin B1
AKT	Protein kinase B
ALL	Acute lymphoblastic leukaemia
Ang	Angiopoietin
ATM	Ataxia Telangiectasia Mutated
ATP	Adenosine triphosphate
BCA	Bicinchoninic acid
BMI	Body mass index
BRCA	Breast cancer gene
BSA	Bovine serum albumin
C	Cirrhosis
Cdc42	Cell division control protein 42 homolog
cDNA	Complementary DNA synthesis
CFA	Colony formation assay
c-Kit	KIT proto-oncogene receptor tyrosine kinase
c-Met	Tyrosine-protein kinase Met
CNV	Copy number variation
CpG	Cytosine-phosphate-guanine
Ct	Cycle threshold
ΔCt	Delta Ct (Ct value of target gene minus Ct value of the housekeeping gene)
CTL	Cytotoxic T lymphocytes
CTLA-4	Cytotoxic T-lymphocyte-associated protein 4
cyt C	Cytochrome C
dCCA	Distal cholangiocarcinoma
DCs	Dendritic cells

2-DG	2-Deoxy-D-glucose
DMEM	Dulbecco's Modified Eagle's Medium
DMRs	Differentially methylated regions
DMSO	Dimethyl sulfoxide
DNA	Deoxyribonucleic acid
DNMT3A	DNA methyltransferase 3 alpha
dNTP	Deoxy nucleotide triphosphate
EASL	European Association for the Study of the Liver
EC50	Half maximal effective concentration
eCCA	extrahepatic cholangiocarcinoma
ECL	Enhanced chemiluminescence
EGFR	Epidermal growth factor receptor
ETC	Electron transport chain
$FADH_2$	Flavin adenine dinucleotide
FBS	Foetal bovine serum
FDA	Food and Drug Administration
FGFR	Fibroblast growth factor receptor
FLT3	Fms-related tyrosine kinase 3
g	Gravitational force
G	Group
GDP	Guanosine diphosphate
GEFs	Guanine nucleotide exchange factors
GLUT	Glucose transporter
GTP	Guanosine triphosphate
Gy	Gray
HBV	Hepatitis B virus
HCV	Hepatitis C virus
HCC	Hepatocellular carcinoma
HGFR	Hepatocyte growth factor receptor or c-Met
HIF-1	Hypoxia-inducible factor 1
HK2	Hexokinase 2
HNPCC	Hereditary nonpolyposis colorectal carcinoma
HR	Homologous recombination

HPRT	Hypoxanthine guanine phosphoribosyltransferase
hr	Hour
IC50	50% inhibitory concentration
iCCA	Intrahepatic cholangiocarcinoma
ICI	Immune checkpoint inhibitor
ID	The identification number
IGFR	Insulin-like growth factor receptor
IR	Ionising radiation
ISLE	Identification of clinically relevant synthetic lethality
kb	Kilo base
KD	Knock down
LDH	Lactate dehydrogenase
LDHA	Lactate dehydrogenase A
LDHB	Lactate dehydrogenase B
LDHC	Lactate dehydrogenase C
LHBD	Lactate dehydrogenase D
LINE	Long-interspersed nuclear elements-1
lncRNA	Long non-coding RNA
M	Molar
mAb	Monoclonal antibody
5mC	5-Methylcytosine
MCT	Monocarboxylate transporter
MEK	Mitogen-activated protein kinase
MET	Mesenchymal-epithelial transition
miRNA	Micro RNA
min	Minute
ml	Millilitre
mM	Millimolar
mo	Month
mRNA	Messenger RNA
mTOR	Mammalian target of rapamycin
MTT	3-(4,5-dimethylthiazol-2-yl)-2,5-diphenyltetrazolium bromide
NAD^+	Nicotinamide adenine dinucleotide plus

NADH	Nicotinamide adenine dinucleotide (NAD) + hydrogen (H)
NADPH	Nicotinamide adenine dinucleotide phosphate
NAFLD	Non-alcoholic fatty liver disease
ncRNA	Non-coding RNA
nm	Nanometre
NM	Normal medium
NMF	Non-negative matrix factorisation
OD	Optical density
OCT1	Organic cation transporter 1
OS	Overall survival
OXPHOS	Oxidative phosphorylation
P	Phosphate group
PARP	Poly (adenosine diphosphate [ADP]–ribose) polymerase 1
PBS	Phosphate-buffered saline
pCCA	Perihilar cholangiocarcinoma
PCR	Polymerase chain reaction
PD-L1	Programmed cell death-ligand 1
PD-L2	Programmed cell death-ligand 2
PDGFR	Platelet-derived growth factor receptor
PEI	Percutaneous ethanol injection
PFS	Progression-free survival
piRNA	PIWI RNA
PM	Physiological medium
PVDF	Polyvinylidene difluoride
r^2	R-squared
Rac1	Ras-related C3 botulinum toxin substrate 1
RAF	Rapidly accelerated fibrosarcoma
RET	Rearranged during transfection
RFA	Radiofrequency ablation
RFU	Relative fluorescent unit
RLU	Relative luminescent unit
RNA	Ribonucleic acid
rpm	Revolutions per minute

RPMI-1640	Roswell Park Memorial Institute medium 1640
RT	Radiotherapy
RT-qPCR	Reverse transcription-quantitative polymerase chain reaction
RYBP	RINGl and YYl binding protein
SD	Standard deviation
SDS	Sodium dodecyl sulfate
SEER	The Surveillance, Epidemiology, and End Results
SEM	Standard error of the mean
shRNA	Short hairpin RNA
siRNA	Small interfering RNA or short interfering RNA
SIRT	Selective internal radiotherapy
SLGs	Synthetic lethal genes
ssDNA	single strand DNA
STAT	Signal transducer and activator of transcription
SIRT	Selective internal radiation therapy
SL	Synthetic lethality
SLG	Synthetic lethal gene
SRB	Sulforhodamine B
STAT	Signal transducer and activator of transcription
TAAs	Tumour-associated antigens
TACE	transarterial chemoembolisation
TBST	Tris-buffered saline with tween
TCA	Tricarboxylic acid
TCGA	The Cancer Genomes Atlas
Th1	T helper type 1
TIAM1	T-cell lymphoma invasion and metastasis-inducing protein 1
TIE	Tyrosine kinase with immunoglobulin-like and EGF-like domains
TKI	Tyrosine kinase inhibitors
TLR4	Toll-like receptor-4
TSS	Transcription start site
UK	the United Kingdom
U.S.	The United States
USA	The United States of America

µl	Microlitre
µM	Micromolar
V	Volt
vs	Versus
VEGFR	Vascular endothelial growth factor receptor
WHO	World Health Organisation

Chapter I

Introduction

1.1 Cancer

Cancer can be described as an abnormal mass of cells which can divide uncontrollably, are invasive, and expand into adjacent organs or other parts of the body. **Fig. 1.1** displays the number of new cancer cases (left pie chart) and cancer-related deaths from the most prevalent cancers worldwide in 2020 (right pie chart). For liver cancer it is noteworthy that the number of yearly deaths recorded is almost equivalent to the number of yearly new cases diagnosed. Consequently it is the sixth most common cancer diagnosed but the third most common cause of cancer-related death [**https://gco.iarc.fr/today/data/factsheets/ cancers/39-All-cancers-fact-sheet.pdf**].

1.2 Recent updates on cancer statistics in the United Kingdom

In the UK, there will be 3.5 and 4 million individuals living with cancer by 2025 and 2030, respectively. Furthermore, that number is predicted to rise until it reaches almost 5.3 million by 2040. This rise is caused in part by the UK's aging and expanding population, as well as advances in cancer detection and care [**https://www.macmillan.org.uk/dfsmedia/1a6f23537f7f4519bb0cf4c45b2a629/9468-10061/2022-cancer-statistics-factsheet**].

Liver cancer is the 18th most prevalent malignancy, making up 2% of all new cancer cases (around 17 cases per day) in the UK. It is the 15th and 20th most prevalent cancer, with about 4,100 and 2,100 new cases per year among men and women from 2016-2018, respectively. People between the ages of 85 and 89 are most likely to get liver cancer. The most common type of liver cancer in women is intrahepatic bile duct carcinoma, and the most common type of liver cancer in men is hepatocellular carcinoma [**https://www.cancerresearchuk.org/health-professional/cancer-statistics/statistics-by-cancer-type/liver-cancer**].

Liver cancer is the 8th leading cause of cancer-related mortality, accounting for 3% of all cancer-related deaths. There are approximately 5,800 liver cancer deaths annually, or 16 cases per day with about 2,300 and 3,600 deaths per year among females and males from 2017-2019, respectively. Currently, liver cancer is the 10th most prevalent cause of cancer deaths. Those between the ages of 85 and 89 have the highest liver cancer mortality rates [**https://www.cancerresearchuk.org/health-professional/cancer-statistics/statistics-by-cancer-type/liver-cancer#heading-One**].

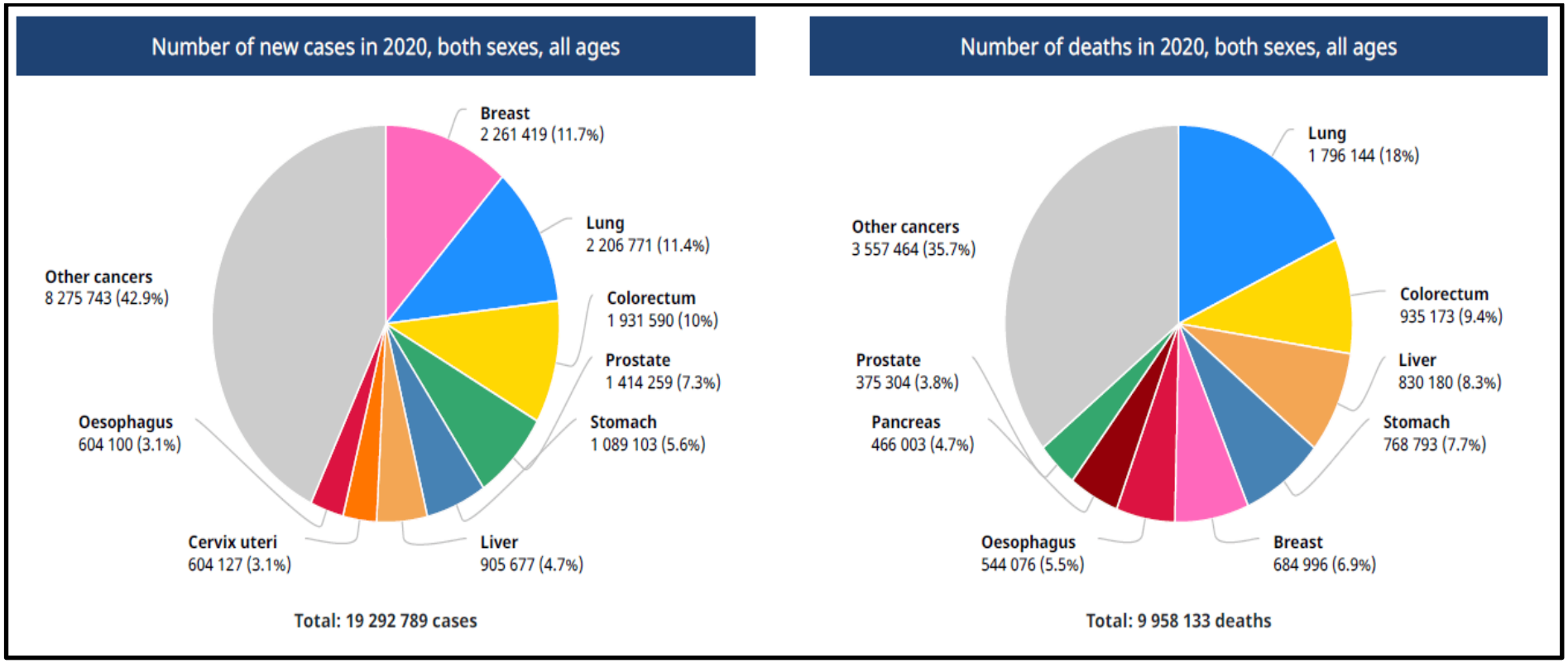

Figure 1.1 The global incidence of new cases and deaths from common cancer types in both sexes and all ages in 2020 [**https://gco.iarc.fr/today/data/factsheets/ cancers/39-All -cancers-fact-sheet.pdf**].

In England, between 2013 and 2017, 38.1% and 12.7% of liver cancer patients survived at least one- and five-years following diagnosis, respectively. Nearly eight out of ten (78%) liver cancer patients diagnosed in the disease's earliest stages will survive at least one year, compared to only one out of five (20%) patients diagnosed at the disease's most advanced stage. In England and Scotland, the five-year relative survival rate for men with liver cancer is below the European average, while it is comparable in Wales and Northern Ireland. In England and Scotland, the five-year relative survival rate for women with liver cancer is lower than the European average, whereas it is comparable in Wales. It should be noted that obesity, smoking, infection, and alcohol are thought to account for 23%, 20%, 10%, and 7% of cases, respectively. And 49% of liver cancer cases may be preventable [**https://www.cancerresearchuk.org/health-professional/cancer-statistics/statistics-by-cancer-type/liver-cancer#heading-Two**].

From 1997 to 2017, primary liver cancer was frequent in both sexes in the UK, with males being afflicted at a greater incidence than women. From 2014 to 2017, both sexes experienced a plateau in incidence. Scottish males had the highest incidence and fatality rates in the UK. Across all patients in the UK, 1-, 2-, and 5-year survival rates were 40%, 27%, and 14%, respectively (**Fig. 1.2)**. Although survival rates have improved, existing treatments are inadequate, and novel targeted therapies are desperately required [**Burton et al., 2021**].

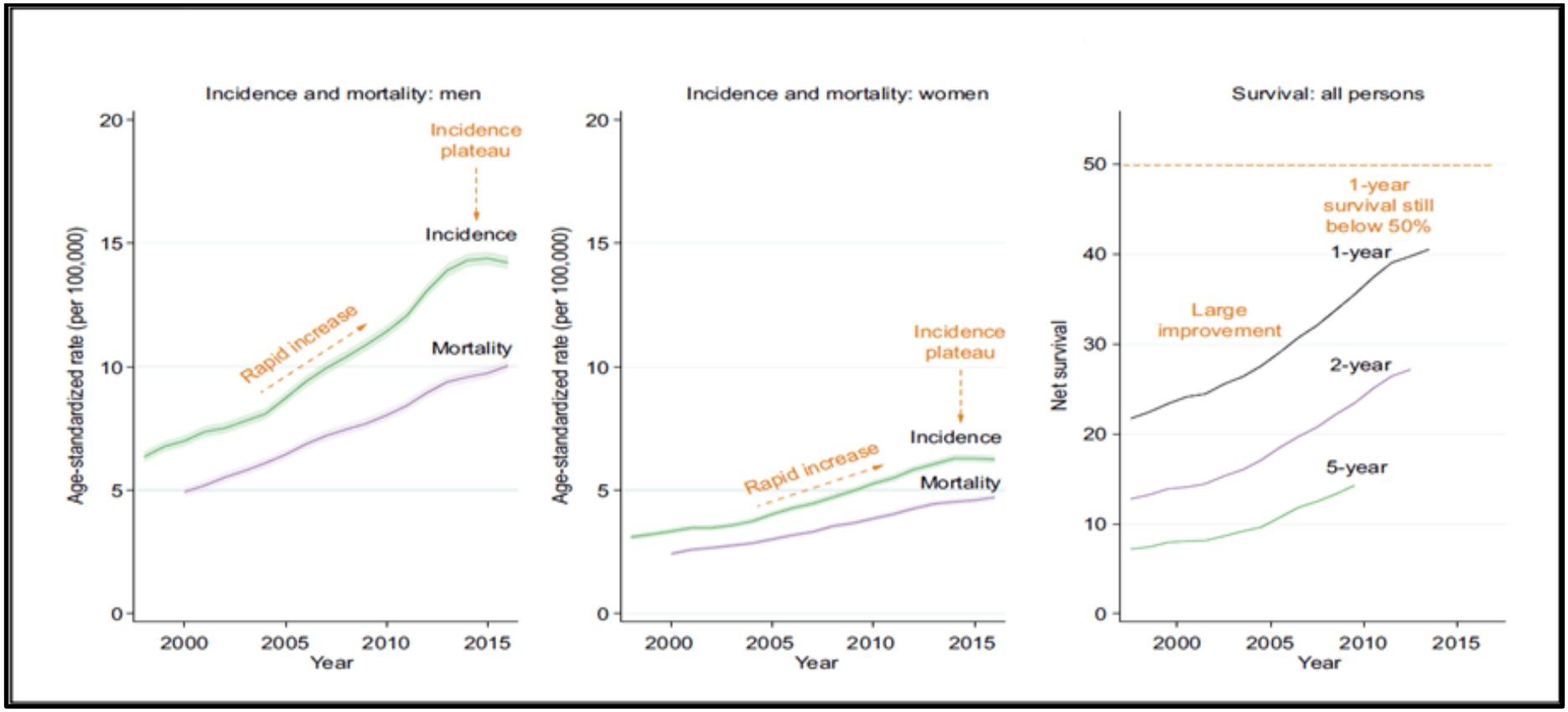

Figure 1.2 The primary liver cancer incidence and mortality rates in the UK during 1997-2017 [Burton et al., 2021].

1.3 Recent updates on cancer statistics in Thailand

According to the World Health Organisation (WHO), liver cancer was the most common cancer among Thai men and females in 2020, accounting for 27,394 cases. The most prevalent kinds of cancer in males are liver (18,268; 19.6%), lung (15418; 16.5%), colorectum (10,660; 11.4%), prostate (8,630; 9.2%), non-Hodgkin lymphoma (3,738; 4%), and other cancers (36,711; 39.3%), respectively. In women, the most prevalent cancers are those of the breast (22,158; 22.8%), colorectum (10,443; 10.7%), cervix uteri (9,158; 9.4%), liver (9,126; 9.4%), lung (8,295; 8.5%), and other cancers (38,031; 39.1%), respectively. [**https://gco.iarc.fr/today/data/factsheets/populations/764-thailand-fact-sheets.pdf**].

1.4 Liver cancer types

Liver cancer encompasses several different cancer types, including hepatocellular carcinoma (HCC), cholangiocarcinoma (CCA), mixed hepatocellular cholangiocarcinoma (HCC-CCA), fibrolamellar carcinoma (FLC), and the juvenile neoplasm hepatoblastoma. HCC is the most frequent type of primary liver cancer, followed by CCA, with the others accounting for less than 1%. **Fig. 1.3** illustrates the basic structure of the liver. 60% to 80% of the total liver mass is made up of hepatocytes. Structurally, these cells are arranged in lobules that can be further subdivided into functional zones or regions [**Sia et al., 2017**].

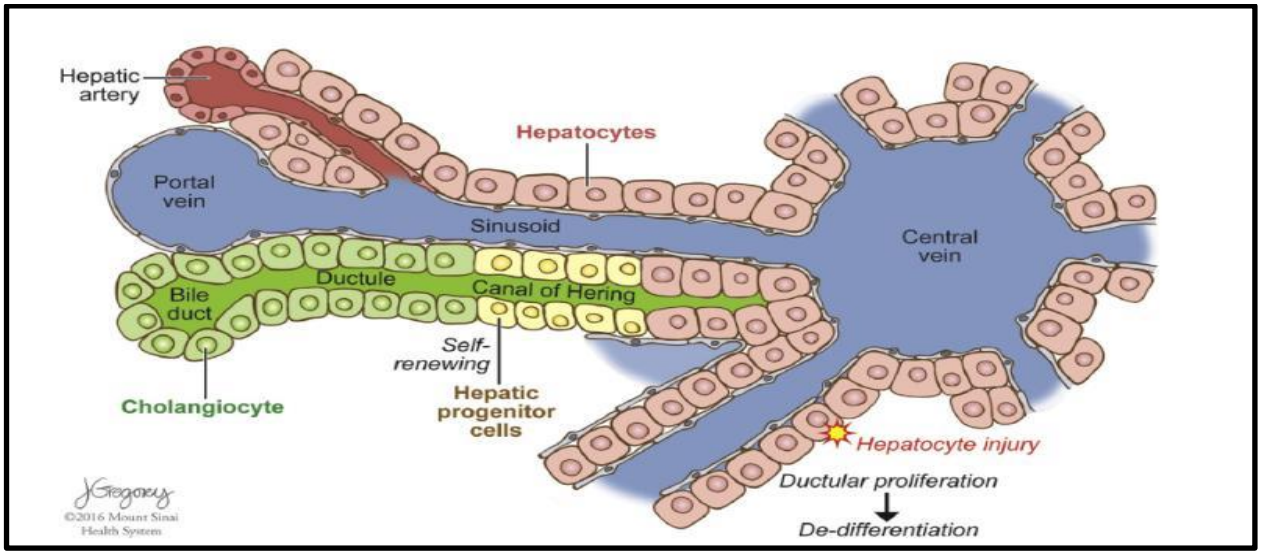

Figure 1.3 The anatomy of the liver's lobules and the site of the liver cancer cell's genesis. The intrahepatic anatomy of the liver lobule as well as the site of hepatic cells that produce liver tumours. The liver may develop HCC, CCA, and mixed HCC-CCA depending on the transformation event and the kind of cell undergoing neoplastic transformation. The branches of the biliary tree (or canals of Hering) are assumed to be location to hepatic stem or progenitor cells [**Sia et al., 2017**].

1.4.1 Hepatocellular carcinoma

Hepatocellular carcinoma (HCC) is a hepatocyte-derived cancer, and it is the most prevalent type of primary liver cancer, accounting for 75-85% of all cases [**Bray et al., 2018**]. The incidence of liver cancer, particularly the HCC subtype, has increased significantly over the past two decades. This might be related to advances in screening and diagnostic procedures. Furthermore, increasing the survival rate of cirrhotic patients may promote HCC development [**Rashed et al., 2020**]. Less than half of patients survive one year after being diagnosed with primary liver cancer [**Burton et al., 2021**]. Mostly, HCC develops in patients with pre-existing chronic liver disease and inflammation, such as liver cirrhosis. [**Llovet et al., 2021; Galun et al., 2022**].

1.4.2 Cholangiocarcinoma

Cholangiocarcinoma (CCA) is the second most common type of liver cancer accounting for 10-15% of primary liver cancer. The CCA is made up of a wide mixture of epithelial cells that are found throughout the biliary system [**Sarcognato et al., 2021; Hewitt et al., 2022**]. The incidence is increasing globally, and treatment outcomes are very poor, with a 5-year survival rate of under 5% [**Byrling et al., 2016**]. Age over 65, obesity, and diabetes mellitus are the common risk factors for CCA. Infectious diseases such as liver flukes, HBV, HCV, and HIV can also lead to the development of CCA. Some drugs, toxins, and chemicals (smoking, alcohol, dioxin, nitrosamines, asbestos, isoniazid, oral contraceptives) and inflammatory diseases (biliary tract stone disease, liver cirrhosis) have also been reported to increase the risk of CCA development [**Banales et al., 2016**].

As indicated in **Fig. 1.4A,** CCA can be divided into two groups based on anatomical location: intrahepatic cholangiocarcinoma (iCCA) and extrahepatic cholangiocarcinoma (eCCA). The eCCA can be further divided into perihilar cholangiocarcinoma (pCCA), and distal cholangiocarcinoma (dCCA) (**Fig. 1.4B**). The iCCA is classified into three subtypes: (**i**) mass forming (**ii**) periductal-infiltrating, and (**iii**) intraductal (**Fig. 1.4C**) [**Byrling et al., 2016; Lendvai et al., 2020; Kodali et al., 2021; Hewitt et al., 2022**].

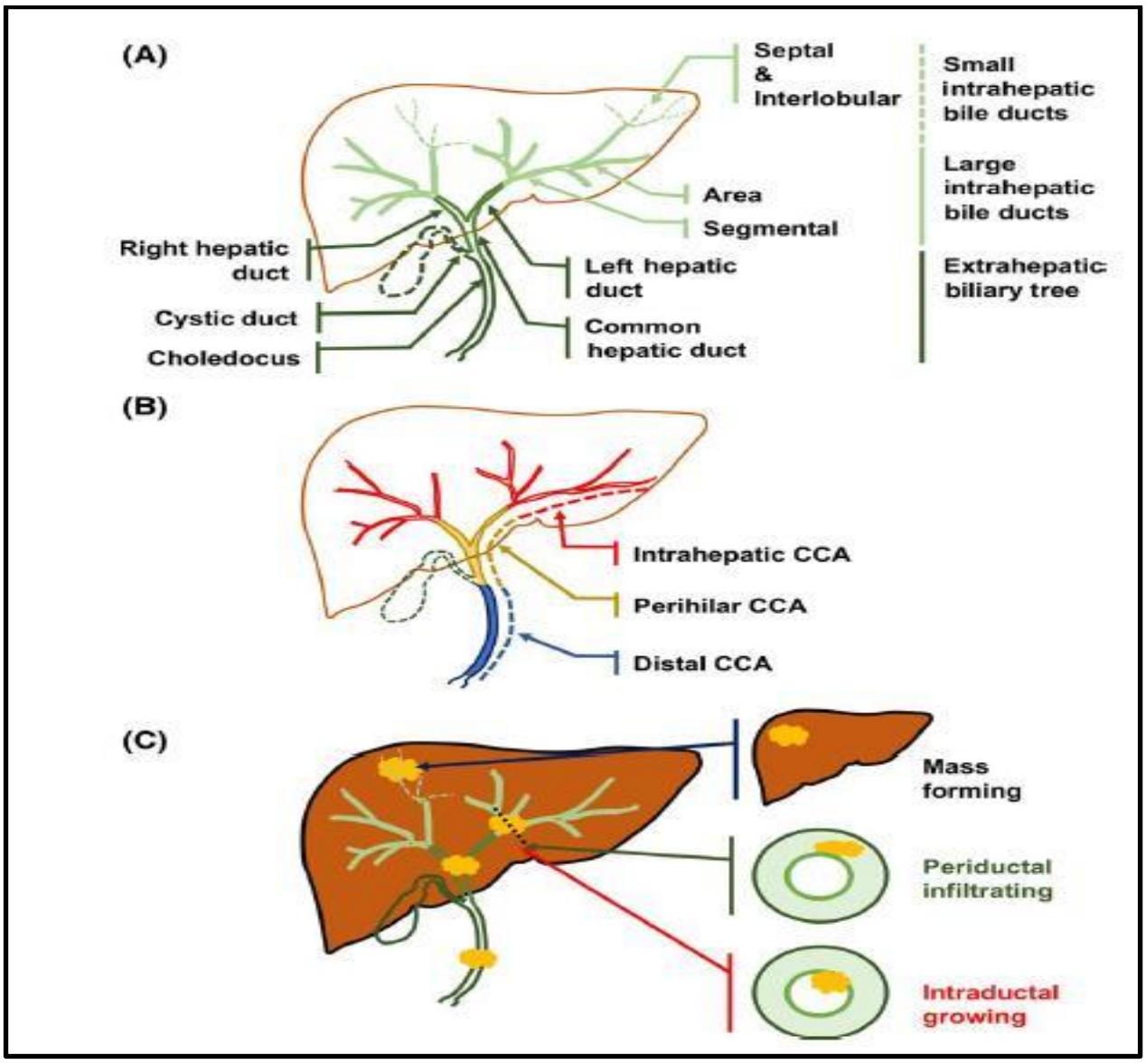

Figure 1.4 Cholangiocarcinoma classification based upon anatomical localisation. (**A**) The biliary tree divided into two subgroups; the intrahepatic (large and small intrahepatic bile ducts, **light green**) and extrahepatic parts (**dark green**). Small intrahepatic bile ducts are classified into septal & interlobular bile ducts whereas large intrahepatic bile ducts are classified into area and segmental bile ducts. The extrahepatic biliary tree comprises the right and left hepatic ducts, the common hepatic duct, cystic duct**,** choledocus, and gallbladder. (**B**) Cholangiocarcinoma (CCA) is divided into three groups based on where it is located: intrahepatic (**red**), perihilar (**orange**), and distal CCA (**dark blue**). Intrahepatic CCA (iCCA) is present close to the second-order bile ducts. (**C**) Based on its outward appearance, iCCA might exhibit one of three development patterns: mass-forming, periductal infiltrating, or intraductal growing [**Kendall et al., 2019**].

The incidence of CCA varies greatly across the global illustrating the exposure to various risk factors. In East Asia, where iCCA accounts for 85% of primary liver cancers [**Banales, et al., 2016**]. The highest rates occur in the Northeast of Thailand (>80 per 100,000), where the liver flukes (*Opisthorchis viverrine* and *Clonorchis sinensis*) are endemic and CCA is the primary liver cancer (over 80%), followed by South Korea (>7 per 100,000) and China (>7 per 100,000). In contrast, Western countries including Italy, the UK, the USA, France, and Canada show a lower rate than Asia (3.36, 2.17, 1.67, 1.3, and 0.35 per 100,000, respectively) (**Fig. 1.5**) [**Bergquist et al., 2015; Banales et al., 2016**].

As with HCC, many CCA patients have advanced disease at the time of diagnosis, making them incurable. All iCCA and eCCA forms had median survival times of 5 to 12 months for patients who underwent no surgical procedure. A multimodality therapy strategy may be used for unresectable lesions. At all disease stages, higher survival rates were seen with multimodality treatment compared with the single technique treatment with resection, chemotherapy, or radiation therapy. This was especially true for pCCA, the application of multi-modality techniques that has received the greatest attention. An aggressive strategy is warranted since these tumours present at an early stage but have a poor survival rate. In contrast to pCCA, where chemotherapy was combined with surgery, iCCA had a higher median survival rate. A probable rationale is that smaller malignancies that are accessible to complete resection might have had a better likelihood of effective surgery, or have a reduced risk for invasion or recurrence. These malignancies frequently manifest at a later stage, requiring the development of efficient early detection techniques [**Waseem and Tushar, 2017**].

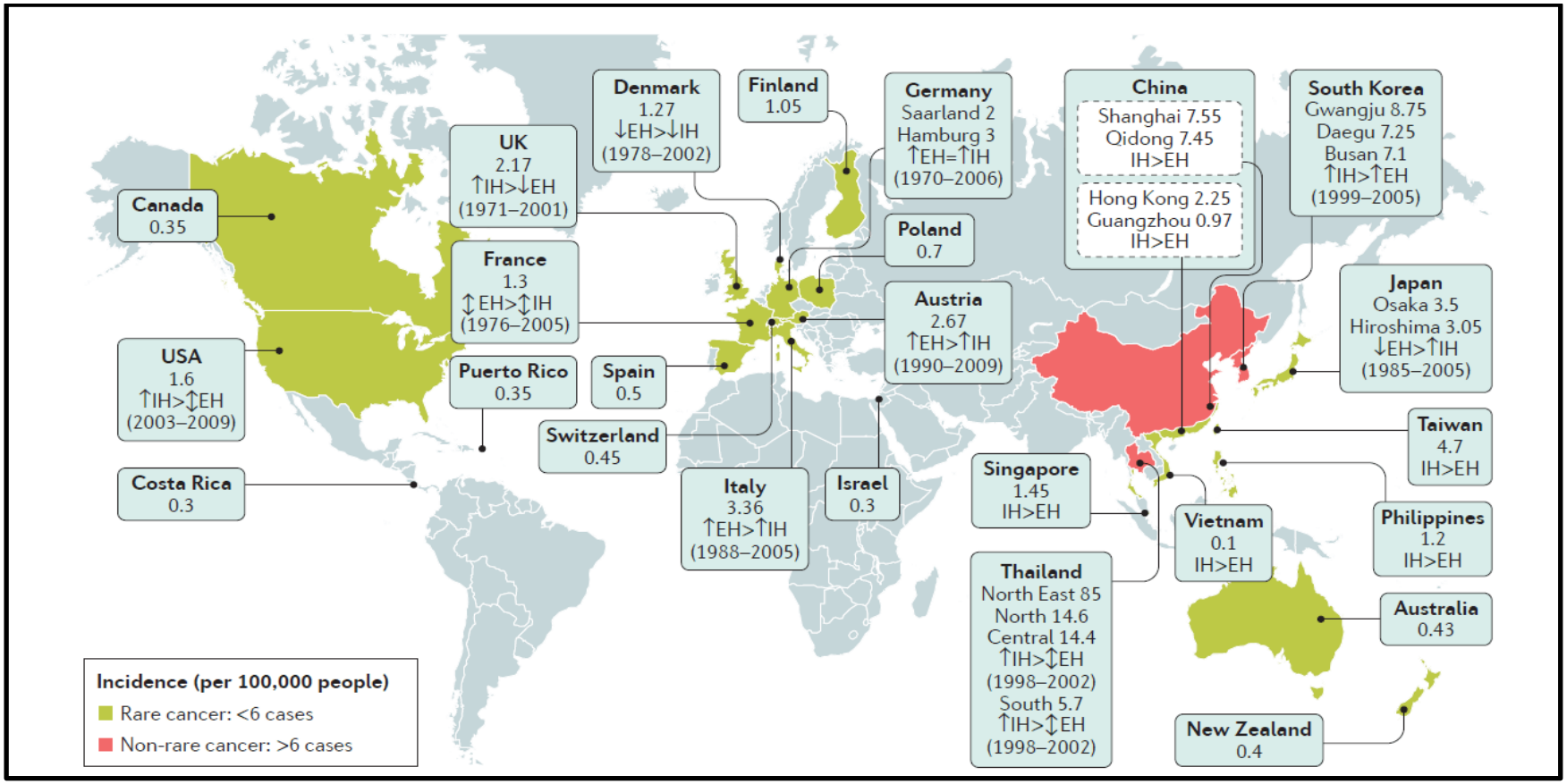

Figure 1.5 The worldwide prevalence of cholangiocarcinoma. IH: intrahepatic cholangiocarcinoma. **EH**: extrahepatic cholangiocarcinoma [**Banales, et al., 2016**].

1.4.3 Combined hepatocellular cholangiocarcinoma

Combined hepatocellular-cholangiocarcinoma (cHCC-CCA) is a rare kind of liver cancer that combines HCC and CCA, accounting for 0.87-1.3 percent of all primary liver malignancies [**O'Connor et al., 2014**]. Wang and colleagues [**Wang et al., 2019**] utilised The Surveillance, Epidemiology, and End Results (SEER) database (1973–2004) and found that in 2000 and 2014, the incidence rates of cHCC-CCA were 0.26 and 0.59 per 1,000,000, respectively. Similarly, the incidence-based mortality rate for cHCC-CC increased from 0.17 per one million in 2000 to 0.46 per one million in 2014. The cHCC-CCA survival rate was 7–11 months (median 9 months). Moreover, the 1-year, 3-year, and 5-year survival rates were 43.4%, 21.5%, and 17.1%, respectively. Infections with the HBV and HCV, cirrhosis, and male are widely reported as risk factors. cHCC-CCA is characterised by the simultaneous presence of two different morphological patterns of HCC and iCCA (HCC and iCCA are seen in separate sections of the same liver, at distinct locations, or are connected with the same tumour). However, their clinical manifestations are identical. Additionally, cHCC-CCA is more aggressive than HCC and/or iCCA alone and has a very poor prognosis [**Cutolo et al., 2022**]. The progression free survival after locoregional therapy (transarterial chemoembolisation, microwave ablation, radiofrequency ablation) is lower for cHCC-CCA patients than in either HCC or CCA [**Mukund et al., 2022**]. Wang et al compared the result of three treatment options and found that liver transplantation improved the highest survival time of cHCC-CCA than surgical resection and local destruction whereas no surgery showed the poorest outcome [**Wang et al., 2019**].

1.4.4 Fibrolamellar carcinoma

Fibrolamellar carcinoma (FLC), a rare kind of liver cancer that makes up 0.4–0.5% of cases, is more commonly found in young adults who do not have cirrhosis or hepatitis. Additionally, men are more likely than women to develop this type of cancer. The majority of treatments continue to be surgical, but systemic therapeutic has been established and are currently the subject of ongoing clinical trials [**Aryan et al., 2022**]. FLC patients, in contrast to HCC, typically lack underlying risk factors (such as HBV/HCV infection or liver cirrhosis) and they are more often identified in young people, presenting without distinct symptoms. Furthermore, FLC patients may benefit more from aggressive surgical therapy, such as liver transplants or resections, as the cancer typically progresses slowly [**Bacinschi et al., 2021**].

1.4.5 Hepatoblastoma

Hepatoblastoma is a kind of juvenile tumour that mostly affects children above the age of five years old [**Sia et al., 2017**]. This rare kind of liver cancer accounts for 1% of all paediatric malignancies [**Feng et al., 2019**] and is thought to arise from hepatocyte precursors [**Lo'pez-Terrada et al., 2014**]. The incidence increased from 1.89 per million in 2000 to 2.16 in 2015. The 5-, and 10-year survival rates were over 80% [**Feng et al., 2019**]. Because there is no worldwide standard categorisation, even general pathologists find it difficult to establish a diagnosis [**Jeong et al, 2022**].

1.5 Hepatocellular carcinoma, epidemiology, geography, and risk factors

Over 900,000 people worldwide were diagnosed with liver cancer in 2020 [**see Fig. 1.1**], and HCC accounts for the 3rd highest cause of cancer-related death [**Vogel et al., 2022**]. The HCC incidence shows substantial global variation, largely attributed to differences in HCC risk factors such as as hepatitis B (HBV) or hepatitis C virus (HCV) infections, alflatoxin, excessive alcohol consumption, non-alcoholic fatty liver disease (NAFLD).

Both HBV and HCV are major risk factors for the development of HCC. The geographical distribution of HCC incidence, as well as the key aetiological factors involved in hepatocarcinogenesis, are affected by geography. East Asia has the greatest rate of HCC, as seen in **Fig. 1.6**, with Mongolia having the highest rate worldwide. HBV is the predominant aetiological factor in most regions of Asia (excluding Japan), Andean Latin America, Western Africa, and Oceania. In contrast, HCV is the most common cause of infection in Western Europe, North and South America, North Africa, and Japan.

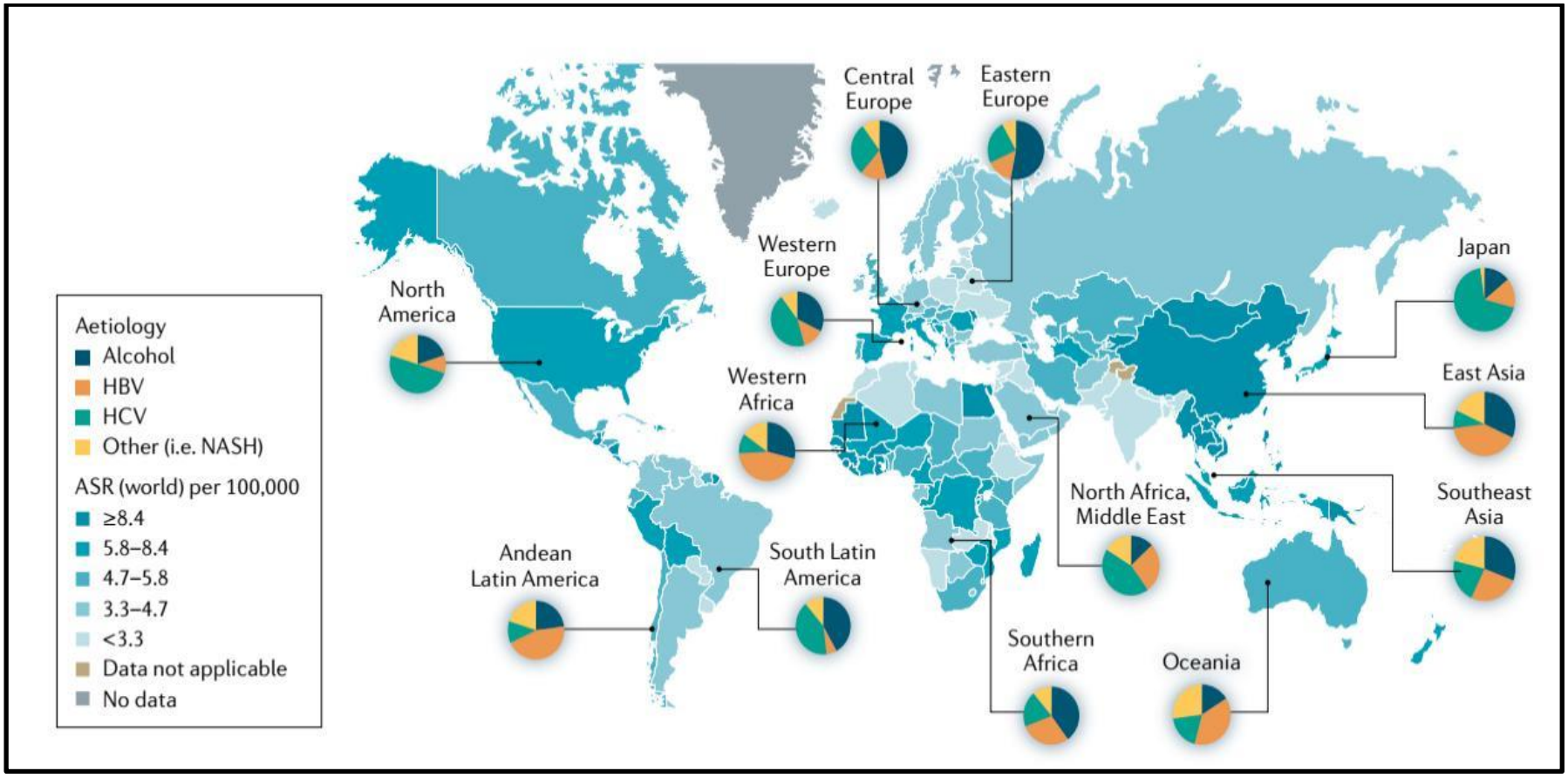

Figure 1.6 The global distribution of HCC by geography and etiology.

HBV: Hepatitis B virus. **HCV**: Hepatitis C virus. **NASH**: Non-alcoholic steatohepatitis. **ASR**: age-standardised incidence rate [**Llovet et al., 2021**].

1.5.1 Hepatocellular carcinoma and alcohol consumption

Alcohol-related liver disease is the most common kind of chronic liver disease globally, contributing for 30% of HCC cases and HCC-specific fatalities [**Ganne-Carrié and Nahon, 2019**]. Heavy alcohol consumption can result in acute or chronic hepatitis, and cirrhosis, all of which can contribute to the development of HCC. The use of alcohol has been related to a three to tenfold increase in the incidence of HCC [**Matsushita and Takaki, 2019**]. Furthermore, alcohol correlates with other variable factors that increase the risk of HCC, such as HBV and HCV infection, diabetes, and smoking. There are several suggested mechanisms by which alcohol may promote liver cancer, including acetaldehyde's carcinogenic effects and the generation of reactive oxygen species due to excessive iron build-up in the liver [**Zhu et al., 2022**].

1.5.2 Hepatocellular carcinoma and aflatoxin

Aflatoxin is produced by *Aspergillus flavus* and *Aspergillus parasiticus* and is a toxic carcinogen. This poisonous toxin, a secondary metabolite produced by some filamentous fungus or mold, is regarded as the most serious dietary risk factor for both humans and animals. Aflatoxin is found in the soil and food crops and exposure to this toxin is an important risk factor for HCC development. There are around 20 distinct forms of aflatoxins found in nature, the most dangerous of which is aflatoxin B1 (AFB1) [**Mungamuri and Mavuduru, 2020**]. WHO has recognised AFB1 as one of the most dangerous natural category 1A carcinogens. AFB1 toxicity in cells and tissues is mediated a wide variety of effects, including cell cycle arrest, reduction of cell proliferation, activation of apoptosis, oxidative stress, endoplasmic reticulum stress, and autophagy [**Li et al., 2022**], genetic mutations, and epigenetic modifications that lead to HCC [**Mungamuri and Mavuduru, 2020**].

1.5.3 Hepatocellular carcinoma and non-alcoholic liver fatty disease

NAFLD is a complicated metabolic condition that is on the rise across the world and it is one of the important risk factors of HCC development [**Grgurevic et al., 2021**] with or without cirrhosis [**Younossi and Henry, 2021**]. The prevalence of NAFLD is associated with obesity, metabolic syndrome, and type 2 diabetes [**Lazarus et al., 2021**]. Younossi and Henry reported that obese patients with a body mass index (BMI) more than 30 kg/m^2 had a two-fold increased risk of HCC, whereas a BMI greater than 35 kg/m^2 was associated with a four-fold increased risk. Furthermore, type 2 diabetes doubles the risk of HCC and increases the risk of mortality from HCC by 1.5 times. However, the risk of HCC rises five-fold if a patient has both the metabolic syndrome

and type 2 diabetes [**Younossi and Henry, 2021**]. From June 2015 to May 2020, Pinyopornpanish and colleagues investigated 392,800 individuals with NAFLD from 26 U.S. healthcare databases and discovered that the prevalence of HCC in non-cirrhotic and cirrhotic NAFLD patients was 4.6 and 374.4 per 10,000, respectively. Furthermore, older men with a history of smoking and diabetes were at greater risk of HCC. So, cirrhosis is the main reason why people with NAFLD are more likely to get HCC [**Pinyopornpanish et al., 2021**].

1.6 Hepatocellular carcinoma treatments

The treatment outcomes for HCC patients are generally poor, and over 70% of patients present with disease that is incurable by current therapies. Ding and Wen utilised the SEER database to identify 80,347 HCC patients of all stages from 1988 to 2015. The SEER findings show an improvement in survival for HCC patients from 1988 to 2015, which might be attributed to developments in early detection and improved therapy (**Fig. 1.7**) [**Ding and Wen, 2021**].

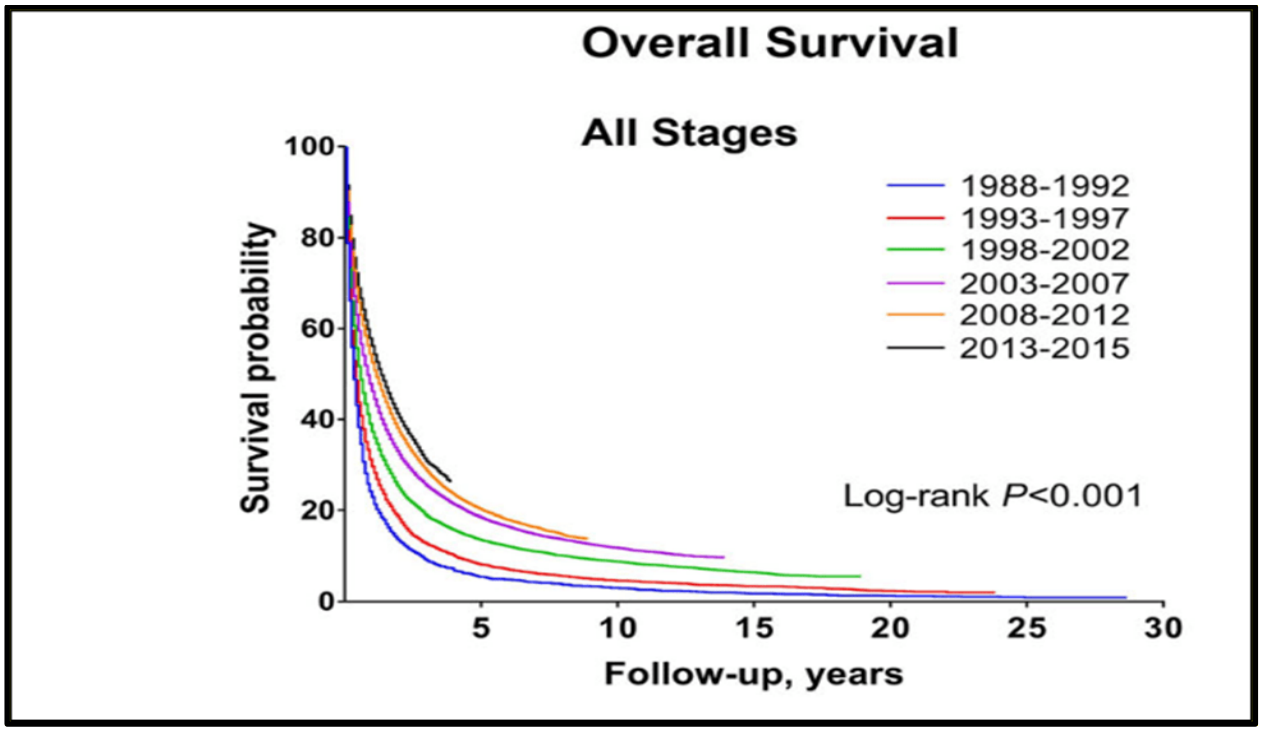

Figure 1.7 Overall survival of all stage of HCC patients using the Surveillance Epidemiology and End Result (SEER) database of 80,347 patients from 1988 to 2015. The overall survival was calculated by Kaplan-Meier method [**Ding and Wen, 2021**].

There are multiple options for HCC treatments, for example, resection, liver transplantation, radiofrequency ablation (RFA), radiation therapy, chemotherapy, microwave, percutaneous ethanol injection (PEI), immunotherapy, transarterial chemoembolisation (TACE), and selective internal radiation therapy (SIRT) [**Niu et al., 2021**]. Unfortunately, only few of those results in major improvements in outcome for late-stage disease patients. The American Association for the Study of Liver Disease (AASLD) guideline advises liver resection as the first choice for HCC treatment in patients with a relatively healthy liver. However, this is not recommended in cases of early-stage disease who have cirrhosis and poor liver function. Furthermore, in advanced stages of HCC, since risk of recurrence is substantial, resection is not recommended especially HCC patients with cirrhosis [**EASL, 2018; Heimbach et al., 2018**]. Manzini's group compared eight sets of guidelines and concluded that all guidelines advised resection as the first option for HCC patients with healthy liver who did not have cirrhosis [**Manzini, 2017**]. The European Association for the Study of the Liver (EASL) guidelines state that surgery is the best way to treat HCC cancer but limited to patients in very early or early stages. However, the EASL guideline also recommends that liver transplantation may be considered for HCC patients with end-stage liver disease who would alive for less than a year without transplantation. The EASL treatment recommendations for HCC with cirrhosis are shown in **Fig. 1.8** [**EASL, 2018**].

One of the most serious issues for patients suffering with HCC is its "late detection". Although numerous HCC treatments are available, most patients' options are restricted due to advanced stage illness, metastasis, tumour size, and liver functions, all of which impact treatment decisions [**Lee et al., 2015; Marrero et al., 2018**]. Treatment goals for such late-presenting patients are often palliative, with an emphasis on extending lives and improving quality of life rather than curing. Patients detected at an early stage, on the other hand, have a better chance of long-term survival because, unlike late-stage illness, therapeutic alternatives are accessible. As a result, researchers will have a huge challenge in developing novel treatment options for HCC during the next two decades.

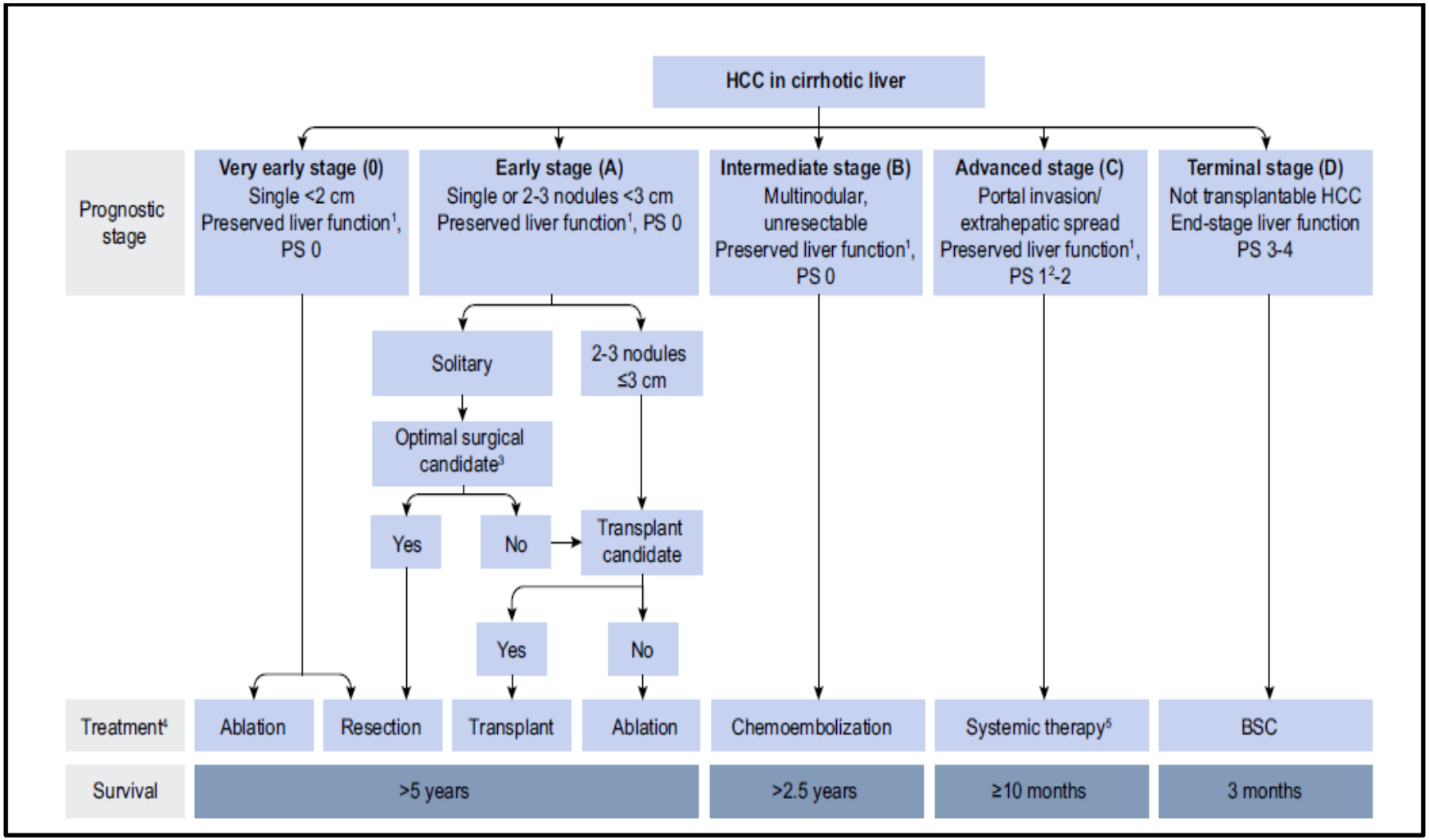

Figure 1.8 An updated clinical practical guideline for HCC in cirrhotic liver [EASL, 2018].

1.6.1 Systemic therapy

Over the past decade, targeted therapy has resulted in ground-breaking advancements in advanced HCC. These drugs destroy tumours by changing important cellular signalling mechanisms, such as inhibit angiogenesis or cell cycle progression. Currently, clinical studies are investigating the combination of immune checkpoint inhibitors (ICIs) which has demonstrated stronger anticancer benefits in some studies [**Tan et al., 2022; Vafaei et al., 2022**]. **Fig. 1.9** illustrates how the molecular targeted therapy for HCC inhibits the downstream signals necessary for cell survival, proliferation, differentiation, migration, and angiogenesis **[Niu et al., 2021**].

The number of systemic drugs that have been approved for treating HCC, such as multityrosine kinase inhibitors (sorafenib, lenvatinib, regorafenib, and cabozantinib), anti-angiogenic antibody drugs (ramucirumab and apatinib), and immune checkpoint inhibitors (nivolumab and pembrozilumab). These medications can be used alone (nivolumab or pembrolizumab) or in combination (ipilimumab in combination with nivolumab or atezolizumab in combination with bevacizumab) [**Bruix et al., 2021; Llovet et al., 2022; Zhang et al., 2022**]. Now, approximately 50% of HCC patients are treated with systemic therapy [**Llovet et al., 2022**].

1.6.1.1 Tyrosine kinase inhibitors

Systemic therapy by tyrosine kinase inhibitors (TKIs) increased the overall survival (OS) of HCC patients. The TKIs are divided into two lines; the first line is sorafenib and lenvatinib. The others are regorafenib and cabozantinib. These drugs are used for unresectable HCC [**Bruix et al., 2021; Vogel et al., 2021**]. As mentioned earlier, nearly half of HCC patients are treated with systemic therapy, which is often used with TKIs, anti-angiogenesis drugs (ramucirumab), and immune checkpoint inhibitors (atezolizumab, ipilimumab, nivolumab, and bevacizumab) [**Bruix et al., 2021; Llovet et al., 2022**; **Zhang et al., 2022**].

Figure 1.9 The molecular targeted therapy for HCC. The key mechanisms include inhibiting tyrosine kinase activity in the intracellular domain of the receptor tyrosine kinase or directly blocking the transmission of downstream signals essential in cell survival, proliferation, differentiation, migration, and angiogenesis [**Niu et al., 2021**].

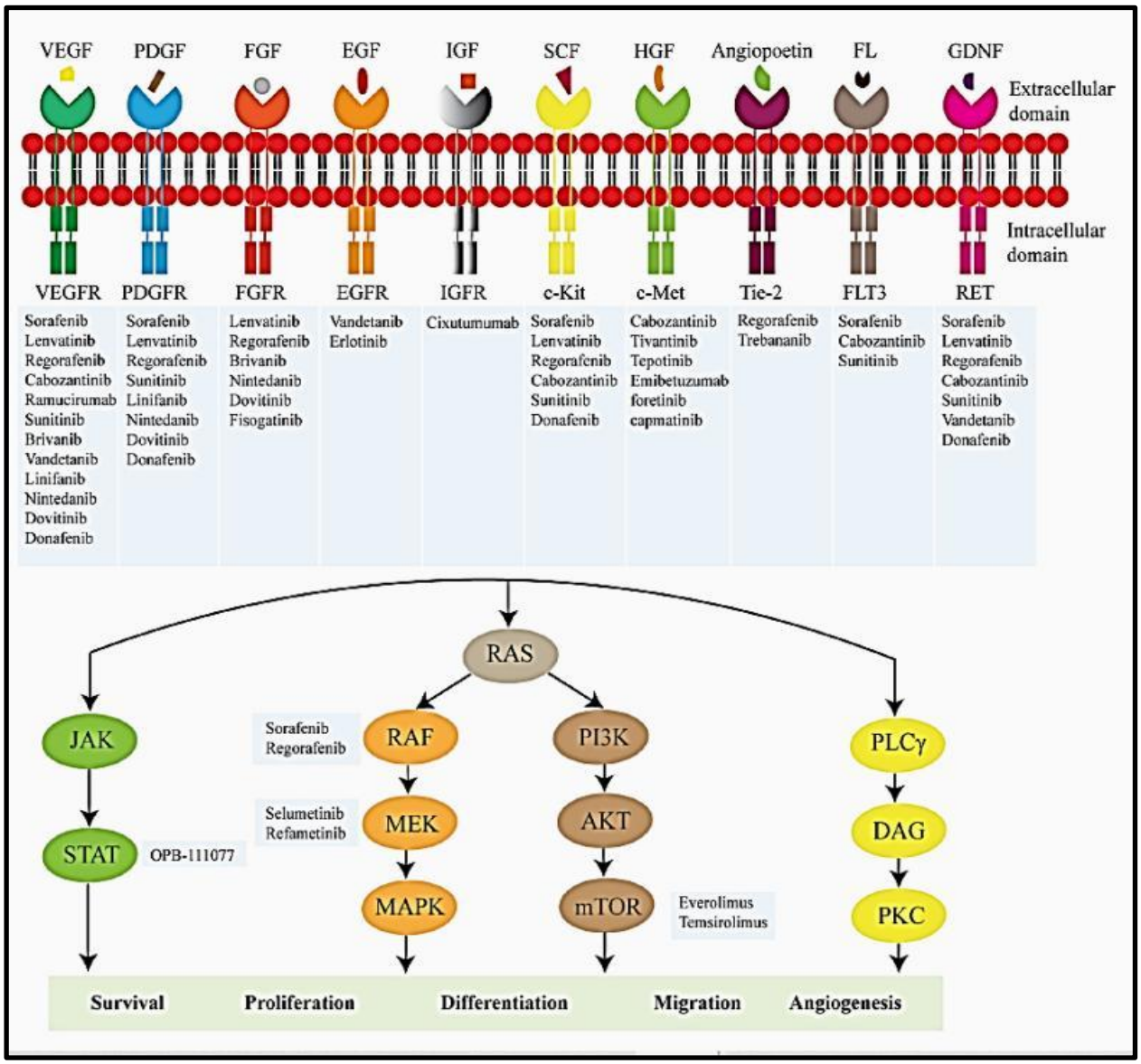

VEGRF: vascular endothelial growth factor receptor, **PDGFR:** platelet-derived growth factor receptor, **FGFR:** fibroblast growth factor receptor, **EGFR:** epidermal growth factor receptor, **IGFR:** insulin-like growth factor receptor, **c-Kit:** KIT proto-oncogene receptor tyrosine kinase also known as stem cell factor receptor or CD117, **HGFR:** hepatocyte growth factor receptor or **c-Met:** tyrosine-protein kinase Met, **Tie-2:** tyrosine kinase with immunoglobulin-like and EGF-like domains 2, **FLT3:** Fms-related tyrosine kinase 3, **RET:** rearranged during transfection, **RAF:** rapidly accelerated fibrosarcoma**, MEK:** mitogen-activated protein kinase**, STAT:** signal transducer and activator of transcription**, and mTOR:** mammalian target of rapamycin.

1.6.1.1.1 Sorafenib

Until recently, there have been no effective systemic treatment for advanced hepatocellular carcinoma patients. In 2007, the U.S. Food and Drug Administration (U.S. FDA) authorised sorafenib as the first drug for unresectable HCC [**Peek and Reddy, 2008**]. Sorafenib, a urea analogue, is an oral multi-TKI, inhibits tumour growth by blocking tyrosine kinases receptors such as VEGF receptor-1 (VEGFR-1), VEGFR-2, VEGFR-3, platelet-derived growth factor receptor-ß (PDGFR-ß), as well as the inhibition of downstream RAF/MEK/ERK signalling cascade [**Raoul et al., 2017**]. It is widely used but extends survival by a modest median of just 10 weeks [**EASL, 2018].** Until now, only sorafenib and lenvatinib, have been authorised as first-line treatments for unresectable or metastatic HCC [**Saung et al., 2021; Zhang et al., 2022**]. In addition, a combination of atezolizumab and bevacizumab [**Zhang et al., 2022**], and nivolumab and ipilimumab [**Saung et al., 2021**] have been approved for HCC patients. **Fig. 1.10** illustrates additional individual or combination drug development pipelines for HCC patients.

1.6.1.1.2 Lenvatinib

Lenvatinib belongs to the TKI drugs that target vascular endothelial growth factor receptor 1 (VEGFR1), VEGFR2, VEGFR3, fibroblast growth factor receptor 1 (FGFR1), FGRF2, FGRF3, FGRF4, and PDGFR. Lenvatinib, like sorafenib, is now commonly used for advanced or unresectable HCC [**Hatanaka et al., 2021; Yang et al., 2021**]. In HCC patients, it had a lower progression rate and a longer progression-free survival (PFS) than sorafenib, but not OS [**Cheng et al., 2017; Cabibbo et al., 2020; Moawad et al., 2020**].

1.6.1.1.3 Regorafenib

Regorafenib is a TKI used as a second-line treatment for advanced HCC. Regorafenib was approved by the U.S. FDA in May 2017 as a second-line treatment for patients with advanced HCC who had previously been treated with sorafenib. Because its structure is similar to sorafenib, it may target a number of kinases involved in tumour angiogenesis, growth, and metastasis, such as VEGFR1, VEGFR2, VEGFR3, PDGFR, and FGFR [**Yang et al., 2021**].

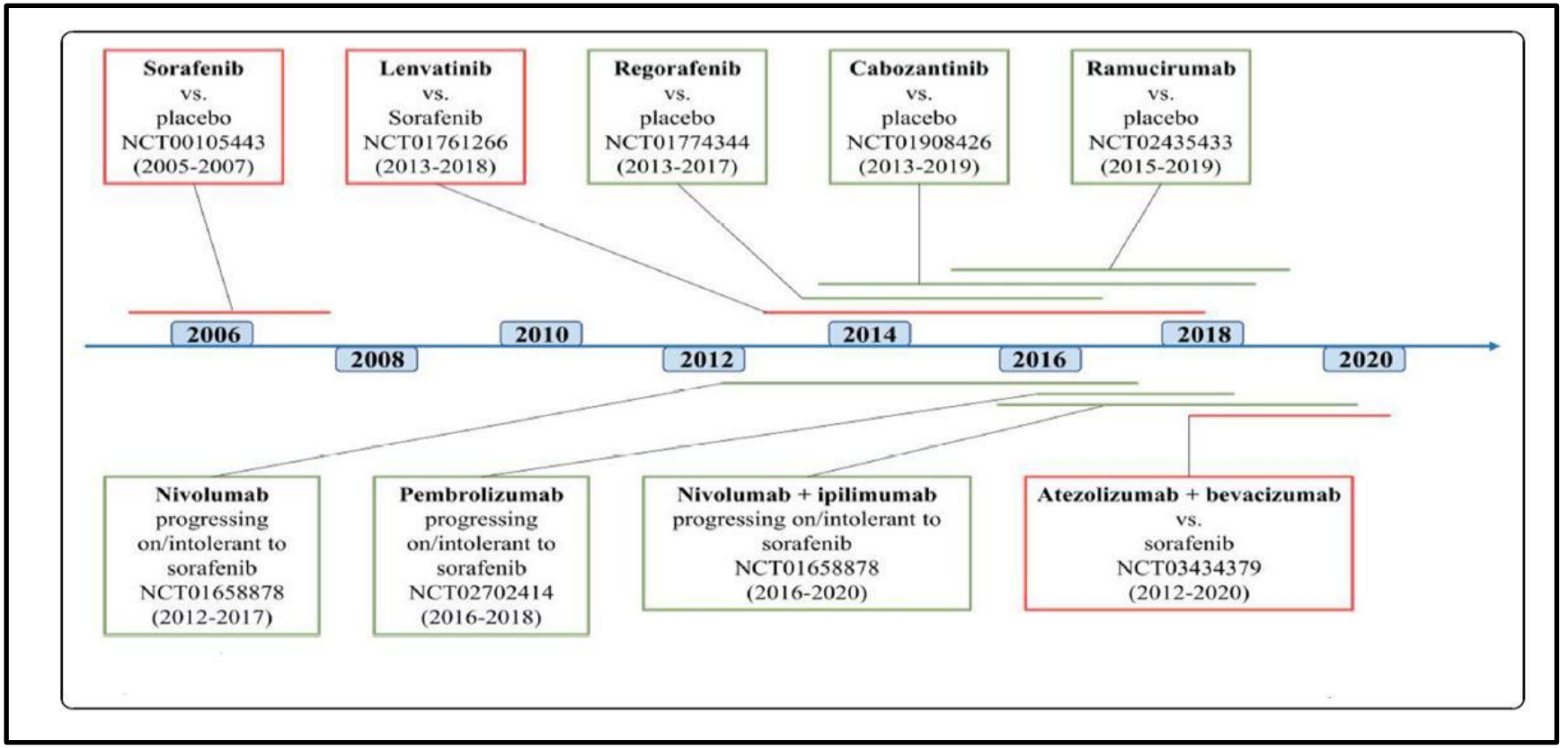

Figure 1.10 Drugs currently approved for HCC, as well as the timing of pivotal clinical trials. The lines on the timeline represent the time between the start of the actual study and FDA approval. First-line therapies are represented by **red boxes**, while second-line therapies are represented by **green boxes** [**Zhang et al., 2022**].

1.6.1.1.4 Cabozantinib

Cabozantinib was approved by the U.S. FDA in 2012 for the treatment of medullary thyroid cancer. In 2019, the U.S. FDA approved cabozantinib for the treatment of HCC patients with acquired resistance to sorafenib. Cabozantinib is a tyrosine kinase inhibitor, which can inhibit proteins involved in tumorigenesis and angiogenesis, such as VEGFR1-3, mesenchymal-epithelial transition (MET), anexelekto, and angiopoietin receptors TIE-2. This drug was approved by U.S. FDA since January 2019 [**Trojan, 2020; Yang et al., 2021**]. Cabozantinib is currently being researched for multiple lines of HCC therapy, particularly in conjunction with immune checkpoint inhibitors.

1.6.1.2 Anti-angiogenesis drugs

Tumour angiogenesis plays an important role in tumour development, progression, and metastasis. As a result, there is a considerable deal of interest in creating antiangiogenic treatments. Hypoxia is the primary starting component of tumour angiogenesis, resulting in increased levels of VEGF, angiopoietin (Ang) 1, Ang2, hypoxia-inducible factor 1 (HIF-1), and other proteins in hypoxic cells [**Qi et al., 2022**].

Over-expression of angiogenic factors and inhibition of anti-angiogenic factors are crucial mediators of tumour-induced blood supply, which results in increased tumour vascular burden and abnormal blood vessels. Due to the very vascular character of HCC, anti-angiogenic therapy is now advised for advanced stage of HCC [**Moawad et al., 2020**]. VEGF, PDGF, tyrosine kinase with immunoglobulin-like and EGF-like domains (TIE) are crucial factors in the angiogenesis produced by HCC**.** Thus, inhibiting tumour angiogenesis may therefore lower the blood flow essential for tumour development, and tumour cell proliferation will stop owing to a shortage of nutrients and growth hormones required to sustain the production of newly created blood **vessels [Ebadi et al., 2014**].

1.6.1.2.1 Ramucirumab

Ramucirumab is a humanised recombinant IgG1 monoclonal antibody that selectively binds to VEGFR2 to prevent the binding of VEGF-A, VEGF-C, and VEGF-D and suppresses endothelial cell proliferation and migration triggered by tumour angiogenesis-related ligands [**Yang et al., 2021**]. This drug was approved in 2019 by the U.S. FDA for the treatment of advanced HCC patients with α-fetoprotein level ≥ 400 ng/mL (identifying a sub-group with poor prognosis, more likely

to derive benefit) who have previously received sorafenib [**Zhu et al., 2019; Choucair et al., 2021**] or after sorafenib treatment [**Finn et al., 2022**].

1.6.1.2.2 Apatinib

Apatinib is a TKI that inhibits proliferation and migration of endothelial cells by blocking VEGFR2 and inhibit tumour angiogenesis [**Yang et al., 2021**]. Zheng's team analysed the effects of apatinib in 178 patients with advanced HCC from 2017 to 2020 (24-month follow-up) and discovered that it had similar PFS results to sorafenib [**Zheng et al., 2022**]. Zhang's group discovered that patients with sorafenib-resistant advanced HCC caused by the HBV may live longer if they get apatinib therapy following supportive care. This is particularly true for people who have fewer liver tumours and extrahepatic spread [**Zhang et al., 2020**].

1.6.1.3 Immune checkpoint inhibitors

Immune checkpoint inhibitors (ICIs) have transformed the treatment of HCC over the past five years. The FDA has approved this regimen because studies comparing it to sorafenib have demonstrated that atezolizumab and bevacizumab together increase OS. Recent studies have shown that durvalumab with tremelimumab is more effective than sorafenib and the combination of atezolizumab and cabozantinib in improving PFS. The FDA has also approved pembrolizumab monotherapy and the combination of nivolumab and ipilimumab as a second-line treatment for cancer based on efficacy evidence [**Llovet et al., 2022**].

Fig 1.11 shows that ICIs work by blocking the inhibitory receptors on the T-cell membrane, which reverses T-cell weakness found in cancer and thereby boosts antitumor immune response [**Okoye et al., 2017**]. Current ICIs target the PD-1 (or its ligand PD-L1) and CTLA-4 pathways, both of which play essential roles in autoimmune regulation [**Delire et al., 2022**]. The current ICIs and their specific targets for HCC patients are listed in **Table 1.1**.

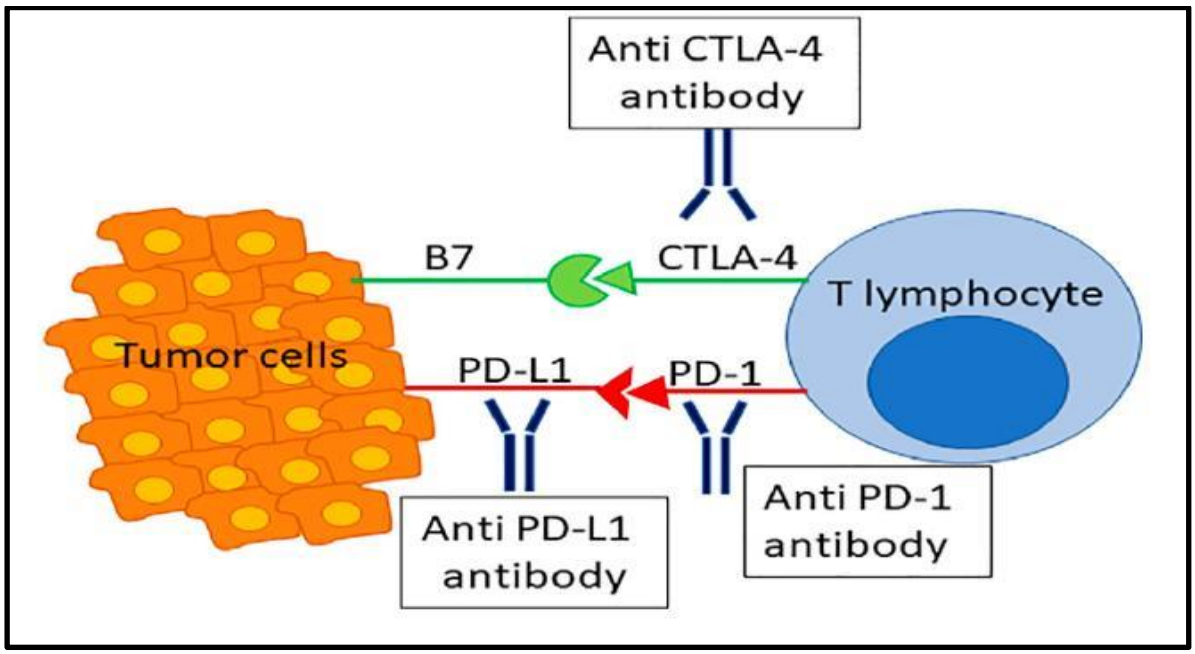

Figure 1.11 The mechanism of immune checkpoint inhibitors. The scheme represents the immunotherapy targeted at the PD-1 (or its ligand, PD-L1) and CTLA-4 pathways, which play important roles in autoimmune regulation. PD-1: programmed cell death protein 1. **PD-L1**: programmed cell death ligand 1. **CTLA-4**: cytotoxic T-lymphocyte-associated protein 4 [**Delire et al., 2022**].

Table 1.1 Updated immune checkpoint inhibitors [**Katariya et al., 2022**].

Class	Name	FDA Approval for HCC	FDA HCC Indication
PD-1	Nivolumab	Yes 22 September 2017	HCC previously treated with sorafenib
	Pembrolizumab	Yes 9 November 2018	HCC previously treated with sorafenib
	Sintilimab	No	NA
	Camrelizumab	No	NA
PD-L1	Atezolizumab	No	NA
	Avelumab	No	NA
	Durvalumab	No	NA
CTLA-4	Ipilimumab	No	NA
	Tremelimumab	No	NA
Combo	Nivolumab + Ipilimumab	Yes 10 March 2020	HCC previously treated with sorafenib
	Atezolizumab + Bevacizumab	Yes 29 May 2020	Unresectable or metastatic HCC
	Durvalumab + Tremelimumab	No	NA

Data from FDA.gov.

1.6.1.3.1 Nivolumab

Nivolumab, the first humanised IgG4 monoclonal antibody against programmed cell death protein 1 (PD-1) that restores host immunological function against tumour cells by competitively inhibiting PD-1 immune checkpoint signalling [**Fan et al., 2022**]. This drug was approved for the treatment of advanced HCC in December 2020 and is suggested for use as a second-line therapy for advanced-stage HCC following sorafenib failure [**Yau et al., 2019**; **Kim et al., 2020**]. However, since post-marketing studies were unable to demonstrate a benefit for HCC patients previously treated with sorafenib, nivolumab was withdrawn from the market in 2021 [**Lemery and Pazdur, 2022**].

1.6.1.3.2 Pembrozilumab

Pembrolizumab is a humanised monoclonal antibody that binds selectively to IgG4 (κ isotype) that blocks PD-1 interacting to its ligands PD-L1 and PD-L2 [**Kudo, 2019**].
Pembrolizumab was efficacious and well tolerated in patients with advanced HCC who had previously had sorafenib treatment and was licensed by the FDA in 2018 as a second-line drug for the treatment of advanced HCC after sorafenib therapy [**Zhu et al., 2018; Verset et al., 2022**]. Furthermore, in the absence of systemic treatment, pembrolizumab demonstrated sustained anticancer efficacy, a good OS, and a good safety profile **[Verset et al., 2022**], similar to the prior data [**Zhu et al., 2018]**, or patients who had not previously undergone immunotherapy [**Benson et al., 2021**].

1.6.1.3.3 The combination of atezolizumab and bevacizumab

In late May 2020, the U.S. FDA authorised atezolizumab (an PD-L1 monoclonal antibody) in combination with bevacizumab (an anti-VEGF monoclonal antibody) as the first-line therapy for advanced HCC [**Trojan, 2020; Wang et al., 2021**]. These combination drugs surpassed sorafenib in terms of OS and PFS in patients with advanced HCC [**Finn et al., 2020**]. The place of TKIs in the second-line setting following atezolizumab and bevacizumab is not acknowledged due to a lack of evidence from clinical studies [**Decraecker et al., 2021**].

1.6.2 The future trends of systemic therapy

The future trend of systemic therapy specifically with advanced HCC are the combination of TKI with ICI such as atezolizumab vs cabozantinib, nivolumab vs ipilimumab, and lenvatinib vs pembrolizumab [**Gordan et al., 2020**]. As demonstrated in **Table 2**, the Markov model was used to evaluate the effectiveness of sequence systemic treatment of 15 regimens to evaluate the advantages (median OS) and drawbacks (severe side effects) compared with the worst sequence of sorafenib-ramucirumab in advanced HCC. The first-line medicine lenvatinib was used, followed by the second-line drug nivolumab, which had the best outcomes as measured by the median OS (27 months). The sequence treatment of the first- and second-line drugs of lenvatinib and pembrolizumab showed a good outcome with 25 months of OS. In contrast, the least effective treatment order was first-line sorafenib followed by second-line ramucirumab or regorafenib or cabozantinib (18 months of median OS [**Cabibbo et al., 2020**].

Table 1.2 Treatment regimens' efficacy and safety based on overall survival median [**Cabibbo et al., 2020**].

Treatment Sequence	Median OS (mo)
Lenvatinib-Nivolumab	27
Lenvatinib-Pembrolizumab	25
Atezolizumab plus Bevacizumab-Nivolumab	24
Sorafenib-Nivolumab	23
Atezolizumab plus Bevacizumab-Pembrolizumab	23
Lenvatinib-Ramucirumab	22
Lenvatinib-Regorafenib	22
Lenvatinib-Cabozantinib	22
Sorafenib-Pembrolizumab	20
Atezolizumab plus Bevacizumab-Ramucirumab	20
Atezolizumab plus Bevacizumab-Regorafenib	20
Atezolizumab plus Bevacizumab-Cabozantinib	20
Sorafenib-Cabozantinib	18
Sorafenib-Regorafenib	18
Sorafenib-Ramucirumab	18

OS: overall survival **Mo**: month

1.6.3 Vaccine

As previously stated, patients with advanced HCC have limited therapy choices, the majority of them are based on systemic therapy of TKIs, ICIs, and anti-angiogenesis drugs. However, current therapies for advanced-stage HCC are unsatisfactory and do not prevent recurrence. As a consequence, other approaches such as vaccinations are being considered as potential strategies for addressing this problem, with the potential to enhance clinical results when used in conjunction with currently authorised systemic drugs. Cancer vaccines are aimed at stimulating an enhanced immune response through the activation and proliferation of T cells, especially cytotoxic T lymphocytes (CTL), which precisely target and destroy cancer cells, resulting in a better therapeutic outcome for the patient. Currently, several tumor-associated antigens have been identified in HCC. However, the majority of these antigens are not specific to HCC. Hence, only a few of them have the potential to develop into vaccines such as peptide-based and dendritic cell based-vaccine [**Khong and Overwijk, 2016; Wang et al., 2021; Repáraz et al., 2022**]. HCC vaccines can be divided into four categories; cell-based, virus-based, peptide-based, and nucleic acid vaccine.

1.6.3.1 Peptide-based vaccine

Cancer vaccines based on epitope peptides have the power to evoke humoral and cellular immune responses against tumour antigens such as tumour-specific antigens or tumour-associated antigens. This type of vaccine is composed of a peptide or a combination of linked or free peptides, as well as adjuvants that aid in their stabilisation and enhance its immunogenicity [**Khong and Overwijk, 2016; Abd-Aziz and Poh, 2022**]. The type of cancer and the patient's immunological characteristics determine which peptide is best suited for developing a cancer vaccine. Despite this, because of their ease of use, peptide vaccines are widely used in the treatment of diseases, including HCC. The common HCC antigens such as alpha-fetoprotein (AFP), glypican-3, Forkhead Box M1, heat shock protein 70, and Wilms' Tumour-1 [**Charneau et al., 2021; Ni, 2022**]. **Table 1.3** displays examples of peptide vaccine development for HCC therapy in clinical trials.

Table 1.3 Clinical trials for HCC vaccine with published results [Repáraz et al., 2022].

Vaccine	Patient Inclusion Criteria	Patients (n)	Immune Response (%)	Clinical Response CR/PR/SD/PD	Observations
AFP HLA-A*02 restricted peptides+IFA	AFP+ tumors from (stage IV patients)	6	66	0/0/0/6	Increased CTL response
AFP HLA-A*24:02 restricted peptides+IFA	Stage B/C tumors	15	33	1/0/8/6	Increased CTL response
GPC3 HLA-A*24:02 and HLA-A*02- restricted peptides+IFA	Advanced or metastatic HCC	33	91	0/1/19/13	Antitumor efficacy
GPC3 HLA-A*24:02 and HLA-A*02- restricted peptides+IFA	Patients undergone curative resection Vaccines as Adjuvant therapy	41	85	Not applicable	Improved recurrence rate
Gv1001 peptide + GM-CSF + cyclophosphamide	Advanced-stage HCC with no previous antitumor treatment	37	0	0/0/17/20	None clinical nor detected immunological response
DCs pulsed with AFP HLA-A*02 restricted peptides	Stage IV patients pretreated with surgery and/or chemotherapy	10	60	0/1/0/9	No objective clinical responses
DCs pulsed with fused recombinant proteins (AFP, MAGE-1 and GPC-3)	After surgical resection and locoregional therapy	12	92	Not applicable	Trend to improved survival
DCs pulsed with autologous tumor lysate	Advanced HCC	31	0 *	0/4/17/10	Improved survival
DCs pulsed with autologous tumor lysate	Unresectable HCC	8	62	0/0/4/3	Immune response generation
DCs pulsed with hepatoma cell-line (HEP-G2) lysate	No other therapeutic option	35	11.4	0/1/6/18	Evidence of antitumor efficacy

Clinical trials with no published results have been excluded. CR (complete response), PR (partial response), SD (stable disease), PD (progressive disease). * immunologic response measurement was not appropriate.

1.6.3.2 Dendritic cells-based vaccine

Dendritic cells (DCs) are the most efficient antigen-presenting cells in the human immune system. They originate from hematopoietic cells in the bone marrow. DCs play a key role in not only activating innate immunity but also triggering CTL-mediated adaptive immunity. DCs may recognise infections, tissue damage signals, and tumour antigens and subsequently travel to secondary lymphoid organs, where they deliver antigens and activate T cells. DCs may cause a variety of immune responses, including T helper type 1 (Th1), Th2, regulatory T cells, and Th17. DCs come in a variety of phenotypes and locations. They form a cellular system that is dispersed throughout the body and is in charge of immune monitoring [**Castell-Rodríguez et al., 2017**]. Furthermore, mature DCs have been shown to increase the cytotoxic activity of natural killer cells (NKs), which function as innate immune effector cells to remove pathogen-infected or tumour cells [**Constantino et al., 2017; Shang et al., 2017; Jeng et al., 2022**]. DC-based vaccines have become a promising immunotherapy for treating different types of cancer, including HCC, because of these qualities.

To date, there are no HCC vaccines development utilising peptide-based or DCs-based technologies that have been utilised to treat HCC patients. Finding a fresh solution to the HCC issue in the twenty-first century will be challenging.

1.7 Common genetic alterations in HCC

Genomic instability, somatic mutations, single-nucleotide polymorphisms, and dysregulated signalling pathways, have been associated with the onset and progression of HCC. A better comprehension of the genetic alterations that play important roles in HCC could lead to the identification of potential driver mutations and the discovery of early diagnostics and novel therapeutic targets against HCC [**Niu et al., 2016**].

1.7.1 Genomic instability

Genomic instability is one of the hallmarks of cancer and usually refers to an increase in the rate at which abnormalities occur within the genome. There are many types of genomic instability, such as chromosomal instability, which refers to the rapid change in chromosome structure and quantity in cancer cells as compared to normal cells. Other types of genomic instability include microsatellite instability (defined by an increase or decrease in the number of oligonucleotide repeats present in microsatellite sequences) and forms of genomic instability characterized by higher frequencies of base pair mutations [**Negrini et al. 2010**].

Due to global hypomethylation (**described in section 1.8**), long-interspersed nuclear elements-1 (LINE1) are activated in various epithelial cancers including HCC [**Burns et al., 2017; Schauer et al., 2018**]. These activated LINE1 elements contribute towards genomic instability by carrying out insertional mutagenesis and genomic rearrangements [**Schauer et al., 2018; Shukla et al., 2013**].

1.7.2 Somatic mutation

Somatic mutations are caused by errors during the repair or replication of damaged DNA. Such errors in the germline enhance genetic variation by serving as a substrate for natural selection, which drives evolution. The rate of germline mutation is determined by genetics and is influenced by a number of factors such as environmental constraints and population size. Mutation rates cannot be decreased to zero since doing so would preclude future evolutionary change and would have fitness consequences for the organism owing to the extensive repair and replication systems required [**Vijig and Dong, 2020**].

Fig. 1.12 illustrates the various forms of DNA damage that occur on a regular basis in every cell, such as base modification, single- or double-strand DNA breakage, and crosslinks. Errors in DNA repair and replication, on the other hand, result in *de novo* mutations ranging from

single-nucleotide variations to chromosomal abnormalities. Mutations, unlike DNA damage, are irreversible and hence unavoidably accumulate over time [**Vijig and Dong, 2020**].

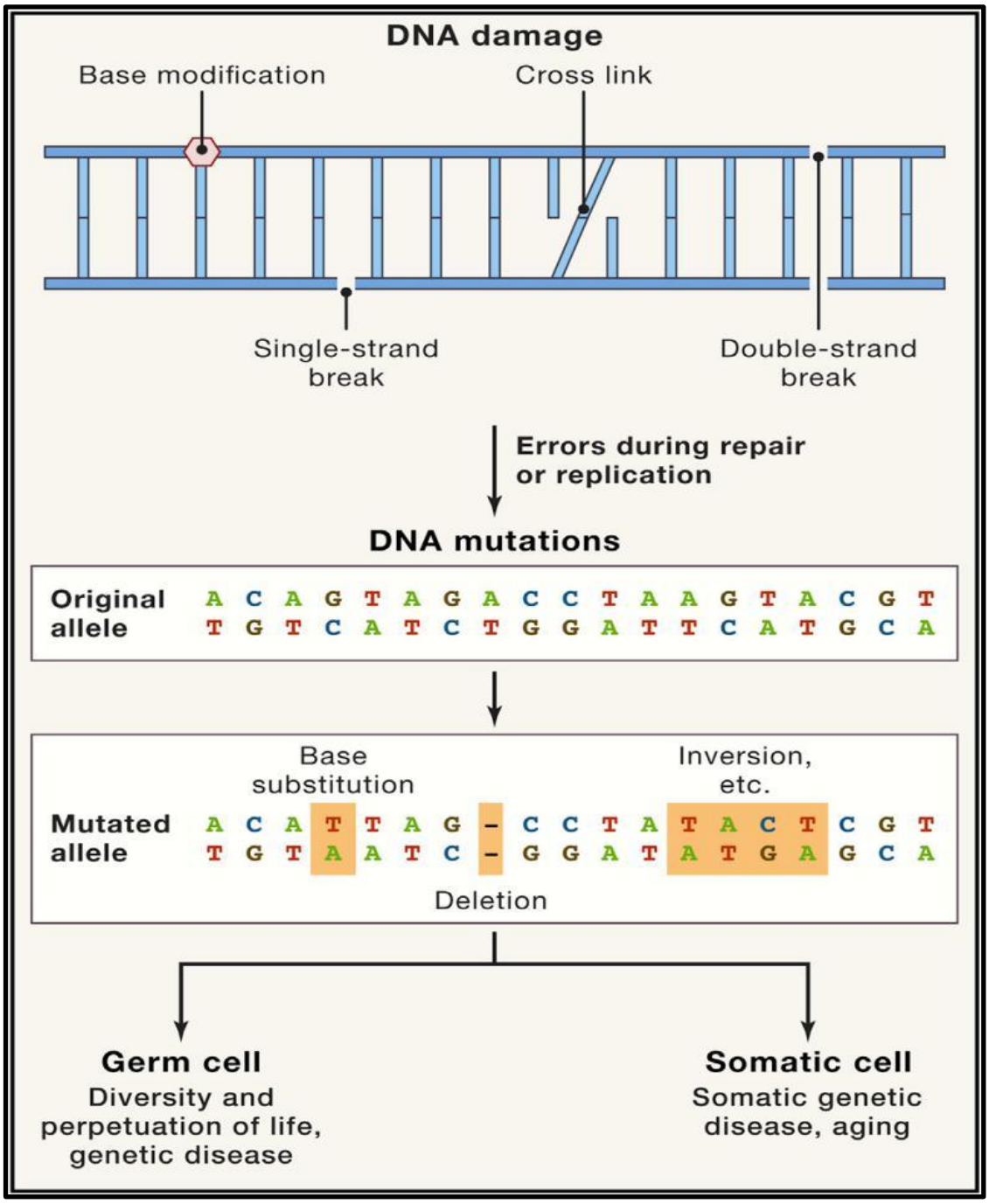

Figure 1.12 Somatic DNA mutation causes and effects [Vijig and Dong, 2020].

1.7.3 Copy number variation

Copy number variations (CNVs) are a kind of genomic variation that is poorly understood. Human carry two copies of a gene; one comes from paternal and another one from maternal. However, only one copy may be present and on the other hand three or more than three copies may also be present. The basis for this alteration is mostly duplications and deletions, ranging in size from a few hundred base to several mega base compared to a reference genome [**Giri and Mohapatra, 2017; Zhou et al., 2017; Pös et al., 2021**].

Gene amplification (increase in copy number) and deletion (loss in copy number) are prevalent in cancer cells and contribute to cancer cell proliferation, sensitivity, and resistance to therapy. Trastuzumab (Herceptin®), the first targeted precision medicine, was developed to treat breast cancer patients with HER2 gene amplification. Oncogenes, genes that promote cancer growth, such as HER2 often have an aberrant rise in gene count. In contrast, genes that slow the growth of cancer (tumour suppressor genes) may be deleted from the genome by gene deletion [**https://www.oncomine.com/blog/detecting-copy-number-variants-in-the-cancer-genome**].

HCC is a multistep, multifactorial process characterized by frequent aberrant gene modifications, including as CNVs [**Niu et al., 2016**]. Furthermore, CNVs have been demonstrated to promote oncogene overexpression and tumour suppressor gene inactivation in a variety of cancers, including HCC [**Shahrisa et al., 2021**]. Large-scale amplifications and deletions of chromosomal arms or whole chromosomes characterise the CNV landscape in HCC genomes (amplified: 1q, 5p, 6p, 8q, 17q, 20q, and Xq or deletion: 4p-q, 8p, 13p-q, 16p-q, 17p, 21p-q, and 22q) [**Kan et al., 2013**]. Amplification of *PRKDC* gene in HCC has been shown to be associated with resistance to TACE and radiotherapy [**Cornell et al., 2021**]. Thus, understanding the functions of CNVs is thus critical for HCC prevention, therapy, and prognosis prediction [**Bian et al., 2021**].

1.8 Epigenetics

In eukaryotic cells, genomic DNA is compacted into chromatin within the nucleus. The chromatin further condenses to form chromosomes which exhibit regions of differential accessibility of the DNA sequence for transcription factors and other DNA binding proteins that control the activation or repression of transcription of specific genes [**Bardhan and Liu, 2013; Chen et al., 2014**]. The DNA folding mechanism starts with the DNA being wrapped around the octamer core of histone proteins (basic proteins which binding with the negative charge of the DNA chain) to form nucleosomes. There are multiple levels of chromatin packaging such as the formation of condensed chromosome structures during cell division, the chromatin coils further condense to form chromosomes (**Fig. 1.13**) [**Jansen and Verstrepen, 2011**].

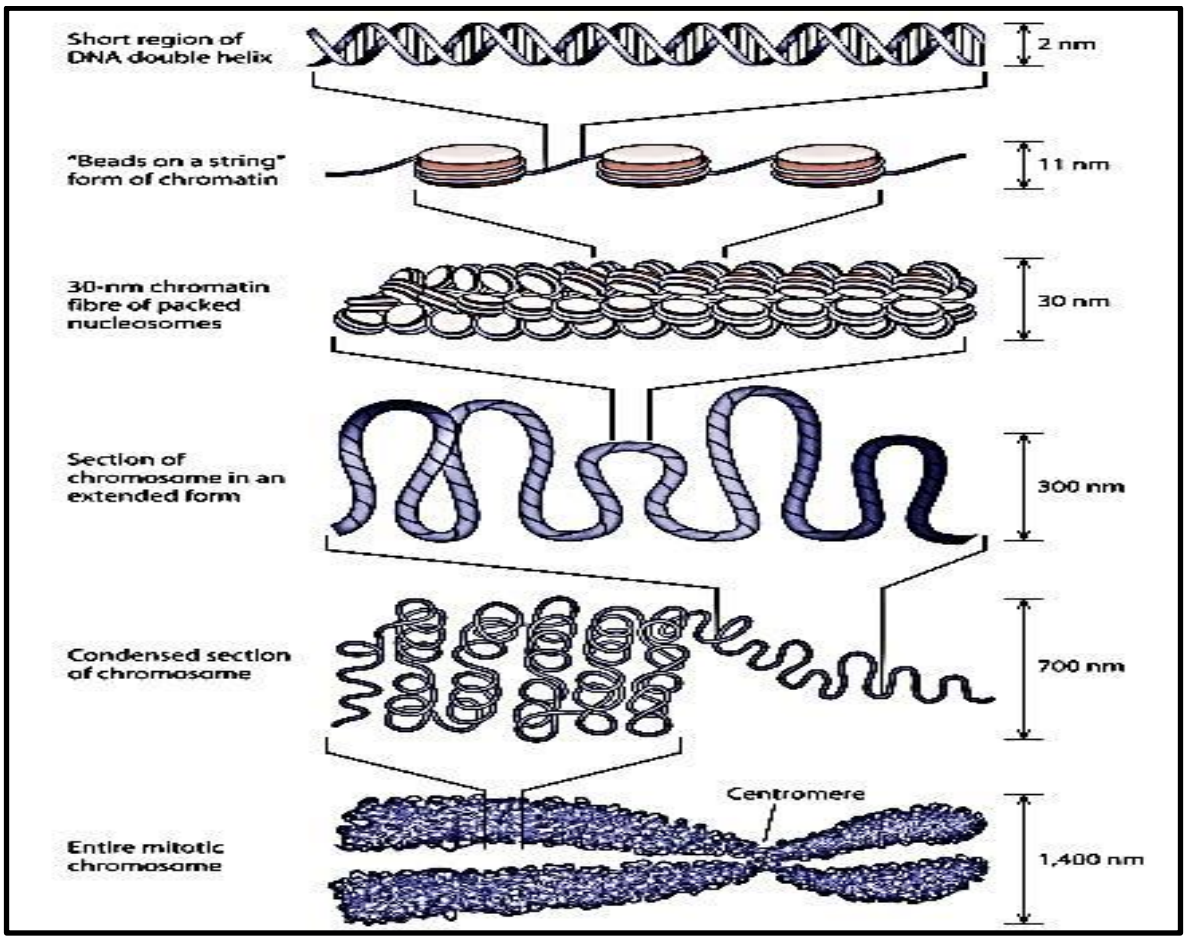

Figure 1.13 Chromatin structure in eukaryotic cells [**Jansen and Verstrepen, 2011**].

The concept of epigenetics was first proposed by Conrad Waddington in 1942 [**Waddington, 1942**]. Epigenetics can be defined as a heritable change in gene expression without alteration of the primary DNA sequences [**Ma et al., 2014**]. Epigenetic changes are clonally heritable from mother cell to daughter cell during cell division, although trans-generational epigenetic inheritance is rare [**Issa, 2011**]. Although all cells contain the same genetic information, all genes are not activated simultaneously in all cell types. This is due to the influence of epigenetics mechanisms which regulate gene expression to allow differential expression in different cell types [**Moore et al., 2013**]. Thus, epigenetic changes are crucial in maintaining cellular identity, but have relatively little role in inheritance between generations. The main mechanisms of epigenetics are DNA methylation, histone modifications and non-coding RNA-mediated epigenetic regulation [**Dawson and Kouzarides, 2012**].

1.8.1 DNA methylation

DNA methylation involves the methyl (CH_3) group from S-adenosylmethionine (SAMe) being transferred to the fifth position of cytosine ring in a CpG dinucleotides site to form 5'-methyl-cytosine by one of a family of DNA methyltransferase enzyme (DNMT1, and DNMT3a, DNMT3b) (**Fig. 1.14A**) [**Gal-Yam et al., 2008; Braghini et al., 2022**]. In the mammalian genome, around 70% of cytosines in CpG dinucleotides are methylated. However, most of the genome is deficient in CpG sites and these sites are much rarer than would be predicted based on the overall GC content1of the genome. The exception to this is short stretches of DNA, known as CpG islands (CpGIs) which have a much greater density of CpG sites. Approximately 60% of human genes have CpGIs (represent 1-2% of human genome) in their promoter region, usually overlapping the transcriptional start site. These promoters associated CpGIs are mostly unmethylated in normal cells. In contrast, hypermethylation in these regions at a very high frequency occurs in all cancer types [**Fukushige and Horii, 2013; Braghini et al., 2022**]**.** The model of DNA methylation patterns in normal and cancer cells is shown in **Fig. 1.14B.** In short, during cellular transformation there is a redistribution of the DNA methylation pattern; sporadic CpG sites in the bulk of DNA become hypomethylated while many CpGIs become hypermethylated.

In mammals, DNA hypermethylation by *de novo* DNA methyltransferase (DNMT) at CpG-rich regions or CpGIs at promoter region are essential for normal cell development of mammals during embryogenesis [**Issa et. al., 2011; Li and Zhang, 2014**], normal growth and development [**Williamson et al., 2015**]. However, this process may be interrupted by cancer. DNA methylation is typically maintained by DNMT1 when cells divide, ensuring genome stability through multiple cell divisions. Thus, DNA methylation patterns represents epigenetic inheritance. In addition, DNA methylation plays a crucial role in developmental process of X-chromosome inactivation and genomic imprinting in mammals [**Li and Zhang, 2014**].

1.8.2 Histone modification

The nucleosome is the basic unit of chromatin which comprises of 8 (octamer, a pair of each protein) histone proteins (H2A, H2B, H3, and H4, overall positive charge) which are wrapped tightly with 146 base pairs of DNAs (overall negative charge) (**Müller-Knapp, and Brown, 2004; Zhang and Reinberg, 2018**]. It is well established that multiple modification of histones can occur, particularly in the tail regions which protrude from the histone octamer that can influence overall chromatin architecture and gene expression, for example; (**1**) histone acetylation of lysine by histone acetyl transferases which can unwind the DNA from the nucleosomes, resulting in gene activation, (**2**) histone phosphorylation of threonine, serine, and tyrosine by kinases can change the chromatin structure, and (**3**) histone methylation of lysine and arginine by methyltransferases can activate or deactivate gene expression depending on the site and other histone modifications in that region for example, either methylation or acetylation of lysine 4 on histone H3 (H3K4) can activate gene expression while methylation of lysine 9 or 27 on histone H3 can recruit repressive complexes. [**Müller-Knapp, and Brown, 2004; Kouzarides, 2007; Bannister and Kouzarides, 2011**]. The sites of histones modification are shown in **Fig 1.15**. Thus, histone modifications are crucial in controlling gene expression, chromatin structure and DNA repair.

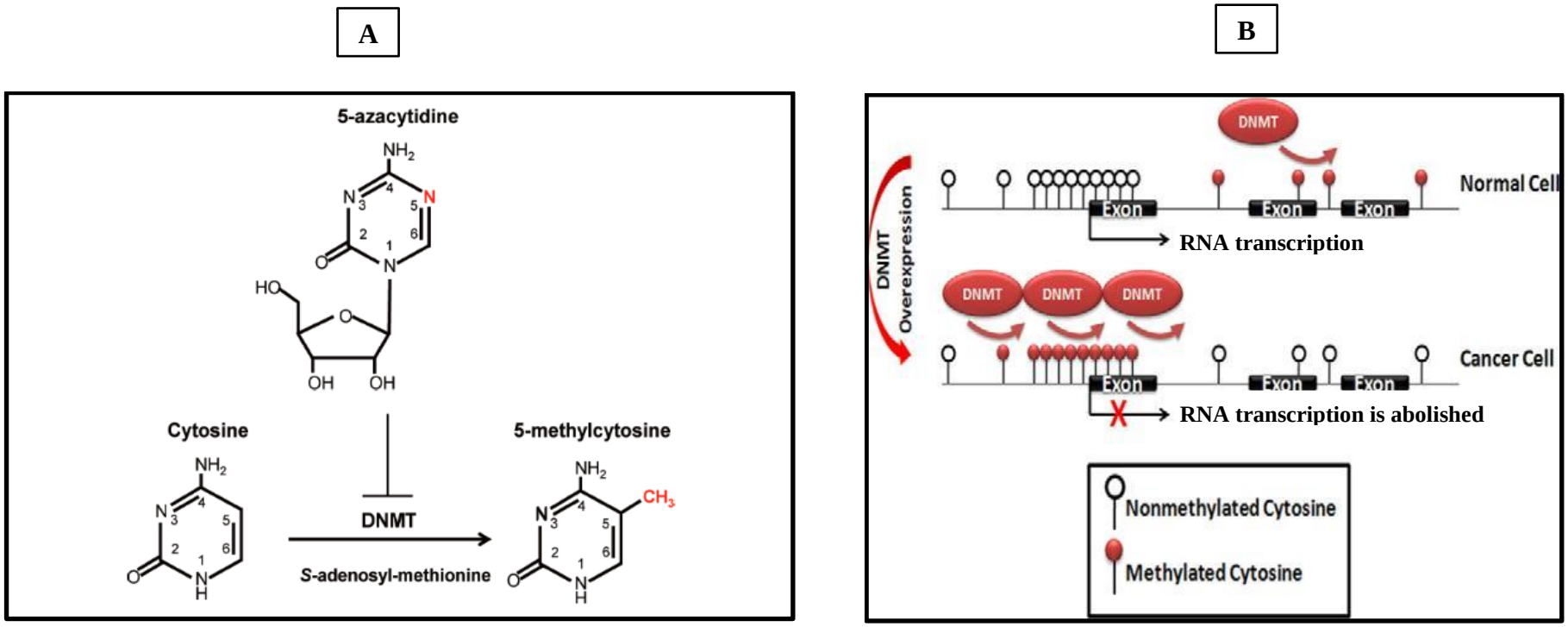

Figure 1.14 DNA methylation. (**A**) Methylation of cytosine by DNA methyltransferases (DNMTs**)** to the 5 position of cytosine ring which can be blocked by 5-azacytidine [**Fukushige and Horii, 2013**]**.** (**B**) The model of DNA methylation in normal and cancer cells [**Muntean and Hess, 2009**]

.

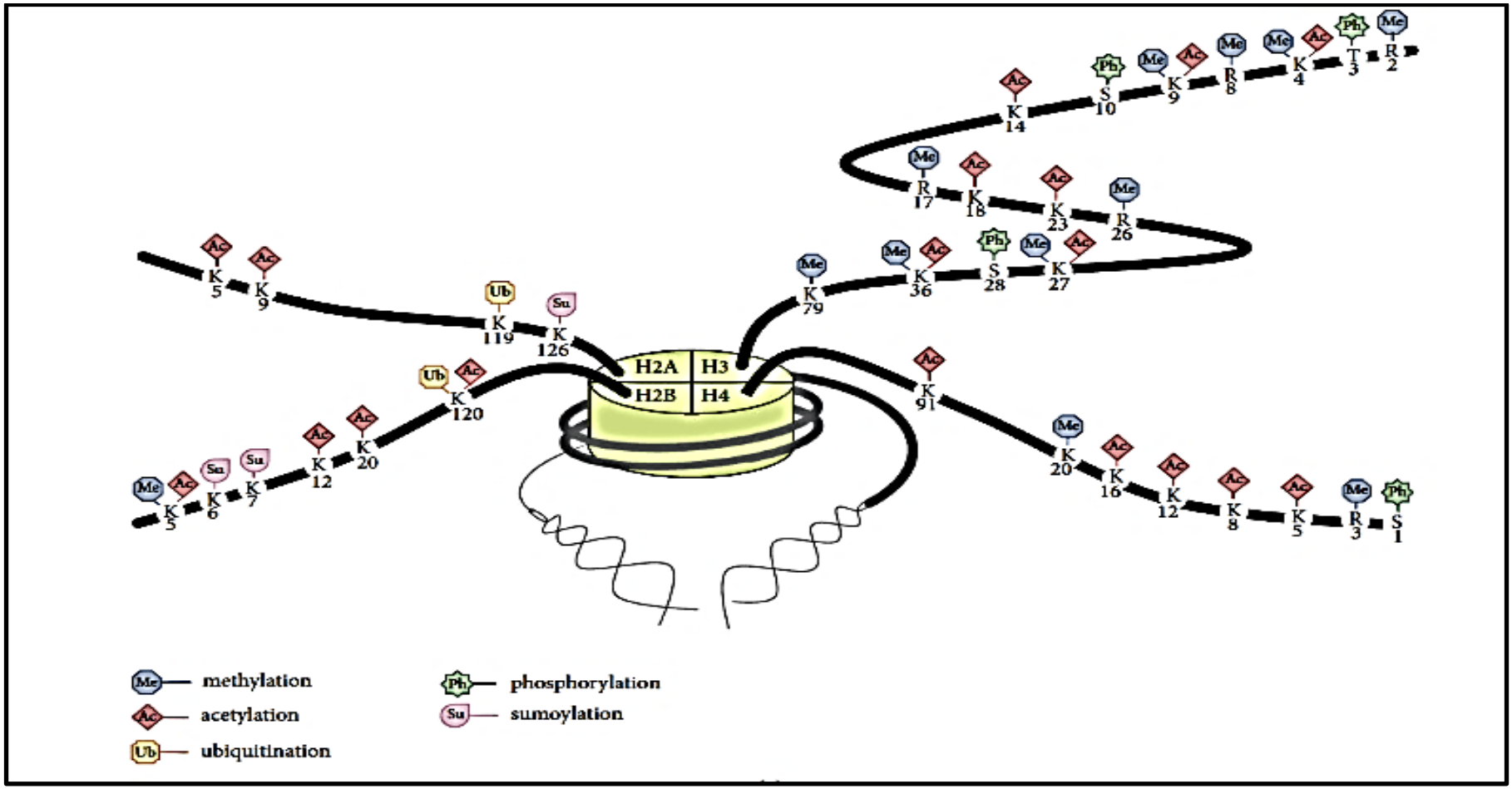

Figure 1.15 Histone can be modified by methylation, acetylation, phosphorylation, ubiquitination, and sumoylation [**Araki and Mimura, 2017**].

1.8.3 Non-coding RNA-mediated epigenetic regulation

Non-coding RNA (ncRNA) is widely recognised for its role in the regulation of many diseases such as HCC [**Ding, 2018**], and it is now well established as having crucial roles in the maintenance of cellular homeostasis and functionality [**Ratti et al., 2020**]. The ncRNA members are ranging from small to long RNA which consists of small RNA (18-24 nucleotides), microRNA (miRNA), and long non-coding RNA (lncRNA, >200 nucleotides). Small RNA can control chromatin modification and structure without involving RNA interference (RNAi). Small and lncRNA play an important role to regulate gene expression, the stability of genome, and the defense mechanism against foreign genetics [**Holoch and Moazed, 2015**]. The mechanism occurs when small non-coding RNA (ncRNA) or lnc RNA interacts with the protein involved in the epigenetic process, leading to gene expression inhibition (**Fig. 1.16)**, please read Morris publication for more details [**Morris et al., 2015**]. MicroRNAs are small RNA molecules that influence gene expression at the translational level by binding to the 3-untranslated region of the targeted messenger RNA (mRNA) and resulting a block in translation and/or destruction of the transcript [**Ratti et al., 2020**]. However, miRNAs have been shown to interact with other areas such as the 5′ UTR, coding sequences, and gene promoters. MiRNAs can also initiate translation or control transcription under specific situations [**ÓBrien et al., 2018**].

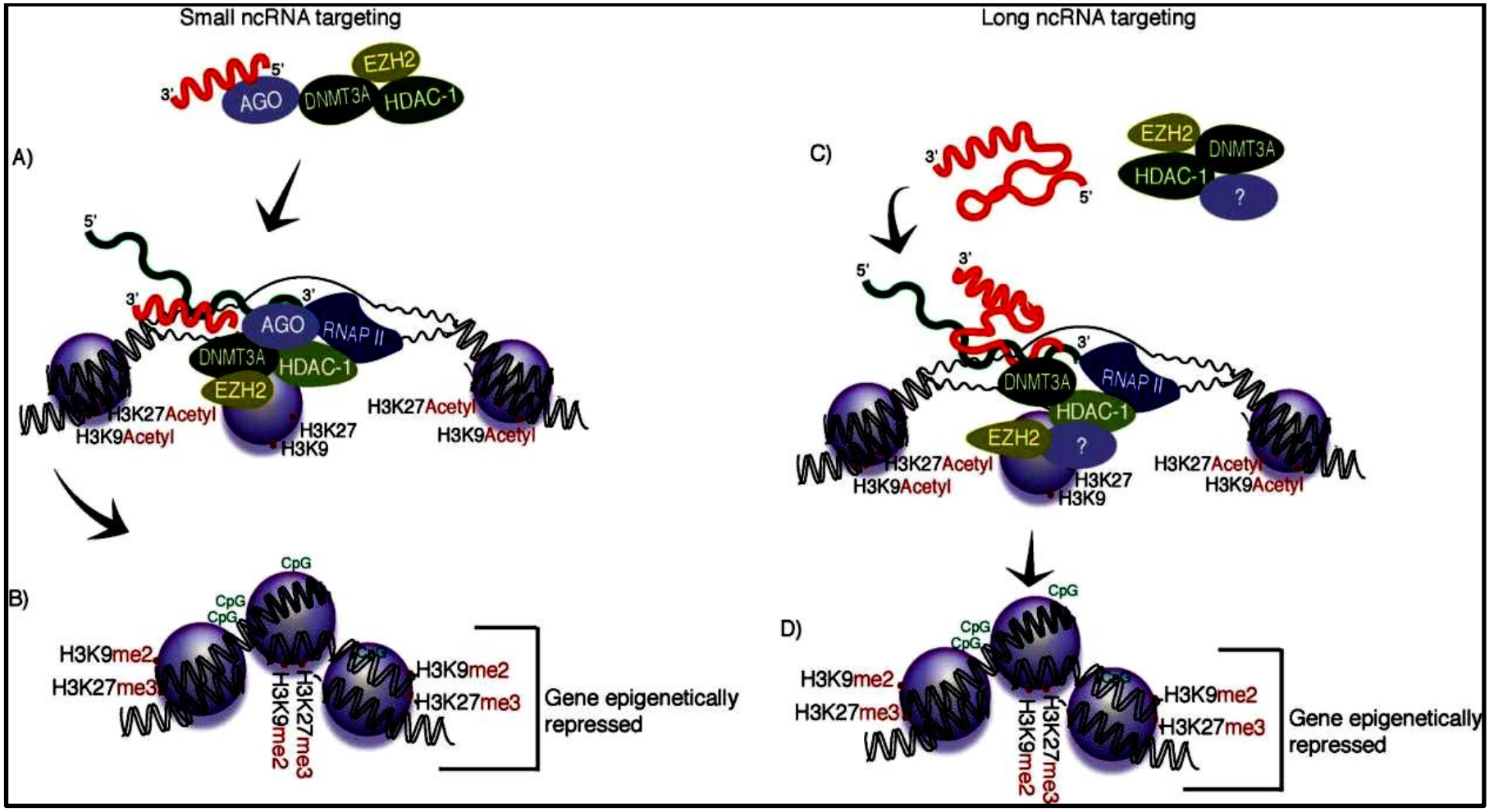

Figure 1.16 Non-coding RNA silencing. **(A**) and **(B)**, Small non-coding RNAs form complexes with transcriptional genes, resulting in gene silencing (gene repression) **(C)** and (**D)**, long non-coding RNAs interact with DNMT3A and repress transcription [**Morris et al., 2015**].

1.9 DNA methylation and gene silencing

DNA methylation does not change the genetic information, but it is important in gene silencing or repression of gene transcription [**Issa, 2011; Williamson et al., 2015**]. The two main mechanisms for gene silencing associated with promoter methylation are direct inhibition of binding of the transcription factors or recruitment of transcriptional corepressor molecules via methyl-CpG binding proteins (MBPs) that bind the methyl-CpG sites leading to chromatin compaction and repressing transcriptional activities [**Fukushige and Horii, 2013**] (**Fig. 1.17**). DNA methylation plays an essential role in chromatin stability, genetic imprinting, gene expression, [**Zhang and Xu, 2017**], and X chromosome inactivation [**Klustein et al., 2016**]. However, abnormalities in the DNA methylation pattern have been widely observed in cancer, aging, metabolic disorders, neurological disorders, and autoimmune disease [**Klustein et al., 2016**]

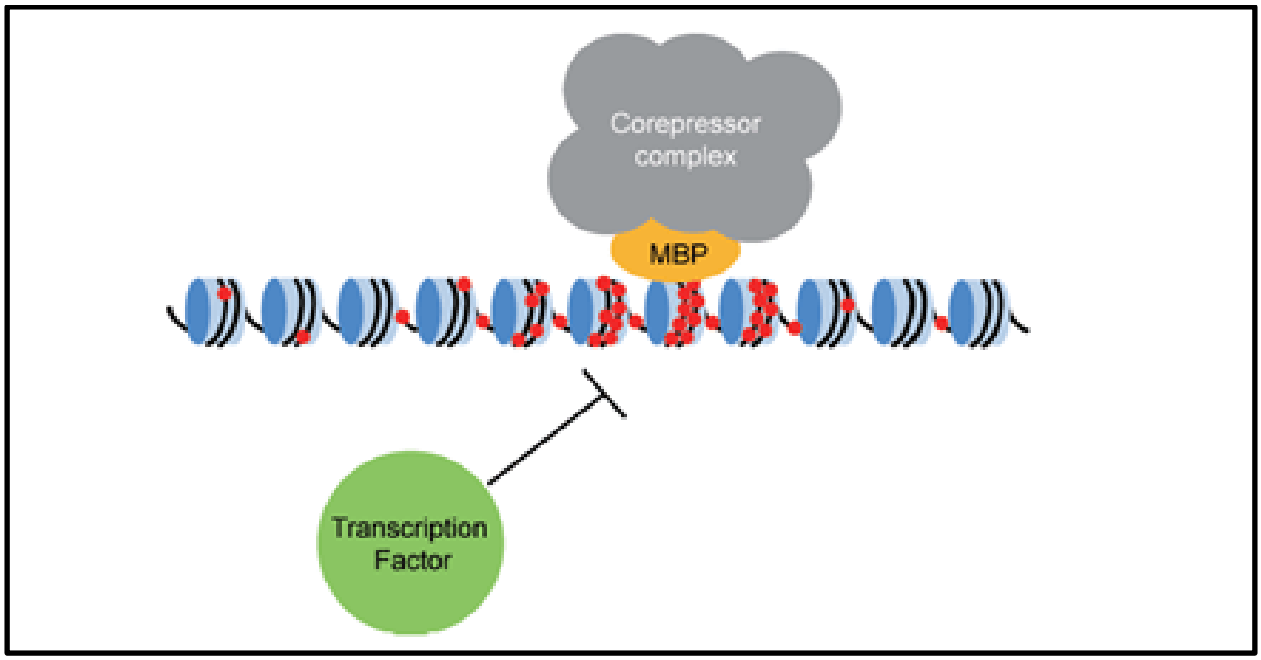

Figure 1.17 Illustrate the mechanism of transcriptional silencing. One of the mechanisms to inhibit transcription by blocking the binding of transcription factor with its recognition site by DNA methylation and MBPs (methyl-CpG binding proteins) [**Fukushige and Horii, 2013**].

1.10 DNA methylation in cancer

Cancer cells frequently exhibit global hypomethylation but simultaneously exhibit higher methylation at CpGIs, and, as result, silencing of gene expression [**Issa et al., 2004**]. Aberrant DNA hypermethylation is very common in cancer cells, resulting in widespread hypermethylation of CpGIs. These hypermethylated CpGIs can be found at tumour suppressor genes, DNA repair proteins, pro-differentiation factors, cell cycle control regulators, and anti-apoptotic factors development [**Fukushige et al., 2013**]. Thus, DNA hypermethylation leads to inhibition of the transcription of various genes involved in cell growth, proliferation, and development. The pattern of altered DNA methylation in cancer cells is specific to each tumour type and may represent different pathophysiological processes, stage of the disease which can be used as a biomarker of cancer [**Esteller et al., 2005; Gao et al., 2008**]. Moreover, DNA methylation biomarkers might have the benefit over genetic and protein markers. This is because the amount of aberrant DNA methylation of specific CpGIs are higher than those of genetic defects (a few numbers of genes are mutated). Therefore, detection of aberrant DNA methylation is potentially important indicator of cancer for risk assessment, early detection, prognosis, and predicting therapeutic responses [**Fukushige et al., 2013**]. Breast cancer gene 1 (*BRCA1*) was one of the first genes shown to be frequently targeted by hypermethylation as a key step in cancer development. The *BRCA1 gene* is a tumour suppressor gene that, plays a key role in carcinogenesis of breast and ovarian cancer. Inactivation of *BRCA1* gene may occur in hereditary cancer through inheritance of gene mutations [**Nindrea et al., 2018**]. However, studies revealed that this gene is highly methylated in sporadic, non-familial breast cancer and that hypermethylation, not mutation, is the predominant mechanism leading to *BRCA1* inactivation in 10-30% of sporadic cases [**Cho et al., 2015; Nindrea et al., 2018; Vos et al., 2018**]. Similarly, *MLH1*, a DNA mismatch repair (*MMR)* gene has been associated with familial colon cancer. Loss of activity of the *MMR* genes (*MLH1, PMS2, MSH2,* and *MSH*6) leads to microsatellite instability which can be observed in hereditary nonpolyposis colorectal carcinoma (HNPCC). Furthermore, most cases of HNPCC can be attributed to inheritance of mutation in *MMR* genes, predominantly *MLH1* or *MSH2* [**Caja et al., 2020**]. Around 15% of colorectal cancers are thought to develop in part due to defective function of the DNA MMR [**Sinicrope et al., 2011**] and in such sporadic cases loss of MMR activity is most frequently due to *MLH1* hypermethylation.

1.11 DNA methylation in HCC

In HCC, like other cancer types, hypermethylation of CpGIs has been shown to be common and often includes well established tumour suppressor genes, such as *RASSF1A*, *APC*, and *CDH1* as shown in **Fig. 1.18**. [**Ozen et al., 2013**]. Zhang et al reported that CpGI in these promoters of *RASSF1A* were highly methylated in HCC patients, but not normal liver tissues [**Zhang, 2002**]. Furthermore, *RASSF1A* was highly methylated in stage I and II in early stage of HCCs and can be used to discriminate between HCC and non-HCC tissues [**Moribe et al., 2009**]. The identification and understanding of the DNA methylation changes in the CpGIs related to gene promoters in HCC will be useful and be used for the development of molecular biomarkers for screening, prognosis prediction, early diagnosis, and monitoring treatment efficacy for HCC.

1.12 DNA methylation as a predictor of response or resistance to treatment

DNA methylation levels and pattern can be used to estimate survival, prognosis, diagnosis, progression, and response to therapy [**Hatzimichael et al., 2014**]. Several studies have revealed that DNA methylation can be used as a candidate for cancer therapy. One of the most well know is 5-Azacytidine, a potent DNMT inhibitor. U.S. FDA approved for the treatment of myeloid malignancies. After 5-Azacytidine incorporated into the DNA, leads to DNA hypomethylation [**Yang et al., 2010**].

At present, chemotherapy, RT, or combination of chemoradiation is commonly used in cancer therapy, however, some patients are resistant to these therapies. And initially sensitive patients often develop resistance during their treatment. Although ionising radiations (IR) can kill cancer cells by damaging DNA, the DNA can also be repaired. Moreover, cancer cells can be resistant to anticancer drugs and escapes programmed cell death through DNA methylation leading to inactivation of genes involved in response to DNA damage. It has been reported that hypermethylation of *RUNX3* in human esophageal cancer [**Sakakura et al., 2007**], as well as *RASSF1A*, *RASSF2*A and *HIN-1* in oral squamous cell carcinoma [**Huang et al., 2009**] are associated with increased radioresistance. Whereas hypermethylation of *NR4A3* and *WIF1* induce cisplatin resistance in gastric carcinoma [**Choi et al., 2017**]. It has been reported that DNA methylation inhibition by zebularine increased radiosensitivity of multiple tumour cell lines (Mia-PaCa, Du145, and U251) and U251 xenografts in mice [**Dote et al., 2005**]. Moreover, DNA methylation at *ATM* gene in HNCCP cell line (HCT-116) increased radiosensitivity [**Zhu et al., 2018**].

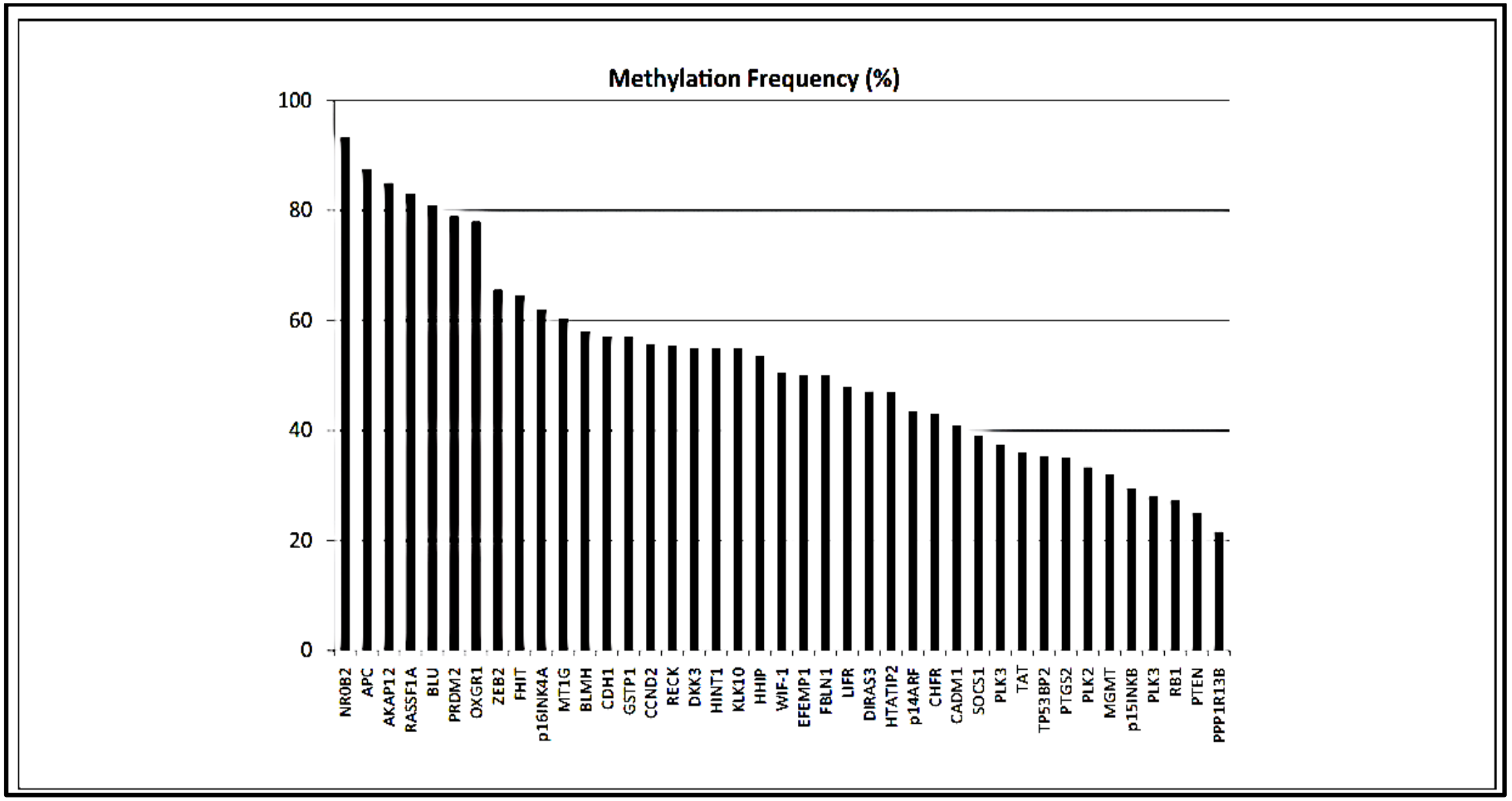

Figure 1.18 Most frequency of methylated genes at promoter in HCC [Ozen et al.

Although in some cell lines, DNA methylation inhibition led to increased resistance, suggesting methylate loci can be involved in both increased and decreased radiosensitivity. The effect of DNA methylation on radiosensitivity is shown in **Table 1.4**.

1.13 Synthetic lethal genes in cancer

Synthetic lethal gene (SLG) describe interdependency between two genes which causes cell death if both genes are inactivated but not individual inactivation. In contrast, if only one of two genes are inactivated the cell remain alive [**Lee et al., 2018**]. The model of SGL is shown in **Fig. 1.19**. Synthetic lethality has become a potential option for development of novel cancer treatments. Identification of synthetic lethal partner genes for disrupted tumour suppressor genes or activating oncogenic mutations can allow specific targeting of cancer cells [**Wang et al. 2017**].

1.13.1 The examples of synthetic lethal genes in cancer

In normal cells, both base- excision repair and homologous recombination (HR) are available for the repair of damaged DNA (**Fig. 1.20A**). A good example of SLGs concept are *PARP* and *BRCA1/2* genes partners. The reason behind this is that PARP is required for repair of single strand DNA (ssDNA) breaks. If these are not repaired before DNA replication, then replication across the single strand break will create a double stand break. This would normally be repaired by HR. Thus, in *BRCA1/2* deficient cells (**Fig. 1.20B**) treated with a PARP inhibitor (**Fig. 1.20C**), there is an accumulation of unrepaired ssDNA breaks, which will become dsDNA breaks at replication. These double strand DNA breaks either do not get repaired or are repaired by an error prone mechanism (non-homologous end joining). This results in cell death due to the accumulation of damaged DNA (**Fig. 1.20D**).

Table 1.4 Effect of methylated DNA related radiosensitivity [Zhu, 2018].

Gene	Methylation site	Tumor	Cell line	Methylation status	P-radiosensitivity	T-Radiosensitivity
ERCC1	Promoter	Glioma	MGR1	Demethylated	Resistant	-
			MGR2	Methylated	Sensitive	-
			SF767	Methylated	Sensitive	-
			T98G	Demethylated	Resistant	-
ATM	Promoter	Colorectal carcinoma	HCT-116	Methylated	Sensitive	Resistant
			LoVo	Demethylated	Resistant	-
			RKO	Demethylated	Resistant	-
		Glioma	U87	Methylated	Sensitive	Resistant
			T98G	Demethylated	Resistant	Resistant
			U118	Demethylated	Sensitive	Sensitive
RASSF1A	Promoter	Pancreatic carcinoma	MiaPaca	Hypermethylated	Resistant	Sensitive
		Glioblastoma	U251	Hypermethylated	Resistant	Sensitive
		Prostate carcinoma	DU145	Hypermethylated	Resistant	Sensitive
		NPC	CNE2	Hypermethylated	Resistant	Sensitive
			SUNE2	Hypermethylated	Resistant	Sensitive

P-radiosensitivity: primordial radiosensitivity

T-radiosensitivity: radiosensitivity after treatment with methyltransferase inhibitor

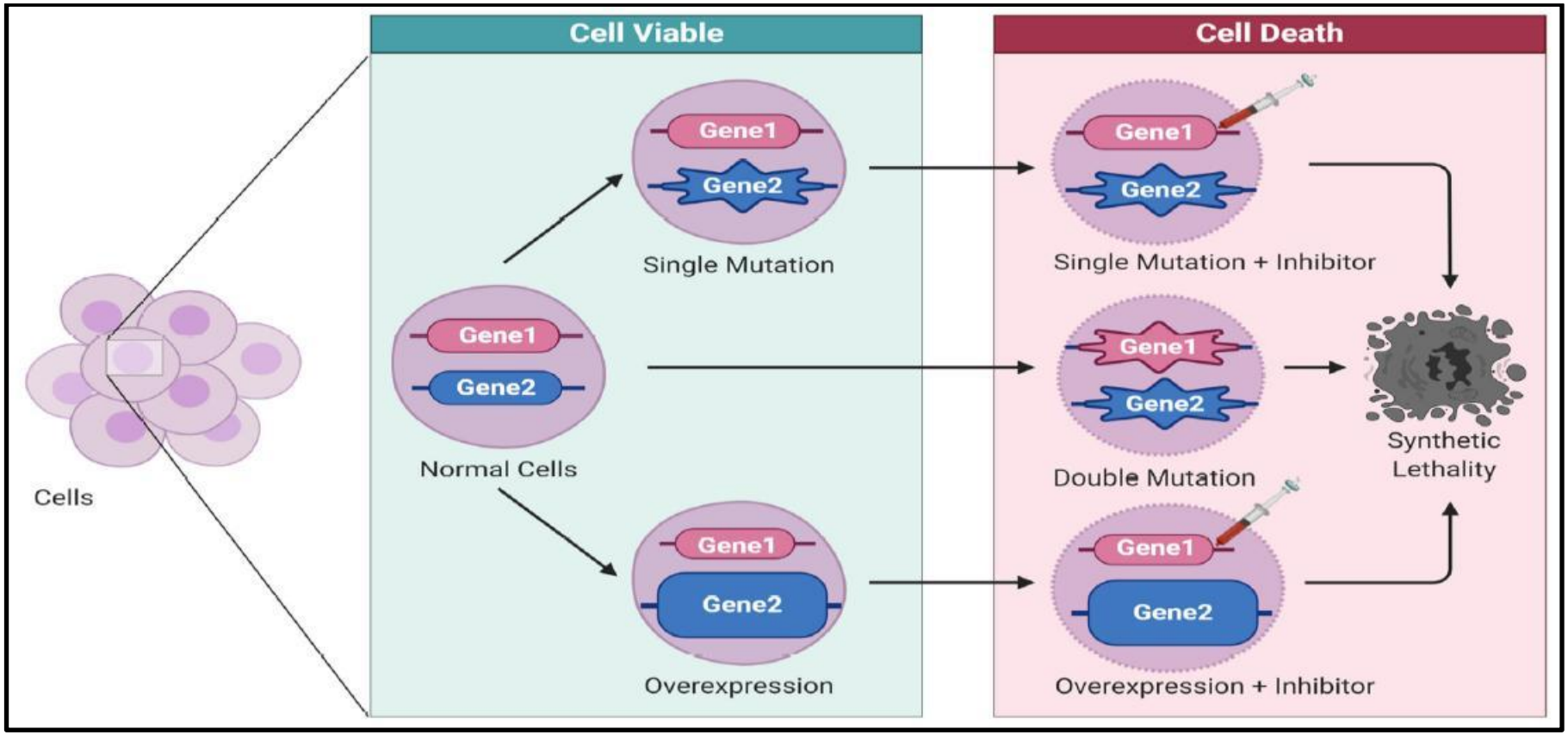

Figure 1.19 The synthetic lethal gene interaction. The two genes are synthetic lethality when inactivation of both genes leads to cell death. In contrast, mutated gene or overexpression alone is not lethal. Tumour suppressor gene mutation or oncogene overexpression in tumour cells could result in gene activation [**Topatana et al., 2022**].

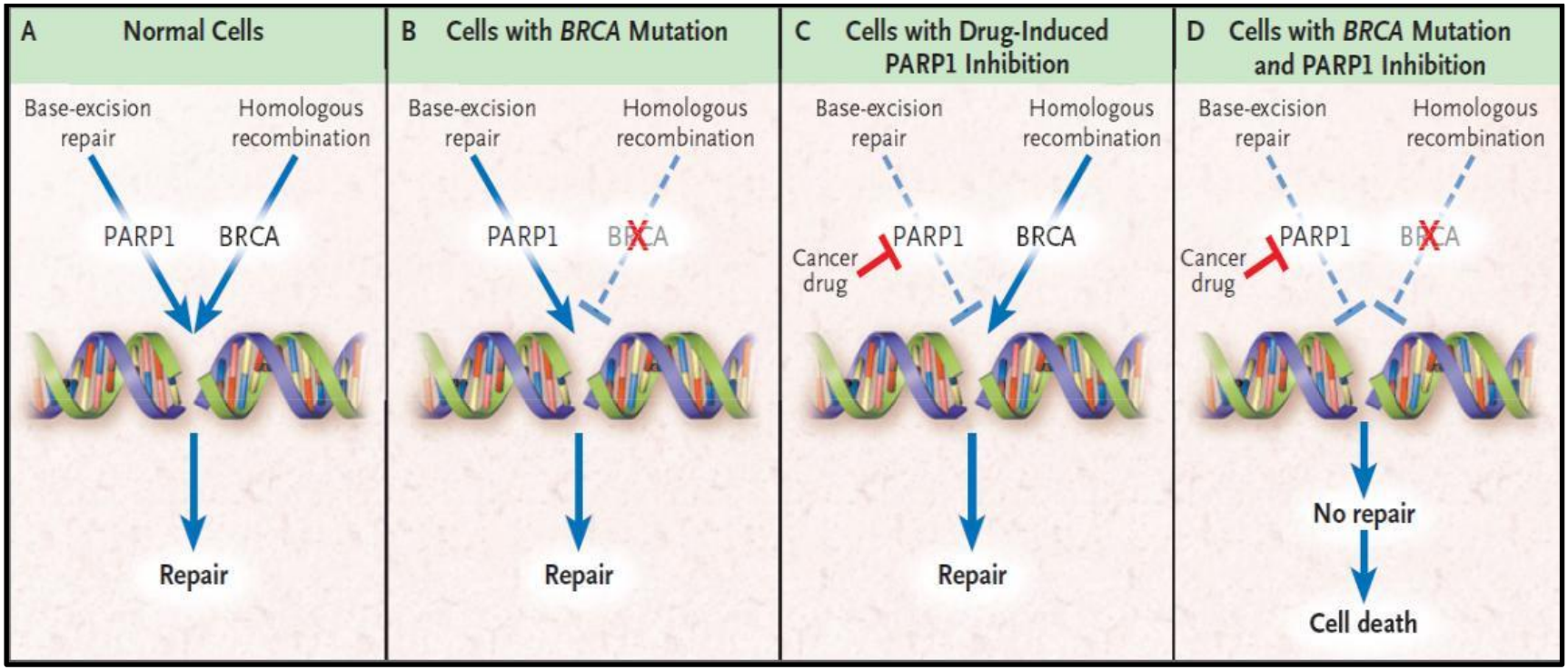

Figure 1.20 The mechanism of synthetic lethality induced cell death via PARP inhibition [Iglehart and Silver, 20

1.13.2 Different approaches to identify synthetic lethal genes

There have been multiple reports of SLG pairs being discovered. Lee and colleagues used tumour molecular profiles, patient clinical data, and gene phylogeny relationships to identify synthetic lethality interaction using an approach that they termed identification of clinically relevant synthetic lethality (ISLE). They discovered that ISLE-identified synthetic lethality interactions can predict drug response to a wide range of drugs *in vitro* and *in vivo*, establishing the basis for rational drug combination design [**Lee et al., 2018**]. Apaolaza and coworkers identified synthetic lethality by employing metabolomic approaches based upon the genetic Minimal Cut Sets concept that integrates genetic and nutritional interactions that promote cells proliferation. When simultaneous inactivation stopped biomass synthesis but individual inactivation did not, that was a sign of a synthetic lethal pair [**Apaolaza et al., 2022**]. One approach for screening for synthetic lethality in cancer is use of RNAi libraries. Hölzen and colleagues used a knockdown technique based on miR-E to target all genome-encoded proteases to identify proteases as synthetic lethal partners of PI3K inhibition in murine breast cancer stem cells (PyMG-816 and PyMG-TA). They were able to discover 181 proteases that altered the sensitivity of murine breast cancer cells to low-dose PI3K inhibition using this method. They verified 12 protease hits in breast cancer cells using separately created inducible knockdown cell lines. They came to the conclusion that Usp7, Metap1, and Metap2 are synthetic lethal partners of protease/PI3K inhibition in breast cancer cells. This might assist enhance breast cancer treatment in the future [**Holzen et al., 2022**]. Schwalbe and his colleagues have developed a new bioinformatics pipeline (integrating genome-wide DNA methylation/gene expression data) to identify 21 SLG pairs candidate in acute lymphoblastic leukaemia [**Schwalbe et al., 2021**]. Liu and colleagues proposed the SL^2MF technique as a novel synthetic lethality model that learns latent representations of genes from observed SL data using logistic matrix factorization [**Liu et al., 2020**]. However, other different synthetic lethality approaches have been reported such as Synthetic Lethality Bio Discovery Portal using computational approach to predict synthetic lethal interactions from hallmark cancer pathways by mining cancer's genomic and chemical interactions. [**Deng et al., 2019**], and a rapid inhibitor screening pipeline based on simple growth inhibition screenings that take use of synthetic lethality [**Muscato et al., 2022**].

Synthetic lethality approaches have resulted in SLGs pairings that hold the possibility of more effective and more tumour-specific therapies for many malignancies. Given the desperate need for improved therapeutic options for HCC patients, identifications of SLGs targets that are relevant in HCC would be a potentially great benefit. Thus, our group employed Schwalbe's workflow employing publically accessible data of genome-wide DNA methylation and gene expression data to discover potential synthetic lethality candidates in HCC patients. For functional analysis, the SLGs candidate will be examined using short interfering RNA and an inhibitor to determine whether they exhibit properties consistent with synthetic lethality and could serve as effective therapeutic targets for HCC patients.

Excision, radiofrequency ablation, and transplantation are only effective in the early stages of HCC. Furthermore, existing therapy at all stages of HCC are insufficient. In contrast, several synthetic lethality approaches have resulted in SLGs pairings that hold the possibility of focused therapy for many malignancies [**Huang et al., 2020; Setton et al., 2021**].

1.14 The aims of this study

1.14.1 To identify *in vitro* models to validate potential SLGs for specific subgroups of HCC patients.

1.14.2 To functionally assess the identified genes in cell lines to validate their synthetic lethality.

1.14.3 To evaluate the potential of the identified SLGs as potential biomarkers for treatment stratification or sensitisation.

Chapter II

Materials and Methods

2.1 Mammalian cell culture

Hepatocellular carcinoma (HCC) cell lines HepG2, Huh-7, PLC/PRF-5, and cholangiocarcinoma SK-Hep1 are routinely cultured with Dulbecco's Modified Eagle's /Ham F12 medium (Sigma, UK). Hepatocellular carcinoma SNU182 cell line is routinely propagated in Roswell Park Memorial Institute medium 1640 (RPMI-1640). Immortalised hepatocyte (HHL5) is propagated in Dulbecco's modified Eagle's medium/high glucose supplemented with 1% non-essential amino acid (Sigma-Aldrich, UK). All mediums were supplemented with 10% fetal bovine serum (Gibco, Brazil), 100 U/ml penicillin and 100 µg/ml streptomycin (Sigma), and 1% L-glutamine (Sigma). Cells were incubated at 37˚C in humidified incubator with 5% CO_2.

The MycoAlert Mycoplasma Detection Kit (UK) was regularly used to check for mycoplasma contamination, and all cell lines exhibited negative results. All HCC cell lines had also underwent authentication (Northgene, UK), and the result were a 100% match to the expected short tandem repeat patterns for each cell line.

2.2 Determinaiton of toxicity of NSC23766, GNE-140, 2-Deoxy-D-glucose, and metformin

2.2.1 Cytotoxicity of a specific RAC1 inhibitor NSC23766

HepG2, Huh-7, SK-Hep1, SNU182, PLC/PRF-5, and HHL5 cell lines were seeded at 2,000 cells/well into 96-well plates. After incubating overnight at 37 ^{0}C, 5% CO_2, added NSC23766 at a concentration of 0, 25, 50, 75 and 100 µM in a final volume of 200 µl. Cells were performed with MTT, SRB, CellTox™ green cytotoxicity, and Caspase-Glo® 3/7 apoptosis assay at the time indicated within that figures or tables.

2.2.2 Cytotoxicity of lactate dehydrogenase inhibitor GNE140

HepG2, Huh-7, SK-Hep1, SNU182, PLC/PRF-5, and HHL5 cell lines were seeded and incubated overnight at standard conditions. Added GNE-140 (Selleck, USA, 25 mM in 50% DMSO in PBS, filtered sterile, aliquoted, and kept in -20 ^{0}C) at concentrations of 0, 0.2,1,5, 25, and 50 µM in a final volume of 100 µl. Cell viability MTT assay, CellTox™ cytotoxicity assay, and RealTime-Glo™ MT cell viability assay was evaluated after treatment as indicated time in the chapter result.

2.2.3 Cytotoxicity of glycolysis inhibitor 2-Deoxy-D-glucose (2-DG)

HepG2, Huh-7, SK-Hep1, SNU182, PLC/PRF-5, and HHL5 cell lines were seeded and incubated overnight**,** added 2-DG (stock 1 M in PBS, filtered sterile, aliquoted, and kept in -20 ^{0}C, Sigma) at a concentration of varies from 0-25 µM depending on the sensitivity of each cell line to this inhibitor in a final volume of 100 µl. Cell viability MTT assay and Incucyte® live cell analysis was performed after treatment as indicated time in the relevant chapter.

2.2.4 Cytotoxicity of oxidative phosphorylation inhibitor metformin

HepG2, Huh-7, SK-Hep1, SNU182, PLC/PRF-5, and HHL5 cell lines were seeded and incubated overnight. Metformin was added (stock 1 M, filtered sterile, aliquoted, and kept in -20 ^{0}C, Acros Organics, UK) at a concentration varying from 0-25 µM depending on the sensitivity of each cell lines to this inhibitor in a final volume of 100 µl. Cell viability MTT assay and Incucyte® live cell analysis was performed after treatment at different times as indicated in the chapter result.

2.2.5 Drug synergy of 2-Deoxy-D-glucose and metformin

HepG2, Huh-7, SK-Hep1, SNU182, PLC/PRF-5, and HHL5 cell lines were seeded and incubated overnight, added 2-DG, metformin, and combination of both 2-DG and metformin at 0,1,2,4 mM in a final volume of 100 µl. SRB assay was performed at 144 hrs of treatment. Data were evaluated using Combenefit free software available from **https://www.cruk.cam.ac.uk/ research-groups/jodrell-group/combenefit**.

2.3 Cell proliferation MTT assay

MTT (3-[4,5-dimethylthiazol-2-yl]-2,5 diphenyl tetrazolium bromide) assay is widely used to measure cell proliferation to determine cytotoxicity of various drugs. This assay relies on the dehydrogenase enzyme in mitochondria of viable cells metabolite tetrazolium salt MTT into insoluble formazan crystals [**https://link.springer.com/content/ pdf/10.1007/978-1-61779-080-5_20.pdf**].

The MTT assay was performed to assess cell growth and proliferation. Briefly, 10 µl of MTT solution (5 mg/ml in PBS, aliquoted, and kept at -20 ^{0}C, abcam) was added into each well, and incubated at 37 ^{0}C for at least 4 hrs. The medium was discarded and replaced with 150 µl of DMSO to dissolve the formazan crystals. The optical density (OD) was measured at a wavelength of 570 nm using a microplate reader (Blustar Omega, BMG Labtech) using DMSO as the blank.

2.4 Estimation the protein content by SRB assay

The sulforhodamine B assay or SRB assay had been developed to measure cytotoxicity drug screening (**Skehan et al., 1990**). This method is relied on the binding of the dye to amino acid residues of fixed cells under mild acidic conditions. Contrary, the biding dyes will be extracted from the cells under basic conditions. At the end point of treatment, cells were fixed by adding 50 µl of cold Carnoy's fixative solution (1:3 of acetic acid:methanol, kept in fridge) on the top of medium and incubated overnight at 4 ^{0}C. Discarded the solution and washed 5 times quickly with distilled water to remove the fixing reagent and serum protein. Let air dried and stored the plates for the next step.

Next, stained the dried wells with 40 µl of 0.04% SRB in 1% acetic acid for 40 minutes at room temperature. Washed the staining plates 5 times quickly with 1% acetic acid to remove the dye excess. Tapped the plates on a paper towel to remove any remaining dye. Kept the washing time to a minimum to reduce desorption on protein-bound dye and allowed the plate to air dry until no further moisture was visible. Bound SRB dye-protein was solubilized by adding 200 µL of 10 mM unbuffered Tris base per well. The OD was measured at 570 nm in a microplate reader (FLUOstar Omega, BMG Labtch) using 10 mM unbuffered Tris base solution as a blank.

2.5 CellTox™ green cytotoxicity assay

Cytotoxicity was evaluated by adding (25 µl/well) with CellTox™ green cytotoxicity assay (Promega) was dissolved in culture medium at a ratio of 0.125:1,000 after four days post treatment. The relative fluorescent unit (RFU) was measured from 4-6 days of treatment. The relative fluorescent unit (RFU) was assessed by measuring the fluorescence signal at 485 nm (excitation) and 520 nm (emission) using medium as a blank.

2.6 RealTime-Glo™ MT cell viability assay

The RealTime-Glo™ MT cell viability assay (Promega) was evaluated (following the CellTox™ green cytotoxicity assay at 144 hrs after drug treatments) by adding 25 µl (0.25:1,000)

of this reagent and incubating for 1 hr. The relative luminescent unit (RFU) was measured using a microplate reader.

2.7 Apoptosis induction of NSC23766

The mechanism of cell death via apoptosis induction of NSC23766 was determined by Caspase-Glo® 3/7 apoptosis assay kit (Promega). HepG2, Huh-7, SK-Hep1, SNU182, PLC/PRF-5, and HHL5 cell lines were seeded 5,000 cells. After being exposed with NSC23766 for 48 hrs, added Caspase-Glo® 3/7, incubated 1 hr before measuring relative luminescent unit (RLU) with a microplate reader.

2.8 Clonogenic assay

To perform this assay, cells were seeded at low densities at 1,000 - 4,000 cells into 100 mm^2 petri dish depending on plating efficiency of each cell lines, and left around 2 weeks for the cell to form colonies after exposed with radiation or drugs. At the ended of treatment, washed colonies once with PBS, and fixed and stained at with 1-2% crystal violet (dissolved in 25% methanol in deionised water) for at least 1 hr. Only SNU182 was stained with 2% crystal violet for at least 2 hrs. Removed the dyes by washed the plate gently with tap water and let air dry overnight. The visible blue-purple colonies were counted utilising colony counter (ColCount™ , Oxford Optronix, UK). **Fig. 2.1** illustrated the clonogenic assay processes.

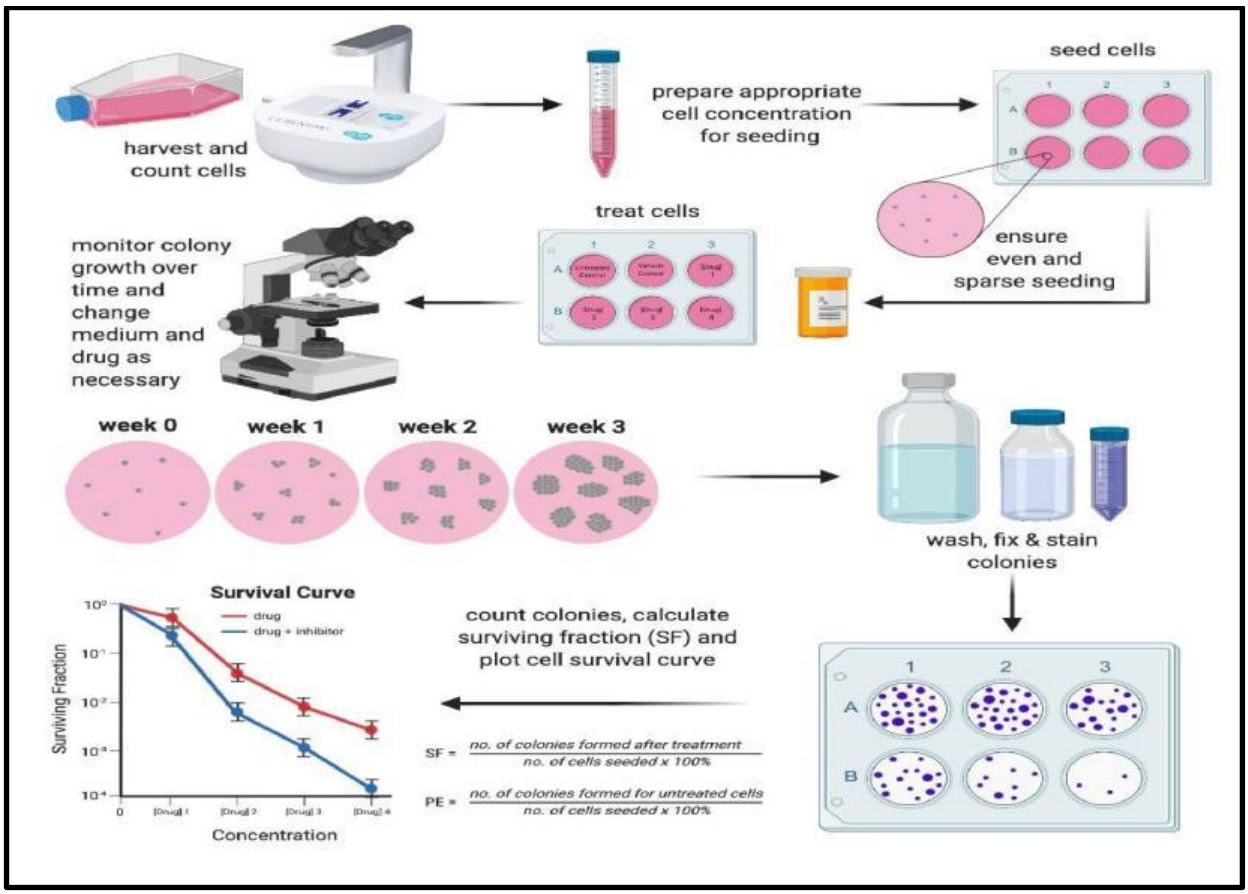

Figure 2.1 The summary of clonogenic assay protocol. Data were plotted in a line graph as a survival fraction vs drug concentrations or radiation exposure at different doses (accessed from **https://cytosmart.com/resources/resources/clonogenic-assay-what-why-and-how**).

2.9 siRNA transfection of mammalian cells

siRNA was used to silent the target gene using *Trans*IT-X2® transfection reagent (Mirus) to deliver siRNA into the cells.

2.9.1 Knockdown of *TIAM1* gene

Cell were seeded at 8 x 10^4 cells per well into 12-well plates. After being cultured overnight, the cells were expected to be 60–80% confluent. This is to ensure that the cells are actively dividing during the post-transfection period and reach the appropriate cell density. The transfection was carried out according to the manufacturer's instructions. Briefly, the transfection reagent was warmed to room temperature and vortexed gently before use. The complex of siRNA and transfection reagent was prepared by adding 250 µl of medium (serum and antibiotic-free) into sterile microtubes and adding siRNA or a negative control at a final concentration of 50 nM. 7.5 µl of *Trans*IT-X2 transfection reagent (Mirus) was added and mixed gently. This was then incubated

for 20 to 30 minutes at room temperature to form the complex before being added drop-wise to the cell cultures in 12 well plates (**Table 2.1**). The culture plates were gently rocked back and forth and from side to side to ensure the equal distribution of the complexes throughout the wells. The transfected cells were cultured for 48 hrs before further analysis via RT-qPCR. The list of siRNAs used in this project has been summarised in **Table 2.2**.

Table 2.1 The conditions for siRNA transfection with *Trans*IT-X2 for one well of 12-well plates.

Composition	Amount (µl)
Medium (antibiotics and serum free)	**250**
***TIAM 1* siRNA/Non-targeting siRNA/negative control siRNA (10 µM stock), final 50 nM**	**13.6**
***Trans*IT-X2**	**7.5**
Complete growth medium	**1,000**

Table 2.2. The list of siRNA used for transfection and control.

siRNA	Company
***TIAM 1* siRNA (h) sc-36669**	**Santa Cruz Biotechnology**
siRNA Duplexes All stars negative control siRNA, 20 nmol, #1027281	**Qiagen**
Non-targeting siRNA siGENOME #1, D-001210-01-05	**Dharmacon**

2.9.2 Cell proliferation after *TIAM 1* gene knockdown

Cells were seeded at 2,000 cells/well into a 96-well plate. After overnight incubation, the complex of *TIAM1* or non-siRNA with 0.3 µl *Trans*IT-X2 was added to each well. Untreated and mock (only *Trans*IT-X2 transfection reagent) was included as controls. Cell proliferation was determined with the MTT assay (Sigma, USA) at 6 days post-transfection. 10 µl MTT solution (5 mg/ml in PBS) was added directly into each well and incubated at 37 ^{0}C for at least 4 hrs. At the end of time period, the solution was removed and 150 µl DMSO was added to dissolve formazan crystals, shaken for 5 minutes before measurement of optical density (OD) at 570 nm using a microplate reader (FLUOstar, Omega). Each experiment has been done with three-four replications and at least three independent experiments were implemented before data analysis. The conditions for transfection in 96-well plates was displayed in **Table 2.3**.

Table 2.3 The conditions for targed *TIAM 1* gene knockdown with *Trans*IT-X2 for one well of 96-well plate.

Composition	Amount (µl)
Medium (antibiotics and serum free)	**9**
***TIAM* 1 siRNA/Non-targeting siRNA/negative control siRNA (10 µM stock), final 50 nM**	**0.25**
***Trans*IT-X2**	**0.3**
Complete growth medium	**92**

2.10 Protein extraction and quantification

Cell pellets were dissolved in 40–100 µl of lysis buffer, depending on the size of the pellets and vortexed until the cells were completely resuspended. The cell suspension was heated at 100 ^{0}C for 10 minutes and placed on ice. The lysate solution was sonicated (Soniprep 150, UK) at a magnitude of 6 (three times for ten seconds each) with at least one-minute rest interval. Samples were kept on ice at all times during sonication. If the lysate was still viscous, sonication was repeated. Centrifuged at 13,000 x g for 10 minutes at 4 ^{0}C. The supernatant was collected into new microtubes and stored at -20 ^{0}C or -80 ^{0}C before use.

Protein quantification was carried out with Pierce™ BCA protein assay kit (ThermoFisher Scientific) according to the manufacturer's instructions. The standard curve was prepared according to the sample protocol but using 10 µl of BSA standard solutions ranging from 0-2.0 mg/ml. The average 562 nm absorbance measurement of the blank was subtracted from the measurements of all other individual standard BSA and samples. Protein concentrations of samples were determined from the standard curve.

2.11 Western blotting

30-50 µg of protein was mixed with a loading dye at 1:1 ratio, heated at 100 ^{0}C for 10 minutes before loaded into the 4-15% Mini PROTEAN® TGX™ precast gel (Biorad). The gels were run at 80 V for 30 minutes followed by 100 V until the first dye reaches to the bottom of the gel (approximately 60 – 70 minutes). Proteins were transferred onto a PVDF membrane (Biorad). The membrane was blocked in 5 ml of 5% milk or 5% BSA in TBST for at least 1 hour, with gentle shaking. The membrane was incubated with the primary antibody according to the manufacturer's instruction at 4 ^{0}C overnight with gentle rocking. The membrane was washed three times for 10 minutes each in TBST before incubating with diluted polyclonal goat anti-mouse immunoglobulin-HRP conjugated antibody (Dako, Denmark) or goat anti-rabbit immunoglobulin-HRP conjugated antibody (Dako, Denmark) at a ratio of 1:1,000 to 1:2,000 in 5% milk or 5% BSA in TBST for 1 hour in room temperature. The membrane was washed three time with TBST before developing the blots with enhanced chemiluminescence (ECL) detection reagents (ECL reagent, SignalFire™, Cell Signaling Technology). Then, the membrane was covered with plastic wrap before exposed the membrane to ChemiDoc™ MP imaging system (Biorad). The work flow of western blotting has summarised in **Fig. 2.2**, and the list of antibodies for western blotting was displayed in **Table 2.4.**

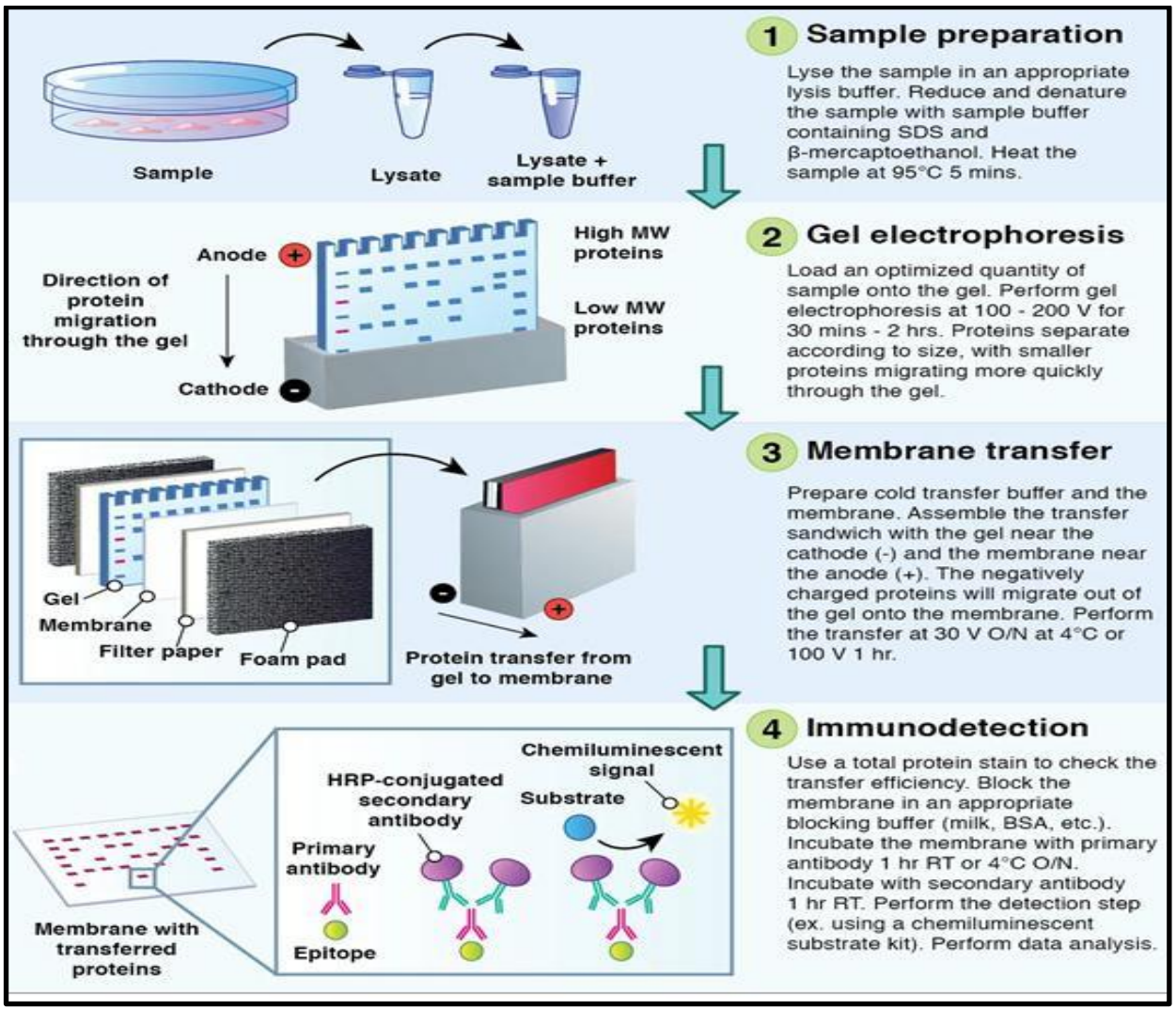

Figure 2.2 The summary of the western blot experiment [https://www.angibodies.com/western-blotting].

Table 2.4 Antibodies used in western blotting.

Antibody	Species	Company	Dilution
RAC 1/2/3 (G-2)	Mouse	Santa Cruz Biotechnology # SC514583	1:1,000
LDHB	Mouse	Abcam # ab85319	1:5,000
Tubulin	Mouse	Sigma #9026	1:5,000
Polyclonal Goat anti-rabbit immunoglobulin HRP	Rabbit	Dako	1:2,000
Polyclonal Goat anti-mouse immunoglobulin HRP	Mouse	Dako	1:2,000

2.12 RNA extraction and quantification

Total RNA was extracted using the total RNA purification kit (Norgenbiotek, Canada) according to the manufacturer's instructions. Briefly, the cell pellets were removed from the -80 ^{0}C freezer and warmed down to room temperature, tapping until the cells were dispersed. The cells were lysed by adding 350 µl of Buffer RL and incubated at room temperature for 5 minutes. 200 µl of ethanol was added and vortexed briefly (around 10 seconds). The next step was the binding of RNA with the resin in mini spin-column. The solution was transferred into the column equipped with collection tubes, and centrifuged at 3,000 x g (~ 6,000 rpm) for 1 minute. The flowthrough was discarded and 400 µl of Wash Solution A was added to the column and centrifuged at 14,000 rpm for 1 minute. and the columns were washed again with Wash Solution A (as above) 3 times. The columns were then centrifuged for 2 minutes. The columns were transferred to microcentrifuge tubes and 30-50 µl of Elution Solution A was added to the columns followed by centrifugation for 2 minutes at 200 x g (~2,000 rpm) and 1 minute at 14,000 x g. The RNA concentration was estimated by NanoDrop® Spectrophotometer (ND-1000, NanoDrop Technologies, USA).

2.13 cDNA preparation

High capacity cDNA reverse trascription kit (appliedbiosystems) was used for complementary DNA synthesis (cDNA). The protocol was followed by manufacturer**'s** instruction. Briefly, mixed reverse transcriptase buffer, dNTP, reverse transcriptase random primers, and RNA template as showed in **Table 2.5**. Adjusted to 20 µl with nuclease-free H_2O. Performed the reaction on ice all the time. The thermal cycling was performed by PCR as displayed in **Table 2.6**. After thermal cycle has been finished, the cDNA was diluted with 80 µl nuclease-free H_2O (total 100 µl) before reverse transcription-quantitative polymerase chain reaction (RT-qPCR) analysis.

Table 2.5 The reagents used for cDNA synthesis with normal PCR.

Reagent	Volume (µl)
Reverse transcriptase buffer (10X)	**2.0**
Reverse transcriptase random primers (10X)	**2.0**
25X dNTP Mix (100 mM)	**0.8**
RNA template	**Add RNA solution equivalent to 1 µg**
Nuclease-free H_2O	**Adjust to a final volume of 20.0**

Table 2.6 Thermal cycling conditions for normal reverse transcription.

Settings	Step 1	Step 2	Step 3	Step 4
Temperature (^{0}C)	**25.0**	**37.0**	**85.0**	**4.0**
Time (min)	**10.0**	**120.0**	**5.0**	**∝**

2.14 RT-qPCR

Each well of the 384-well PCR plate (Life Tenhnologies, UK) consisted of 8.0 µl of master mixed [5.0 µl of Syber green (Invitrogen), 0.2 µl of 10 µM primer (forward and reverse (Eurofins genomics), and 2.8 µl DEPC water or nuclease free water], and 2 µl of cDNA template or housekeeping genes. Spun to mix (Mini plate spinner, MPS 1000, Labnet) before performed by RT-qPCR machine (QuantStuio 7 Flex, appliedbiosystems). **Table 2.**7 summarises the primers used in RT-qPCR, and **Table 2.8** displays the RT-qPCR conditions.

Table 2.7 The primer sequence used for RT-qPCR

Gene	Forward	Reverse
TIAM1	**GAAGGACTTTGTCTTCTGCC**	**ATGGCGGTGATCCAGTTTTC**
LDHB	**GAAGAAGAGGCAACAGTTCC**	**GCCACAATTTTAGGTGTCTGA**
HPRT	**TTGCTTTCCTTGGTCAGGCA**	**ATCCAACACTTCGTGGGGTC**
RAC1	**GAAAATGTCCGTGCAAAGTGG**	**CTTCAGTTTCTCGAT CGT GTC**

Table 2.8 RT-qPCR conditions

Setting	Hold stage		PCR stage (40 cycles)		Melt curve stage (continuous)		
Temperature (^{0}C)	**50.0**	**95.0**	**95.0**	**60.0**	**95.0**	**60**	**95.0**
Time (min)	**2.00**	**10.00**	**0.15**	**1.00**	**0.15**	**1.00**	**0.15**

2.15 X-ray irradiation

To investigate the radiotoxicity, cells were seeded and incubated overnight in a 96-well plate before being exposed to 0–8 Gray (Gy) of X-ray (Glumay RS320, UK). Cell viability was determined by MTT, SRB, and CFA at the indicated time post-irradiation.

2.16 Genome-wide DNA methylation analysis in HCC cell lines

Genome-wide DNA methyaltion analysis of four HCC cell lines (HepG2, Huh7, PLC/PRF-5, and SNU182) was used to assess similarities between HCC cell lines and HCC subgroup 2 of HCC patient samples. The DNA methylation analysis was peformed using Infinium MethylationEPIC BeadChip arrays.

2.16.1 Infinium MethylationEPIC BeadChip arrays

The Infinium MethylationEPIC assay quantifies methylation at single CpG sites, providing high resolution for understanding epigenetic changes. This assay enables researchers to investigate the biological role of DNA methylation in normal and cancer DNA samples. Each array format covers 99 percent of Reference Sequence with multiple probes per gene. The well-established Infinium® Assay is used to examine CpG methylation in bisulfite converted genomic DNA as shown in **Figure 2.3** [**Bibikova et al., 2009; Bibikova et al., 2011; https;//www. illumina.com**]. We used this technology to examine DNA methylation in four HCC cell lines for classification these cell lines fall into the novel subgroup specific to DNA methylation pattern.

2.16.2 Infinium MethylationEPIC data analysis

The Infinium MethylationEPIC array employs bisulfite conversion and Illumina® technology. Bisulfite treatment converts unmethylated cytosines to uracil wherease 5-methylcytosine (5mC) bases are unchanhged [**Olova et al., 2018**]. Using site-specific probes, Infinium HD array technology assesses the ratio of fluorescent signals from methylated and unmethylated probes on the array. This can then be used to calculate the methylation fraction for the interrogated locus [**Bibikova et al., 2011**]. To analyse the result from Infinium MethylationEPIC array, R studio version 3.5.3. was used to perform DNA mehtylation analysis.

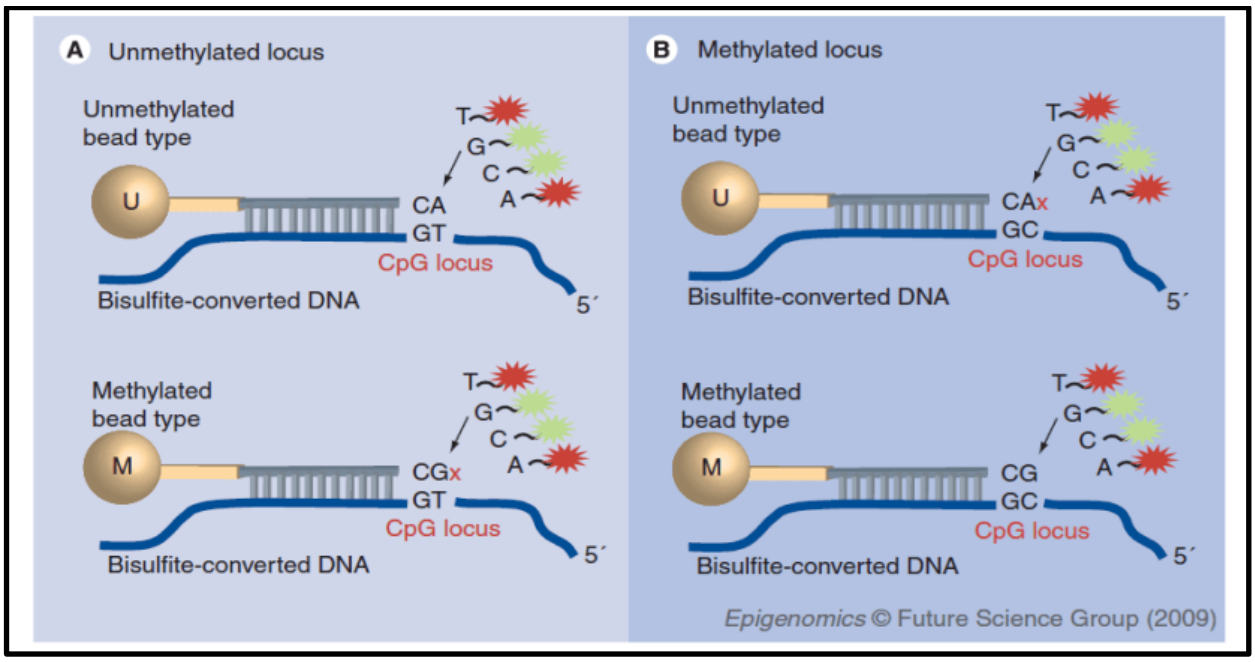

Figure 2.3 Illustrate the Infinium Methylation assay scheme. (**A**) The CpG locus of interest is unmethylated, which incorporate with an unmethylated bead (U probe), resulting in base extension (strong singal). The unmethylated locus has a single base mismatch to the methylated bead (M probe), resulting in base extension inhibition (low signal). (**B**) The CpG locus of interest is methylated, which would produce the converse result. The methylated bead (M probe) expresses the signal, whereas the unmethylated bead (U probe) does not. The methylation score, which is displayed as a β value, indicates the degree of methylation status (the ratio of fluorescent signal from the methylated probe to the overall intensities) [**Bibikova et al., 2009**].

2.16.3 Genome-wide DNA methylation Arrays of HCC cell lines

Bisulfite conversion was performed using the Zymo EZ-96 DNA methylation kit (Zymo Research). Genome-wide DNA methylation was quantified in all samples using the Infinium MethylationEPIC BeadChip array, which evaluates genome-wide CpG methylation at over 850,000 sites and carried out at the Wellcome Trust Clinical Research Facility, University of Edinburgh (Edinburgh, UK) and data analysis was performed by Lalchungnunga. Raw methylation data from MethylationEPIC arrays for all test and control samples were processed using the minfi Bioconductor package version 1.28.4 in R studio version 3.5.3. The single-sample (ssNoob) method was used for normalisation [**Fortin et al., 2017**]. Probes with a detection p-value>0.01 and cross-reactive probes (i.e., probes which cross-hybridize between autosomes and sex chromosomes) were removed [**Chen et al., 2013**]. After processing, 820,139 probes remained for the childhood paired samples (n=820,134 of these passed quality control in the adult samples). Methylation values were

transformed to β values, which range from 0 (0% methylation) to 1 (100% methylation), representing methylation intensity [**Du et al., 2010**].

2.16.4 Identification of differential methylation in HCC

Differentially methylated regions (DMRs) were identified using the DMRcate R package with the default settings [**Peters, 2016**]. Briefly this identifies regions of 2 CpG sites or greater, with an average β value difference of > 0.2. The lambda value (maximum distance allowed between neighboring CpG sites) was set at 1000 bp. Identification of candidate synthetic lethal genes, based on our previously published approach [**Scwalbe et al., 2021**], is described in more detail in **Section 3.2 of Chapter 3**.

2.17 Statistical analysis

All experiments were performed in at least three independent experiments in triplicate or quadruplicate before data analysis. Statistical significance was performed using a two-sample t-test assuming equal variances or One-way ANOVA with Dunnett's multiple comparisons test. Some multiple comparisons were made using t-test rather than ANOVA because the necessary statistical package to perform ANOVA was not available in a personal computer.

Chapter III

Identification of *in vitro* model to validate potential synthetic lethal genes in HCC and functional assessment of *TIAM1* as a potential synthetic lethal gene

3.1 Synthetic lethality

Synthetic lethality has emerged as an alternative approach as targeted therapy in cancer. Therefore, identification and confirmation of synthetic lethality partner genes in particular cancers or cancer subtypes can open up promising new approaches for more effective and less toxic therapies.

3.2 A novel bioinformatic pipeline to identify synthetic lethal genes utilising genome-wide DNA methylation and gene expression data

Recently, our lab established a novel approach for identification of subtype- specific synthetic lethal genes (SLGs), which utilises genome-wide DNA methylation/gene expression data. Initially this was used to identify SLGs in acute lymphoblastic leukaemia (ALL), and medulloblastoma. However, it is probable that the proposed method could be applied to multiple cancer types for identification of SLGs candidates [**Schwalbe et al., 2021**].

The process is described in **Fig. 3.1** using ALL as an example where genome-wide DNA methylation [**Nordlund et al., 2013**; **Gabriel et al., 2015]** and expression **[Haferlach et al., 2010**] data was derived from ALL. The approach depends on identification of genetic/molecular subtype specific differences. Initially, DNA methylation in one specific subgroup is compared to DNA methylation in all other subgroups combined. A differentially methylated region (DMR) is a region where the DNA methylation pattern differs among multiple samples. Many DMRs are correlated with tissue-specific gene expression. Alteration in the methylation status of DMRs can potentially be used to find genes that differ between normal and cancer cells [**Chen et al., 2016**]. Various DMR- finding methods utilising bioinformatics approaches had been reported [**Jaffe et al., 2012**; **Pedersen et al., 2012**; **Robinson et al., 2014**; **Bucher and Beck, 2015; Chen et al., 2016**] which have different benefits and limitations. Our team used the DMRcate method to predict DMRs across the genome. The benefits of this software over other methods had been summarised by Peters and co-worker's publication **[Peters et al., 2015**]. DMRcate-derived DMRs were chosen based on the beta value distributions with in a range of 0.00 to 0.99 (0 and near 1) to measure DNA methylation levels based on Infinium methylation arrays. Initially, the subtype under study (subtype of interest) was compared with all other subtypes grouped together and DMRs identified based on a difference in beta value of 0.2 (equivalent to 20% methylation). In this study, DMRs were defined as containing 2 or more CpG sites. Subsequently, the DMRs were further analysed to identify the region of biggest difference (again with at least 2 CpG sites). The minimum difference

at the region of maximal change can be varied. We typically used a beta value difference of ≥ 0.3 or 0.4, depending on the extent of methylation differences between the sample sets under study and the purity of the tumour samples (**Fig. 3.1A**). DMRs retained at this stage are then compared to all other subtypes individually (**Fig. 3.1B**). Only those that show differences of greater than the set beta value compared with every other subtype were taken forward (i.e., only if the methylation difference is truly specific for the subtype being assessed). Finally, DMRs retained at this stage were assessed for their association with gene expression (**Fig. 3.1C**). Initially, the gene mapping closest to the DMR was identified (DMRs mapping >20 kb from a gene transcription start site were excluded from further analysis). Expression of the associated gene was then assessed to identify those exhibiting subtype specific increased expression (i.e., significantly higher expression in the subtype of interest versus all other subtypes). DMRs/genes passing all of these criteria were taken forward as candidate SLGs. This approach was able to identify SLGs in both haematological (ALL) and solid (medulloblastoma) tumours with a very high level of specificity [**Schwalbe et al., 2021**].

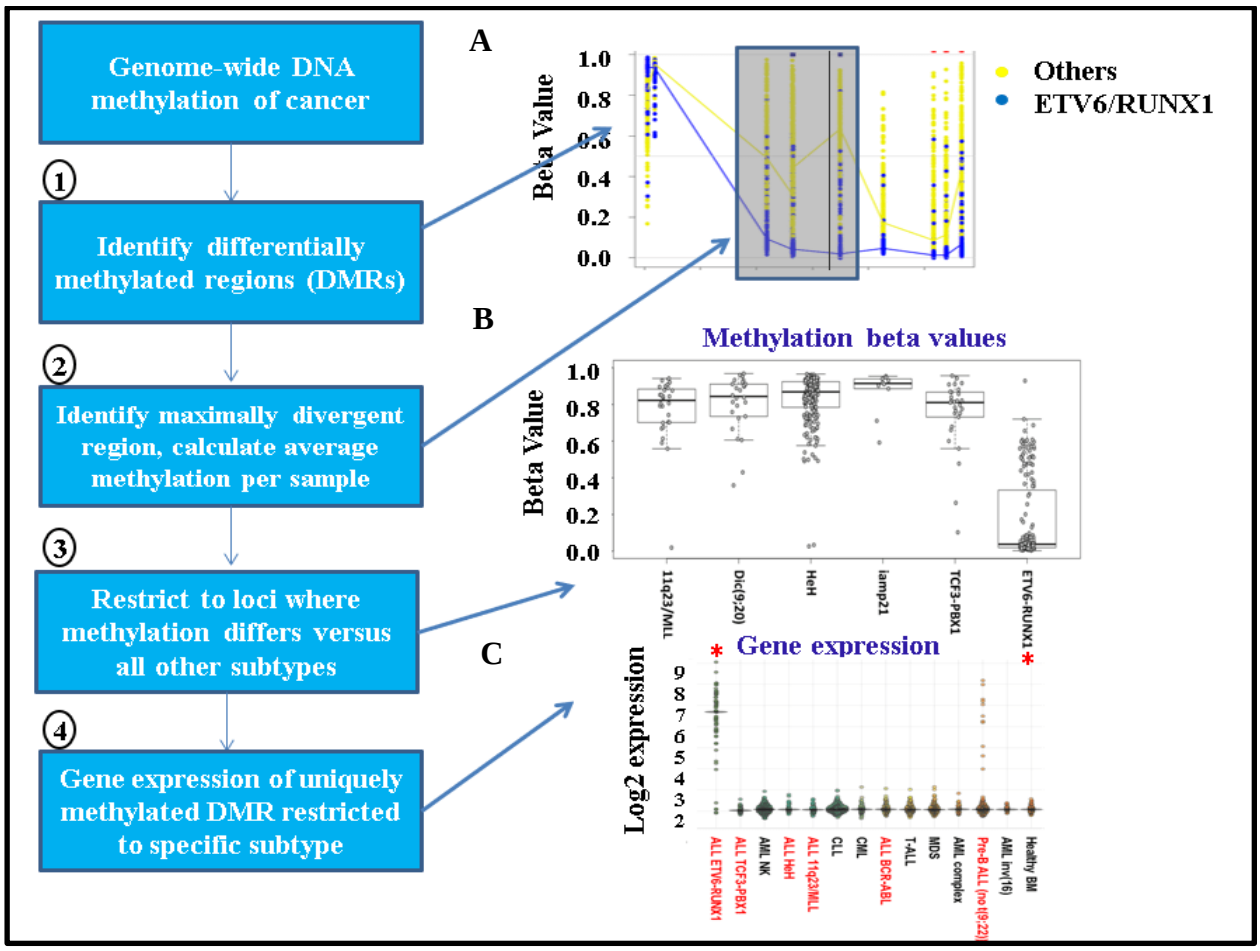

Figure 3.1 A diagram outlining the bioinformatics pipeline for the identification of SLGs candidate. **(1)** The DMRs for a specific subtype of cancer are identified using DMRcate software. **(2)** Identify the maximally divergent region (must contain at least 2 CpG sites). **(3)** This is then compared with all other subtypes of cancer under study **(4)** Expression analysis of DMR-linked genes between the subtype of interest and all other subtypes. **A**: Example of identification of region of biggest change (including 3 CpG sites from an original DMR of 9 CpG sites). **B:** DNA methylation compared between subtype of interest and individual subtypes at region of biggest change. **C:** Gene expression data of each subtype, showing subtype specific increased expression of the linked gene [**reproduced from Schwalbe et al., 2021**].

3.3 Identification of synthetic lethal genes in HCC using the bioinformatics pipeline

The strategy described above is specifically designed to identify SLGs in a subgroup-specific manner and this process has been successfully employed for a number of cancers such as medulloblastoma and ALL [**Schwalbe et al., 2021**]. Therefore, stratification of HCC patients into subgroups was required to allow this approach to be utilised for HCC.

A number of approaches have been attempted to classify HCC into subtypes, including molecular subtypes [**Kuma et al., 2011; Goossens et al., 2015; Chaisaingmongkol et al., 2017; Rebouissou and Nault, 2020; Wu et al., 2020**], histological subtypes [**Lo, 2019**], and immunological subtypes [**Giraud et al., 2021**]. However, this has not resulted in a consensus molecular subgrouping of HCC. To overcome this deficit, our group had stratified HCC patients based on genome-wide DNA methylation of primary HCC samples. We used non-negative matrix factorization (NMF) algorithm, described by Lee and Seung [**Lee and Seung, 1999**] to allow clustering of HCC patients into subgroups. The analysis was performed using a publicly available data set of 224 HCC samples, analysed using Illumina 450K methylation beadchip arrays, that had been collected as part of the HEPTROMIC Consortium [**Villanueva et al., 2015**]. This analysis could identify five potential subgroups (subgroup 1-5 or G1-G5) based upon differential DNA methylation (**Fig. 3.2**).

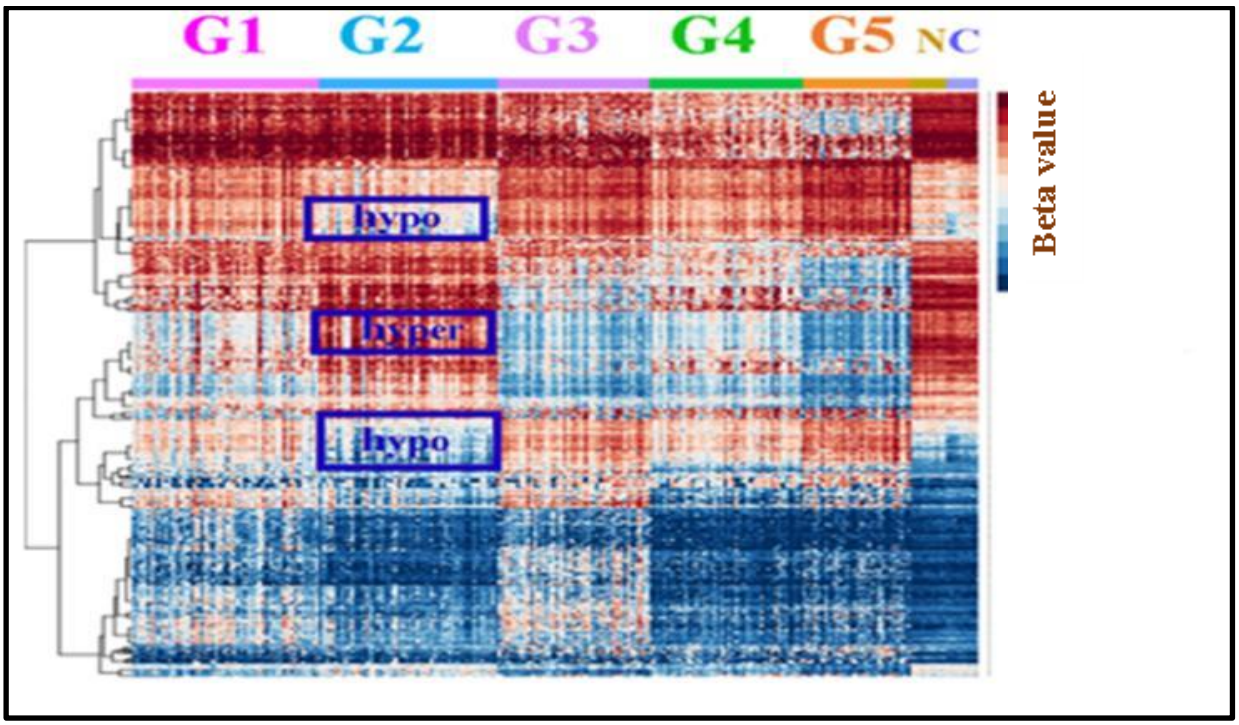

Figure 3.2 Heat map of DNA methylation at CpG sites in HCC, normal hepatocytes and cirrhosis samples. 450K methylation beadchip data for a set of 224 primary HCC samples [**Villanueva et al., 2015**] was used for NMF analysis to allow the identification of subclusters. This analysis supported the potential existence of 5 methylation-based HCC subgroups. The figure shows clustering based upon the 10,000 most differentially methylated probes and regions of methylation difference that are specific for subgroup 2 (versus the other four HCC clusters) are highlighted in blue boxes. **G**: Group (1 to 5). N: normal hepatocytes. **C**: Cirrhosis.

However, the extent of methylation differences between the subgroups was limited. Subgroup 2 was the most clearly separated by the NMF analysis (**Fig. 3.2, highlighted in dark blue boxes**) and had clear regions of methylation that differed from the other 4 subgroups. By contrast, as can be seen in **Fig. 3.2**, the other four subgroups largely lacked significant regions of methylation that were truly subgroup specific.

Subsequently, we applied the novel bioinformatic approach (**see Fig. 3.1, Schwalbe et al., 2021**) to identify potential SLGs in HCC using the newly identified methylation-based subgroups. This approach allows the identification of subgroup specific SLGs by integrating analysis of genome wide DNA methylation and gene expression data, as described above. This analysis identified two candidate SLGs for HCC subgroup2; lactate dehydrogenase B (*LDHB*) (**Fig. 3.3A**) and T-cell lymphoma invasion and metastasis 1 (*TIAM1*) (**Fig. 3.3B**).

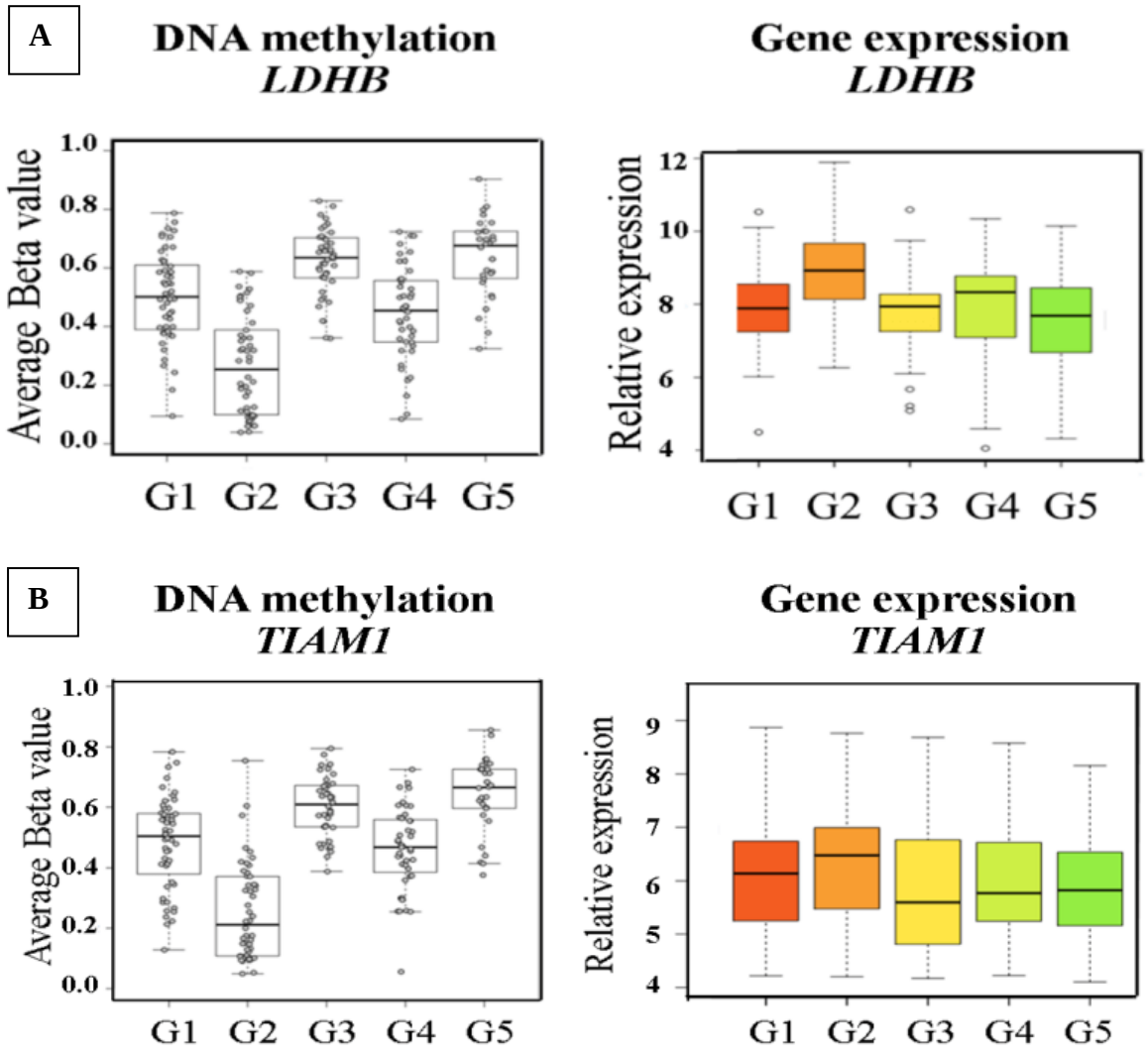

Figure 3.3 DNA methylation and gene expression of *LDHB* (A) and *TIAM1* (B) genes in primary HCC patients. G1-G5 refers to HCC subgroups. Box plots for DNA methylation represent average of beta values for CpG sites identified as the region of maximal difference within DMR corresponding to the indicated gene. Beta value 1.0 is equivalent to 100% methylation, and 0.0 is equivalent to 0 % methylation. Box plots for gene expression representing log2 transcript levels of the indicated gene in HCC subgroups.

Consistent with the expected pattern for SLGs, both *LDHB* and *TIAM1* exhibit significantly lower methylation in subgroup 2 than the average of all other combined subgroups and also lower than any of the other individual subgroups. This is associated with a corresponding higher expression, which is again specific for subgroup 2. No other SLG candidate was identified thus subsequent functional analysis was focussed on *TIAM1* and *LDHB*.

3.4 Lactate dehydrogenase B

LDHB is an enzyme encoded from *LDHB* gene. The main function of this enzyme is to convert lactate to pyruvate in anaerobic glycolysis pathway. More details of LDHB are described in **section 4.5.2**

3.5 T-cell lymphoma invasion and metastasis 1 (TIAM1)

TIAM1 is a member of Dbl-family guanine nucleotide exchange factors (GEFs) and activates Rho-GTPase substrates. It has ability to activate Ras-related C3 botulinum toxin substrate 1 (RAC1). TIAM1 catalyses the conversion of RAC1 inactive GDP-bound form to active GTP-bound form, whilst GTPase-activating proteins (GAPs) hydrolyse RAC1-GTP-form to RAC1- GDP-form, as a result RAC1 is inactivated [**Zheng et al., 2001**]. Activation of RAC1 through TIAM1 results in the polarisation of the cytoskeletal, actin polymerisation, membrane ruffles, tight junction formation, microtubule (MT) stabilization, and cell spreading [**Iden and Collard, 2008; et al., 2019**].

TIAM1 is overexpressed in various cancer types and is reported to influence the metastatic process of many cancer types [**Ding et al., 2014**; **Ding et al., 2018**], promote cell proliferation [**Zhou, 2017**], tumorigenesis *in vivo* [**Huang et al., 2013**] progression of tumours [**Wang et al., 2014**] including hepatocarcinogenesis [**Ding et al., 2009**], and reduced the survival rate in HCC patients [**Ding, 2009**]. Upregulation of TIAM1 enhances cell proliferation, migration, and invasion of the human HCC cell line, MHCC97L, both *in vivo* and *in vitro* [**Liu et al., 2014**].

3.6 Chapter aims

3.6.1 Identification of *in vitro* models representing HCC subgroup 2.

3.6.2 To evaluate *TIAM1* as a potential SL gene for HCC subgroup 2.

3.7 Results

3.7.1 *TIAM1* and *LDHB* gene expression analysis in HCC-related cell lines

To allow initial testing of the candidate SL genes HCC cell lines were characterised in terms of expression of *TIAM1* and *LDHB.* Cell lines which correspond to subgroup 2 were predicted to exhibit low methylation/high expression of both *TIAM1* and *LDHB* genes), while cell lines corresponding to any of the other subgroups should exhibit high methylation/low expression of both *TIAM1* and *LDHB*.

Expression analysis for *TIAM1* and *LDHB* was carried out in four HCC cell lines HepG2, Huh-7, PLC/PRF-5, SNU182, and two liver derived non-HCC cell lines SK-Hep1, and immortalised, non-transformed, HHL5 cells by RT-qPCR. The data showed that two of the HCC cell lines (SNU182 and PLC/PRF-5) expressed higher messenger RNA (mRNA) level of both *TIAM1* (**Fig. 3.4A**) (Ct value =25-28) and *LDHB* (**Fig. 3.4B**) (Ct value = 26-28) than other two HCC cell lines (HepG2 and Huh 7) which exhibited very low expression of these two genes (Ct value = 35-38). Based on the expression data SNU182 and PLC/PRF-5 cells can be potential representative of HCC subgroup 2. On the other hand, HepG2 and Huh-7 cells can be potential representative of HCC non-subgroup 2. The two remaining non-HCC cell lines (SK-Hep1and HHL5) exhibited very similar expression to SNU182 and PLC/PRF-5. However, these two cell lines are not HCC, therefore, we clustered them into non-HCC subgroup.

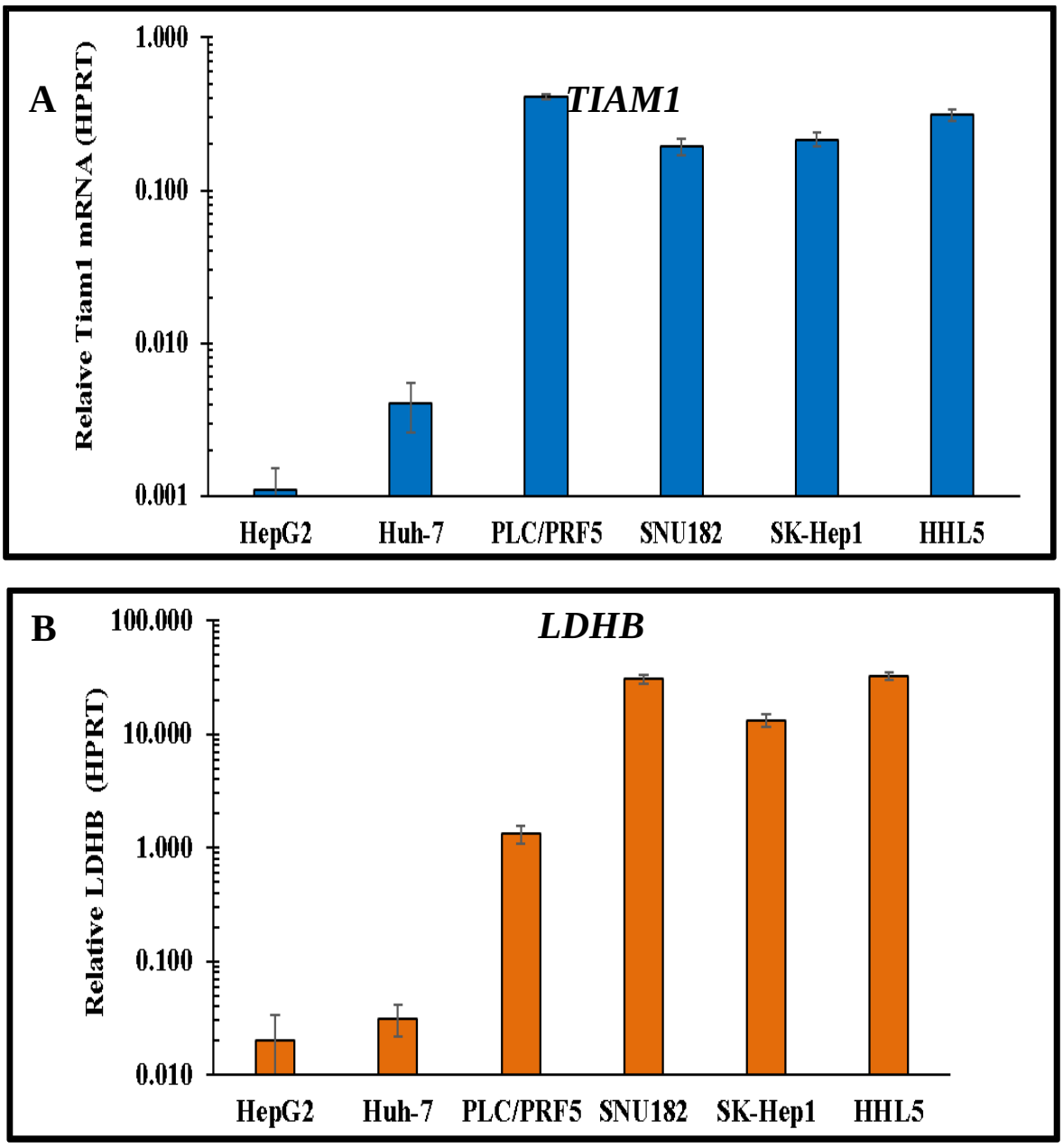

Figure 3.4 Relative *TIAM1* and *LDHB* gene expression normalised with internal hypoxanthine phosphoribosyl transferase (*HPRT*). (**A**) The relative *TIAM1* expression compared with *HPRT* (n = 6-11), and (**B**) the relative *LDHB* expression compared with *HPRT* (n = 4-5). Data are calculated as $2^{-\Delta Ct}$, and values are shown as mean ± SEM. ΔCt is the Ct value of targeted *TIAM1* or *LDHB* gene minus Ct value of the housekeeping gene (*HPRT*).

3.7.2 DNA methylation data of HCC cell lines

The goal of this study was to compare the DNA methylation profiles of the four HCC cell lines across the same loci as the primary HCC samples. Genomic DNA from the four HCC cell lines were analysed using Infinium MethylationEPIC array to obtain genome-wide DNA methylation patterns in order to compare it with HCC patient's profile. We specifically looked at identified DMRs in HCC subgroup 2 versus other HCC samples (**Table 3.1**), including the DMRs associated with *TIAM1* (**Fig. 3.5A**) and *LDHB* (**Fig. 3.5B**). For both genes, DNA methylation across the identified DMRs was lower in both presumptive HCC subgroup 2 cell lines compared to both the predicted non-subgroup 2 cell lines. Furthermore, the extent of the genomic region exhibiting differential methylation between the groups of cell lines exactly matched the DMRs identified in the primary samples, further supporting the definition of SNU182 and PLC/PRF5 as subgroup 2 cell lines.

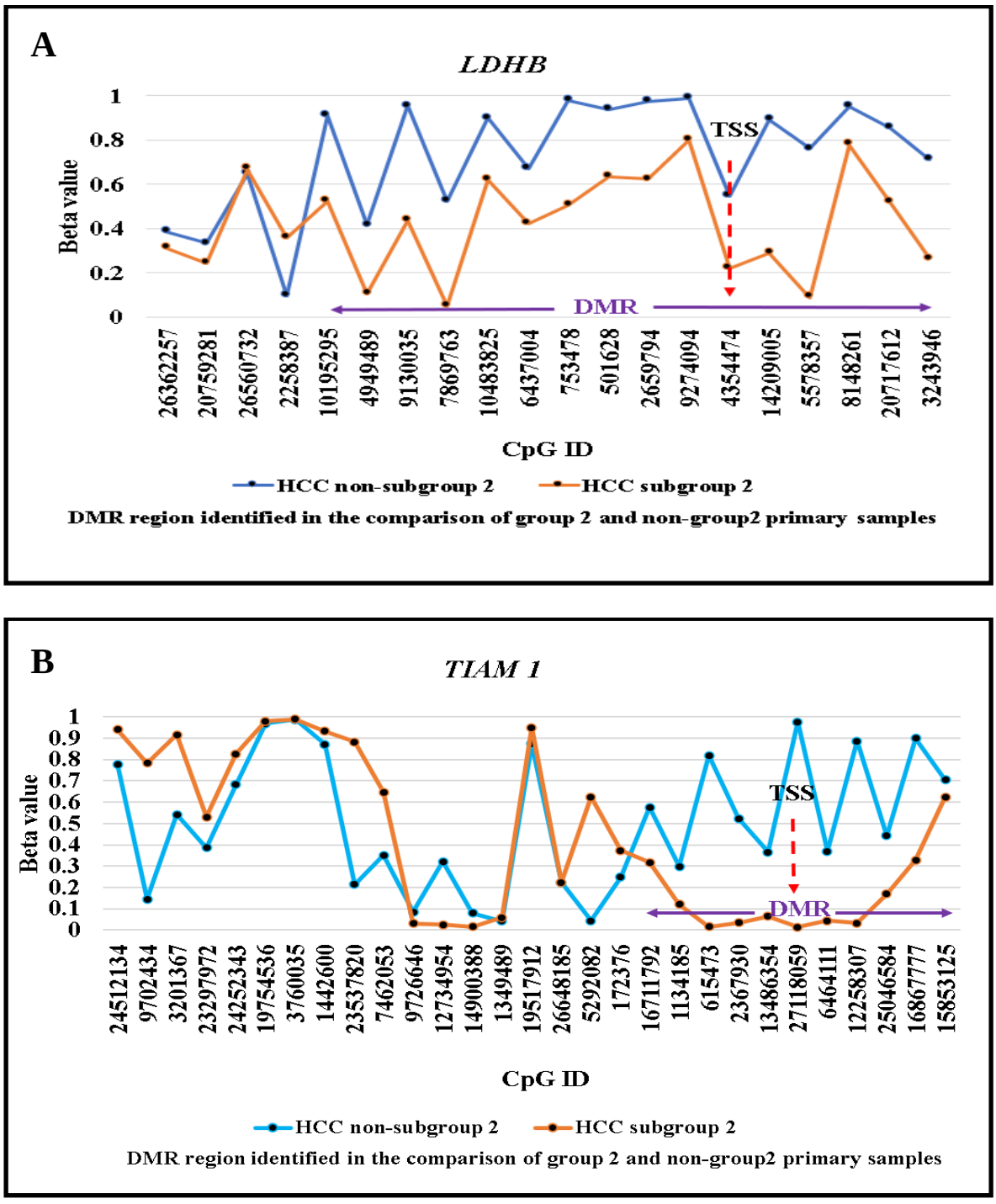

Figure 3.5 DNA methylation levels at DMR and non-DMR of two candidate SLGs - *LDHB* (A) and *TIAM1* (B) using Infinium MethylationEPIC array. ID: The identification number refers to the location of individual CpG which can be used as reference database (CpG loci lack of nomenclature). **TSS**: transcription start site.

Although *LDHB* and *TIAM1* were the only two SLGs candidates identified in HCC subgroup 2, a number of other loci exhibited clear differences in methylation that were strongly associated with subgroup 2 samples in the primary analysis. For example, DMR located at the *ZFP36* gene. As shown in **Fig. 3.6**, the presumptive HCC subgroup 2 cell lines exhibited lower beta values at the *ZFP36* DMR compared to HCC non-subgroup 2 lines. Again, the extent of the differential methylation matched the limits of the DMR identified in the primary samples. Unlike for *TIAM1* and *LDHB* (**see Fig. 3.5**), the DMR for this gene does not overlap the transcriptional start site and consistent with this *ZFP36* is not differentially expressed in HCC subgroup 2 (hence why it was not considered as a SLG candidate). **Table 3.1** summarises the methylation status of HCC subgroup associated DMRs in the predicted subgroup 2 and non-subgroup 2 HCC cell lines.

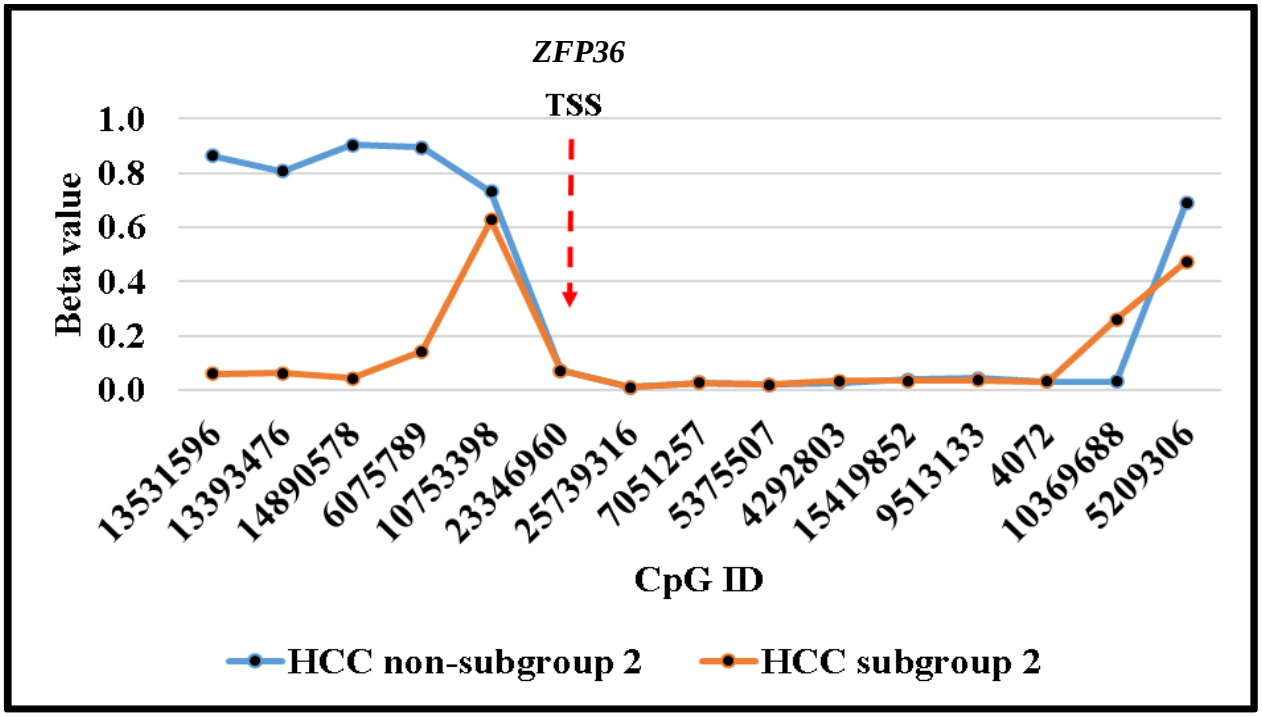

Figure 3.6 DNA methylation level at the *ZFP36* loci derived from Infinium MethylationEPIC array. Reduced methylation is specifically present in the predicted HCC subgroup 2 cell lines at the 4 CpG sites in the DMR identified in the primary HCC samples. The DMR is distal to the TSS (closest CpG site is 2686 bp upstream of the TSS).

Table 3.1 DNA methylation of 7 loci which show clear difference between HCC subgroup 2 and non-subgroup 2 of primary samples.

Gene	Reduced methylation in DMR			
	HCC non-subgroup 2		HCC subgroup 2	
	HepG2	Huh-7	PLC/PRF5	SNU182
TIAM1	No	No	Yes	Yes
LDHB	No	No	Yes	Yes
ZFP36	No	No	Yes	Yes
STAP2	No	Yes	Yes	Yes
SFXN3	Yes	Yes	Yes?	Yes
PROCA1	No	No	No	No
NR5A2	No	No	No	No

Yes: DNA methylation matches the pattern in subgroup 2 primary HCC samples.
No: DNA methylation does not match the pattern in subgroup 2 primary HCC samples
Yes? methylation is similar to, but not identical to, subgroup 2 primary HCC samples.

Thus overall, the results of the methylation analysis support the use of PLC/PRF-5 and SNU182 as model systems for functional analysis of the HCC subgroup 2 SLG candidates. The characteristics of cell lines used in this project is summarised in **Table 3.2**.

Table 3.2 Characteristics of cell lines.

Cell lines	Cell Type	*TIAM1* methylation	*TIAM1* expression	*LDHB* methylation	*LDHB* expression	HCC Subgroup
SNU182	HCC	Hypo	++	Hypo	++	2
PLC/PRF-5	HCC	Hypo	++	Hypo	+	2
HepG2	HCC	Hyper	-	Hyper	-	Non-subgroup 2
Huh-7	HCC	Hyper	-	Hyper	-	Non-subgroup 2
SK-Hep1	Cholangiocarcinoma	Hypo	++	Hypo	++	Non-HCC
HHL5	Immortalised hepatocyte	Hypo	++	Hypo	++	Non-HCC

TIAM1 and *LDHB* expression were determined by RT-qPCR.
DNA methylation was determined by Infinium MethylationEPIC array.
Hypo: low promoter methylation. Hyper: high promoter methylation.
Immortalised hepatocyte HHL5 derived from healthy primary liver tissue which was infected with retrovirus vector LXSN16E6E7 on Moloney's mouse leukaemia virus [**Clayton et al., 2005**]

3.7.3 Impact of *TIAM1* gene knockdown with siRNA on HCC-related cell lines

3.7.3.1 Assessment of *TIAM1* gene knockdown (KD) by RT-qPCR

To evaluate the effect of *TIAM1* on cell proliferation, we knocked down (KD) the *TIAM1* transcript using *TIAM1* specific siRNA. Non-silencing siRNA was also used as a control. RT-qPCR analysis was performed 48 hours post siRNA transfection. The results showed significant reductions (~75-85%) of *TIAM 1* mRNA levels in PLC/PRF-5 (**Fig. 3.7A**), and SNU182 (**Fig. 3.7B**) compared with control non-silencing-siRNA (non-siRNA). Knockdown of *TIAM1* in HCC non-subgroup 2 cell lines (HepG2 and Huh-7) could not be assessed as neither cell line expresses detectable levels of *TIAM1* (however, these cell lines were included in the functional analysis as controls for off-target effects). *TIAM1* mRNA was also decreased (~75-85%) in both SK-Hep1(**Fig. 3.7C)** and HHL5 **(Fig. 3.7D)** post siRNA transfection. These finding indicate that treatment with *TIAM1* siRNA was able to induce a substantial KD of the target in all the *TIAM1* expressing cell lines.

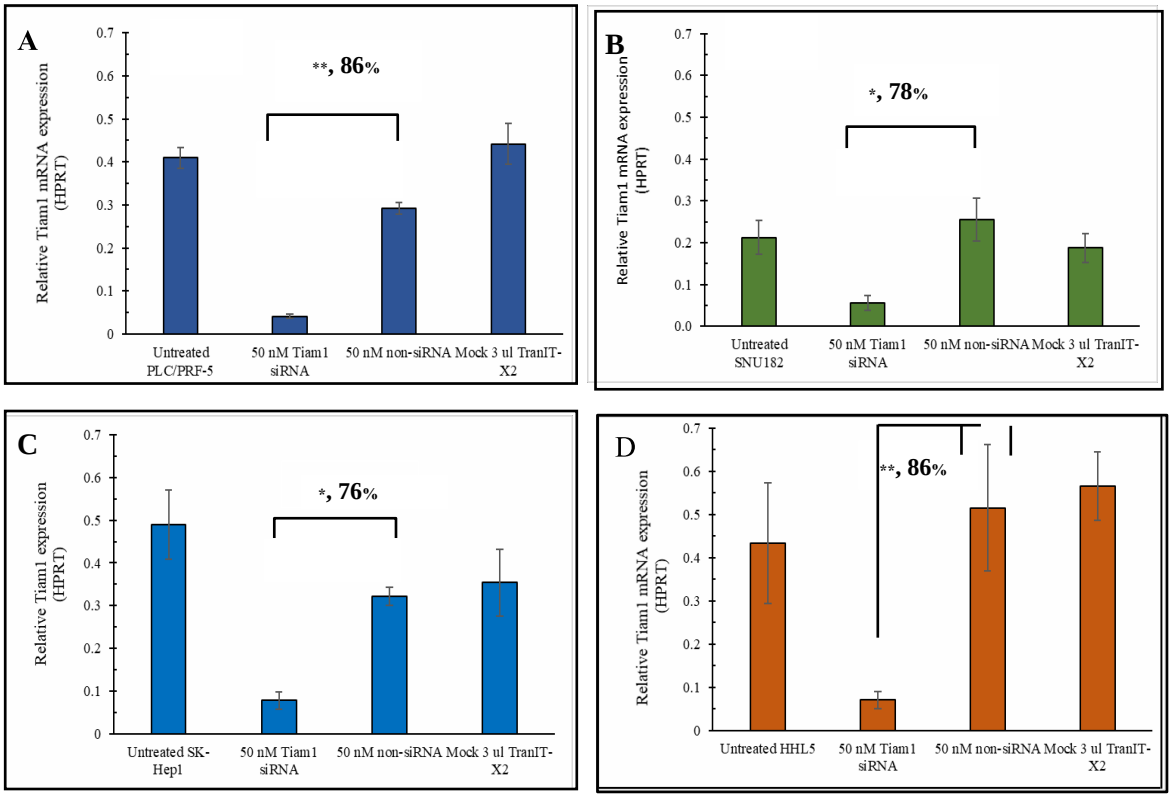

Figure 3.7 RT-qPCR results of cells 48 hrs post-transfection with indicated siRNAs or control conditions. (**A**) PLC/PRF-5 (n=3), (**B**) SNU182 (n=4), (**C**) SK-Hep1 (n= 3) and (**D**) HHL5 (n=2). All cell lines were transfected with 50 nM siRNA: 3 µl *Trans*IT-X2® reagent. Cells were harvested 48 hours post-transfection followed by cDNA synthesis and assessment of *TIAM1* expression using RT-qPCR. Data were calculated as $2^{-\Delta Ct}$ relative to the house keeping control *HPRT*. Value is shown as mean ± SE and statistical comparisons were carried out by using a two-sample t-test assuming equal variances. * $P < 0.0005$, ** $P < 0.00005$.

3.7.3.2 The impact of *TIAM1* gene knockdown on cell proliferation

3.7.3.2.1 Cell proliferation after *TIAM1* gene knockdown in HCC subgroups

Following the previous experiment, we carried out siRNA mediated KD of *TIAM1* mRNA followed by determination of comparative cell growth by MTT assay. The data found that the knockdown of *TIAM1* by *TIAM1* siRNA (50 nM) inhibited cell proliferation rate of PLC/PRF-5 (**Fig. 3.8A**) and SNU182 (**Fig. 3.8B**) by just over 30% after 144 hrs ($p<0.05$).

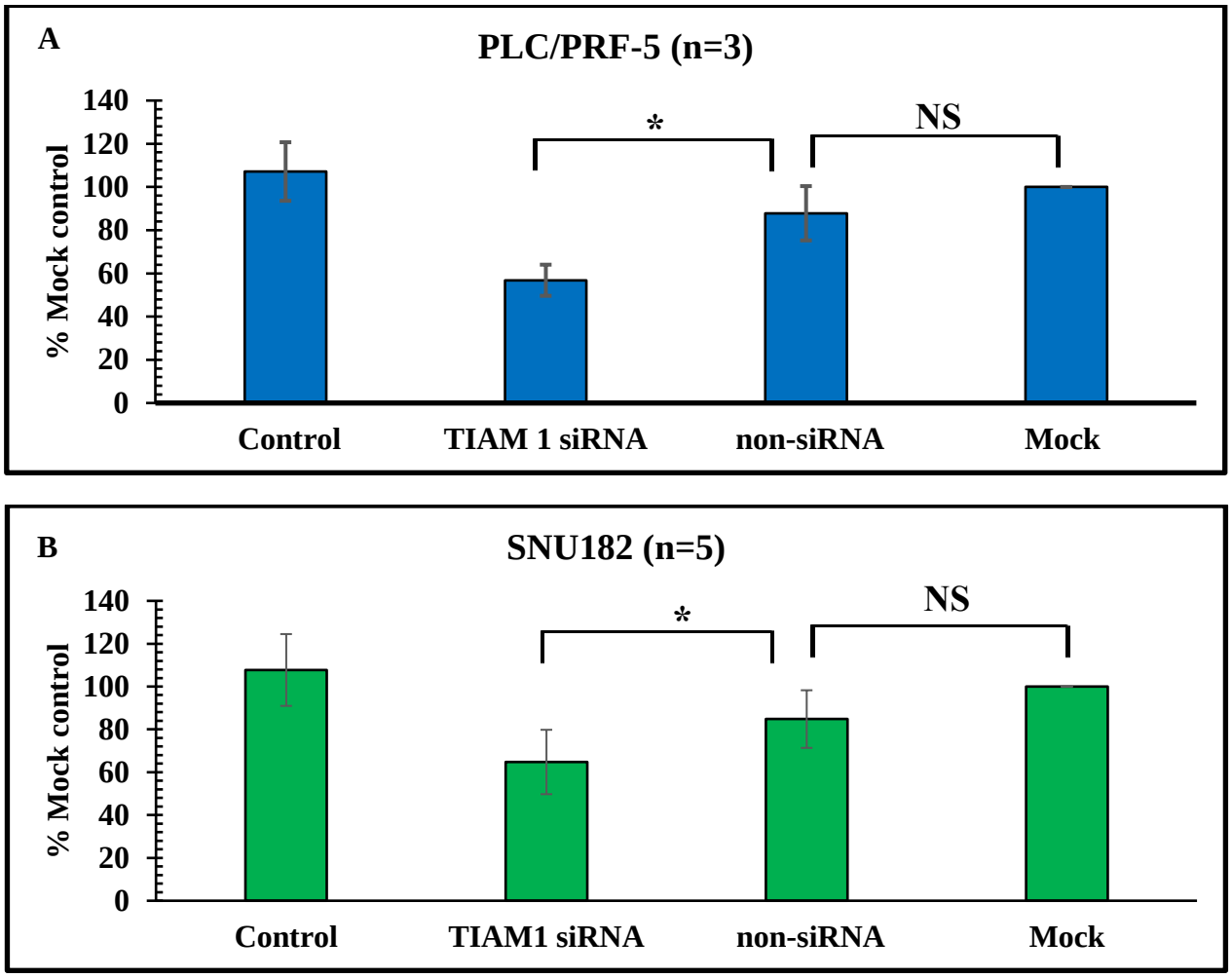

Figure 3.8 MTT assay to assess cell proliferation following knocking down of *TIAM1* gene in HCC subgroup 2 cell lines. Levels of viable cells 144 hrs after *TIAM1* KD were assessed by MTT assay. (**A**) The knockdown of *TIAM1* by *TIAM1* siRNA (50 nM) inhibited cell proliferation of PLC/PRF-5 by around 30% ($P < 0.05$), after 144 hrs post-KD. (**B**) The proliferation rate of SNU182 was reduced by approximately 36% ($P < 0.05$) with the same KD conditions as PLC/PRF-5. Statistical comparisons were carried out by using a t-test, two-sample assuming equal variances. non-siRNA: non-silencing siRNA. NS: not significant. Data are mean ± SD.

HepG2 and Huh-7 were also transfected with siRNA targeting *TIAM1* mRNA. As these cell lines do not express *TIAM1*, this was performed as a control for any potential off-target effects of the siRNA. Cell proliferation of HepG2 (**Fig. 3.9A**) and Huh-7 (**Fig. 3.9B**) was not significantly different between cells transfected with *TIAM1* siRNA or non-siRNA ($P > 0.3$) suggesting that there are no further off-target effects specifically due to the *TIAM1* siRNA. However, Huh-7 cells exhibited high non-specific toxicity (i.e., non-silencing control transfection resulted reduction in cell numbers in comparison with the mock control) making interpretation of the specific impact of the *TIAM1* siRNA difficult.

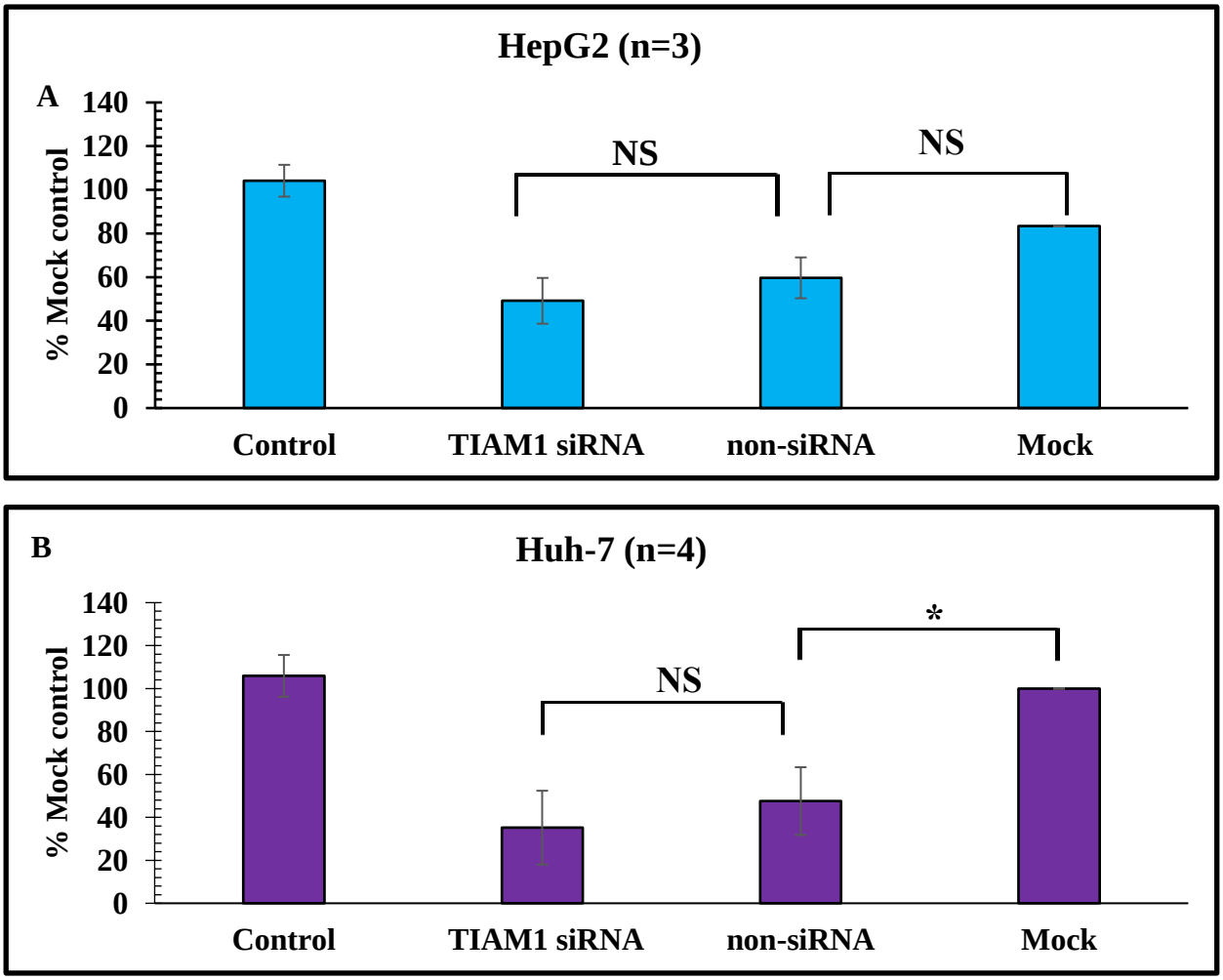

Figure 3.9 Cell proliferation in non-HCC cell lines after *TIAM1* gene knockdown. siRNA: short interfering RNA. **Non-siRNA**: non-silencing siRNA. **Mock**: transfection conditions that include transfection reagent but not siRNA. **NS**: not significant. Data are mean ± SD. *$P < 0.005$.

3.7.3.2.2 Cell proliferation after *TIAM1* gene knockdown in non-HCC subgroups

Cell proliferation after knockdown of *TIAM1* in non-HCC cell lines SK-Hep1 and HHL5 was assessed under the same conditions as above to see whether influence of TIAM1 KD on cell proliferation was specific to HCC subgroup 2 or not. *TIAM1* siRNA mediated KD reduced cell proliferation of SK-Hep1 **(Fig. 3.10A**) whilst it did not show the effect in HHL5 proliferation rate (**Fig. 3.10B**). The lack of a significant impact in HHL5 cells is consistent with the loss of *TIAM1* specifically effecting HCC subgroup 2 as compared with non-transformed hepatocytes. However, SK-Hep1 exhibited a similar reduction in proliferation after knockdown suggesting that *TIAM1* may have a role in proliferation and/or survival in other cancer types.

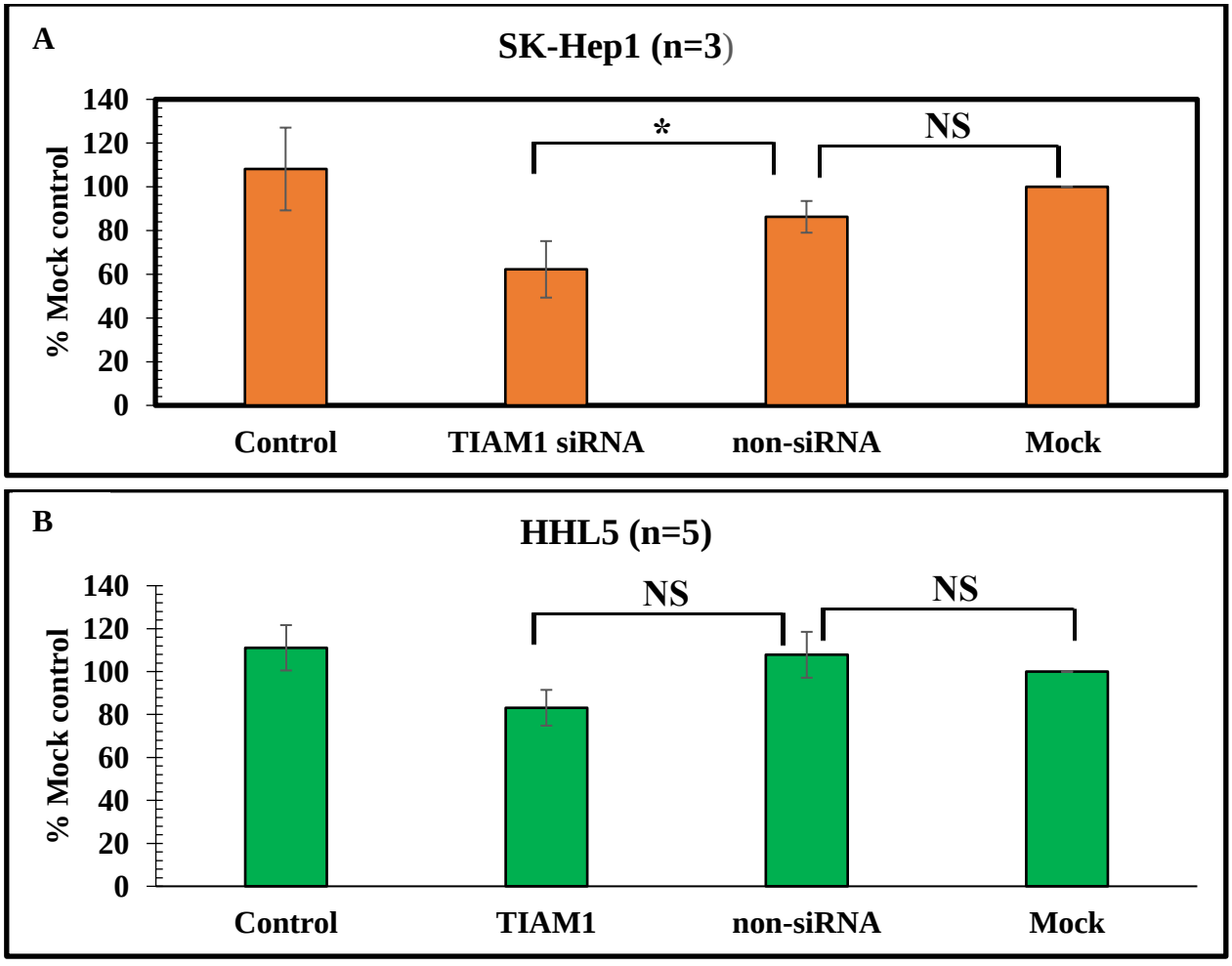

Figure 3.10 Cell proliferation in non-HCC cell lines after *TIAM1* gene knockdown. (**A**) Represent data of transfected reduction around 35 % in SK-Hep1 (n=3). (**B**) Cell proliferation reduction in HHL5 did not different between *TIAM1* siRNA and non-siRNA KD at 50 nM (n=5) Data are mean ± SD.*P<0.05. **siRNA**: short interfering RNA. **Non-siRNA**: non-silencing siRNA. **Mock**: transfection conditions that include transfection reagent but not siRNA. **NS**: not significant.

3.7.4 Relative sensitivity of *TIAM1* gene expressing and non-expressing cell lines to RAC1 inhibition with NSC23766

3.7.4.1 Sensitivity of NSC23766 estimated by MTT cell viablility assay

NSC23766, a specific RAC1 inhibitor, has been reported to block the interaction of TIAM1 with RAC1[**Ruffoni et al., 2019**]. Thus, to assess the possibility that loss of TIAM1 was acting through loss of RAC1-signalling, sensitivity of the cell lines towards NSC23766 was evaluated. In addition to acting as confirmation of the siRNA mediated knockdown, this approach also had the advantage of overcoming the difficulties due to non-specific toxicity following transfection with siRNA and thus allowing all cell lines to be assessed. The cell lines were treated with various doses of NSC23766 and its impact on cell proliferation assessed using the MTT assay. The effect of NSC23766 on the three subgroups indicated that NSC23766 inhibited cell growth of all cell lines in a dose- and time-dependent manner, however, the extent varied between the subgroups. As shown in **Fig. 3.11**, HCC subgroup 2 cell lines SNU182 (**Fig. 3.11A**) and PLC/PRF-5 (**Fig. 3.11B**) were found to be the most sensitive to the inhibitor, compared with non-HCC subgruoup2 (HepG2; **Fig. 3.11C**, and SK-Hep1; **Fig. 3.11D**), and the cell lines belonging to other subgroups. Interestingly, the non-HCC cell lines HHL5 **(Fig. 3.11E**), and SK-Hep1 (**Fig. 3.11F**) showed lower sensitivity to the inhibitor although the level of *TIAM1* expression is similar to HCC subgroup 2, suggesting the increased sensitivity may be specific for HCC subgroup 2 and not simply reflective of the presence or absence of *TIAM1* expression, which is in line with the concept of synthetic lethality. The cytotoxicity of this compound on HCC and non-HCC cell lines is summarised in **Table 3.3**.

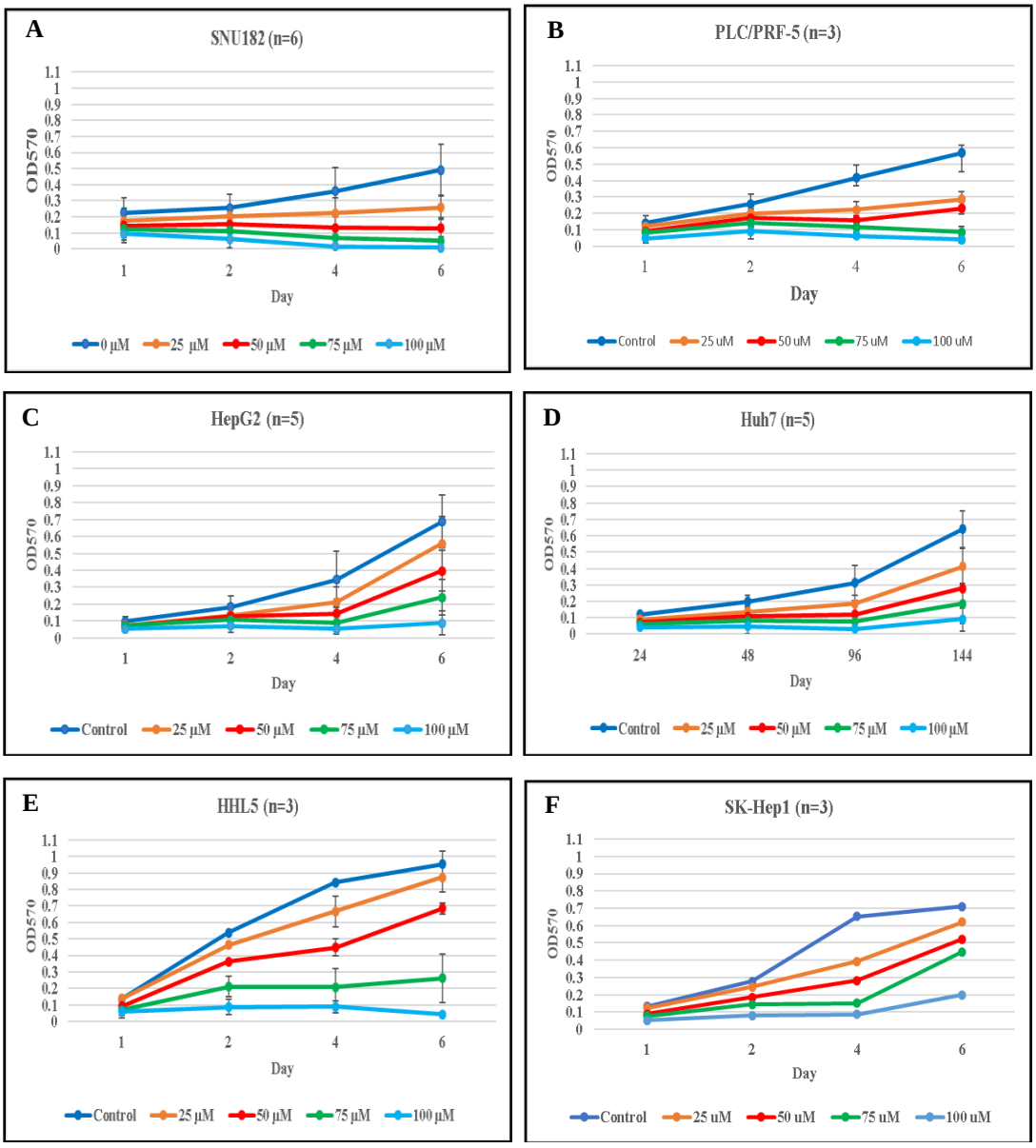

Figure 3.11 The cytotoxicity of NSC23766 on HCC and non-HCC cell lines assessed by MTT assay. After incubating cells overnight, NSC23766 at 0 - 100 µM was added. The MTT assay was performed at 1, 2, 4, and 6 days after the drug was added. Data represent as mean ± SD of at least 3 independents studies.

Table 3.3 The cytotoxicity of NSC23766 on HCC and non-HCC subgroup determined by MTT assay.

Cell lines	HCC subgroup	IC50 (μM) MTT assay	Significance (Compared with SNU182)	P value with SNU182	Significance (Compared with PLC/PRF-5)	P value with PLC/PRF-5	N
SNU182	2	27.84 ± 5.20	-	-	No	0.5559	6
PLC/PRF-5	2	24.84 ± 0.91	No	0.5559	-	-	3
HepG2	Non-subgroup 2	57.08 ± 9.61	Yes	<0.0001	Yes	<0.0001	5
Huh-7		49.90 ± 0.11	Yes	<0.0001	Yes	<0.0001	3
SK-Hep1	Non-HCC	76.74 ± 1.16	Yes	<0.0001	Yes	<0.0001	3
HHL5		61.60 ± 5.89	Yes	<0.0001	Yes	<0.0001	3

IC50 was calculated from Prism software.
Data are shown as mean ± SD. One-way ANOVA with Dunnett's multiple comparisons test.

3.7.4.2 CellTox™ green cytotoxicity assay

3.7.4.2.1 Validation of the sensitivity and linearity of CellTox™ green cytotoxicity assay

The MTT assay cannot distinguish between dead and viable cells. Thus, the CellTox™ assay was used to quantify dead cells through the binding of the fluorescent dye with the DNA of dead cells, whereas the dye cannot pass freely through the cell membrane of viable cells. Thus, the proportion of fluorescent signals reflect the toxicity of the test compounds. However, before utilising this assay, it is necessary to assess the sensitivity and linearity of the assay for the cell lines being used. This analysis revealed a direct relationship between the total number of dead cells (killed with the lysis solution provided with the kit) and the fluorescent signal, which increased proportionally with the number of dead cells with the r-squared (r^2) for all cell lines over 0.97 (**Fig. 3.12**). This result indicated that this assay is reliable for testing cytotoxicity with good linearity in the cell lines used for this study.

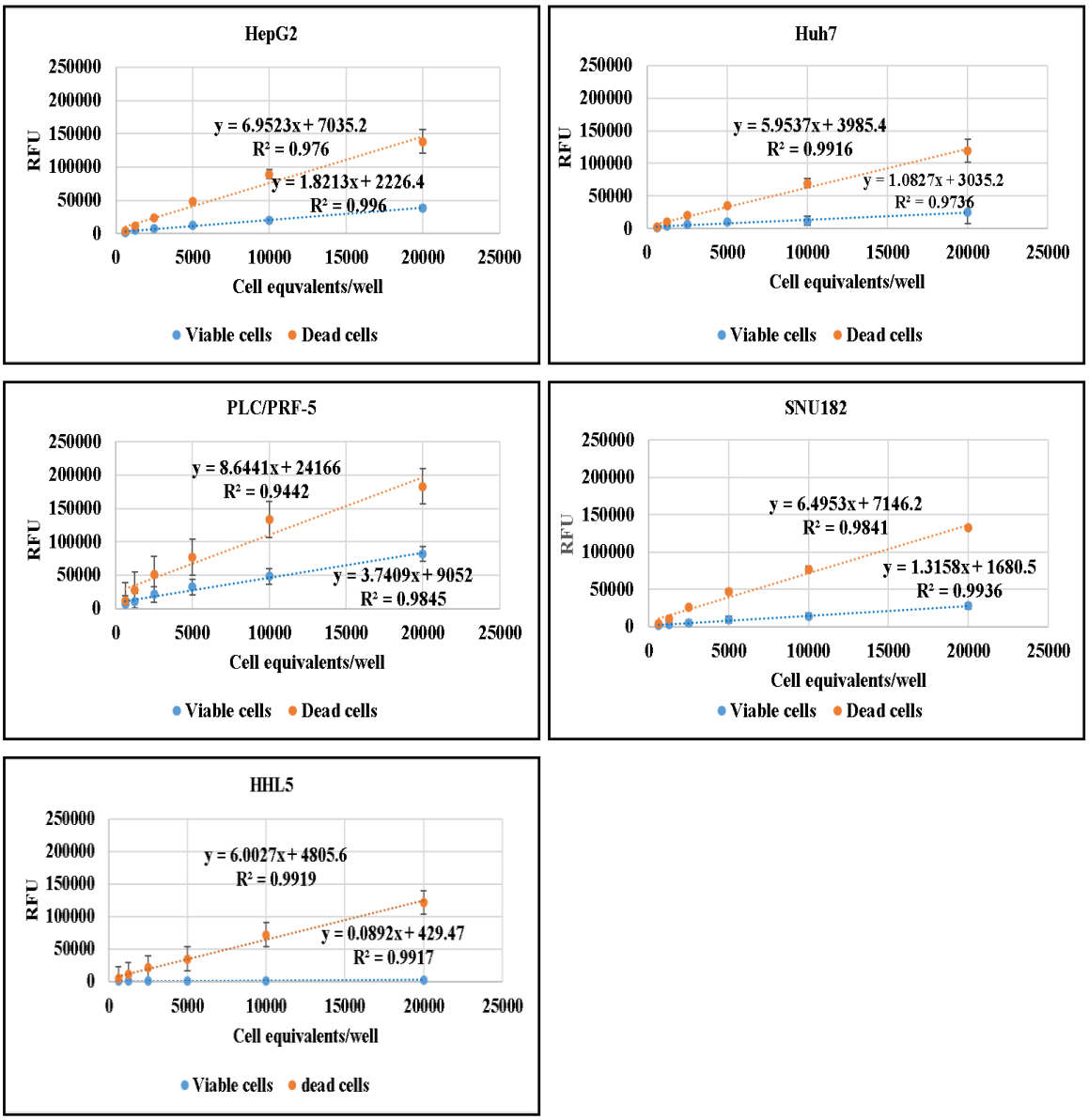

Figure 3.12 Validation of sensitivity and linearity of CellTox™ green cytotoxicity assay. The intensity of the fluorescence signal reflects relatively the number of dead cells. The colour represents dead (**blue**) or viable (**brown**) cells. Fluorescence was measured using a microplate reader after 15 minutes of incubation. The excitation wavelength is 485 nm, and the emission wavelength is 520 nm. RFU: relative fluorescent unit. Data are mean ± SD of onc experiment (triplicate).

3.7.4.2.2 Cytotoxicity of NSC23766 on hepatocellular carcinoma

Having established the linearity/sensitivity of the assay as described above, it was then used to assess cytotoxicity of NSC23766 on the HCC cell lines. NSC23766 showed high impact on PLC/PRF-5 and SNU182 determined cells growth rate by MTT assay. The sensitivity of these cell lines to this inhibitor could be due to reduced proliferation or increased rates of cell death/toxicity. Thus, CellTox™ green reagent was used to assess toxicity 48 hrs post treatment with varying doses of NSC23766. This analysis found that NSC23766 treatment did not result in high levels of cell death. For five of the six cell lines there was no clear evidence of induction of cell death even when exposed to doses that were several times higher than IC50 values. The only exception was SNU182, where clear induction of cell death was seen after exposure to 120 μM of NSC23766. However, even in this cell line, cell death was only seen at doses greater than those previously shown to completely inhibit cell growth (compare effect of 50 μM NSC23766 in **Fig. 3.11A** versus the lack of cell death after exposure to 60 μM in **Fig. 3.13**).

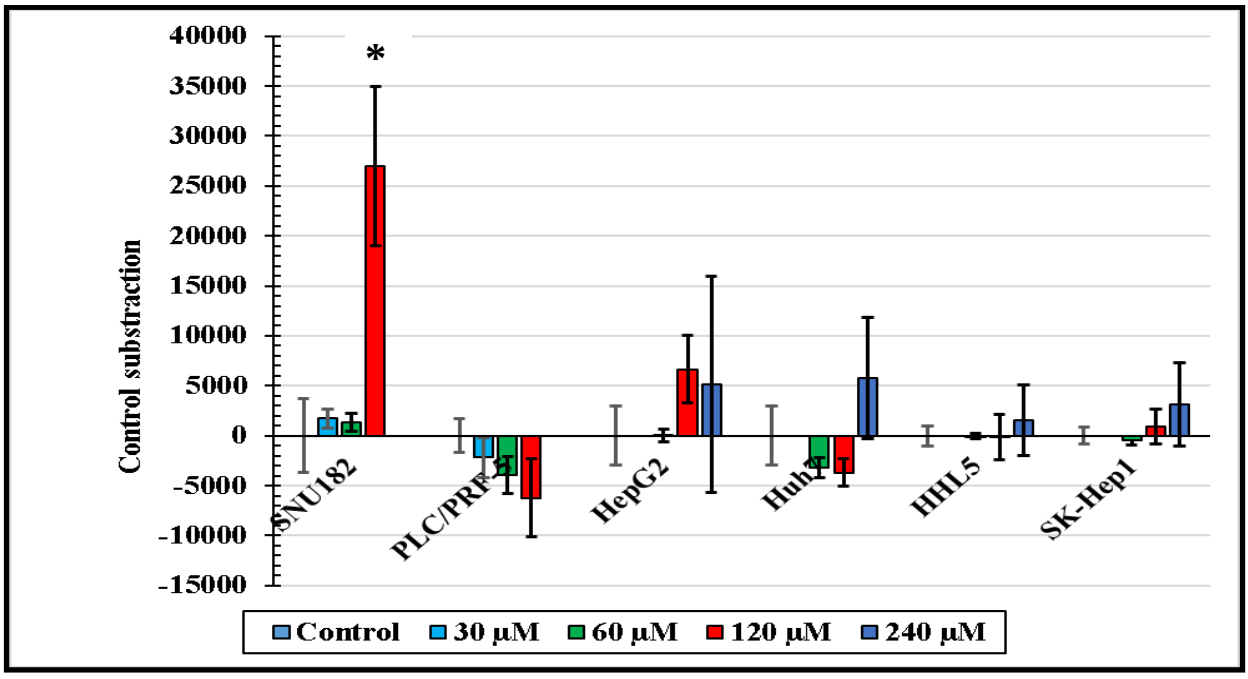

Figure 3.13 The cytotoxicity of NSC23766 on HCC and non-HCC cell lines determined by CellTox®. After 48 hrs, cell cytotoxicity was assessed by measuring the fluorescence signal. Data were normalised with the control group by subtraction the fluorescent signal of treatment with the untreated control ± SD. N=2. Statistical comparisons were carried out by using a t-test, two-sample assuming equal variances. *P< 0.005.

3.7.4.3 RAC1 expression

The observed differences in NSC23766 sensitivity could be influenced by the level of RAC present in the different cell lines. Thus, western blotting was used to assess the level of RAC expression in HCC and non-HCC cell lines. This result demonstrated that SK-Hep1 had the highest RAC expression. However, there is no discernible difference between PLC/PRF-5, SNU182, and Huh-7. Although HHL5 and HepG2 were expressed at a higher level, the difference was minor (**Fig. 3.14**). Because there was not a specific RAC1 antibody available, RAC expression was assessed using a RAC antibody, which binds RAC1, RAC2, and RAC3.

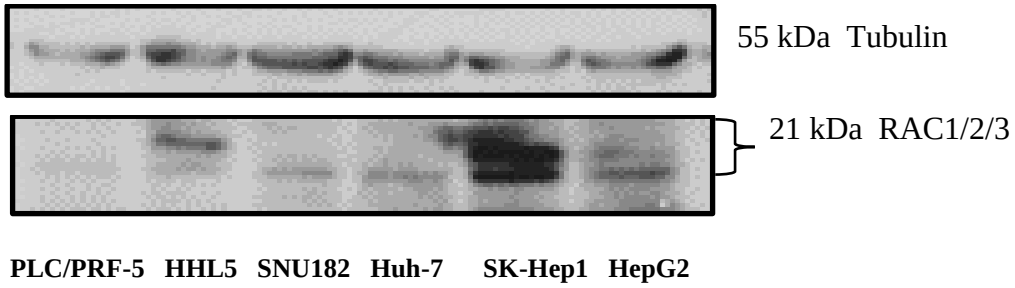

Figure 3.14 Relative expression level of RAC1 was manipulated by western blotting. Photos were taken from ChemiDoc (Biorad).

3.7.4.4 Assessment of apoptosis induction following NSC23766 treatment

To confirm that the lack of cell death identified above was not assay dependent, levels of apoptosis were also assessed, based on caspase activation. Apoptosis was again clearly seen in SNU182, after treatment at 120 μM, but was not detected in any of the other cell lines at any dose (**Fig. 3.15).** Even when PLC/PRF-5 was exposed to a higher dose (480 μM, nearly 20 times the IC50 value), no evidence was found to suport the induction of apoptosis (data not shown). Overall the results suggest that inhibition of RAC1 with NSC23766 was most primarily cytostatic and little evidenvce was seen for induction of cell death (only seen in SNU182 at a dose well above the IC50).

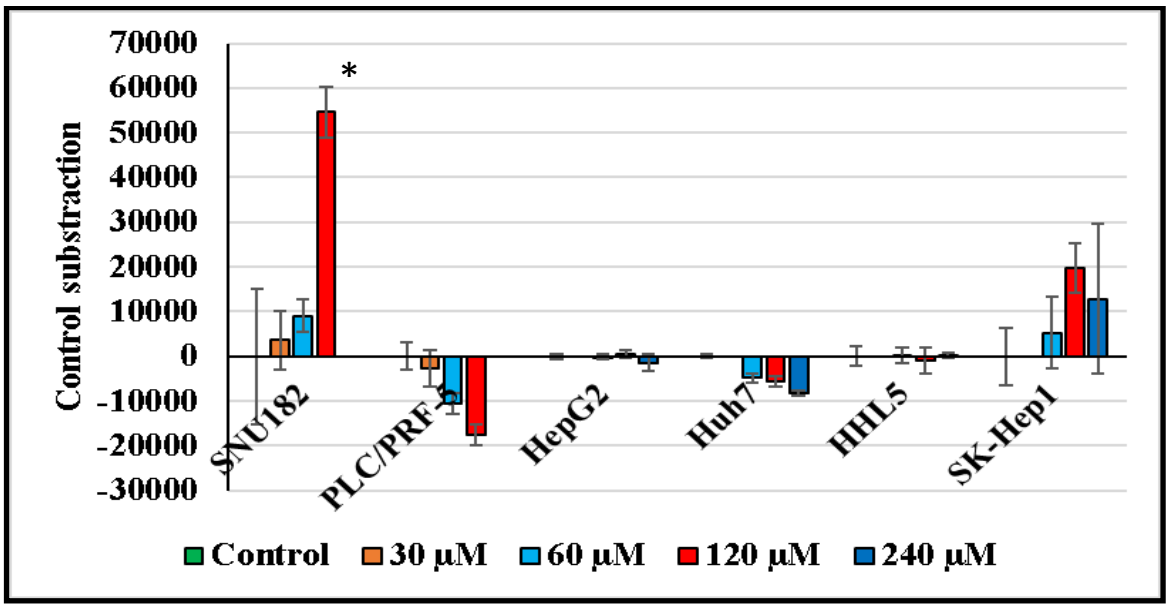

Figure 3.15 The apoptosis induction of NSC23766 on HCC and non-HCC cell lines was evaluated by caspase-Glo® 3/7 apoptosis assay. After 48 hrs of drug added, apoptosis was assessed by measuring the luminescence signal after added Caspase-Glo® 3/7 assay (Promega) for 1 hr. Data is subtracted from control ± SD. N=2. Statistical comparisons were carried out by using t-test, two-sample assuming equal variances. *P < 0.00005.

3.8 Discussion

Most cancers are defined by similarity in morphology or location. However, many can be further subdivided into subtypes based on additional molecular, pathology, or clinical features.

Recently, we have developed a bioinformatic screening approach that utilises such molecular subclassification to enable the identification of SLGs. However, widely accepted molecular subgroups of HCC have not been clearly elucidated.

Various classifications of HCC by molecular, histopathology, clinical, and immunohistochemistry subtypes have been reported. However, those methods consume more budget, time, labour, and require expertise for subclass elucidation. Thus, we applied to use genome wide DNA methylation data equipped with NMF to classify HCC into subgroups.

Several studies have demonstrated that HCC is resistant to chemotherapy and RT [**Cuestas et al., 2005; Guo et al., 2018; Lohitesh et al., 2018**]. As a result, new approaches to HCC treatment are urgently needed. Because thousands of genes are mutated in various malignancies, discovering and validating possible SLGs could be a key approach to allow the development of targeted cancer therapies. By combining genome-wide DNA methylation and gene expression data, our team is the first to use a bioinformatics approach to detect SLGs in HCC samples. As the required datasets are publicly available, this approach can be performed more cheaply and rapidly than previously published approaches such as siRNA screening [**Pathak et al., 2015**], and chemical library, shRNA library [**Thompson et al., 2015**]. Furthermore, the pipeline has been verified in ALL and medulloblastoma with reliable results of the approach [**Schwalbe et al., 2021**]. The result of this method indicated that these HCC clusters exhibited relatively few clusters specific methylation differences, except for subgroup 2. Therefore, synthetic lethal gene analysis was focused primarily on this cluster. Analysis with our bioinformatics pipeline identified two candidate SLGs, *TIAM1* and *LDHB*, within HCC subgroup 2, with no candidates identified in any of the other subgroups.

The methylation data of *TIAM1* in patient samples from HCC subgroup 2 differed considerably from those other subgroups. Although mRNA expression levels were also increased the difference in expression level compared to that of other subgroups was limited **(see Fig. 3.3B)**. However, the difference in expression in tumour cells may be underestimated, as HCC samples typically have relatively high levels of contamination with non-tumour cells. Consistent with this

mRNA expression differed much more markedly between the presumptive HCC subgroup 2 (PLC/PRF-5 and SNU182) and non-HCC subgroup 2 (HepG2 and Huh-7) cell lines, as seen in **Fig. 3.4A**. Additional expression analysis, either using more highly purified primary samples, or immunohistochemical approaches where expression can be assessed specifically in tumour cells would be required to confirm the extent of differential TIAM1 expression.

Screening of *LDHB* and *TIAM1* mRNA expression within HCC cell lines, consistent with the primary data, identified all four cell lines as exhibiting a positive correlation between expression of the two genes. PLC/PRF-5 and SNU182 were positive for both genes (consistent with HCC subgroup 2), while HepG2 and Huh-7 exhibited low/absent expression of both genes (consistent with not being derived from subgroup 2). In addition, the DNA methylation analysis at the two loci also mirrored the patterns seen in the primary samples, with low DNA methylation in SNU182 and PLC/PRF-5 at both loci and high methylation in the two non-expressing cell lines. In addition, the region of differential methylation exactly matched the DMR identified in the primary samples. Similar to the two potential SLGs, the ZFP36 loci also exhibited methylation patterns that match the presumptive definition of the cell lines as subgroup 2 or non-subgroup 2, while there were no loci where HepG2 and Huh-7 were similar to group 2 and SNU/PLC were not, the methylation analysis did identify a number of DMRs where the differences were not replicated in the cell lines. The failure of all loci to mirror the primary samples may represent variability in the primary samples and/or methylation changes that developed during cell culture. Overall, the methylation analysis further supported the likely derivation of SNU/PLC from subgroup 2 and Huh-7/HepG2 as not derived from subgroup 2.

We silenced the *TIAM1* gene in HCC subgroups 2, PLC/PRF-5, and SNU182, as well as non-HCC subgroups (SK-Hep1 and HHL5). Cell proliferation was reduced by more than 30% following the knockdown without off-target effect. The inhibition of RAC1 activity by NSC23766 suppressed cell growth of all six cell lines tested in a dose-and time-dependent manner. HCC subgroup 2 cell lines exhibited the most sensitivity to the inhibitor, consistent with the prediction that TIAM1-mediated RAC1 activation is of particular importance in these cell lines. However, while this is consistent with the hypothesis, the difference in relative sensitivity may not be enough to consider this a viable option for specifically targeting HCC. Interestingly, cytotoxicity and apoptosis induction were seen in one subgroup 2 cell line, specifically with SNU182, but were not observed for another subgroup 2 cell line, PLC/PRF-5. These studies also indicated that NSC23766

is not specific for the inhibition of TIAM1 activation of RAC1 as we can see the sensitivity to this inhibitor in HepG2 and Huh-7 (low/undetectable *TIAM1* gene expression). This suggests that the inhibitor also has inhibitory effects that are independent of TIAM1. Consequently, a more potent and specific inhibitor may be required to fully assess the extent to which targeting TIAM1 can specifically inhibit HCC subgroup 2 cells.

3.9 Limitations and Future directions

3.9.1 The number of HCC cell lines representing HCC subgroup 2 of patient's samples are limited. We have PLC/PRF-5 and SNU182 representing as the members of this subgroup.

3.9.2 Additionally, HCC primary cells exhibit restricted proliferate and subculture times due to its inability to develop adequately. These are the constraints which limit the number of primary samples available for HCC research. As a consequence, alternative approach would be to use cell lines that represent aspects of HCC biology. Other HCC-related cell lines (Huh1 and Hep3B) were screened to see whether they could be segregated among lines that exhibited both the *TIAM1* and *LDHB* genes (potential subgroup 2) and lines that did not express either (potential non-subgroup 2 model). The finding showed that these two HCC cell lines express only *LDHB* gene (data not shown). Therefore, we failed to identify any suitable HCC cell lines representing subgroup 2 and non- subgroup 2 model.

3.9.3 RNAi is an easy and low-cost experiment to knock down the target genes. However, RNAi can have off-target effects. This study demonstrated that the sequence of siRNA we used did not exert an off-target effect in the neg-*TIAM1* gene of non-HCC subgroup 2 HepG2. non-HCC subgroup 2 Huh-7 showed non-specific toxicity. Thus, additional non-HCC subgroup2 cell lines would be required to confirm that the effects are specific for targeting TIAM1 in subgroup 2 cells.

3.9.4 NSC23766 has low ability to inhibit cell proliferation in HCC cell lines. This inhibitor was cytocidal but not cytotoxic to all cell lines at 100 μM, and apoptosis was revealed with only SNU182 after increasing the concentration to 120 μM. This compound had a weak inhibitory effect on MDA-MB-435 breast cancer cells (IC50 = 95 μM) [**Montalvo-Ortiz et al., 2012**]. We have attempted to increase the dose of NSC23766 to 240 μM. However, it did not induce apoptosis in

HCC subgroup 2 PLC/PRF-5. This makes NSC23766 not suitable for further clinical study. Due to the lack of high potency and specificity of RAC1/TIAM1 inhibitor EHop-016 has a high efficiency against breast cancer MDA-MB-435 and MDA-MB-231, the IC50 is 1.1 and 3 μM, respectively [**Montalvo-Ortiz et al., 2012**]. The 1D-142, showed strong activity to two human lung cancer A549 (7.8 μM) and A375 (7.4 μM), colon HT29 (9.0 μM), prostate PC3 (9.3 μM), and MDA-MB-231 (14.6 μM) [**Ciarlantini et al., 2021**]. However, the potency and efficacy of these high potency compounds and the off-target effect have not been investigated in HCC cell lines. Therefore, it should be future elucidated of those with HCC subgroup 2 cell lines. Furthermore, the downstream impact of TIAM1 inhibition such as migration and apoptosis could be evaluated.

Chapter IV

The influence of LDHB status on sensitivity to the metabolic inhibitors 2-Deoxy-D-glucose (2-DG) and metformin

4.1 Gylcolysis pathway

Cancer cells require more glucose for energy production to support cell growth and proliferatation than normal cells. Otto Warburg and co-workers found that the rate of glucose uptake increased dramatically even in oxygen abundance [**Warburg et al., 1924**]. This phenomenon is termed the Warburg effect and is one of the hallmarks of cancer [**Fan et al., 2019**].

The glycolysis pathway is the process of breaking down a six-carbon molecule of glucose into the two three-carbon molecules but requires a glucose transporter (GLUT) to transport glucose across the cell membrane. Glycolysis occurs in cytoplasm and consists of ten steps, producing 4 ATP, 2 NADH, 2 pyruvate and 2 $H^{+,}$, and 2 H_2O. But, it also uses 2 ATP, thus a net gain of 2 ATP is produced per a molecule of glucose [**Kierans and Taylor, 2021**]. The glycyolysis pathway is illustrated in **Fig. 4.1.**

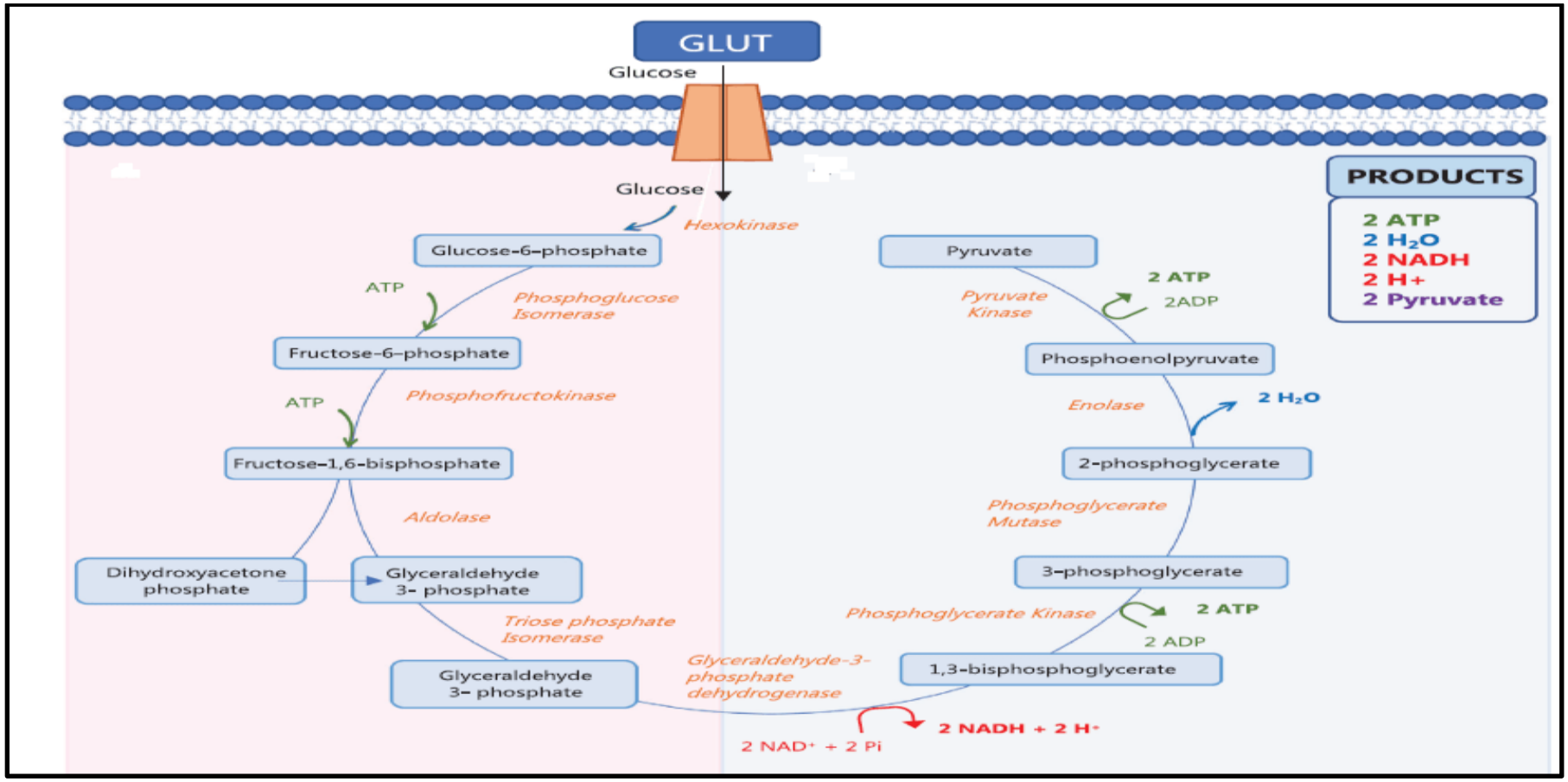

Figure 4.1 The overview of glycolysis pathway. GLUT: Glucose transporters; located within the cellular membrane, they take up glucose from the extracellular space. Through the actions of glycolytic enzymes, glucose is oxidized in a stepwise manner (orange text). The glycolytic pathway requires the investment of two molecules of ATP to oxidize glucose (preparatory phase), which allows for the simultaneous generation of two molecules of NADH, two molecules of H+, two molecules of H_2O, two molecules of pyruvate, and a net gain of two molecules of ATP per unit of glucose (pay-off phase) [**Kierans and Taylor, 2021**].

4.2 The Krebs cycle

The Krebs cycle, also known as the tricarboxylic acid (TCA) cycle, occurs in the mitochondrial matrix and is the primary route for ATP generation under aerobic conditions. This pathway consists of various chemical reactions that begins with pyruvate, which is produced during glycolysis. Pyruvate is metabolism divides into two pathways before entering the Krebs cycle (**Fig. 4.2**):

(1) Pyurvate is conveted to acetyl CoA by pyruvate dehydrogenase.

(2) Pyruvate is changed into oxalocacetate by pyruvate decarboxilase.

This cycle contains eight metabolic reactions (**red text**), and the pathway results in the production of flavin adenine dinucleotide ($FADH_2$, reduced form) and nicotinamide adenine dinucleotide (NAD, oxidised form) (NADH, reduced form). These are then used in the electron transport chain (ETC).

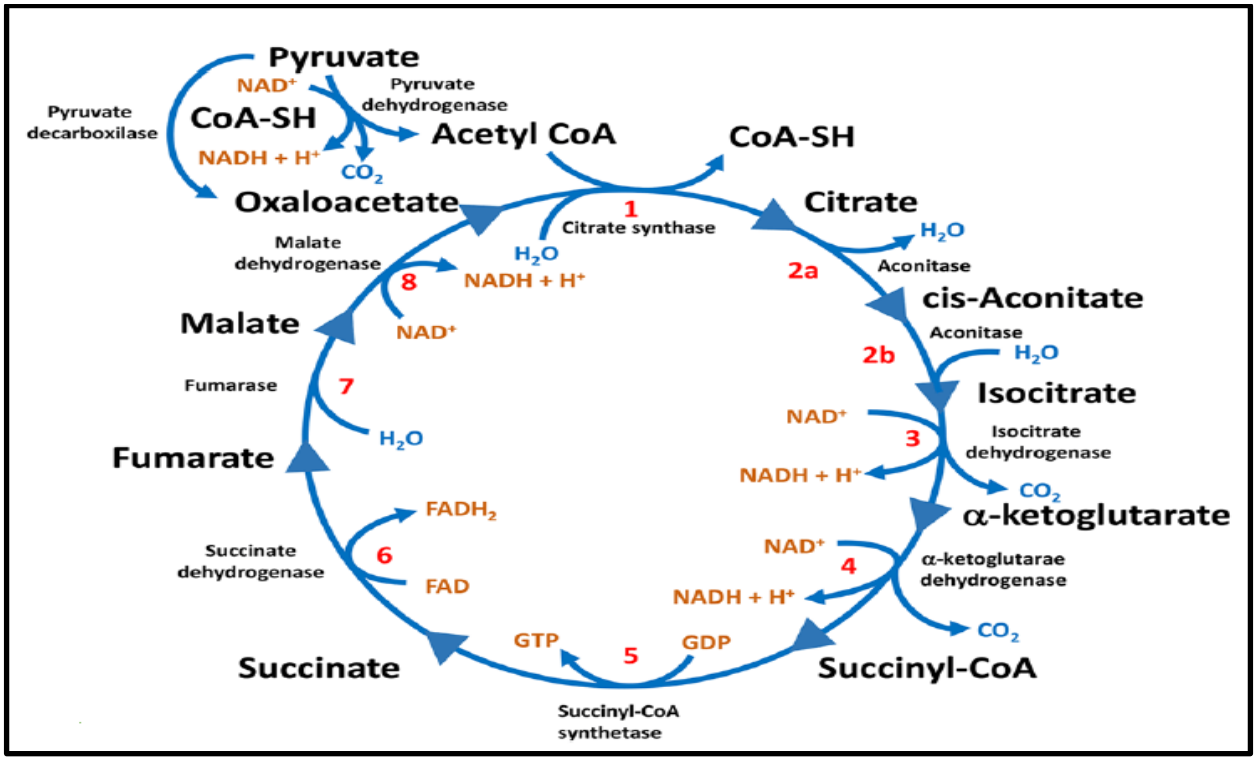

Figure 4.2 Depicts the Krebs cycle. The metabolic reactions are indicated by the red colour The goal of this pathway is to produce electron carriers (NADH and $FADH_2$), which are required for the electron transport chain in mitochondria to generate energy [**Gasmi et al., 2021**].

4.3 Oxydative phosphorylation and electron transport chain

Oxidative phosphorylation (OXPHOS) is an ATP-producing pathway in which electrons are transferred from electron donors (NADH and $FADH_2$ from the Krebs cycle) to electron acceptors (complex I and II) via the ETC (**Fig. 4.3**), which is composed of five protein complexes. Cancer cells have higher glycolysis than normal cells, suggesting that OXPHOS is downregulated in cancers. However, recent studies have shown that OXPHOS can be upregulated in a variety of cancers, including lymphoma, leukemia, melanoma, and pancreatic ductal adenocarcinoma, even when active glycolysis is present [**Bergman et al., 2016; Ashton et al., 2018**]. As a result, OXPHOS inhibitors such as metformin would have the potential to be used as an anti-cancer drug.

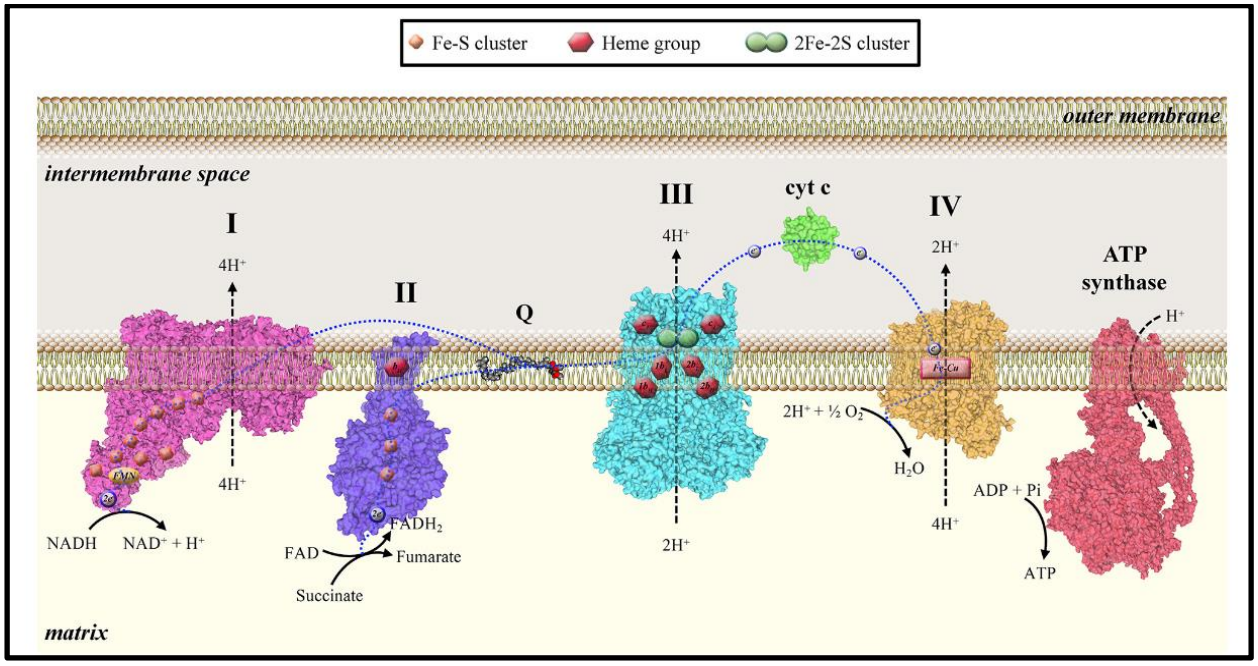

Figure 4.3 Electron transport chain in mitochondria. The ETC is made up of four enzyme complexes (complexes I–IV), coenzyme Q (Q), cytochrome C (cyt C), and ATP synthase. To generate a large amount of protons (H+), ETC oxidises the TCA products NADH (which is transferred to complex I) and $FADH_2$ (which is transferred to complex II). The proton gradient produced by complexes I, III, and IV is then transported to complex V, where ATP synthase produces ATPs [**Branca et al., 2020**].

4.4 Glycolysis and oxydative phosphorylation in normal and cancer cells

Glycolysis is the main pathway for energy production in most cancer cells, whereas OXPHOS is the main pathway in normal cells. It has been shown that glycolysis in cancer cells can be upregulated up to 200 times relative to normal cells [**Akram, 2013**].

Fig. 4.4 Illustrates the efficiency of energy generation in normal and cancer cells. Glycolysis in normal cells under aerobic conditions occurs in the cytoplasm. Then, pyruvate enter into mitochondria and metabolised to acetyl CoA before entering into the Kreb's cycle. Following OXPHOS, a total of 30 or 32 ATP is produced. However, only 2 ATPs are generated via glycolysis under anaerobic conditions per molecule of glucose (**Fig. 4.4A**). In many cancer cells, the majority of glucose is metabolised via the glycolysis pathway and a minority go to the OXPHOS pathway. In addition, a small amount of glucose is converted to precursor molecules (NADPH, pentose, and ribose-5-phosphate) before generating nucleotides; the above process is known as the pentose phosphate pathway (**Fig. 4.4B**). Despite the fact that the "Warburg effect" causes less efficient energy production, various cancer cells use this as their primary energy generation pathway while mitochondrial function is unaffected.

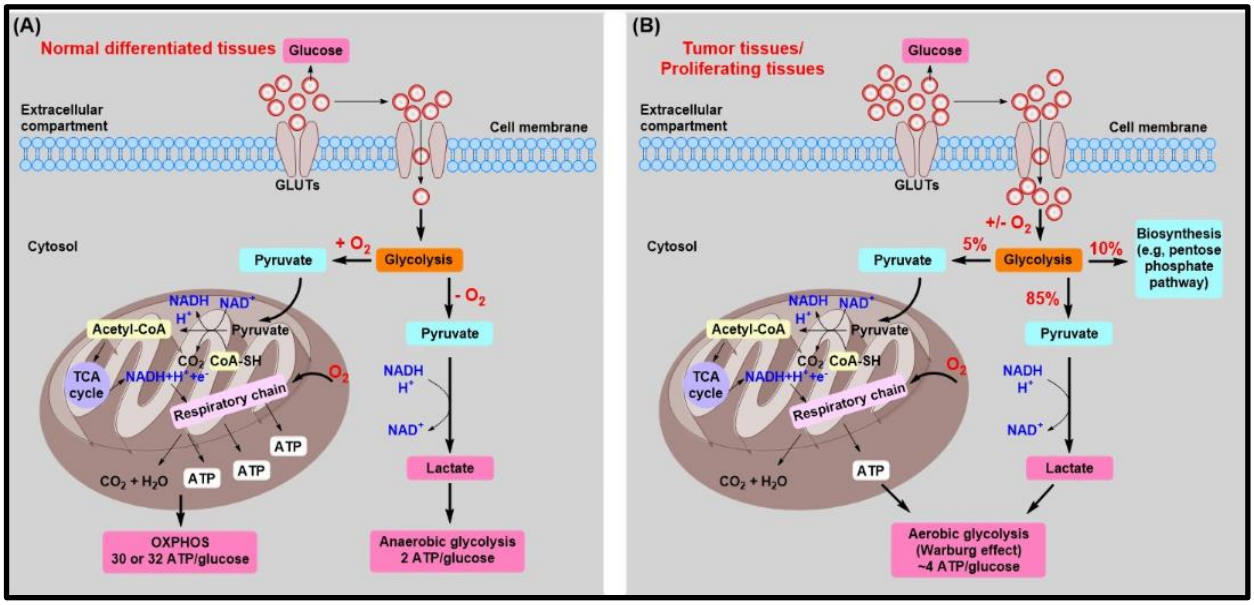

Figure 4.4 Comparion of glycolysis pathway between normal and cancer cells. (**A**) Under aerobic environment in normal differentiated tissues, one molecule of glucose must be converted to two pyruvates in the cell cytoplasm via glycolysis, followed by the TCA cycle to generate CO_2 in the mitochondria. During this process, 30 or 32 ATP molecules are produced. Under anaerobic conditions, however, less pyruvate is transferred to the oxygen-consuming mitochondria, resulting in only 2 ATP molecules produced per molecule of glucose. (**B**) Mitochondrial function is normal in tumours and proliferative tissues, however mitochondrial OXPHOS is minimal in tumour cells. Most glucose (~85%) is converted to pyruvate, and lactic acid, respectively. In order to meet the metabolic requirements of both energy and materials for rapidly growing cells, the minority of glucose is metabolised and enters into OXPHOS (+/- oxygen present). Furthermore, around 10%

of glycolysis products (glucose-6-phospate) serves as precursors for the manufacture of macromolecules (e.g., pentose phosphate pathway) [**Fan et al., 2019**].

As previously stated above, normal cells rely on OXPHOS for energy production because it is more efficient for ATP production than glycolysis [**Zheng, 2012**]. However, it will be important to discover why many cancer types do not use this pathway as their primary source of energy production. At first, it was suggested that this might be due to the impairment of OXPHOS in cancer cells [**Warburg, 1956**]. However, normal mitochondrial function was demonstrated to be present in ovarian and peritoneal cancer tissues [**Lim et al., 2011**] as well as melanoma cell lines [**Scott et al., 2011**]. A key reason might be that metabolites from the pathways have functions in addition to energy generation and are critical for the production of intermediate macromolecules such as nucleic acids, amino acids, and lipids, which are all required for cell growth and survival [**Zheng, 2012**; **Fan et al., 2019**].

As shown in **Fig. 4.5**, Zheng's group summarised the factors that influence cancer cells to use the glycolysis rather than the OXPHOS pathway. In fact, glycolysis and OXPHOS both contribute to the maintenance of cellular energetic balance. Hypoxic environments can lead to the activation of glycolysis through hypoxia-inducible facctor-1α to compensate for OXPHOS malfunction [**Zheng, 2012**]. It has been proposed that changes in both oncogenes and tumour suppressors genes play a key role in cancer's aerobic glycolysis and OXPHOS [**Levine and Puzio-Kuter., 2010**; **Zheng, 2012**]. Increased oncogene expression or inactivation of tumor suppressors may then stimulate glycolysis while inhibiting OXPHOS. [**Zheng, 2012**].

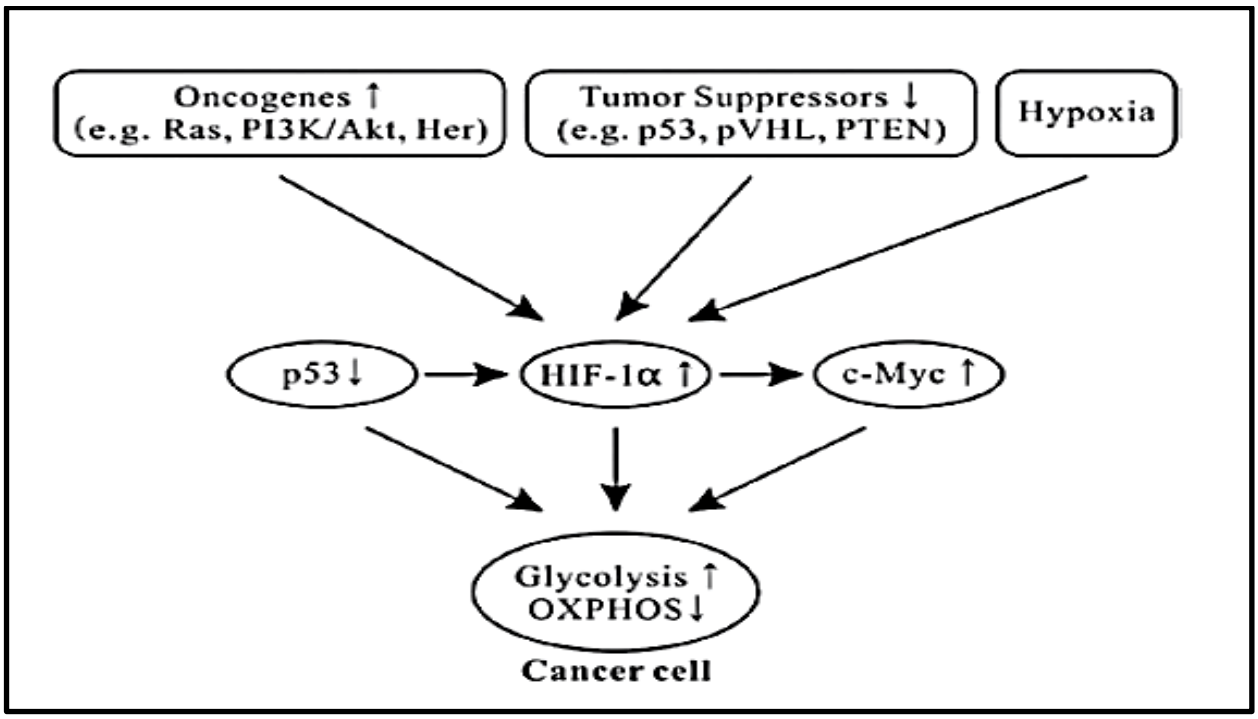

Figure 4.5 Factors influence cancer cells to use glycolysis rather than OXPHOS. The 'triad' of transcription factors responsible for the glycolytic phenotype in cancer is composed of hypoxia-inducible factor (HIF) -1α, c-Myc, and p53. Under normoxic conditions, HIF-1α is activated by oncogenes (e.g. Ras, PI3K/Akt, and Her) or inactivated tumor suppressors (e.g., p53, pVHL, and PTEN) genes. In addition, HIF-1α boosts c-Myc expression. HIF-1α activation could activate glycolysis via hypoxia condition [**Zheng, 2012**].

4.5 Lactate dehygrogenase

The lactate dehydrogenases (LDHs) are primary metabolic enzymes in vertebrates that consist of four subunits (LDHA, LDHB, LDHC, and LDHD). Different combinations of which form the holoenzyme in different tissues. All of these can catalyse the bi-directional conversion of lactate to pyruvate and NADH to NAD+ (**Fig. 4.6**). LDHA, LDHB, and LDHC catalyse L-lactate whereas LDHD utilises D-lactate [**Mishra and Benerjee, 2019**].

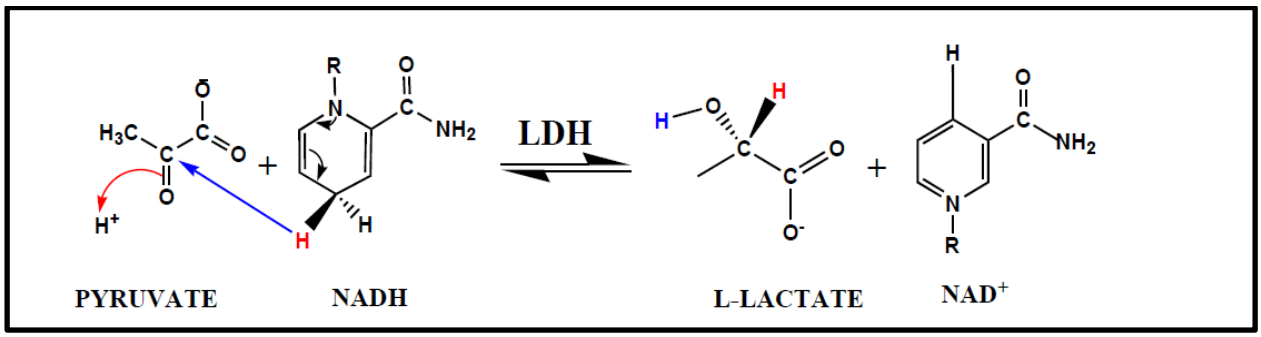

Figure 4.6 The function of lactate dehydrogenase (LDH). The LDH catalyses the reversible conversion of pyruvate to lactate and NADH to NAD+ and vice versa [**Khan et al., 2020**].

4.5.1 Lactate dehydrogenase A

Lactate dehydrogenase A (LDHA) preferentially converts pyruvate to lactate and NADH to NAD+ in anaerobic conditions, resulting in an acidic microenvironment. This condition is thought to promote cancer cell aggressiveness, metastasis, and recurrence [**Urbańska and Orzechowski, 2019; Schwab et al., 2021**].

4.5.2 Lactate dehydrogenase B

When oxygen is abundant, lactate dehydrogenase B **(**LDHB) preferentially converts lactate to pyruvate and NAD+ to NADH. The pyruvate then enters OXPHOS to genrerate energy [**Urbaska and Orzechowski, 2019]**. LHDB is expressed in all tissues, with particularly high levels of expression in heart tissue [**Lv et al., 2019**]. Knocking out of both LDHA and LDHB suppresses tumour growth and increases radiosensitisation in mouse B16F10 and human LS174T tumor cell lines **[Schwab et al., 2021**]. In 2021, Shibata's group published AXKO-0046, a novel LDHB inhibitor with a half maximal effective concentration (EC50) of 42 nM [**Shibata et al., 2021**].

4.5.3 Lactate dehydrogenase C

Lactate dehydrogenase C (LDHC**)** is an LDH family member that is largely specifically expressed in sperm and testes during sexual maturation **[Odet et al., 2011; Cui et al., 2020; Khan et al., 2020]**. Thus, this enzyme is essential for glycolysis and ATP production in sperm flagella [**Odet et al., 2011].** LDHC protein is expressed at low levels in myocardium, liver, kidney, skeletal muscle, and brain [**Cui et al., 2020**], and also expressed in several kinds of human cancer, such as lung cancer, breast cancer, renal carninoma, and melanoma [**Hua et al., 2017; Gupta, 2012; Cui et**

al., 2020; Forkasiewicz et al., 2020; Chen et al., 2021]. Kong and colleagues reported that blocking LDHC with the LDHC inhibitor N-propyl oxamate reduced MDA-MB-231 invasion and migration without inducing apoptosis [**Kong et al., 2016**]. In human, LDHA, LDHB, and LDHC share 84–89% sequence similarities and 69–75% amino acid identities [**Urbańska and Orzechowski, 2019**].

4.5.4 Lactate dehydrogenase D

Lactate dehydrogenase D (LDHD) has been found to be expressed in mitochondria. Previous research has found that the activity of this enzyme is increased in renal cell carcinoma patients [**Wang et al., 2018**], but it role in this type of cancer, and indeed in cancer more widely, is unknown.

4.6 Lactate

Previouly, lactate was thought to be a waste product of aerobic glycolysis, however, now it is known that lactate can be used as an alternative energy source in some cell types. In neurons it is utilised through the “neuron astrocyte lactate shuttle”. Lactate can also be used as a source of gluconeogenesis in the liver and an alternative enegy source for muscles during hard exercise (**Fig. 4.7**).

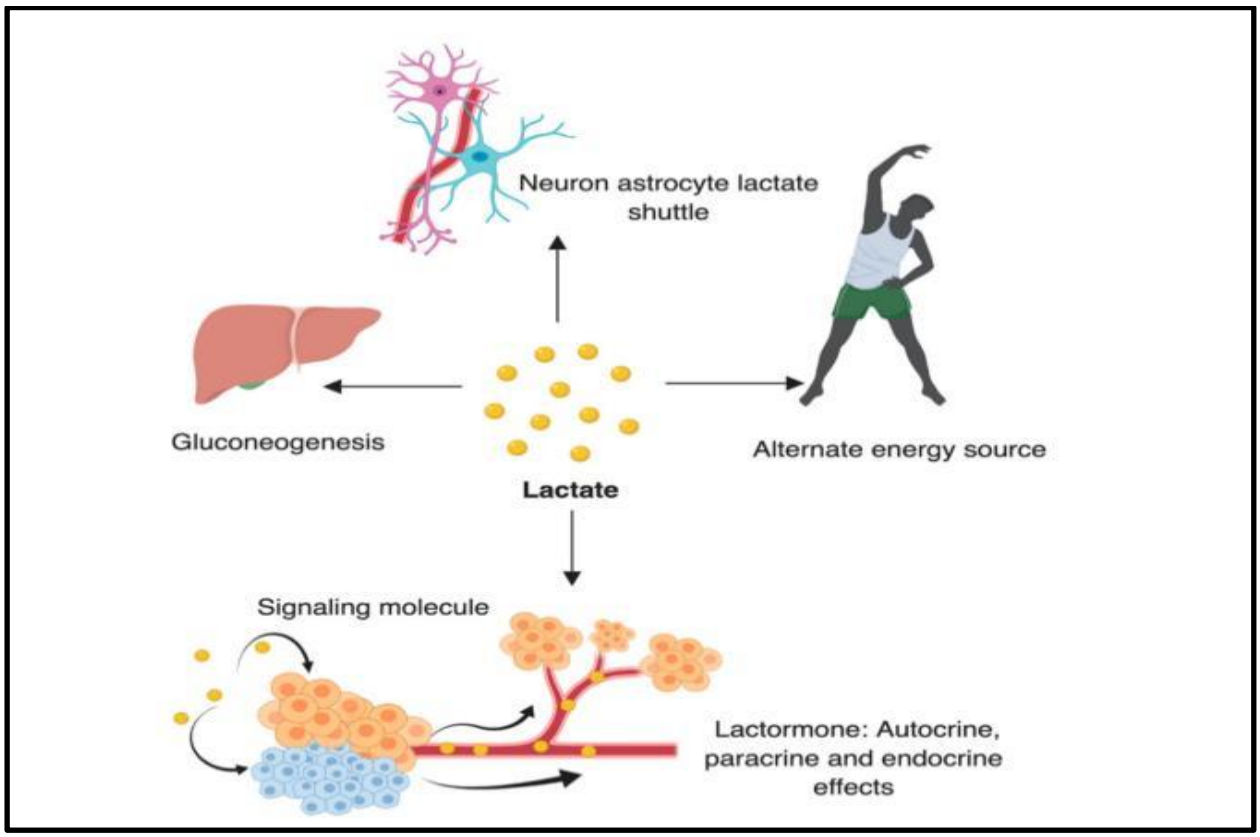

Figure 4.7 Lactate's physiological role in the body. Lactate acts as an alternate fuel in the body during exercise, and acts as an energy source in the brain via the neuron astrocyte lactate shuttle. It is a source of gluconeogenesis and acts as a hormone (lactormone) [**Mishra and Banerjee, 2019**].

Besides normal physiology, oxidative cancer cells can utilise lactate as a fuel source. Lactate is produced in glycolytic cancer cells and excreted into the microenvironment and can be taken up by oxidative cancer cells (**Fig. 4.8**). Brisson et al. reported that LDHB silencing can inhbit cell proliferation in both glycolytic and oxidative cancer cells [**Brissson et al., 2016**]. Therefore, targeting LDHB might have potential as an anticancer approach.

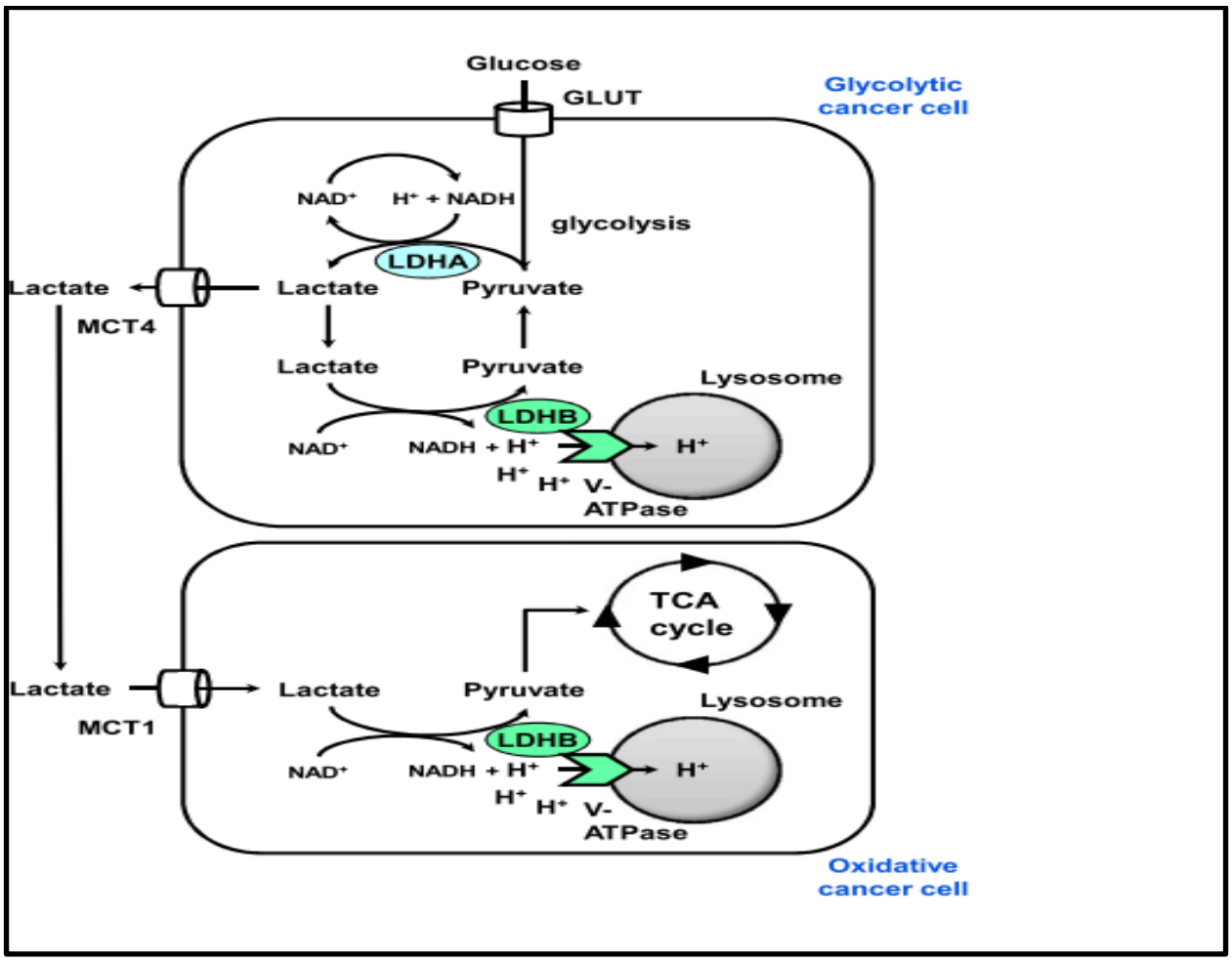

Figure 4.8 Lactate shuttle between glycolytic and oxidative cancer cells. Lactate is not freely transported across the cell membrane, therefore it requires transporter for delivery. Monocarboxylate transporter 4 plays an important role in cellular export, while MCT1 is involved in uptake of lactate [**Brisson et al., 2016**].

4.7 2-Deoxy-D-Glucose

2-Deoxy-D-Glucose (2-DG) is a glucose analogue. It inhibits the hexokinase 2 enzyme and thus blocks glycolysis (**Fig. 4.9**). Inhibition of glycolysis may exhibit greater toxicity on cancer cells, especially cancer cells which are glycolysis dependent for energy generation. We hypothesised that LDHB positive cell lines could catalyse the conversion of lactate to pyruvate, and then pyruvate could subsequently enter into the tricarboxylic cycle (TCA) or OXPHOS to allow the generation of ATP independent of glycolysis. Thus, cells expressing LDHB may be less sensitive to 2-DG-mediated glycolysis inhibition.

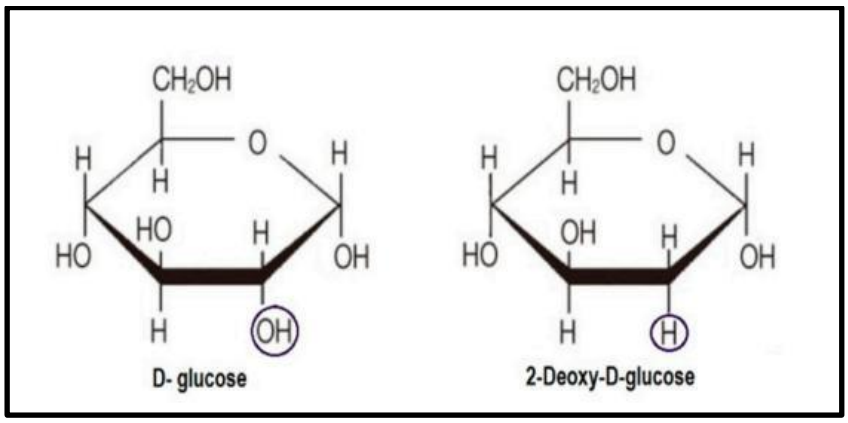

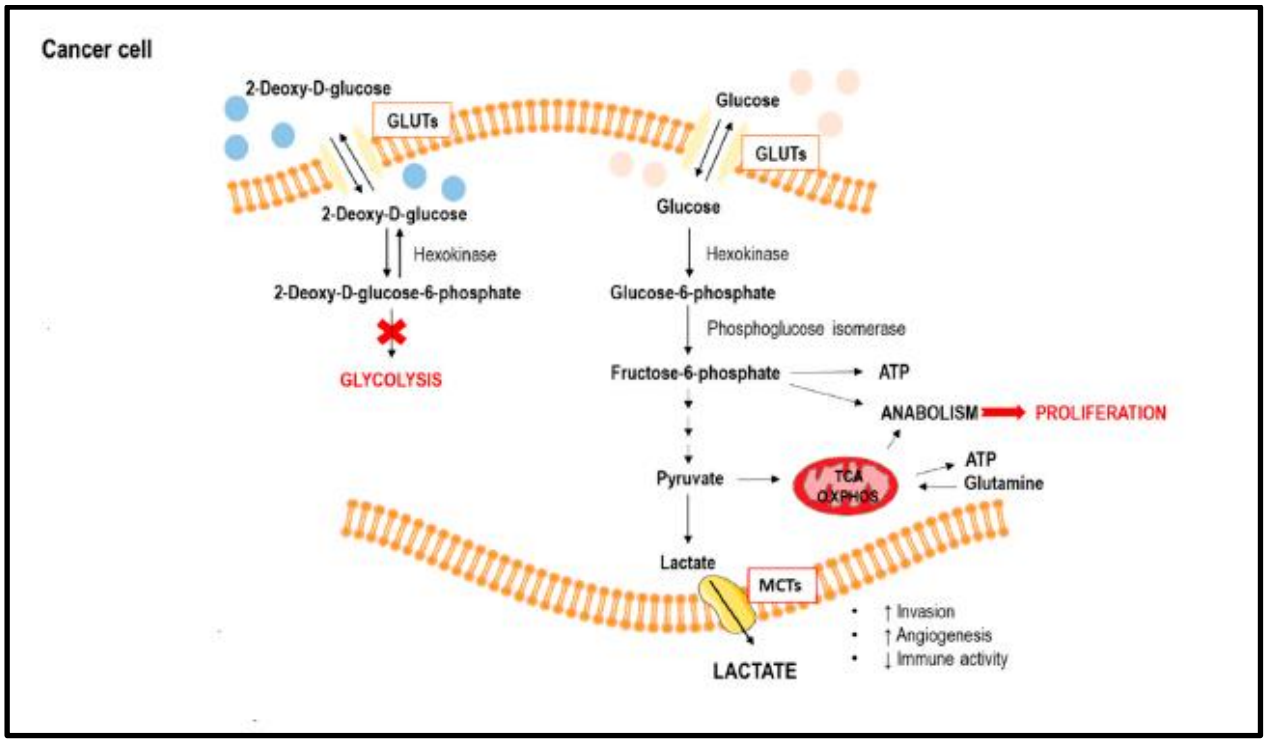

Figure 4.9 The schematic illustration depicts the molecular structure of D-glucose, 2-DG, and the mechanism of 2-DG. In normal glycolysis, glucose is metablolised into lactate, and lactate is excreted from cells by monocarboxylate transporters (MCTs). Both glucose and 2-DG are taken up into the cell by the same glucose transporters (GLUTs) [**Pajak et al., 2020**].

4.8 Metformin

Metformin (1,1-dimethylbiguanide) is a first-line drug for type 2 diabetes mellitus (insulin independent) and was first reported as a treatment for diabetes in 1957 [**Cantoria et al., 2014; Bailey, 2017**]. Metformin is a biguanide derivative that comprises of two molecules of guanidine linked by a nitrogen atom (**Fig. 4.10**).

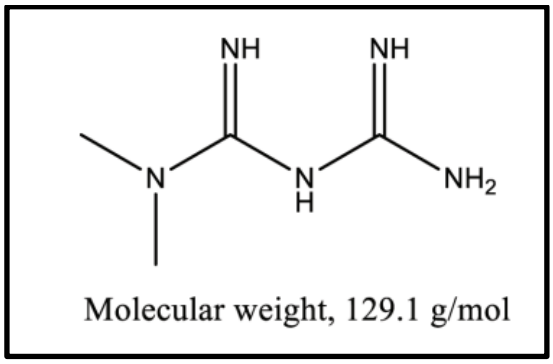

Figure 4.10 The chemical structure of metformin. Metformin is a small molecule drug with a molecular weight of 129.1 g/mol [**Adegbola et al., 2017**].

Metformin enters cells via the organic cation transporter 1 (OCT1) and inhibits the mitochondrial respiratory chain complex 1, resulting in the inhibition of ATP production. As a result, cell growth is halted, apoptosis is induced, and autophagy is activated (**Fig. 4.11**) [**Cerezo et al., 2014; Zhao et al., 2020**].

We hypothesised that LDHB positive cell lines may be more dependent on OXPHOS and so more effected by metformin (LDHB negative lines may have very low levels of OXPHOS and so blocking it may have comparatively little effect).

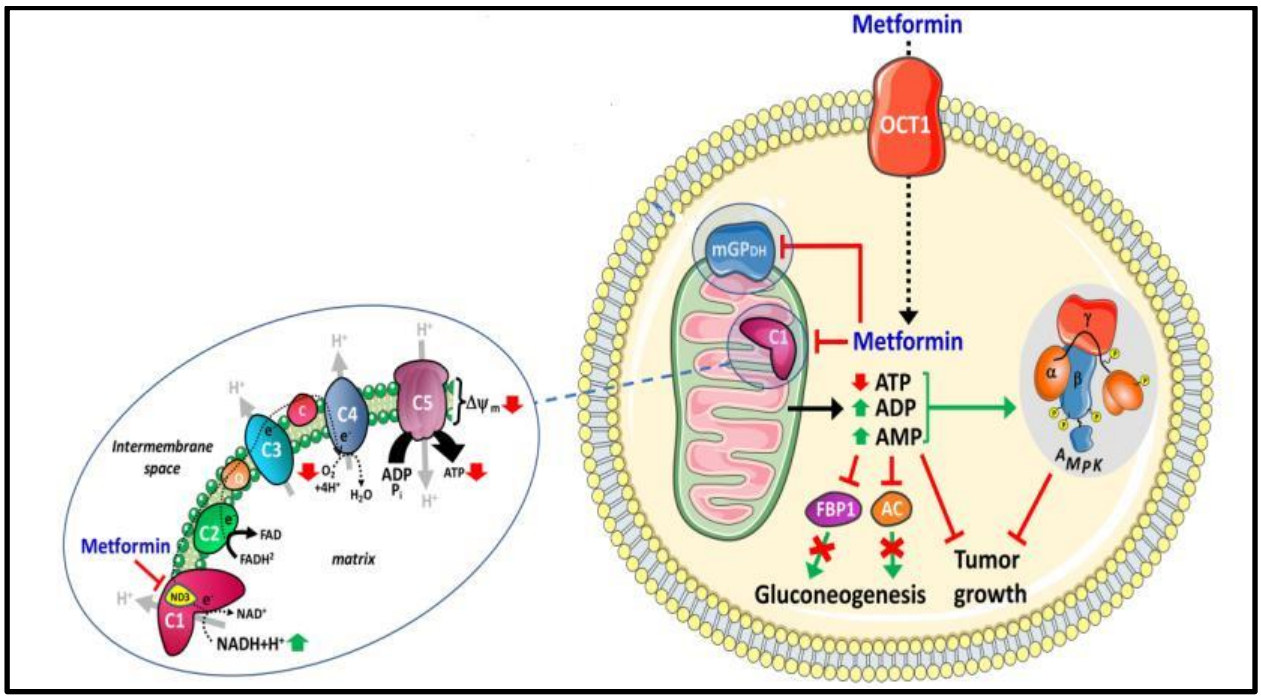

Figure 4.11 The mechanism of action of metformin. Metformin is uptake into the cell via organic cation transporter 1 (OCT1). The respiratory-chain complex 1 in the inner membrane of the mitochondria is then inhibited, resulting in decreased adenosine triphosphate (ATP) production while adenosine diphosphate (ADP) and adenosine monophosphate (AMP) are stimulated. These could be able to suppress gluconeogenesis and tumour growth [**Vial et al., 2019**].

4.9 Chapter aims

4.9.1 To explore LDHB expression in HCC cell lines.

4.9.2 To investigate the impact of inhibition of LDH in HCC cell lines and its dependence on LDH expression levels.

4.9.3 Analysis of the impact of LDHB status on sensitivity of HCC-related cell lines to glycolysis inhibitor 2-DG and the oxidative phosphorylation inhibitor metformin.

4.9.4 Evaluation of the impact of LDHB status on sensitivity of HCC cell lines to treatment with the combination of 2-DG and metformin.

4.9.5 Evaluation of the impact of physiological levels of potential alternative energy sources on response to metabolic inhibitors.

4.10 Results

4.10.1 Expression of LDHB at protein level in the HCC-related cell lines

LDHB expression at the mRNA level was shown in the previous chapter, demonstrating three strongly positive cell lines (SNU182, SKHep1, HHL5), one intermediate positive cell line (PLC/PRF5), and very low expression cell lines (Huh-7 and HepG2) (**see Fig. 3.4B of Chapter III**). Western blotting was then performed to evaluate LHDB protein expression. This revealed high LDHB protein level in SK-Hep1, HHL5 and SNU182 while Huh-7, HepG2 and PLC/PRF-5 showed a very minimal protein level (**Fig. 4.12**). LDHB protein levels in the cell lines were largely consistent with the transcript levels (**see Fig. 3.4B of Chapter III)** except for PLC/PRF-5. PLC/PRF-5 is positive for LDHB at the transcript level (and is thus identified as a group 2 HCC cell line) but LDHB protein expression is almost absent (equivalent to non-group 2 HCC cell lines with undetectable LDHB transcript expression). Since protein is essential for functional impact, in terms of studying the influence of LDHB status on cell lines sensitivity to metabolic interventions, we classified our cell lines into 2 groups: LDHB positive (SNU182, SK-Hep1, HHL5) and LDHB low/negative (Huh-7, HepG2 and PLC/PRF-5). The high level of mRNA but low protein level in PLC/PRF5 suggests that either the mRNA is inefficiently translated or that the LDHB protein is degraded due to post-translational modification in this cell line.

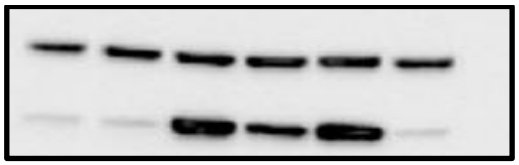

Figure 4.12 LDHB protein expression by western blotting. Protein was extracted using SDS lysis buffer for the respective cell lines. 50 µg of total protein was loaded onto 4-15% gel (Biorad) and probed with antibodies against LDHB and tubulin (as a protein loading control). Picture was taken under luminescent mode (ChemiDoc™ MP Imaging System, Biorad).

4.10.2 Analysis of impact of GNE-140 (LDH inhibitor) on HCC-related cell lines

GNE-140 is a potent LDHA and LDHB inhibitor, having IC50 values of 3 and 5 nM, respectively [**https://www.medchemexpress.com/_R__GNE-140.html**]. Since a specific LDHB inhibitor is not available, we have investigated the effect of this inhibitor within this project to determine whether high LDHB expressing cell lines are more sensitive to this inhibitor than the low LDHB expressing cell lines.

Overall, GNE-140 exhibited relatively low potency against HCC cell lines, and non-HCC cell lines, with little evidence of reduced cell numbers in any of the cell lines except which using higher doses of the drug (25 μM or higher). There was some evidence of sensitivity related to LDHB expression (**see western blot, Fig. 4.12**), as the LDHB positive cell lines HHL5 (**Fig. 4.13A**) and SK-Hep1 (**Fig. 4.13B**) were the most sensitive to the drug. However, while SNU182 (**Fig. 4.13C**) was more sensitive than the other LDHB negative subgroup 2 cell lines (PLC/PRF-5, **Fig. 4.13D**), it was less sensitive than the other two HCC cell lines HepG2 **(Fig. 4.13E**) and Huh-7 **(Fig. 4.13F**). Thus, overall, there was no clear evidence of LDHB-related sensitivities to the inhibitor, particularly in HCC cell lines.

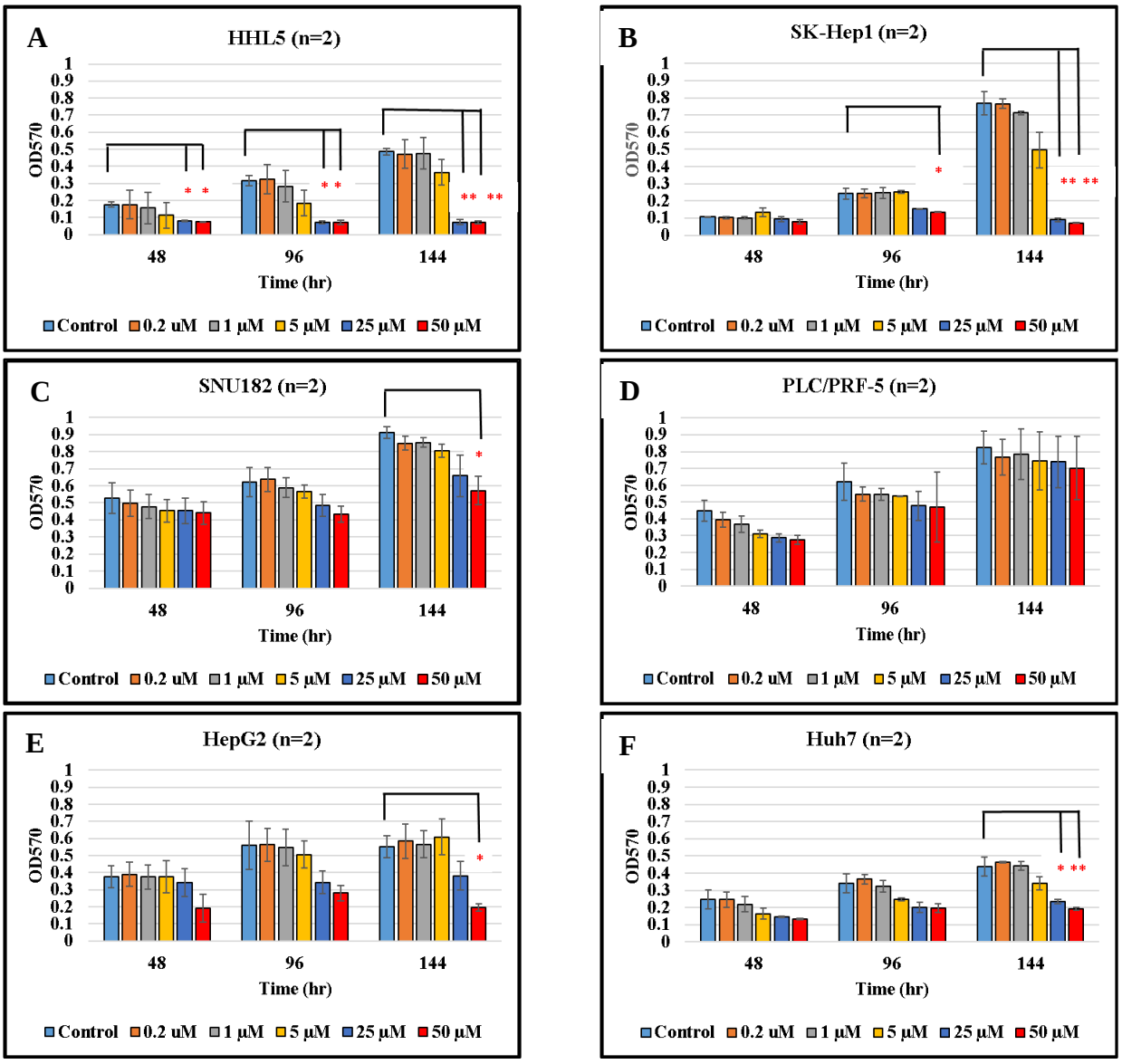

Figure 4.13 The GNE-140 sensitivity to HCC and non-HCC cells. The MTT assay was used to investigate cell proliferation outcomes after 48, 96, and 164 hrs of LDH inhibitor GNE-140 exposure (0-50 µM). The results shown are mean ± SD. *P<0.05. **P<0.005. N=2 of independent studied.

The CellTox™ cytotoxicity assay was used to determine whether the reduction in cell proliferation after exposure to the drug was due to induction of cell death (as opposed to being cytostatic). The data revealed that the inhibitor did not exert a cytotoxic effect to any of the cell lines, even at the highest dose at 50 µM (**bar graph, Fig 4.14**), where there was a clear reduction in cell numbers in the MTT assay (**see Fig. 4.13**). Simultaneously, the RealTime-Glo™ MT cell viability assay (**green line graph, Fig. 4.14**) was used to measure viable cells

at the end of the incubation period. The data revealed that the cytostatic effect was clearly seen in HCC not-subgroup 2 HepG2 and Huh-7 and non-HCC subgroup SK-Hep1 and HHL5 cell lines while it showed minimal effect to HCC subgroup 2 SNU182 and PLC/PRF-5.

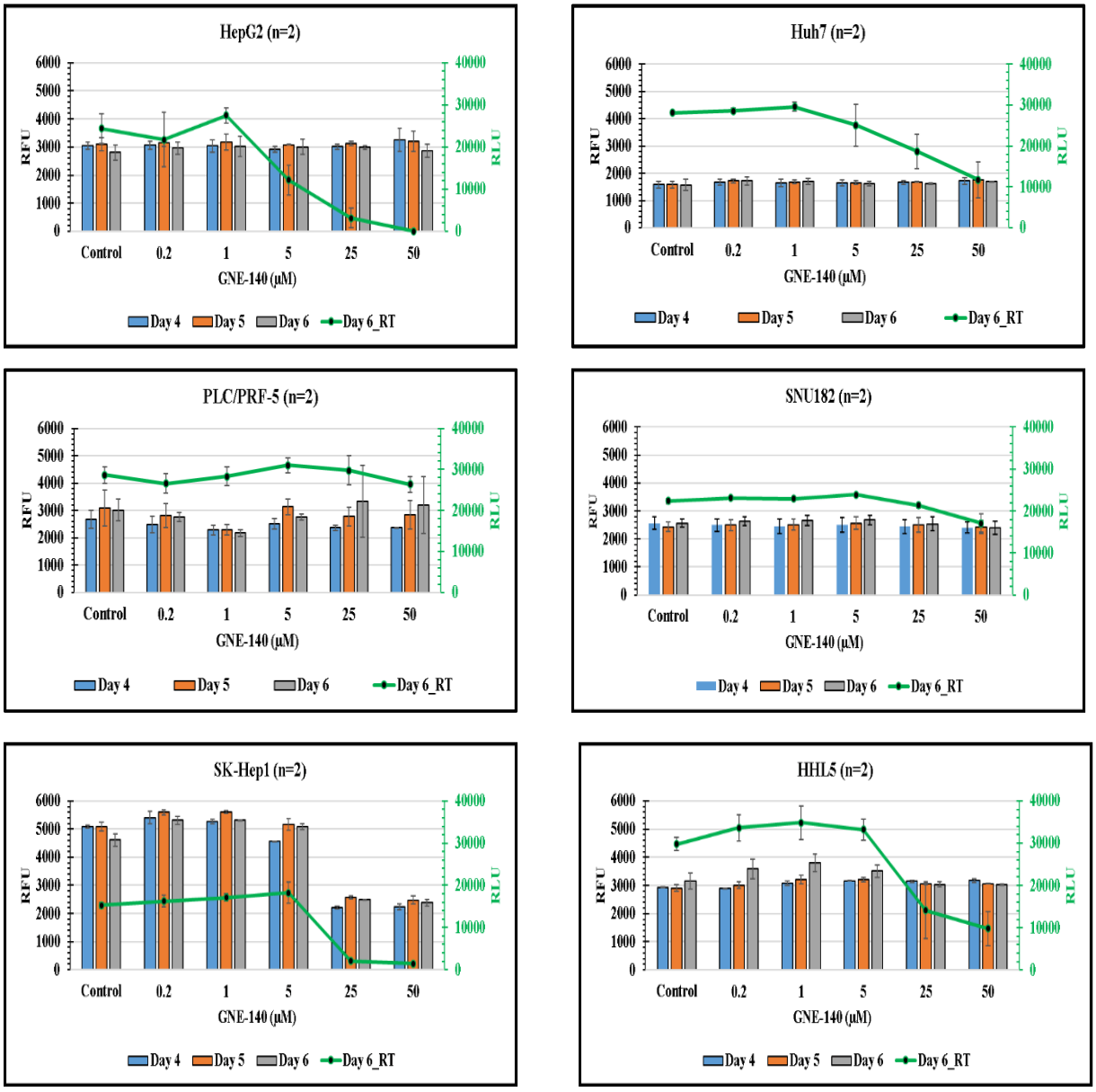

Figure 4.14 The effect of GNE-140 on cell cytotoxicity and cell viability assay. The toxicity of GNE-140 was determined by CellTox™ cytotoxicity (**bar graph**, 0.125 µl reagent: 1,000 µl medium, added 25µl/well). The RFU was measured from 4-6 days of treatment. After RFU measurement on day 6, the cell viability was investigated by adding the RealTime-Glo™ MT assay (**green line graph**, 0.25 µl reagents: 1,000 µl medium, added 25 µl/well) for 1 hr. Data are mean ± SD of duplicate, and two independent studies. RFU: relative fluorescent unit. RLU: relative luminescent unit. RT: RealTime-Glo™ MT cell viability assay.

A comparison of LDHB status and GNE-140 shows that there is no clear link between GNE-140 sensitivity (IC50) and LDHB expression in all cell lines (**Table 4.1**).

Table 4.1 The correlation between GNE-140 sensitivity (expressed in IC50) determined by MTT assay and LDHB expression from western blot.

Cell lines	IC50 (μM)	LDHB status
HepG2	26.55±0.53	+/-
Huh-7	10.73±6.08	+/-
PLC/PRF-5	>50	+/-
SNU182	>50	+++
SK-Hep1	7.70±3.51	+++
HHL5	6.02±0.41	+++

4.10.3 Analysis of the impact of LDHB status on sensitivity of HCC-related cell lines to glycolysis inhibitor 2-DG

Despite the fact that glycolysis is significantly increased in many tumours, therapeutic targeting of glycolysis in cancer patients has not yet been successful, possibly due to tumour cells' metabolic plasticity. Hence, we hypothesised that LDHB positive cell lines may be more able to utilise lactate as an alternative source of energy and thus may be more resistant to the glycolytic inhibitor 2-DG.

HCC cell lines were treated with varying concentrations of 2-DG depending on the sensitivity of each cell line to the drug and assessed to determine if sensitivity was associated with LDHB expression. **Fig. 4.15** illustrates 2-DG sensitivity in HCC and non-HCC cell lines at different dosages. This result shows that there was evidence of a difference in sensitivity related to LDHB expression (**Table 4.2**). The low LDHB expression (**Group A**; HepG2, Huh-7, and PLC/PRF-5) exhibited a greater IC50 than the high LDHB expression (**Group B**; SNU182, SK-Hep1, and HHL5). This difference, however, was not statistically significant (p value = 0.10), although this may be partly reflective of the small sample size. Thus, the results do not rule out the possibility that LDHB-low-expressing cell lines may be more resistant to 2-DG. However, the results do argue against the hypothesis that LDHB expression would allow a bypass of glycolysis and thus increase 2-DG resistance.

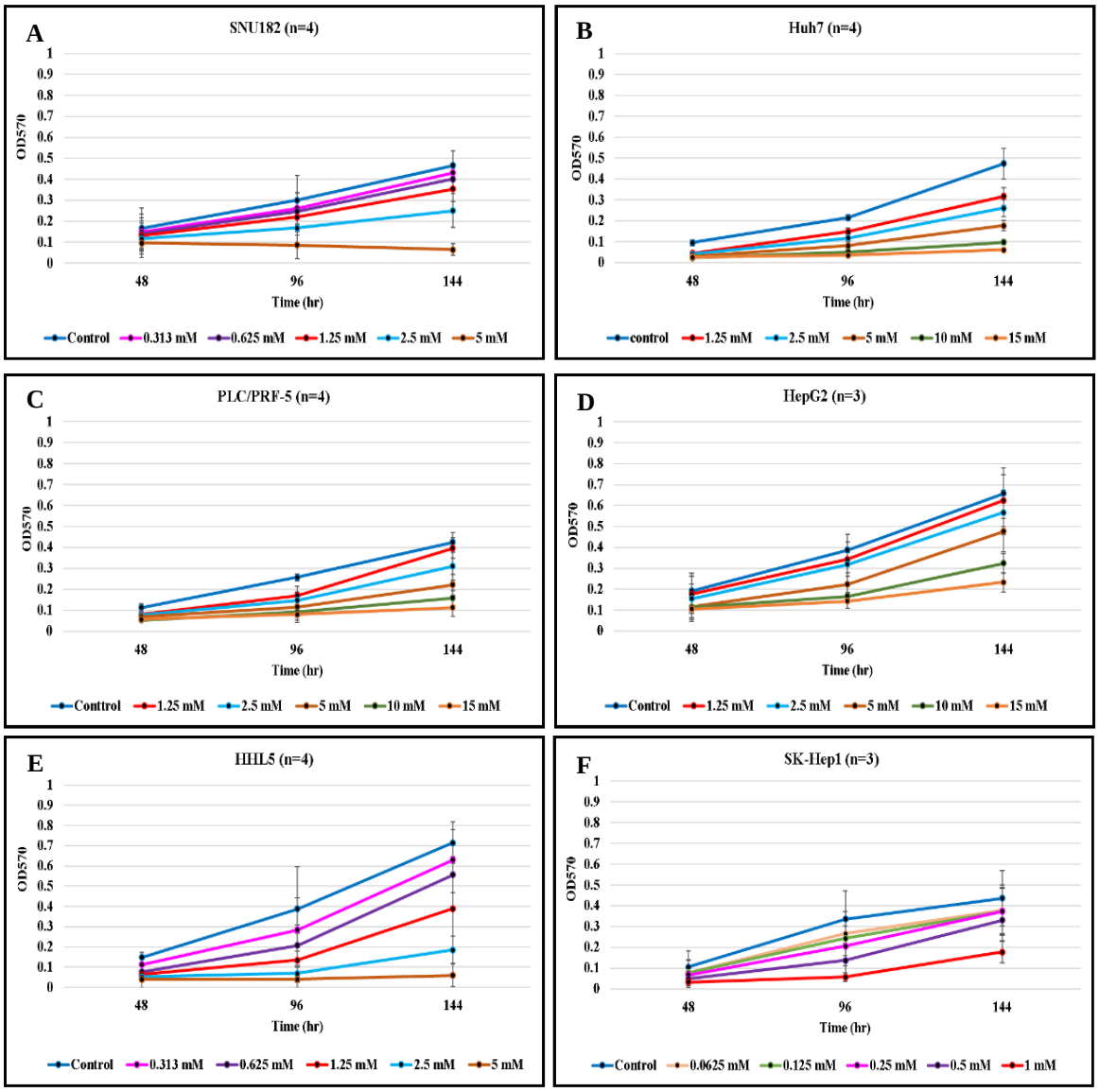

Figure 4.15 Influence of 2-DG on the proliferation of HCC cell lines evaluated by MTT assay. Cells were exposed to 2-DG to a maximum dose of 1 mM (SK-Hep1), 5 mM (SNU-182, HHL5), or 15 mM (Huh-7, PLC/PRF-5, HepG2) and the MTT assay was performed at 48, 96 and 144 hrs after treatment. Graphs represent growth curves of indicated cell lines under different treatment conditions estimated by MTT assay. Because each cell line's sensitivity to the inhibitor varies, the maximum doses were for SK-Hep1 (1 mM), SNU182 and HHL5 (both 5 mM), and HepG2, Huh-7, PLC/PRF (15 mM). Values are mean ± SD of 3-4 independent experiments.

Table 4.2 The IC50 of 2-DG on HCC and non-HCC cell lines determined by MTT assay.

Cell line	IC50 (mM)	Mean IC50 (mM)	LDHB status	P value	Significance between 2 groups	N
HepG2	9.77 ± 1.30	Group A				3
Huh-7	3.09±0.99	6.04±3.41	+/-			4
PLC/PRF-5	5.26 ±1.81			0.1000	No	4
SNU182	2.69 ±0.57	Group B				4
SK-Hep1	0.91 ± 0.05	1.67±0.92	+++			3
HHL5	1.42 ± 0.16					4

The IC50 are calculated from GraphPad Prism 6.
Data are shown as mean ± SD of 3-8 independent studied. Statistic was calculated from t-Test: two-sample assuming equal variances.

The sensitivity of 2-DG on HCC and non-HCC cell lines was further evaluated by IncuCyte®. This system is label-free and collects real-time kinetic data by assessing the surface area occupied by cells during cell proliferation. This study found that 5 mM 2-DG showed the most harmful to SNU182 (high LDHB expression) by stopping cell proliferation at the beginning of treatment (**Fig. 4.16A**), whereas other high LDHB expression (SK-Hep1 (**Fig. 4.16B**), and HHL5 (**Fig. 4.16C**) showed lower sensitivity. PLC/PRF-5 (low LDHB expression) was the most resistant to this inhibitor (**Fig. 4.16D**) than Huh-7 (**Fig. 4.16E**), and HepG2 (**Fig. 4.16F**), respectively. The sensitivity of all cell lines to 5 mM 2-DG is shown in **Fig. 4.16G**, demonstrating that there is no obvious association between sensitivity and LDHB expression, which is consistent with earlier results.

High LDHB expression cell lines (SNU182, SK-Hep1, and HHL5)

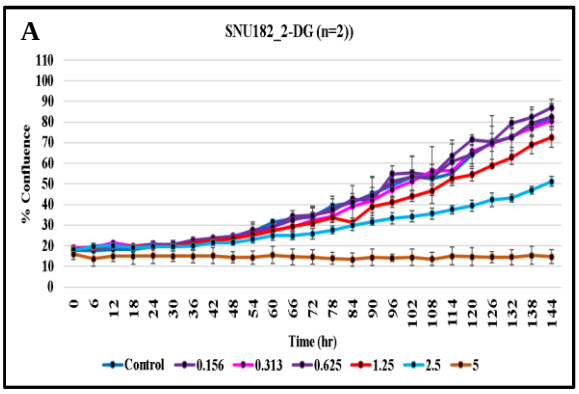

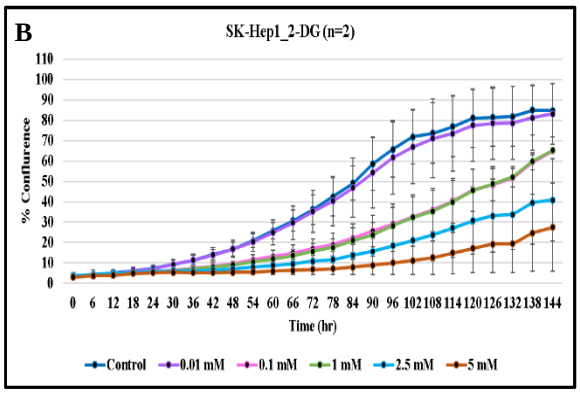

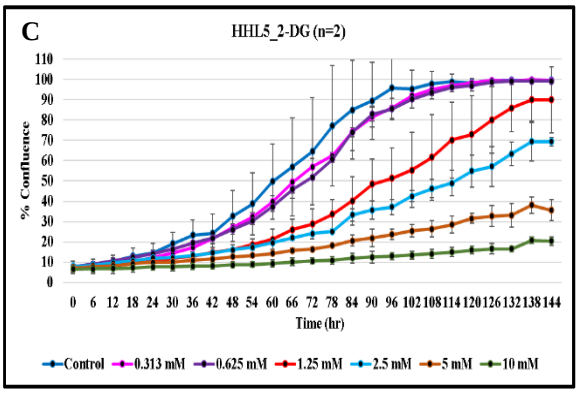

Low/negative LDHB expression cell lines (HepG2, Huh-7, and PLC/PRF-5)

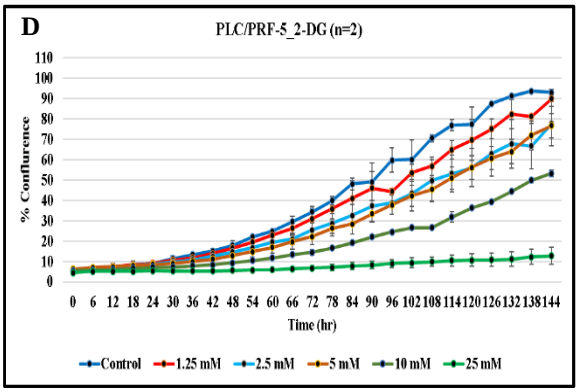

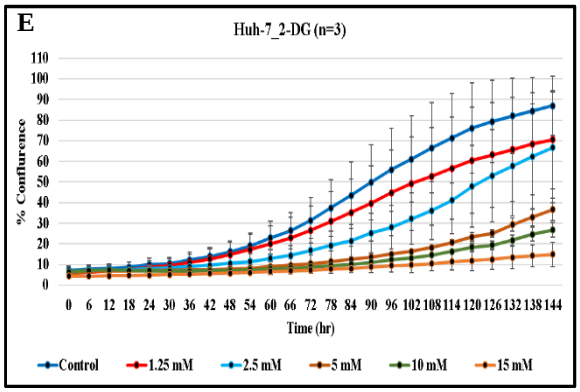

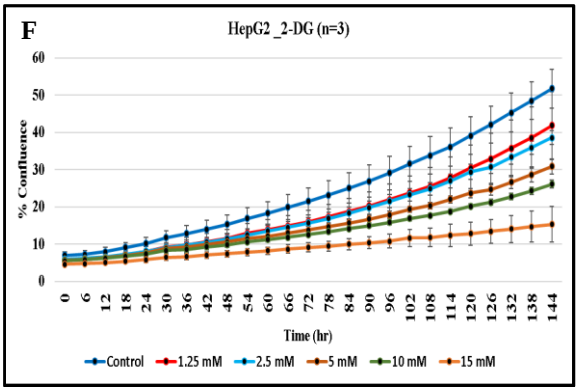

Effect of 5 mM 2-DG on HCC and non-HCC cell lines

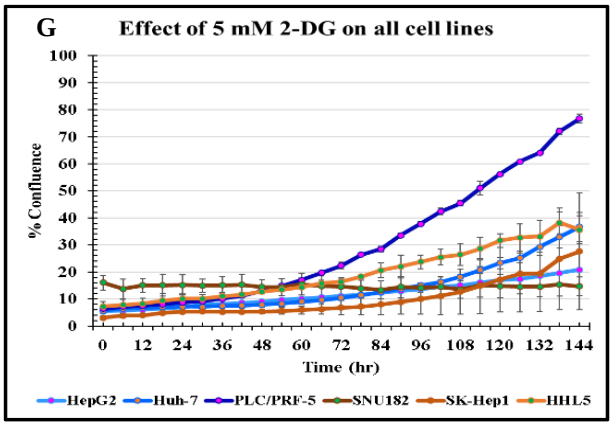

Figure 4.16 The sensitivity to 5 mM 2-DG in HCC and non-HCC cell lines assessed by IncuCyte®. The images were automated taken from four fields imaged/well of 96-well plate, under 10x magnification for every six hrs up to 144 hrs. The percent confluence was calculated automatically at each time point using Incucyte software. Data are mean ± SE of 2-3 independent studied.

4.10.4 Analysis the influence of LDHB status on sensitivity of HCC cell lines to oxidative phosphorylation inhibitor metformin

Like 2-DG, metformin is also a metabolic inhibitor. However, it blocks ATP generation at a later point through inhibition of mitochondrial complex I in the mitochondrial respiratory chain. The anti-proliferative impact of metformin was tested against HCC cell lines and non-HCC cell line using the SRB assay. The SRB assay was used in preference to the MTT assay, as MTT is metabolised by a mitochondrial enzyme. In addition, metformin could inhibit this reaction without necessarily effecting cell proliferation, causing misleading results.

With the exception of PLC/PRF-5, all HCC cell lines were strongly sensitive to metformin, which decreased cell proliferation at 5 mM (**Fig. 4.17**). At 2.5 mM. The inhibitor proved most toxic to immortalised HHL5, preventing cell growth and proliferation, but SK-Hep1 could continue to proliferate at the highest dosage tested at 25 mM.

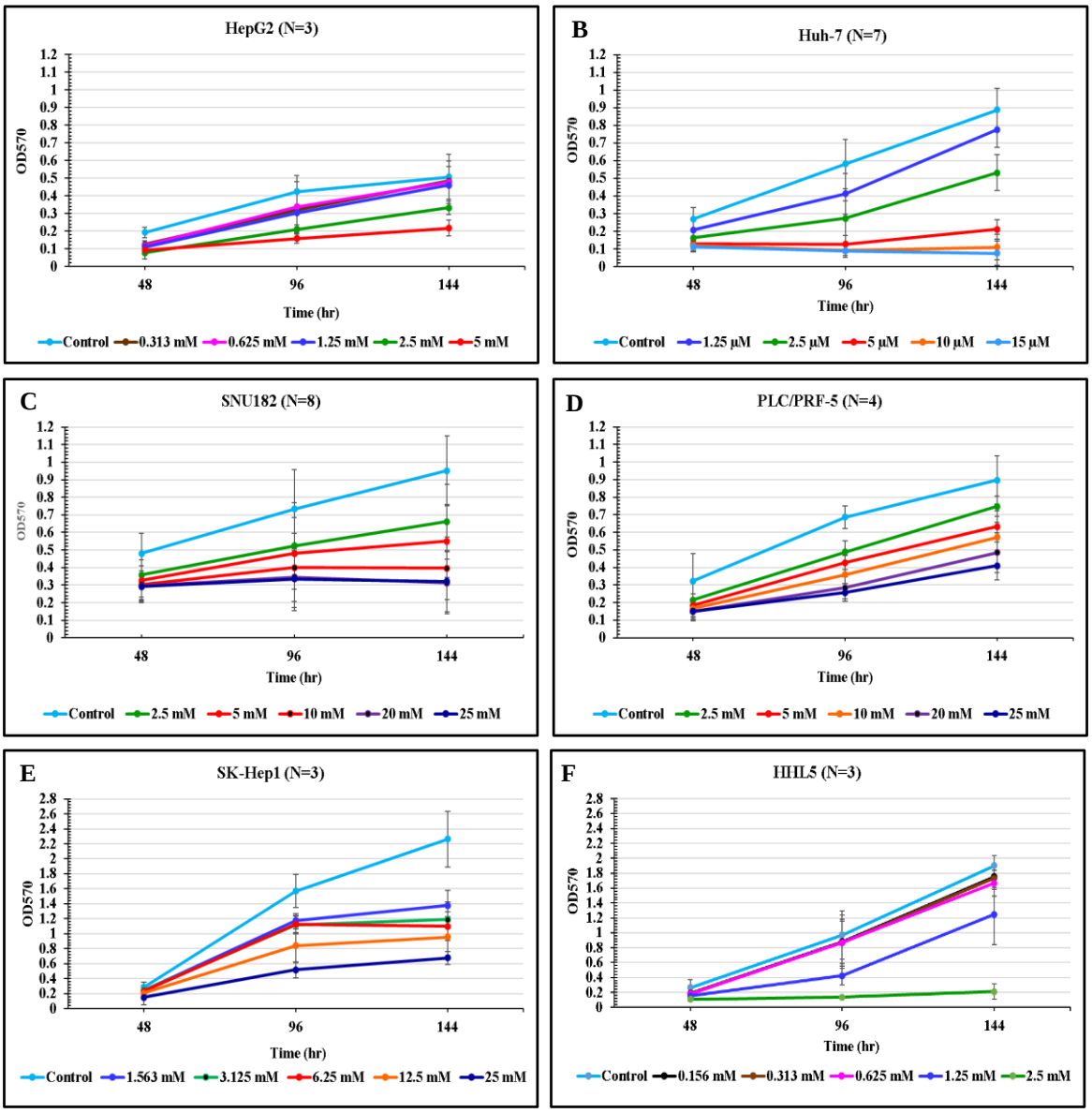

Figure 4.17 The growth-curve of anti-proliferative of metformin on HCC and non-HCC cell lines determined by SRB assay. HCC cells were exposed to metformin to the highest concentration at the concentrations shown. Various concentration ranges were used based on each cell line's response to the drug, which was optimized using Incucyte. Data presents are mean ± SD of at least 3 independents studied. The difference in concentrations used was because of differences in sensitivity of each cell line identified in initial experiments and allowed a clearer determination of doses responses in the individual cell lines.

Again, there was no evidence of a link between metformin sensitivity and LDHB status (p value = 0.434) as shown in **Table 4.3**.

Table 4.3 The IC50 of metformin determined by SRB assay.

Cell line	IC50 (mM)	Mean IC50 (mM)	LDHB status	P value	Significance between 2 groups	N
HepG2	3.69 ± 0.95	Group A				3
Huh-7	3.02 ± 0.50	8.21 ±8.42	+/-			7
PLC/PRF-5	17.93 ± 6.00			0.4340	No	6
SNU182	6.97 ± 3.72	Group B				8
SK-Hep1	2.68 ± 0.59	3.76 ±2.83	+++			3
HHL5	1.62 ± 0.43					3

The IC50 are calculated from GraphPad Prism 6.
Data are shown as mean ± SD of at least three independents studied.
Statistic was calculated from t-Test: two-sample assuming equal variances.

Incucyte was used to test the sensitivity of selected HCC and immortal HHL5 cell lines to metformin in order to confirm the above results. SNU182 (**Fig. 4.18A**) was shown to be more susceptible to metformin than PLC/PRF-5 (**Fig. 4.18B**). 25 mM metformin completely suppressed SNU182 proliferation, but had a much smaller effect on PLC/PRF-5 growth. Metformin inhibited cell growth at 5 mM in HHL5 (**Fig. 4.18C**) which was the most susceptible to this inhibitor than others two HCC cell lines. Thus, the sensitivities of the cell lines in the assay strongly reflected those seen in the SRB assay. Although there was some evidence of increased sensitivity in LDHB expressing cell lines, the increased sensitivity of HHL5 over SNU-182 cells does not support a particular sensitivity related to LDHB expression in HCC cell lines.

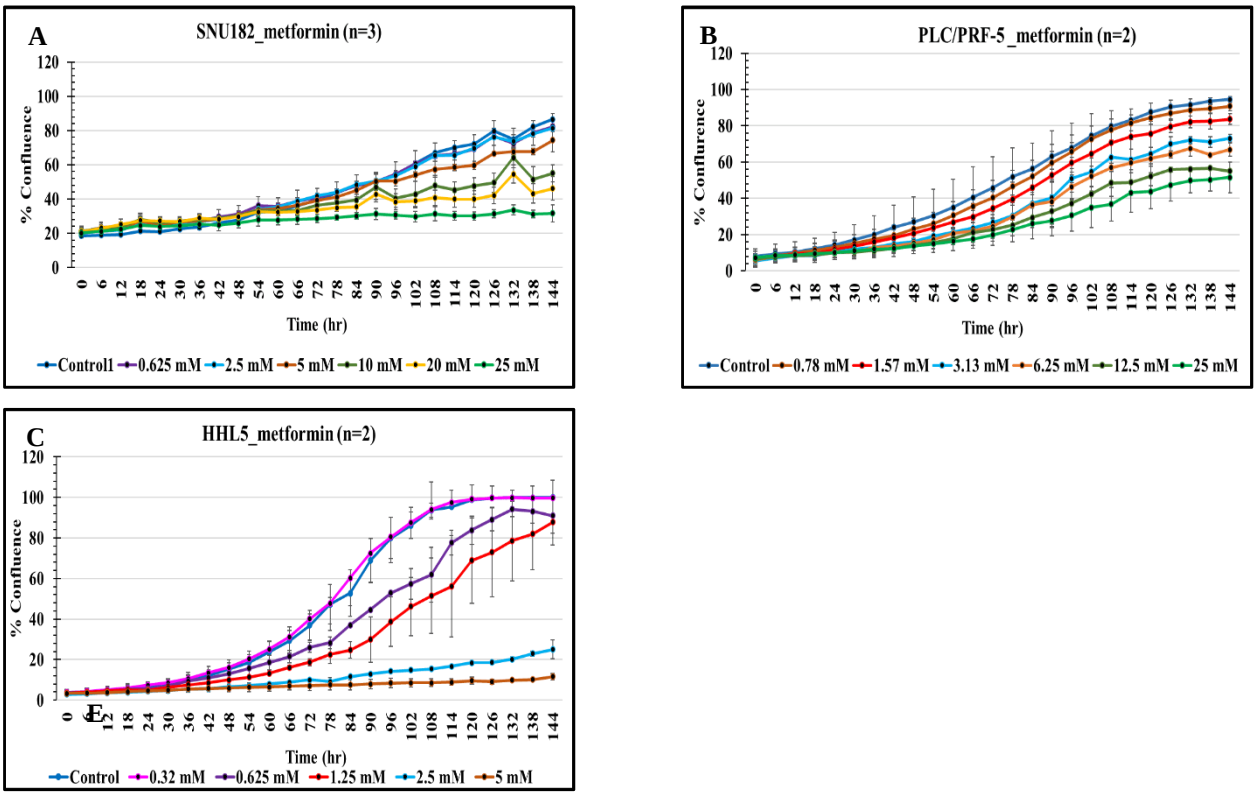

Figure 4.18 The sensitivity of OXPHOS inhibition metformin in HCC and non-HCC cell lines investigated by IncuCyte®. The images were automated taken under 10x objective magnification for every six hrs until reached 144 hrs. The percent confluence was calculated from 2-4 wells of each time point using Incucyte software. Data are mean ± SE of 2-3 independent studied.

4.10.5 Evaluation of LDHB status on sensitivity of HCC cell lines to treatment with the combination of 2-DG and metformin

In this study, any potential synergy between 2-DG and metformin was investigated. To allow assessment of the synergy, HCC and non-HCC cell lines were treated with individual and combinations of both drugs at concentrations of 0, 0.5, 1, 2, and 4 mM (thus giving 25 combinations in total). For four of the cell lines, there was evidence of synergy at multiple dose points, SNU182 (**Fig. 4.19A**), Huh-7 (**Fig. 4.19B**), SK-Hep1 (**Fig. 4.19C**), and HHL5 (**Fig. 4.19D**), while in PLC/PRF-5 there were no dose combinations with significant synergy (**Fig. 4.19E**) (although there did show limited evidence of antagonism) and for HepG2 two combinations gave significant synergy (**Fig. 4.19F**), but this was very limited and the overall pattern did not show reproducible synergy across multiple doses.

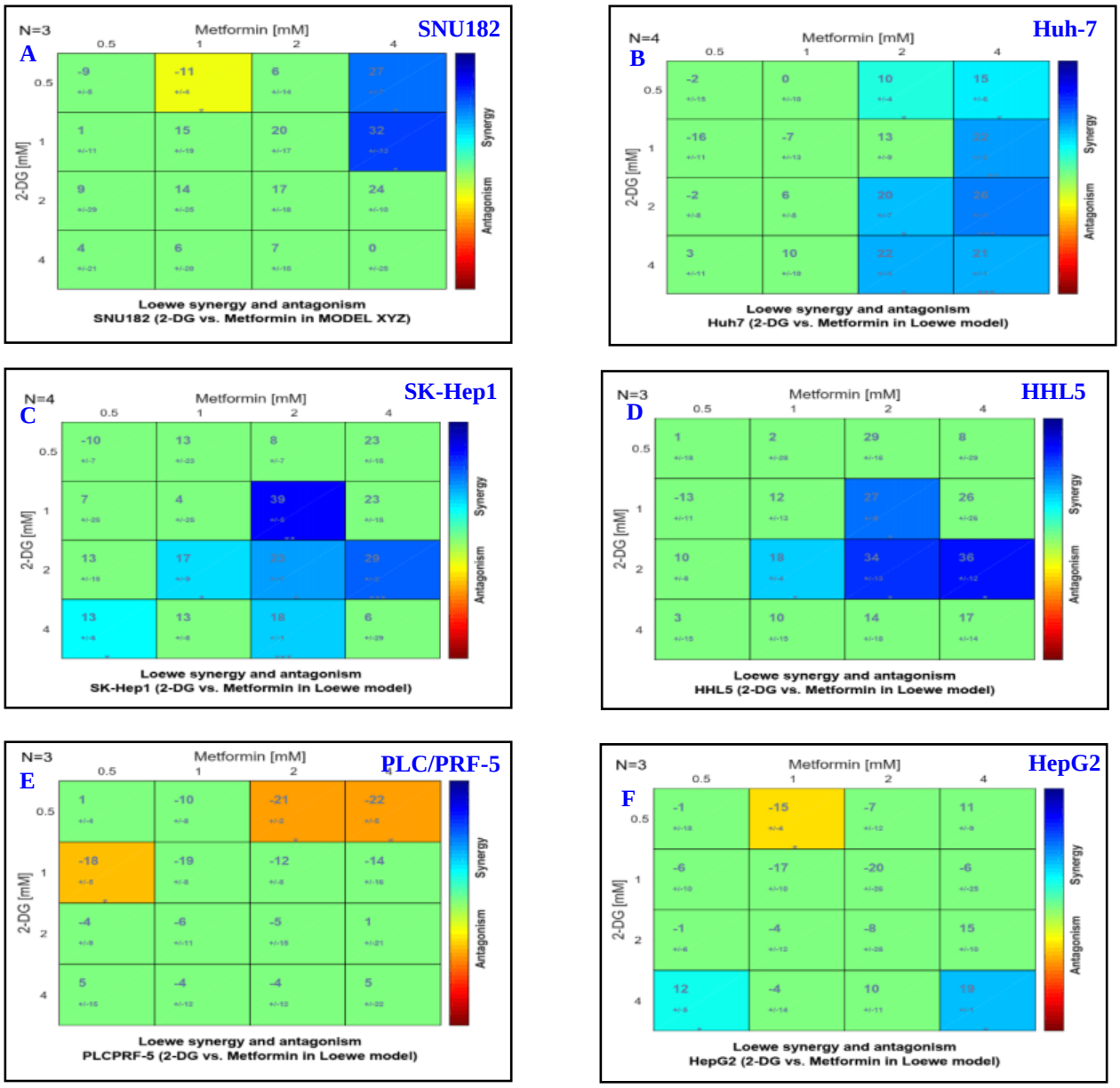

Figure 4.19 Drug synergy interaction of 2-DG and metformin in HCC and non-HCC cell lines evaluated by SRB assay. Drug interactions were investigated after 144 hrs of treatment using the free Combenefit software, specifically with the Loewe model to identify synergy/antagonism in the drugs combination (light/dark blue colour indicate level of synergism whilst yellow/red colour indicate antagonism). The percentage of cytotoxicity SRB assay was calculated from the OD compared with untreated control. Data are mean of % cell cytotoxicity ± SD, summarised from at least three independents studied. *P<0.05. **P<0.005. ***P<0.0005. N=3-4 of independent studied.

4.10.6 Evaluation of LDHB status on sensitivity of HCC cell lines to 2-DG under physiological conditions

A potential confounding factor in this initial analysis is that a number of key metabolites are present at non-physiological concentrations in normal cell growth media. In particular, the media used for growth of the HCC cell lines was approximately 1.78 mM concentration of glutamine. Lactate is not present in the base medium, but will be present in the FBS used to supplement the medium. Although the exact concentration of lactate in FBS has not been reported, we estimated that the media will have about 10 % of normal physiological conditions (as the media has 10 % serum). As glutamine can also be utilised by cells as an alternative energy source, this could mask the potential *in vivo* advantages of expressing LDHB to allow metabolism of lactate as an energy source. The physiological lactate concentration in serum is in the range of 0.5 to 1.5 mM [**Pino and Singh, 2021**]. As a result, lactate was given at a final dose of 1 mM for this experiment. To better reflect the *in vivo* state, the glutamine concentration was lowered to 0.5 mM. When 2-DG was added, we assessed whether LDHB positive cell lines may be able to use supplemented lactate as an energy source to overcome glycolysis inhibition by 2-DG.

To assess whether the 2-DG sensitivity was affected by LDHB status, the six-cell lines were treated with 2-DG in normal medium supplemented with 10 % FBS, 1.78 mM glutamine (hereafter referred to normal medium, **NM**) compared with cultured in 10 % FBS, 0.5 mM glutamine, and 1 mM lactate (hereafter referred to physiological medium, **PM**). Without 2-DG treatment, the cell proliferation of all cell lines was reduced ranging from over 20-70 % in PM compared with NM. While proliferation was reduced in all cell lines, the reduction was high in cell lines with high levels of LDHB expression (SNU182, SK-Hep1, and HHL5, average reduction 65 %) compared with low LDHB expression (HepG2, Huh-7, and PLC/PRF-5, average reduction 39 %) (**Table 4.4**), although this fell just short of statistical significance ($p=0.07$).

Table 4.4 The effect of the mimicing physiological conditions on HCC and non-HCC cell lines investigated by MTT assay.

Cell lines	OD570 at 144 hrs		% Cell proliferation reduction (NM vs PM)	% Average (NM vs PM)	P value	LDHB expression	N
	NM	PM					
HepG2	0.75±0.10	0.32±0.06	56.65	39.49		+/-	2
Huh-7	0.63±0.07	0.5±0.08	21.04		0.07	+/-	2
PLC/PRF-5	0.45±0.10	0.27±0.07	40.77			+/-	2
SNU182	0.60±0.17	0.17±0.06	71.43	65.40		+++	2
SK-Hep1	0.47±0.01	0.18±0.02	61.77			+++	2
HHL5	0.56±0.02	0.21±0.02	63.00			+++	3

MTT assay was measured after 144 hrs post treatment.
Percentage of cell proliferation reduction was calculated by $\{((OD_{NM}-OD_{PM})/OD_{NM})\}$ x100.
Data are representing mean ± SD of 2-3 independent experiments.
NM: normal medium (10% FBS, 1.78 mM glutamine). PM: physiological medium (10% FBS, 0.5 mM glutamine, 1 mM supplemented lactate).

In the parallel, the cell proliferation was performed by fixing the concentrations of 2-DG at 2.5 and 10 mM under NM and PM conditions before MTT analysis. The result of four HCC cell lines (HepG2, Huh-7, PLC/PRF-5, and SNU182) showed that alterations in sensitivity in the different media preparations was restricted to HepG2 (**Fig. 4.20**), where a slight increase in sensitivity was seen in the PM media. In non-HCC subgroup, HHL5 illustrated high sensitivity to both 2 and 10 mM 2-DG, with no difference evident between the NM and PM media. Due to highly toxicity to the non-HCC SK-Hep1 cells, the 2-DG concentrations for this cell line were reduced to 0.5 and 1.0 mM. But again, sensitivity to 2-DG was broadly similar in the NM and PM media.

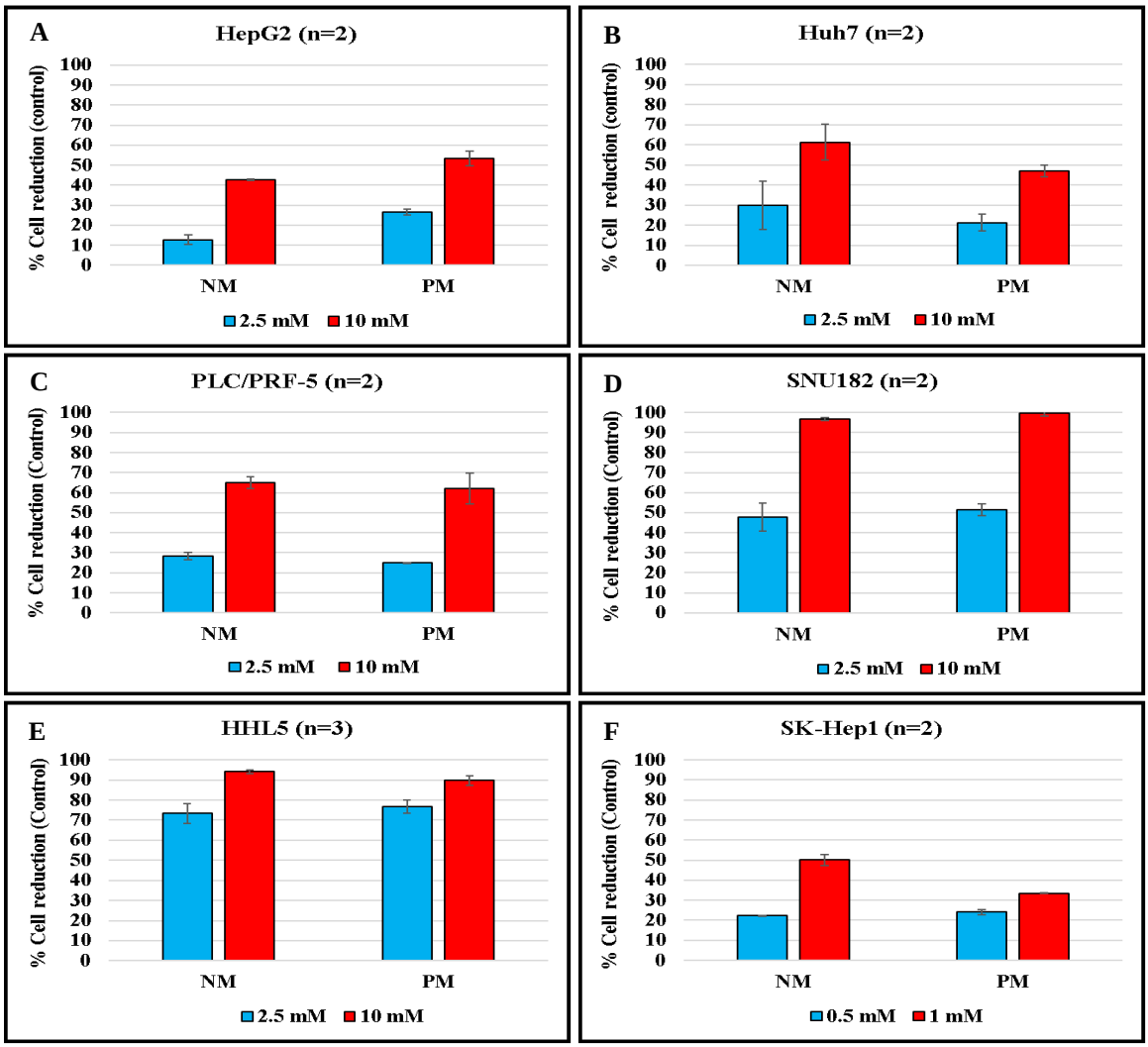

Figure 4.20 MTT assay estimates the sensitivity of HCC and non-HCC cell lines to the glycolysis inhibitor 2-DG under normal and physiological conditions. The percentage of cell reduction was calculated from the treated group compared with the untreated control group of each medium (NM or PM). Percentage of cell proliferation reduction was calculated by {((OD$_{NM}$-OD$_{PM}$)/OD$_{NM}$)} x100. Data are mean ± SD of 2-3 of independent studied.

4.11 Discussion

Although there are several LDH inhibitors that have been studied, many exhibit low potency and off-target effects [**Doherty and Cleveland, 2013; Feichtinger and Lang, 2019**]. On the other hand, some high potency LDH inhibitors (FX11, galloflavin) and RNA interference have been reported. However, to date, none have been approved for clinical use [**Rani and Kumar, 2017**]. Ždralević and co-worker reported that GNE-140 could not inhibit tumour after administered alone or combination with phenformin *in vivo* **[Ždralević et al, 2018].** Data from this study revealed that at HCC cell lines were less sensitive to this inhibitor. At the highest dose of GNE-140 at 50 µM, the drug showed antiproliferative activity (**green line graph, Fig. 4.14**) rather than cytotoxic to the cells (**bar graph, Fig. 4.14**). The effect of GNE-140 showed low potency against HCC cell lines (PLC/PRF-5, and SNU182), or moderate effect to HCC cell lines (HepG2, and Huh-7). This inhibitor also showed high toxicity to non-HCC subgroup SK-Hep1 and immortalised HHL5 (**see IC50 in Table 1**). The HCC subgroup 2 SNU182 cell line was highly sensitive to both glycolysis inhibitor 2-DG (**see IC50 in Table 4.2**) and OXPHOS inhibitor metformin (**see IC50 in Table 3**), but highly resistant to GNE-140 (IC50 > 50 mM, **see Table 4.1**). This line appears to rely on both energy generation pathways, and high LDHB enzyme expression resulted in resistance to the LDH inhibitors GNE-140. In contrast, another HCC subgroup 2 PLC/PRF-5 was sensitive to 2-DG (**see IC50 in Table 4. 2**) but resistant to metformin (**see IC50 in Table 4.3**) and GNE-140 (IC50 > 50 mM, **see Table 4.1**). We investigated the effect of mimicing physiological conditions of lactate and glutamine by supplemented them in medium at 1 and 0.5 mM, respectively. However, the proliferation of all cell lines reduced dramatically (after switching from NM to PM without drug treatment) especially in high LDHB status cell lines, which makes interpretation of the results more challenging (**see Table 4.4**). We have further investigated by adding 2 mM 2-DG to inhibit glycolysis and cultured in NM or PM. The cell proliferation pattern of HepG2 was reduced significantly in PM compared with NM whilst other cell lines did not definitely change. On the other hand, after increasing the dose of 2-DG to 10 mM, the proliferation of SK-Hep1 increase in PM (**see Fig. 4.20**).

Thus, there is no correlation between LDHB status and sensitivity of HCC cell lines to 2-DG in the mimicing physiological conditions.

4.12 Limitations and Future directions

4.12.1 GNE-140 has been reported to inhibit LDHA, LDHB, and LDHC in MDA-MB-231 cells [**Mazzio et al., 2021**]. At 50 μM, this compound was hazardous to all HCC cell lines except PLC/PRF-5 (**see green line in Fig. 4.14**). In addition, this inhibitor showed strong effect on immortalised HHL5 as well. Thus, a potent and selective LDHB inhibitor is needed to further evaluate the effects of LDHB inhibition.

4.12.2 A specific LDHB inhibitor was not available on the market at the time of this study. As a result, we were unable to conduct this experiment with a small molecule that inhibits LDHB specifically. However, the first potent LDHB inhibitor, AXKO-0046 was first published in 2021 [**Shibata et al., 2021**]. It would be useful to investigate the impact of this specific LDHB inhibitor in the HCC cell lines to more thoroughly assess the impact of specific loss of LDHB function. Furthermore, targeted LDHB inhibition by a specific LDHB inhibitor could be used to prove the SLG.

4.12.3 We did not perform siRNA *LDHB* gene knockdown because of limited time. However, knocking down of the *LDHB* gene should be further investigated in HCC subgroup 2, to prove that *LDHB* is respected with the concept of SLG or not.

4.12.4 2-DG and metformin are highly toxic to all HCC cell lines. We could not optimise the dose that highly toxic to HCC cells but not immortalised HHL5 cells. However, more immortalised hepatocyte cell lines or primary hepatocytes should be investigated to verify if the toxicity of these medications is consistent or not.

4.12.5 Assessment of the inhibitors in media with levels of lactate/glutamine more reflective of physiological levels did not demonstrate any evidence of increased survival of LDHB positive cell lines (due to potential use of lactate as an energy source). It is possible that lactate concentrations similar to serum levels do not reflect those found in cancer reported to be up to 10-30 mM [**de la Cruz-López et al., 2019**] and so increased levels of lactate could be assessed to see if these provide a survival advantage for LDHB positive cancer cells.

Chapter V

Investigation of potential radiosensitisation following treatment with 2-DG and metformin in HCC cell lines

5.1 Introduction

Currently, radiotherapy (RT) is one of the major therapeutic approaches for cancers and about 50% of cancer patients receive at least one RT course during their course of treatment [**Baskar et al., 2014**]. Although RT has become more successful in recent decades, radioresistance remains a problem. The evidence of radioresistance has increased in various cancer types over the past two decades, including lung cancer [**Willers et al., 2013**], prostate cancer [**Niamh et al., 2017**] and HCC [**Guo et al., 2018**]. Hence, efforts are been made towards increasing radiosensitivity of tumors by combination treatment or adjuvant therapy. **Fig. 5.1** summarises some methods for improving radiation outcomes by increasing radiosensitivity. For further information, please read Gisbergen's publication [**van Gisbergen et al., 2021**].

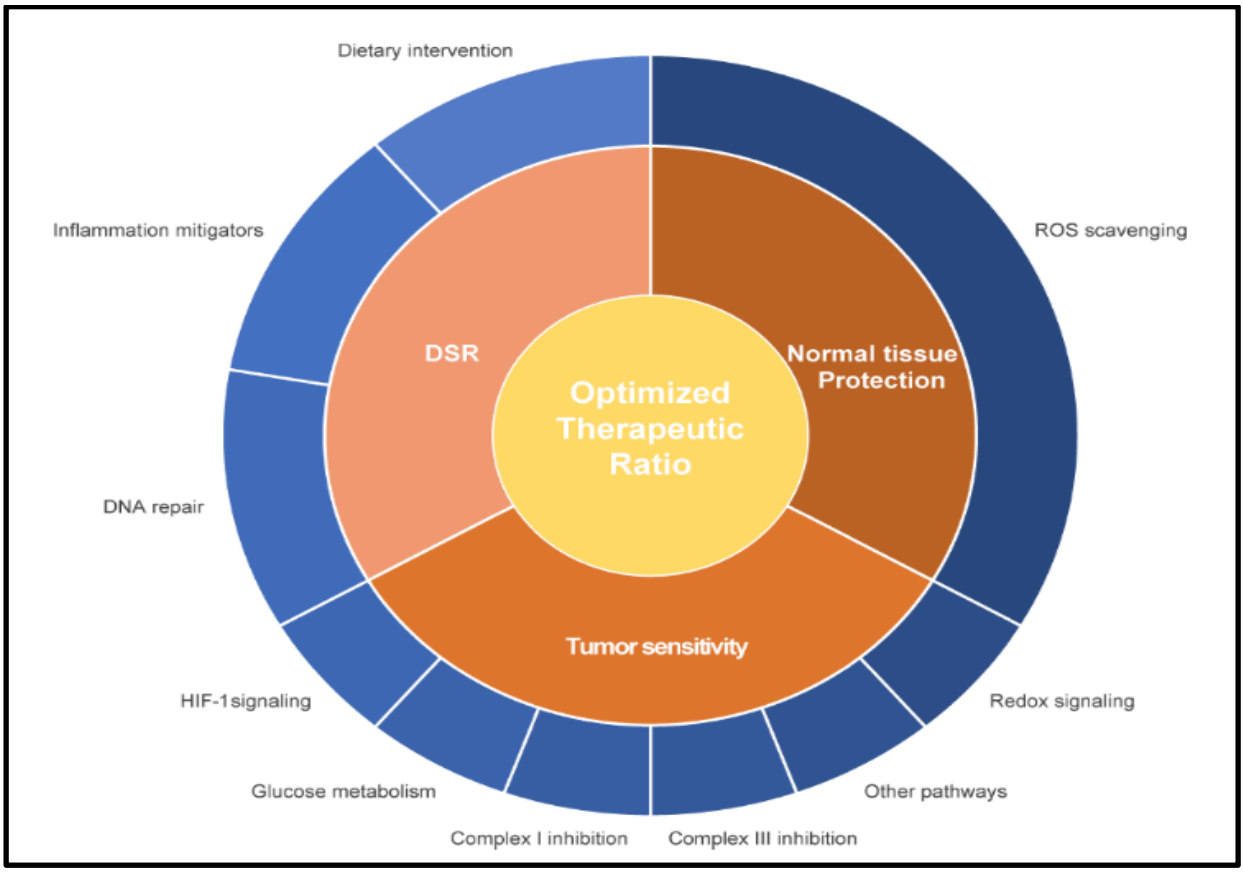

Figure 5.1. Strategies to improve the radiosensitivity in cancer cells. DSR: differential response of normal and cancer cells to stress. ROS: reactive oxygen species. HIF: hypoxia-inducible factor [**van Gisbergen et al., 2021**].

RT has become an alternative treatment option for patients who cannot be treated surgically. Furthermore, advanced stereotactic RT has been developed to deliver minimal radiation

to normal cells while targeting cancer cells. However, in order to improve treatment outcomes, RT may need to be combined with other approaches [**Pérez-Romasanta et al., 2021**]. A promising new approach is the combination of anti-metabolic drug therapy and RT [**Zhang et al., 2020**; **Sun et al., 2022**]. Singh's team found that oral administration of 2-DG (250 mg/kg) before IR was safe and boosted radiosensitivity (5 Gy/fraction/week) in glioblastoma paients [**Singh et al., 2005].** Rao and his colleagues summarised the influence of metformin on RT efficacy by carrying out a systematic review and meta analysis of patients with cancer and diabetes. Overall, metformin appeared to improve the resonse to RT in patients with cancer and diabetes and partly yield survival benefits [**Rao et al., 2018**]. Hence, prospective studies should be carried out to evaluate the benefits of metabolic interventions and RT.

Although sensitivity to metabolic inhibitors (2-DG and metformin) was independent of LDHB status in HCC cell lines (see **Table 4.2 for 2-DG** and **Table 4.3 for metformin** in **Chapter 4**), here we focus on radiosensitisation potential of the metabolic inhibitors 2-DG and metformin and its relationship to LDHB status of the cells to explore LDHB as a potential biomarker for therapeutic efficacy of RT.

5.2 Chapter aim

5.2.1 Evaluate the potential of metabolic inhibitors (2-DG and metformin) as radiosensitisers in HCC cell line models and their relationship to LDHB expression.

5.3 Results

5.3.1 Evaluation of radiosensitivity of HCC cell lines

To investigate the effect of x-ray on the growth of HCC cell lines, cells were seeded in 96-well plates and exposed to radiation ranging from 0 to 8 Gy after plating overnight. The radiotoxicity was investigated using MTT assay after 48, 96, and 144 hrs of radiation exposure. All cell lines demonstrated dose-dependent sensitivity to x-ray in terms of cell proliferation (**Fig. 5.2**).

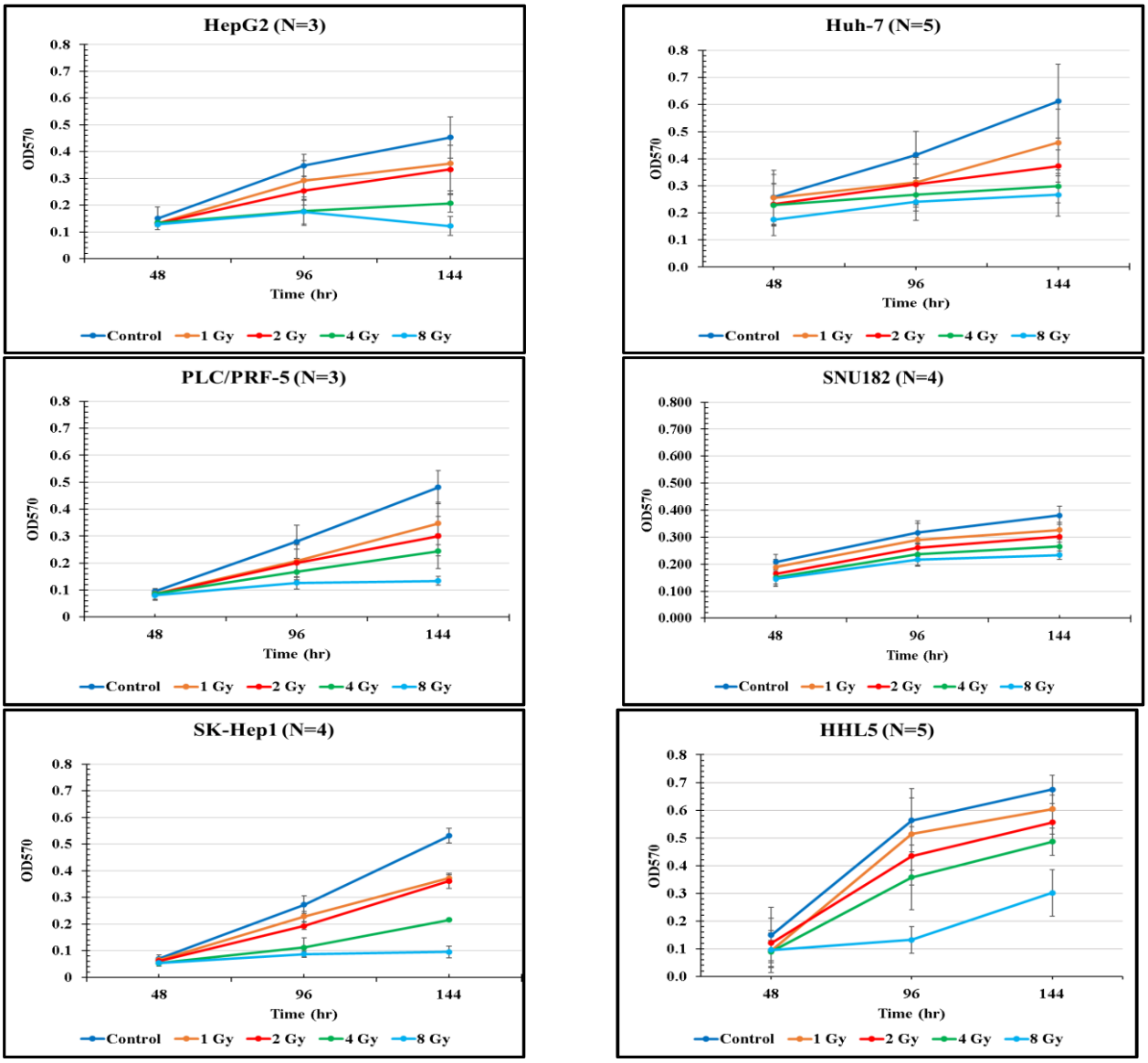

Figure 5.2 The growth curve after x-ray exposure determined by MTT assay. Cells were seeded in a 96-well plate and subjected to various x-ray doses. After 0–8 Gy of x-ray irradiation, cell proliferation was measured at 48, 96, and 144 hrs. The data shown is the mean and standard deviation (SD), with a sample size of 3-6 of independent repeats.

To compare the x-ray sensitivity of the cell lines, cell growth between time points 48 and 144 hrs after irradiation was calculated in terms of % control cell growth. Overall sensitivity to x-ray irradiation was broadly similar across the cell lines. However, at the maximum dose of the study, HepG2 exhibited complete reduction in cell proliferation while the other five cell lines showed some sustained proliferation (~15–40% of control cell growth) even at the highest dose administered (**Fig. 5.3A**).

The SRB assay was performed to confirm these results. Overall, the data was consistent with MTT assay data, i.e., ionising radiation exposure resulted in dose-dependent sensitivity in all the cell lines (**Fig. 5.3B**).

A

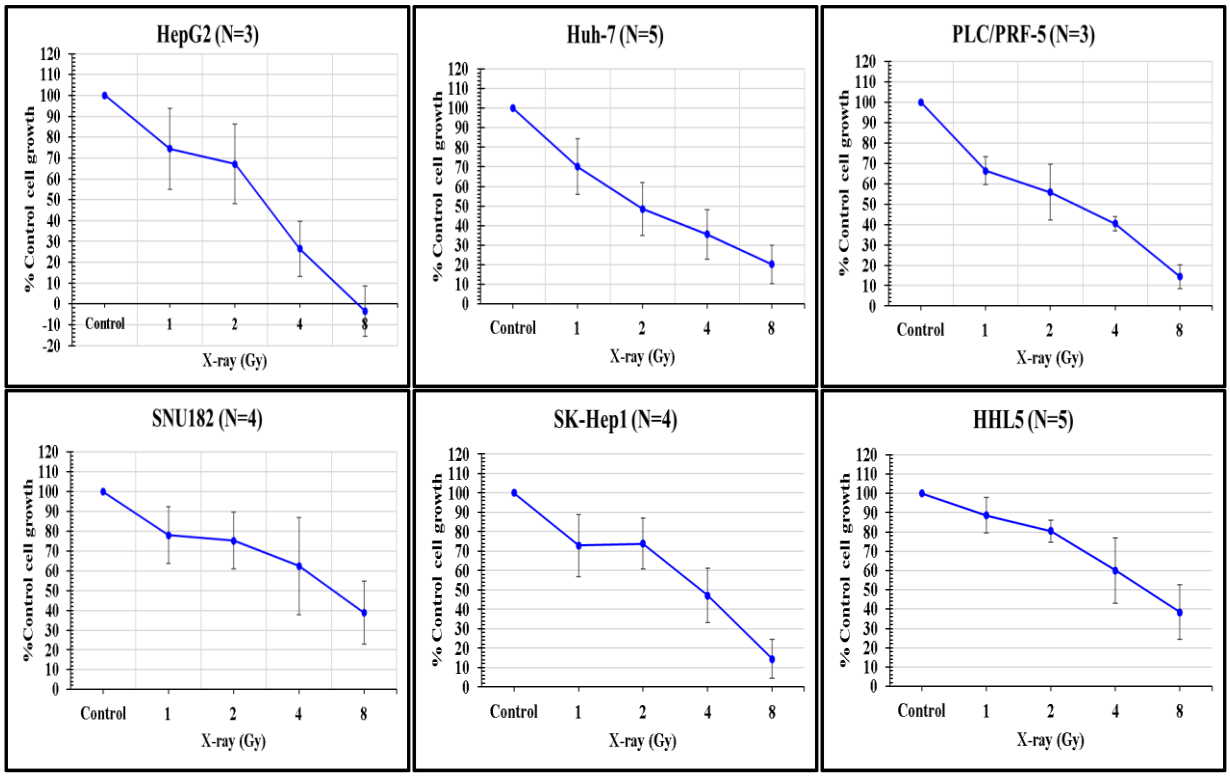

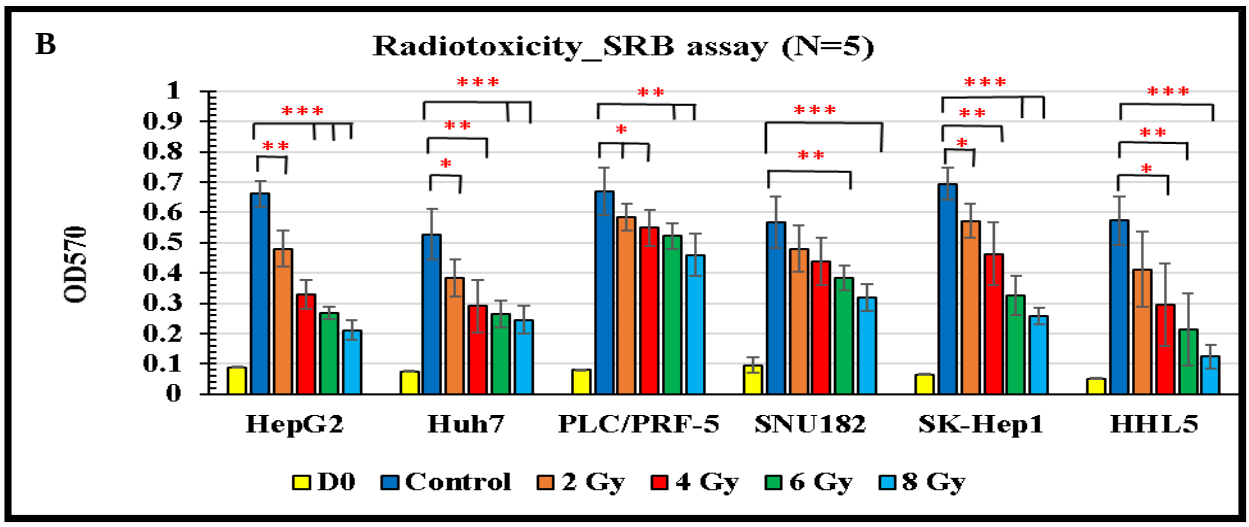

Figure 5.3 MTT (line graph) and SRB (bar graph) asssays were used to compare the x-ray sensitivity of HCC cell lines. (**A**) MTT assay result. %Control cell growth calculated by (ODday6-ODday2) and calculated in percentage compared with control (100%). (**B**) SRB assay was evaluated at day 6 of IR exposure. D0 denote the day after plating overnight and initiating irradiation. The data represents the mean ± SD of at least three independent studies. *P<0.05, **P<0.005, ***P<0.0005.

5.3.2 Assessment of the potential of 2-DG, metformin, and combinations of the two drugs as radio-sensitisers in HCC cell lines

The radiosensitisation potential of 2-DG and metformin for HCC cell lines was investigated by the SRB assay. The doses of these two drugs (0.5 mM 2-DG and 1 mM metformin) were chosen as they resulted in low level toxicity across the cell line panel (**see Fig. 4.15 and 4.16** (2-DG sensitivity) **and Fig. 4.17 and 4.18** (metformin sensitivity) in **Chapter 4**). Amongst the HCC cell lines, only Huh-7 exhibited evidence of potential synergistic interaction between the drugs with and without radiation (bar graph of untreated control compared with mixed drugs, $p<0.05$), although the effect was very limited and may be a primarily additive effect. However, the results did not support synergy between the metabolic inhibitors and radiation exposure, indicated by the ratio of the untreated control to the combination of 2-DG and metformin remaining largely unchanged in at all tested radiation levels (**Fig. 5.3,** only shows cell lines when drug administration resulted in significant growth decreases under either of the radiation settings). In the non-HCC subgroup, there was a significant difference in SK-Hep1 between control and combination drugs with and without radiation ($p<0.0005$). However, the ratio between the signal for the control condition (i.e. no exposure to metabolic drugs) and the signal for either the individual metabolic

inhibitors or the combination of both did not differ at any level of radiation exposure in either Huh-7 or SK-Hep1 cells (**Fig. 5.4**).

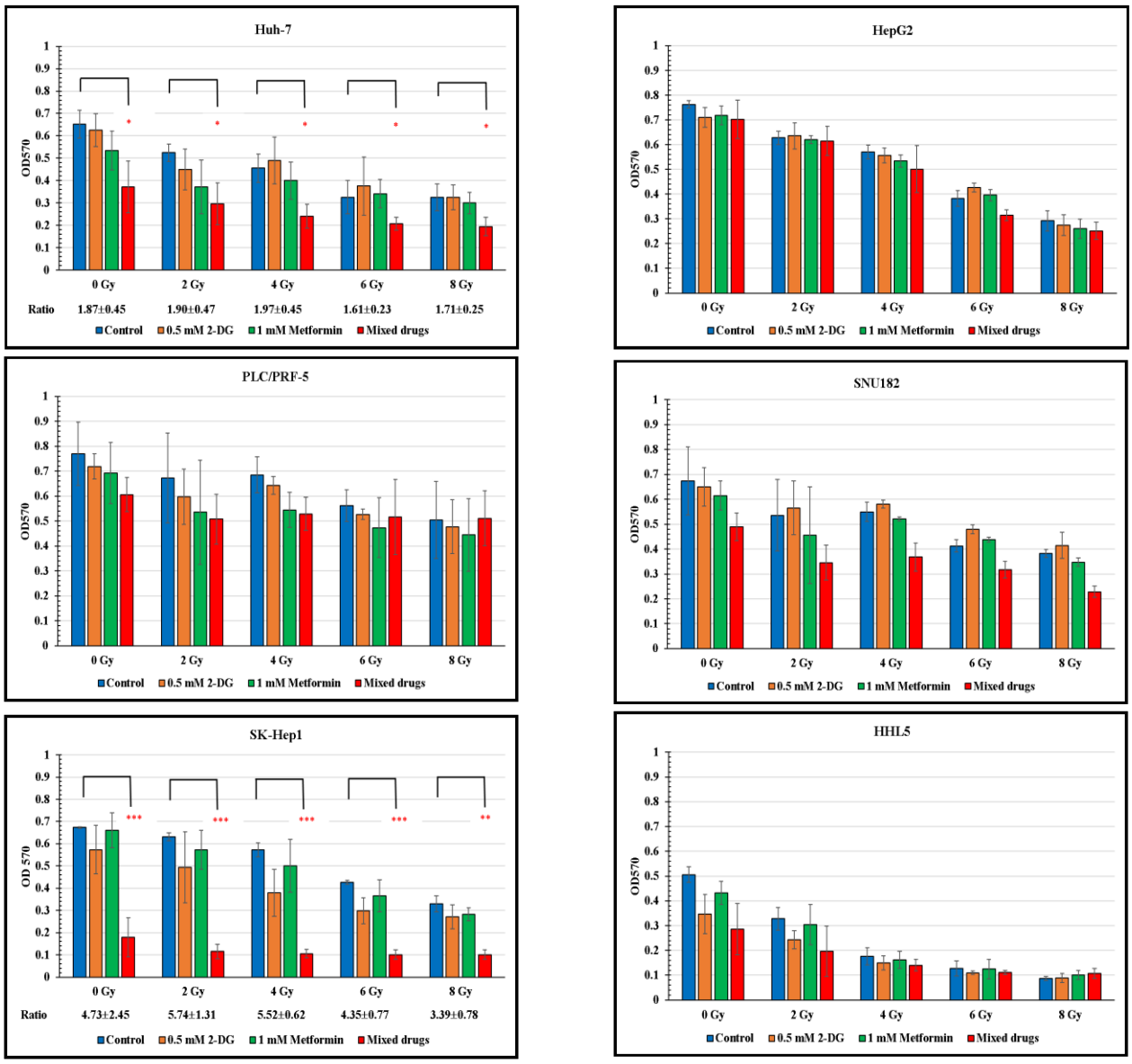

Figure 5.4 The effect of the glycolysis inhibitor 2-DG and the mitochondrial respiratory chain inhibitor metformin administration 24 hrs before irradiation, as evaluated by the SRB assay at 144 hrs. The impact of the glycolysis inhibitor 2-DG and the mitochondrial respiratory chain inhibitor metformin treatment 24 hr before irradiation was determined by the SRB assay after 144 hr post-irradiation.Radiosensitisation was calculated as a ratio by dividing the OD of IR exposure alone (0-8 Gy) by the OD of the combination of 2-DG and metformin plus IR (0-8 Gy).N=3. *P<0.05. **P<0.005. ***P<0.0005.

5.3.3 Assessment of the impact of x-ray irradiation on clonogenic potential of HCC cell lines

The colony formation assay (CFA) is an *in vitro* cell survival assay that evaluates the ability of single cells to survive, reproduce, or divide in order to form colonies. This assay was first described to study the effects of radiation on cancer cell survival and growth, and it has since become a gold standard radiotoxicity method [**Braselmann et al., 2015**]. Hence, we utilised this assay to verify the results obtained by MTT and SRB assays. Since plating effeciency of the cell lines vary, optimal seeding density was detrmined to get sufficient countable colonies (250-1000 per 10cm^2 dish) for each cell line before carrying out the irradiation experiment (**Table 5.1)**. Although HHL5 cells are immortal, they exhibit negligable colony forming ability. Thus, this line is excluded from this study.

Table 5.1 Plating efficiency of HCC cell lines in 10 cm^2 petri dish for 14 days before fixing and staining with 1-2% crystal violet.

Cell line	Seeding density per 10 cm^2 dish (Cells)	Plating efficiency (%)
HepG2	**4,000-6,000**	**13-20**
Huh-7	**4,000-6,000**	**12-19**
PLC/PRF-5	**1,000**	**33-49**
SNU182	**3,000-4,000**	**11-14**
SK-Hep1	**1,500**	**29-35**

Like the MTT and SRB assays, the CFA also demonstrated that radiotoxicity was dose-dependent in these cell lines. For subsequent investigation into radiosensitisation, the 2 Gy dose of x-ray was chosen because it caused considerable toxicity to almost all HCC and non-HCC cell lines ($p<0.05$ for Huh-7, $p<0.005$ for HepG2 and PLC/PRF-5, and $p<0.0005$ for SK-Hep1), except SNU182. Furthermore, this radiation dose was not too harmful, allowing some colony growth to be retained to allow subsequent assessment of any additional impacts of the metabolic inhibitors (**Fig. 5.5**).

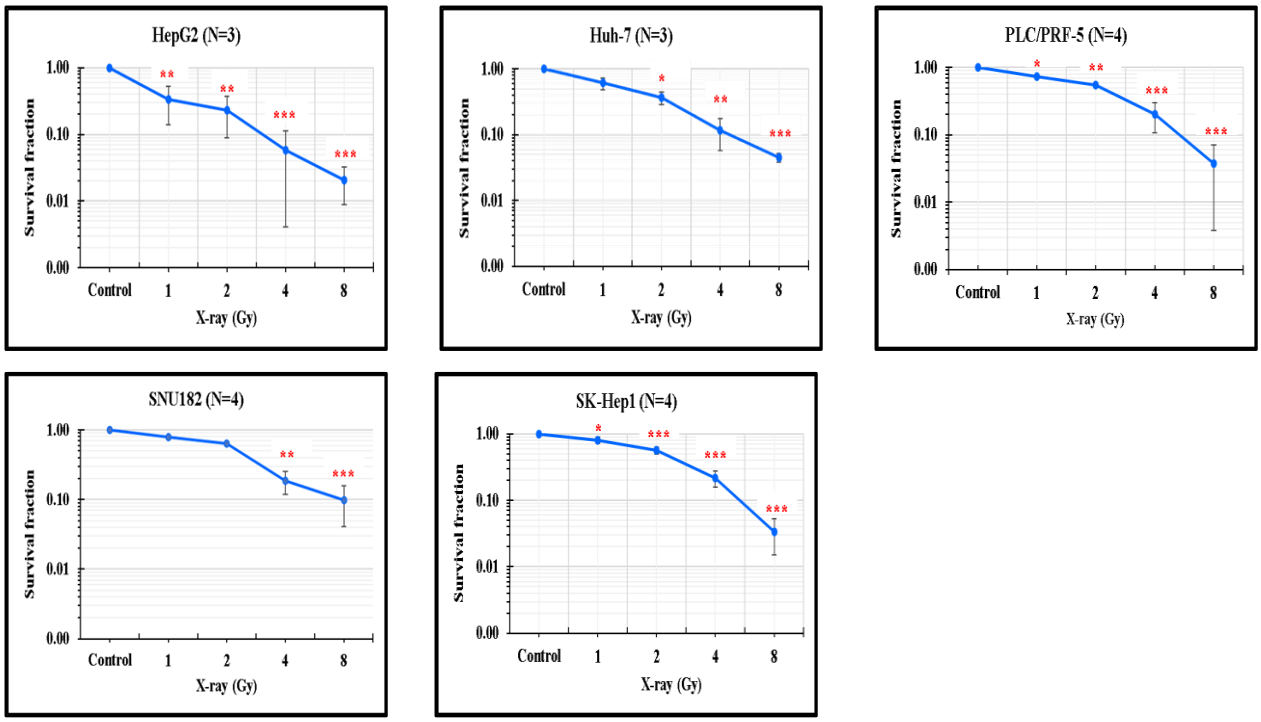

Figure 5.5 Colony formation assay after two weeks of x-ray exposure. Cells were plated overnight in a 10 cm^2 dish before irradiation. Survival fraction is derived by number of colonies in treatment/number of colonies in untreated control. [A colony was defined as a group of cells that is formed by more than 50 cells. *P<0.05, **P<0.005, P<0.0005.

5.3.4 Assessment of the impact of 2-DG, metformin or combination of the drugs on x-ray synergy in terms of the clonogenic potential of HCC cell lines

Having established the impact of radiation alone, CFA was used to assess any potential synergy between radiation and treatment with the metabolic inhibitors. To evaluate the radiosensitisation effect, the ratio of with and without radiation for each condition was calculated. The results showed that none of the individual or mixed compounds had a radiosensitising effect on any of the HCC cell lines that were tested using the ratio that was described earlier ($p>0.05$). The outcome of CFA on radiosensitisation of HCC cell lines corresponds to the SRB assay. In contrast, non-HCC SK-Hep1 cells exhibited radiosensitisation to the mixed drug treatment evaluated by CFA ($p<0.05$) that was not detectable in the SRB assay (**Fig. 5.6**).

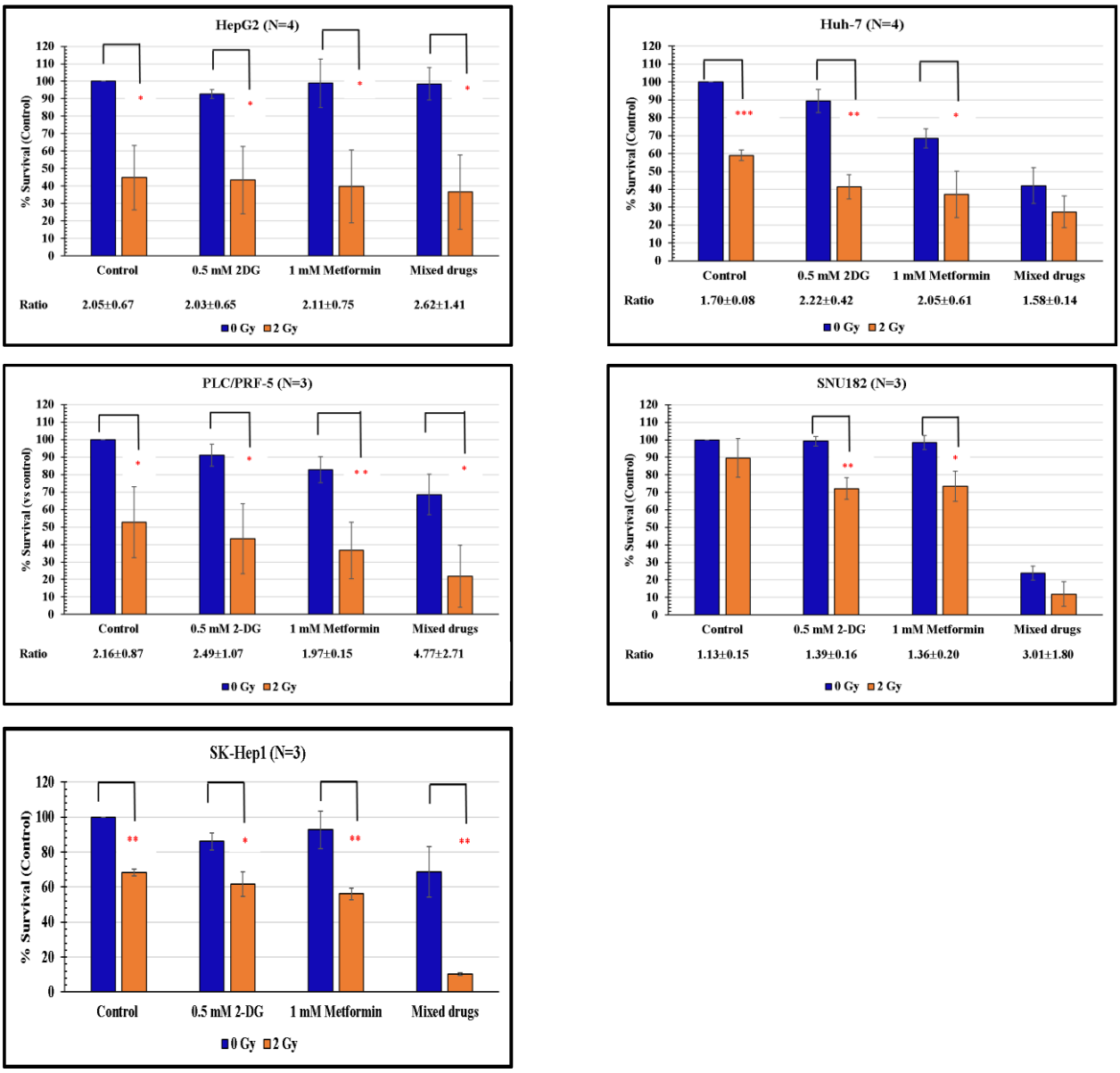

Figure 5.6 The percentage survival graphs of HCC and non-HCC cell lines after irradiation with 2 Gy of x-ray followed by treatment with the indicated drugs determined by CFA. Before drugs were introduced, the cells were irradiated with ionising radiation after plating overnight. The colonies were fixed after 14 days and counted with ColCount™ (Oxford Optonix, UK). %Survival is (the number of colonies of treatment/the number of colonies of untreated control)*100. The ratio is derived by dividing the %survival of treatment without radiation by the %survival of treatment plus 2 Gy of ionising radiation exposure. Data are the mean ± SD of at least-three independent studies. *P<0.05, ** P<0.005, ***P<0.0005.

The combination of both drugs (0.5 mM 2-DG and 1 mM Meftormin) without radiation had a lower impact on CFA in HepG2 and PLC/PRF-5 than non-HCC SK-Hep1 (**see Fig. 5.6**). To determine if any evidence of synergy might be more evident at higher doses, we assessed higher doses of the two metabolic inhibitors (1 mM 2-DG and 3 mM Metformin). As shown in **Fig. 5.7**, 3 mM metformin drastically reduced the number of colonies for both the cell lines with and without radiation. Furthermore, almost no colonies formed after a mixed drug treatment. In these conditions, however, there was no clear indication of synergy between these inhibitors and radiation, although the high toxicity of the combined treatments at these higher doses prevented any relaible assessment of synergy with radiation.

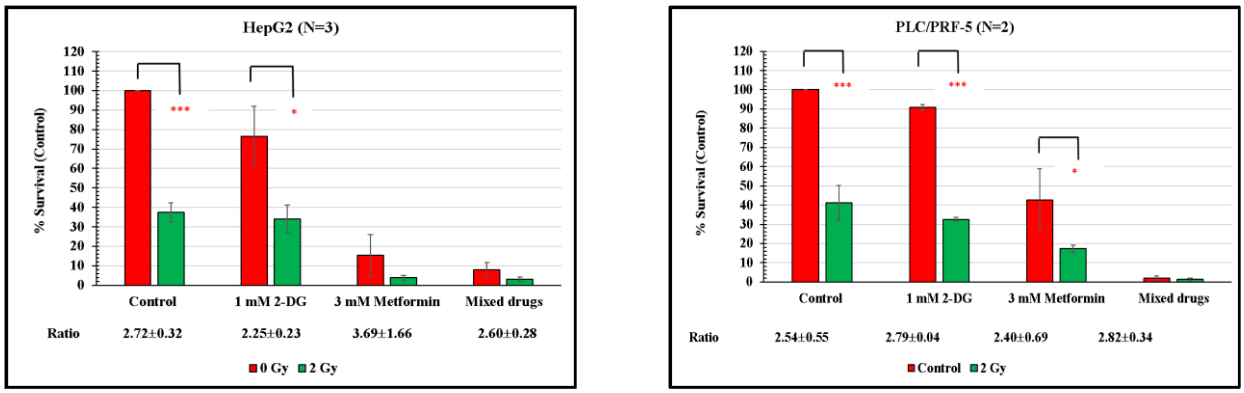

Figure 5.7 Percentage survival of indicated HCC cell lines after exposure to ionising radiation. Cells were pretreated with the indicated doses of metabolic inhibitors. Data are the mean ± SD. N=2-3. *P<0.05, ** P<0.005, ***P<0.0005.

5.4 Discussion

The outcome for HCC patients remains poor, necessitating novel therapeutic approaches. While RT can be helpful in the initial treatment of HCC, advanced HCC is incurable because the previously sensitive tumour develops resistance to radiation. Resistance to radiation therapy is a major clinical issue for patients with various cancers, including HCC [**Willers et al., 2013; Znati et al., 2020; Pérez-Romasanta et al., 2021**]. As a result, there is an urgent need for the development of novel therapeutics that can help patients who will benefit from radiation using radiosensitisers.

Various publications have reported radiosensitisation potential of either 2-DG or metformin in a variety of cancer types, such as pancreatic cancer MiaPaCa2 and Panc-1 [**Wang et al., 2015**], breast cancer MCF7 [**Song et al., 2012**], prostate cancer PC3 [**Rae et al., 2018**], head and neck squamous carcinoma KB [**Sharma et al., 2012**], non-small cell lung cancer H460 [**Sun et al., 2022**], and HCC cell lines (HepG2, and Huh-7) [**Kim et al., 2014; Kim et al., 2016**]. Furthermore, combined inhibition of glycolysis (2-DG) and mitochondrial respiration (metformin) simultaneously promotes radiosensitisation in neuroblastoma and glioma cells [**Nile et al., 2021**]. However, in our study, we have not observed any radiosensitisation effect of either 2-DG or metformin pretreatment, alone or in combination, in any of the tested HCC cell lines.

The discrepancy between our observation and a previous report where metformin enhanced radiosensitivity in HepG2 and Huh-7 could be due to different assays employed in the studies (**Kim et al., 2016**). Kim and colleagues employed the MTT assay; however, it is worth noting that MTT is dependent on mitochondrial activity, which is directly affected by metformin. Hence, we employed the SRB assay instead of MTT. Moreover, for CFA experiments, they employed a higher dose of metformin (10 mM); however, this dose was extremely hazardous to the cell lines in our hands. Even a dose of 3 mM metformin reduced CFA by about 80% in HepG2 cells (**Fig. 5.7);** hence, we did not try higher doses.

To summarise, there was no correlation between radiotoxicity, radiosensitisation and LDHB expression in the HCC and non-HCC cell lines used in this study. However, there are several limitations to this study (discussed below), and thus we cannot rule out the possibility of increased RT in conjunction with metabolic interventions in HCC patients.

5.5 Limitations and Future directions

5.5.1 Although CFA is widely used as a gold standard method for radiotoxicity, however, HHL5 cannot form colonies which we had utilised as a model for normal hepatocytes. As a result, there are no normal cell results to compare with in this assay.

5.5.2 MTT, SRB, and CFA do not directly reflect cell death. Furthermore, the sensitivity of MTT, SRB, and CFA is insufficient, particularly in the case of a few cancer cells that survive after treatment but do not divide or proliferate. Because of the limitations of the methods used, direct approaches to detect cell death should be used to confirm radiotoxicity.

5.5.3 Despite the fact that the combination of two metabolic inhibitors, 2-DG and metformin, was as toxic to two HCC cell lines (Huh-7 and SNU182) as 2 Gy treatment. The result should be confirmed by other methods and extended to more HCC cell lines or patient derived organoids.

5.5.4 Normal cells utilise both OXPHOS (major) and glycolysis (minor) for energy production but cancer cells prefer to use glycolysis as their principal source of energy and biosynthesis. Thus, blocking glycolysis pathways for cancer therapeutics will have an impact on normal cells. Furthermore, cancer cells have the flexibility to switch using a different energy-generating route if one of the pathways is blocked. Thus, alternative targeted tumour metabolism pathways to shutting down energy should be further explored in HCC such as glutaminolysis, and acetate uptake inhibitor **(Fig. 5.8)**.

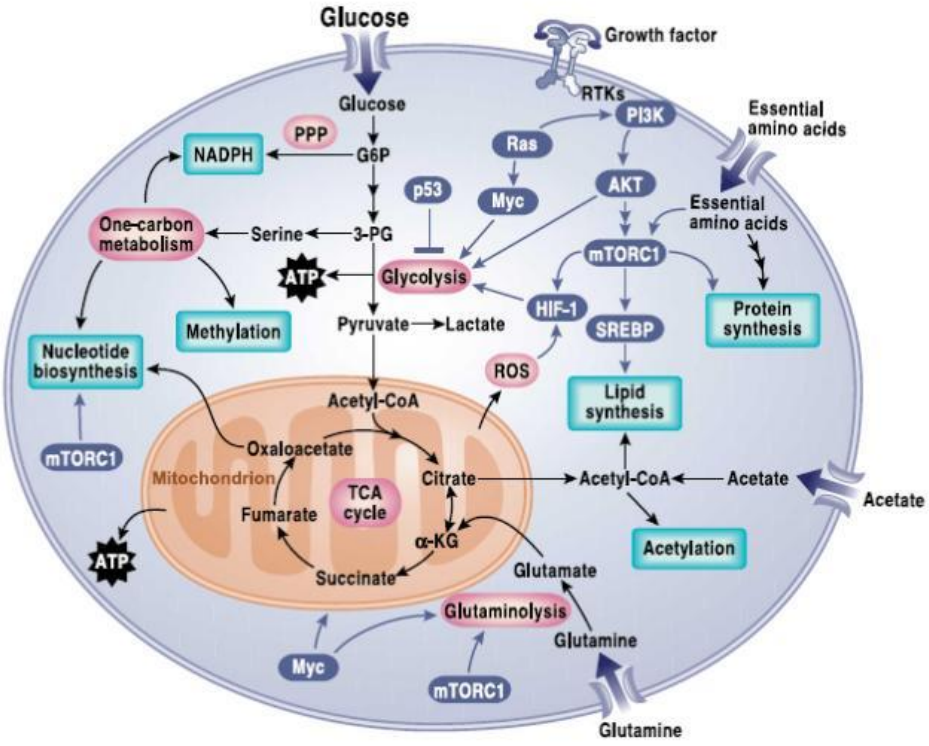

Figure 5.8 Overview of signaling pathway involves cancer metabolism [**Deberardinis and Chandel, 2016**].

Chapter VI

Conclusion and Future Directions

6.1 Conclusion

HCC is one of the most complex diseases, and the existing therapies for HCC patients often have limited effectiveness and high toxicities, and mortality rates are on the rise. Furthermore, almost all HCC patients are diagnosed at a late stage of the disease progression, which limits their therapeutic options. Thus, there is a very clear need for more effective therapies to improve outcomes for HCC patients.

Recent years have seen a dramatic increase in interest in the identification of cancer-specific SLGs to enable the development of more effective and less toxic therapies. To find possible SLGs for particular subgroups of HCC patients, our group used a novel in-house bioinformatics technique. Targeting these genes may result in SL (the destruction of cancer cells while having no effect on healthy cells). We observed that the bioinformatics strategy did not work very effectively, as we didn't detect SLGs for all the subgroups; nevertheless, we identified two potential SLGs in one subgroup of HCC. This thesis is focused on exploring these SLGs (*TIAM1* and *LDHB*) as potential therapeutic targets as individual or combination therapy (with radiation) for HCC.

The TIAM1 protein is a guanine nucleotide exchange factor that is known to regulate RAC1 activity. As RAC1 is known to have important roles in cancer cell growth and in metastasis, regulation via TIAM1 may play an important role in HCC. *TIAM1* siRNA was used to knock down the *TIAM1* gene for the functional analysis. As a result, there was a reduction in proliferation with no off-target effect. However, it exhibited non-specific toxicity in non-HCC subgroup 2 cell lines, hence, additional non-HCC subgroup 2 cell lines are needed to demonstrate that the effects of targeting *TIAM1* in HCC subgroup 2 cells are specific. Furthermore, a specific RAC1 inhibitor (NSC23766) decreased cell growth in PLC/PRF-5 and SNU182 cells (high *TIAM1* gene expression), more effectively than in HepG2 and Huh-7 cells (low or undetectable *TIAM1* gene expression). However, since the inhibitor decreased cell growth even in the cell lines with effectively no *TIAM1* expression, the results indicate off target effect of NSC23766 in HCC cell lines. Furthermore, this inhibitor only caused apoptosis in SNU182, indicating that NSC23766's RAC1 inhibition was primarily cytostatic, with no evidence of cell death activation. Hence, more effective and selective inhibitors such as 1D-142 and EHop-016 may be necessary to adequately analyse the degree to which targeting TIAM1 may specifically inhibit HCC subgroup 2.

LDHB is a catalytic enzyme that participates in the glycolysis pathway, converting lactate to pyruvate, which can then be utilised by the OXPHOS pathway to produce ATP [**Urbańska and Orzechowski, 2019]**. In addition, lactate may be used as a source of gluconeogenesis in the liver [**Mishra and Banerjee, 2019**]. In both glycolytic and oxidative cancer cells, silencing *LDHB* may limit cell proliferation [**Brissson et al., 2016**]. Thus, inhibiting glycolysis and OXPHOS to target cancer metabolism offers an alternative route for targeted cancer treatment.

The glycolysis inhibitor 2-DG [**Tomizawa et al., 2017; Wang et al., 2019; Sasaki et al., 2021**] and the OXPHOS inhibitor metformin [**Xiong et al., 2012; Fujita et al., 2016; Kang et al., 2018; Cunha et al., 2020**] were reported to inhibit proliferation of HCC cells both *in vivo* and in *vitro*. Our findings revealed that both drugs were highly toxic to HCC cell lines but also extremely toxic to immortalised HHL5. While the anti-cancer effects were in keeping with previously reported findings in other cancer types, the therapeutic relevance was called into question since there was no clear difference in sensitivity to the drugs between normal and cancer cells. Thus, effective cancer treatments based on this approach would require alternative inhibitors that could achieve more cancer specificity or be used in combination with other therapeutic approaches with cancer-specific synergies.

Our comparisons of the impact of targeting TIAM1 and LDHB in liver cancer and non-cancer cells did not compare CFA, despite CFA being commonly recognised as the "gold standard" approach for radiotoxicity and radiosensitisation studies. This was because HHL5 cells, which we used as a model for normal hepatocytes, did not form colonies. Therefore, there was no “normal cell” data in the CFA experiments, which was a limitation of these studies.

6.2 Future directions

6.2.1 Expanding the panel of HCC cell lines assessed would be important to clearly demonstrate the preferential sensitivity of *TIAM1*-positive HCC versus *TIAM1*-negative HCC and normal cells. Thus, the identification of additional HCC cell lines with high levels of *TIAM1* and *LDHB* gene expression and global methylation patterns matching HCC-subgroup 2 is required. Furthermore, the analysis could be expanded to other cancer cell types, as many other cancers also show frequent high expression of *TIAM1*, such as small cell lung cancer or neuroblastoma, to determine if synthetic lethal relationships may be preserved across cancer types.

6.2.2 EHop-016 [**Montalvo-Ortiz et al., 2012**] and 1D-142 [**Ciarlantini et al., 2021**] have exhibited strong RAC1 inhibition in numerous cancer types. Hence, these should be tested in HCC subgroup 2 cell lines. Furthermore, the influence of TIAM1/RAC1 inhibition on migration and apoptosis might be studied. Furthermore, drugs that exhibit some degree of selectivity for TIAM1-expressing cancer cells can be used as an initial starting point for structure-based drug development approaches to attempt to develop more specific and potent molecules that may have the potential for increased specificity and a wider therapeutic window.

6.2.3 Because there is currently no confirmatory functional analysis of the *LDHB* gene, screening potential LDHB inhibitors, such as AXKO-0046 [**Shibata et al., 2021**], or silencing the *LDHB* gene by genetic means [**Brisson et al., 2016**], should be investigated further in HCC subgroup 2 cell lines to more clearly determine if it plays a potential synthetic lethal role.

6.2.4 We were unable to optimise a dose of 2-DG and metformin that was very deadly to HCC cells but not to immortalised HHL5 cells. However, other immortalised hepatocyte cell lines or normal hepatocytes should be examined to determine if the sensitivity of normal cells to these agents is consistent.

6.2.5 As we can observe in immortalised HHL5, blocking glycolysis pathways for cancer therapies has an effect on normal cells. Furthermore, cancer cells may switch to a new energy-generating pathway if one of the routes is inhibited. Thus, other targeted tumour metabolic routes for shutting down energy, such as glutaminolysis and acetate absorption inhibitors, should be investigated further in HCC, either as single agents or in combination with other metabolic inhibitors.

References

1. Abd- Aziz N., and Poh CL. Development of peptide- based vaccines for cancer. *Journal of Oncology* 2022, Article ID 9749363. DOI: 10.1155/2022/9749363.
2. Adegbola AJ., Awobusuyi OJ., Adeagbo BA., Oladokun BS., and Owolab AR. *Journal of Exploratory Research in Pharmacology* 2017, 2:78–84.
3. Akram M. Mini- review on Glycolysis and Cancer. *Journal of Cancer Education* 2013, 28:454–457. DOI: 10.1007/s13187-013-0486-9.
4. Apaolaza I., José-Enériz E., Valcarcel LV., Agirre X., Prosper F., et al. A network-based approach to integrate nutrient microenvironment in the prediction of synthetic lethality in cancer metabolism. *PLoS Computational Biology* 2022, 18(3):e1009395. DOI: 10.137/ journ al.pcbi.1009395.
5. Araki Y., and Mimura T. The histone modification code in the pathogenesis of autoimmune disease. *Mediators of Inflammation* 2017, Article ID 2608605. DOI: 10.1155/2017 /2608605.
6. Aryan M., Forrister N., Panchani N., Vashi B., Chowdhury Z., A focused review on recent advances in diagnosis and management of fibrolamellar hepatocellular carcinoma. *Hepatoma Research* 2022, 8:25. DOI: 10.20517/2394-5079.2022.07.
7. Ashton TM., McKenna WG., Kunz-Schughart LA., and Higgins GS. Oxidative phosphorylation as an emerging target in cancer therapy *Clinical Cancer Research* 2018, 24:2482-2490. DOI: 10.1158/1078-0432.CCR-17-3070.
8. Bacinschi X., Zgura AF., Mercan-Stanciu A., Grasu M., Herlea V., et al. Management of diagnosis and treatment in a case of fibrolamellar carcinoma. *Cancer Diagnosis & Prognosis* 2021, 1:23-28. DOI: 10.21873/cdp.10004.
9. Bailey CJ. Metformin: historical overview. *Diabetologia* 2017, 60:1566–1576. DOI: 10. 1007/s00125-017-4318-z.
10. Banales JM., Cardinale V., Carpino G., Marzioni M., Anderson JB., et al. Expert consensus document: Cholangiocarcinoma: current knowledge and future perspectives consensus statement from the European Network for the Study of Cholangiocarcinoma (ENS-CCA). *Gastroenterology and Hepatology* 2016, 13:261-280. DOI: 10.1038/nrgas tro.2016.51.
11. Bannister AJ., and Kouzarides T. Regulation of chromatin by histone modification. *Cell Research* 2011, 21:381-395.
12. Bardhan K., and Liu K. Epigenetics and colorectal cancer pathogenesis. *Cancers* 2013, 5: 676-713. DOI: 10.3390/cancers5020676.

13. Baskar R., Dai J., Wenlong N., Yeo R., and Yeoh KW. Biological response of cancer cells to radiation treatment. *Frontiers in Molecular Biosciences* 2014, 1:24. DOI: 10.3389/fmolb. 2014.00024.
14. Benson AB., *D'Angelica MI., Abbott DE., Anaya* DA., Burgoyne A., et al. Hepatobiliary Cancers, Version 2.2021. *The NCCN Clinical Practice Guidelines in Oncology* 2021, 19(5):541-*565.*
15. Deberardinis RJ., and Chandel NS. Fundamentals of cancer metabolism. *Science Advances* 2016, 2:e1600200.
16. Bergman O., and Ben- Shachar D. Mitochondrial oxidative phosphorylation system (OXPHOS) deficits in schizophrenia: Possible interactions with cellular processes. *The Canadian Journal of Psychiatry* 2016, 61(8):457-469.
17. Bergquist A., and von Seth E. Epidemiology of cholangiocarcinoma. *Best Practice and Research Clinical Gastroenterology* 2015, 29:221-232. DOI: 10.1016/j.bpg.2015.02.003.
18. Bian J., Long J., Yang X., Xu Y., Lu X., et al. Construction and validation of a prognostic signature using CNV- driven genes for hepatocellular carcinoma. *Annals of Translational Medicine* 2021, 9(9):765. DOI: 10.21037/atm-20-7101.
19. Bibikova M., Barnes B., Tsan C., Ho V., Klotzle B., et al. High density DNA methylation array with single CpG site resolution. *Genomics* 2011, 98:288–295.
20. Bibikova M. Le J., Barnes B., Saedinia-Melnyk S., Zhou L., Shen R., and Gunderson KL. Genome-wide DNA methylation profiling using Infinium® assay. *Epigenomic* 2009, 1(1): 177-200.
21. Braghini MR., Re OL., Romito I., Fernandez-Barrena MG., Barbaro B., et al. Epigenetic remodelling in human hepatocellular carcinoma. *Journal of Experimental and Clinical Cancer Research* 2022, 41:107. DOI: 10.1186/s13046-022-02297-2.
22. Branca JJV., Pacini A., Gulisano M., Taddei *N.*, Fiorillo C., et al. Cadmium-induced cytotoxicity effects on mitochondrial electron transport chain. *Frontiers in Cell and Development Biology* 2020, 8:604377. DOI: 10.3389/fcell.2020.604377.
23. Braselmann H., Michna A., Heß J., and Unger K. CFAssay: statistical analysis of the colony formation assay. *Radiation Oncology* 2015, 10:223. DOI. 10.1186/s13014-015-0529-y.
24. Bray F., Ferlay J., Soerjomataram I., Siegel RL., Torre LA., et al. Global Cancer Statistics 2018: GLOBOCAN Estimates of Incidence and Mortality Worldwide for 36 Cancers in 185 Countries. *CA: A Cancer Journal for Clinicians* 2018, 6 8: 394– 424. DOI: 10. 3322/

caac.21492.

25. Brisson L., Bański P., Sboarina M., Michiels C., Copetti T., and Sonveaux P. Lactate dehydrogenase B controls lysosome activity and autophagy in Cancer. *Cancer Cell* 2016, 30:418–431.
26. Bruix J., Chan SL., Galle PR., Rimassa L., and Sangro B. Systemic treatment of hepatocellular carcinoma: An EASL position paper. *Journal of Hepatology* 2021, 75:960–974. DOI: 10.1016/j.jhep.2021.07.004.
27. Burns KH. Transposable elements in cancer. Burns, K. Transposable elements in cancer. *Nature Reviews Cancer* 2017, 17:415–424. DOI: 10.1038/nrc.2017.35.
28. Burton A., Tataru D., Driver RJ., Bird TG., Huws D., et a. Primary liver cancer in the UK: Incidence, incidence-based mortality, and survival by subtype, sex, and nation. *JHEP Reports* 2021, 3:100232. DOI: 10.1016/j.jhepr.2021.100232.
29. Byrling J., Andersson B., Marko-Varga G., and Andersson R. Cholangiocarcinoma – current classification and challenges towards personalised medicine. *Scandinavian Journal of Gastroenterology* 2016, 51(6):641-643. DOI: 10.3109/00365521.2015.1127409.
30. Cabibbo G., Celsa C., Enea M., Battaglia S., Rizzo GEM., et al. Optimizing sequential systemic therapies for advanced hepatocellular carcinoma: A decision analysis. *Cancers* 2020, 12:2132. DOI: 10.3390/cancers12082132.
31. Caja F., Vodickova L., Kral J., Vymetalkova V., Naccarati A., et al. DNA mismatch repair gene variants in sporadic solid cancers. *International Journal of Molecular Sciences* 2020, 21:5561. DOI: 10.3390/ijms21155561.
32. Cantoria MJ., Boros LG., and Meuillet EJ. Contextual inhibition of fatty acid synthesis by metformin involves glucose-derived acetyl-CoA and cholesterol in pancreatic tumour cells. *Metabolomics* 2014, 10:91–104. DOI:10.1007/s11306-013-0555-4 (online version).
33. Castell-Rodríguez A., Piñón-Zárate G.,Herrera-Enríquez M.,Jarquín-Yáñez K., and Medina-Solares I. Dendritic cells: Location, function, and clinical implications. *Biology of Myelomonocytic Cells* 2017, 21-50. DOI: DOI: 10.5772/intechopen.68352.
34. Cerezo M., Tomic1T., Ballotti R., and Rocchi S. Is it time to test biguanide metformin in the treatment of melanoma? *Pigment Cell and Melanoma Research* 2014, 28:8–20.
35. Charneau J., Suzuki T., Shimomura M., Fujinami N., and Nakatsura T. Peptide-ased vaccines for hepatocellular carcinoma: A review of recent advances. *Journal of Hepatocellular Carcinoma* 2021, 8:1035–1054.

36. Chaisaingmongkol J., Budhu A., Dang H., Rabibhadana S., Pupacdi B., et al. Common molecular subtypes among Asian hepatocellular carcinoma and cholangiocarcinoma. *Cancer Cell* 2017, 32:57–70. DOI: 10.1016/j.ccell.2017.05.009.
37. Chen DP., Lin YC., and Fann CSJ. Methods for identifying differentially methylated regions for sequence- and array-based data. *Briefings in Functional Genomics* 2016, 15(6): 485–490. DOI: 10.1093/bfgp/elw018.
38. Chen L., Shu Y., Liang X., Chen EC, Yee SW, et al. OCT1 is a high-capacity thiamine transporter that regulates hepatic steatosis and is a target of metformin. *Proceedings of the National Academy of Sciences of the United States of America* 2014, 111(27):9983–9988.
39. Chen L., Wu Q., Xu X., Yang C., You J., et al. Cancer/testis antigen LDHC promotes proliferation and metastasis by activating the PI3K/Akt/GSK-3β-signaling pathway and the in lung adenocarcinoma. *Experimental Cell Research* 2021, 398:112414. DOI: 10.10 16/j.yexcr.2020.112414.
40. Chen W., Zhu P., Xu H., Hou X., and Guo C. The Association between immune subgroups and gene modules for the clinical, cellular, and molecular characteristic of hepatocellular carcinoma. *Journal of Oncology* 2022, Article ID 7253876. DOI: 10.1155/2022/7253876.
41. Chen Y., Lemire M., Choufani S., Butcher DT., Grafodatskaya D., et al. Discovery of cross-reactive probes and polymorphic CpGs in the Illumina Infinium HumanMethylation450 microarray. *Epigenetics* 2013, 8(2):203-209. DOI: 10.4161/epi.23470.
42. Cheng AL, Finn RS, Qin S, Han KH., Ikeda K., et al. Phase III trial of lenvatinib (LEN) vs sorafenib (SOR) in first-line treatment of patients (pts) with unresectable hepatocellular carcinoma (uHCC). *Journal of Clinical Oncology* 2017, 35(15_suppl: 4001). DOI: 101200/JCO.2017.35.15_suppl.4001.
43. Cho YH., McCullough LE., Gammon MD., Wu HC., Zhang Y. J., et al. Promoter hypermethylation in white blood cell DNA and breast cancer risk. *Journal of Cancer* 2015; 6(9):819-824.
44. Choi SJ., Jung SW., Huh S., Chung YS., Cho H., and Kang H. Alteration of DNA methylation in gastric cancer with chemotherapy. *Journal of Microbiology and Biotechnology* 2017, 27(8):1367-1378.
45. Choucair K., Kamran S., and Saeed A. Clinical evaluation of ramucirumab for the treatment of hepatocellular carcinoma (HCC): Place in therapy. *Onco Targets and Therapy* 2021, 14:5521–5532.

46. Ciarlantini MS., Barquero A., Bayo J., Wetzler D., Traian MMD., and et al. Development of an improved guanidine-based Rac1 inhibitor with in vivo activity against non-small cell lung cancer. *ChemMedChem* 2021, 16:1011 –1021. DOI: 10.1002/cmdc.202000763.
47. Constantino J., Gomes C., Falcão A., Neves BM., and Cruz MT. Dendritic cell- based immunotherapy: A basic review and recent advances. *Immunology Research* 2017, 65: 798–810.
48. Cornell L., Munck JM., Alsinet C., Vilanueva A., Ogle L., and et al. *Clinical Cancer Research* 2014, 21(4): 925–33. DOI: 0.1158/1078-0432.CCR-14-0842.
49. de la Cruz-López KG., Castro-Muñoz LJ., Reyes-Hernández DO., Garcia-Carrancá A., and Manzo-Merino J. Lactate in the regulation of tumor microenvironment and therapeutic approaches. *Frontiers in Oncology* 2019, 9:1143. DOI: 10.3389/fonc.2019.01143.
50. Cuestas ML, Oubiña JR., and Mathet VL. Hepatocellular carcinoma and multidrug resistance: Past, present and new challenges for therapy improvement. *World Journal of Pharmacology* 2015, 4(1):96-116. DOI: 10.5497/wjp.v4.i1.96.
51. Cuestas RF., Rinaldi A., Kandyba EE., Edward M., Willberg C., et al. Liver cell lines for the study of hepatocyte functions and immunological response. *Liver International* 2005, 25:389–402. DOI: 10.1111/j.1478-3231.2005.01017.x.
52. Cui Z., Chen Y., Hu M., Lin Y., Zhang Z., et al. Diagnostic and prognostic value of the cancer-testis antigen lactate dehydrogenase C4 in breast cancer. *Clinica Chimica Acta* 2020, 503:203–209.
53. Cunha V., Cotrim HP., Rocha R., Carvalho K., and Lins-Kusterer L. Metformin in the prevention of hepatocellular carcinoma in diabetic patients: A systematic review. *Annals of Hepatology* 2020, 19:232–237. DOI: 10.1016/j.aohep.2019.10.005.
54. Cutolo C., Aversana FD, Fusco R., Grazzini G., Chiti G., et al. Combined hepatocellular-cholangiocarcinoma: What the multidisciplinary team should know. *Diagnostics* 2022, 12: 890. DOI: 10.3390/diagnostics12040890.
55. Dawson M. and Kouzarides T. Cancer epigenetics: From mechanism to therapy. *Cell* 2012, 150:12-27. DOI: 10.1016/j.cell.2012.06.013.
56. Deberardinis RJ., and Chandel NS. Fundamentals of cancer metabolism. *Science Advances* 2016, 2:e1600200. DOI: 10.1126/sciadv.1600200.

57. Decraecker M., Toulouse C., and Blanc JF. Is there still a place for tyrosine kinase inhibitors for the treatment of hepatocellular carcinoma at the time of immunotherapies? A focus on lenvatinib. *Cancers* 2021, 13:6310. DOI: 10.3390/cancers13246310.

58. Delire B., Martin ED., Meunier L., Larrey D., and Horsmans Y. Immunotherapy and gene therapy: New challenges in the diagnosis and management of drug-induced liver injury. *Frontiers in Pharmacology* 2022, 12:786174. DOI: 10.3389/fphar.2021.786174.

59. Deng X., Das S., Valdez K., Camphausen K., and Shankavaram U. SL-BioDP: Multi-cancer interactive tool for prediction of synthetic lethality and response to cancer treatment. *Cancers* 2019, 11:1682. DOI: 10.3390/cancers11111682.

60. Ding J., and Wen Z. Survival improvement and prognosis for hepatocellular carcinoma: analysis of the SEER database. *BMC Cancer* 2021, 21: 1157. DOI: 10. 1186/ s12885- 021-08904-3.

61. Ding M., Li Y., Yang Y., Che S., Lin Z., et al. Elevated expression of Tiam1 is associated with poor prognosis and promotes tumor progression in pancreatic cancer. *Onco Targets and Therapy* 2018, 11 4367–4375. DOI: 10.2147/OTT.S17142.

62. Ding Y., Chen B., Huang J., Zhang W., Yang H., et al. Overexpression of Tiam1 is associated with malignant phenotypes of nasopharyngeal carcinoma. *Oncology Reports* 2014, 32:607-618. DOI: 10.3892/or.2014.3241.

63. Doherty JR., and Cleveland JL. Targeting lactate metabolism for cancer therapeutics. *Journal of Clinical Investigation*, 2013, 123(9):3685–3692. DOI: 10.1172/JCI69741.

64. Dote H., Cerna D., Burgan WE., Carter DJ., Cerra MA. et al. Enhancement of in vitro and in vivo tumour cell radiosensitivity by the DNA methylation inhibitor Zebularine. *Clinical Cancer Research* 2005, 11(12):4571-4579. DOI: 10.1158/1078-0432.CCR-05-0050.

65. Du P., Zhang X., Huang CC., Jafari N., Kibbe WA., et al. Comparison of Beta-value and M-value methods for quantifying methylation levels by microarray analysis. *BMC Bioinformatics* 2010, 11:587. DOI: 10.1186/1471-2105-11-587.

66. EASL. EASL clinical practice guidelines: Management of hepatocellular carcinoma. *Journal of Hepatology* 2018, 69:182-236. DOI: 10.1016/j.jhep.2018.03.019.

67. Ebadi A., Razzaghi-Asl N., Shahabipour S., and Miri R. Ab-initio and conformational analysis of a potent VEGFR-2 inhibitor: A case study on motesanib. *Iranian Journal of Pharmaceutical Research* 2014, 13(2):405-415.

68. Esteller M. Aberrant DNA methylation as a cancer-inducing mechanism. *Annual Review of Pharmacology and Toxicology* 2005, 45:629-656.
69. Fan T., Sun G., Sun X., Zhao L., Zhong R., and Peng Y. Tumour energy metabolism and potential of 3-bromopyruvate as an inhibitor of aerobic glycolysis: Implications in tumour treatment. *Cancers* 2019, 11:317. DOI: 10.3390/cancers11030317.
70. Fan Y., Xue H., and Zheng H. Systemic Therapy for hepatocellular carcinoma: Current updates and outlook. *Journal of Hepatocellular Carcinoma* 2022, 9:233–263.
71. Feichtinger RG., and Lang R. Targeting L-lactate metabolism to overcome resistance to immune therapy of melanoma and other tumour entities. *Journal of Oncology* 2019: 2084195. DOI: 10.1155/2019/2084195.
72. Feng J., Polychronidis G., Heger U., Frongia G., Mehrabi A., and et al. Incidence trends and survival prediction of hepatoblastoma in children: a population-based study. *Cancer Communications* 2019, 39:62. DOI: 10.1186/s40880-019-0411-7.
73. Finn RS., Qin S., Galle PR., Ducreux M., Kim TY., et al. Atezolizumab plus bevacizumab in unresectable hepatocellular carcinoma. *The New England Journal of Medicine* 2020, 382:1894-905. DOI: 10.1056/NEJMoa1915745.
74. Finn RS., Yau T., Hsu CH., De Toni EN., Goyal L., et al. Ramucirumab for patients with advanced hepatocellular carcinoma and elevated alpha fetoprotein following non–sorafenib systemic therapy: An expansion cohort of REACH-2. *The Oncologist*, 2022, oyac183. DOI: 10.1093/oncolo/oyac183.
75. Forkasiewicz A., Dorociak M., Stach K., Szelachowski P., Tabola R., et al. The usefulness of lactate dehydrogenase measurements in current oncological practice. *Cellular & Molecular Biology Letters* 2020, 25:35. DOI: 10.1186/s11658-020-00228-7.
76. Fortin JP., Triche TJ., and Hansen K. Preprocessing, normalization and integration of the Illumina HumanMethylationEPIC array with minfi. *Bioinformatics* 2017, 33(4):558-560. DOI: 10.1093/bioinformatics/btw691.
77. Fujita K., Iwama H., Miyoshi H., Tani J, Oura K., et al. Diabetes mellitus and metformin in hepatocellular carcinoma. *World Journal of Gastroenterology* 2016, 22(27):6100-6113. DOI: 10.3748/wjg.v22.i27.6100.
78. Fukushige S. and Horii A. DNA methylation in cancer: A gene silencing mechanism and the clinical potential of its biomarkers. *Tohoku Journal in Experimental Medicine* 2013, 229:173-185.

79. Gabriel AS, Lafta FM, Schwalbe EC, Nakjang S, Cockell SJ, Iliasova A, et al. Epigenetic landscape correlates with genetic subtype but does not predict outcome in childhood acute lymphoblastic leukemia. *Epigenetics* 2015, 10:717–726.

80. Galun D., Mijac D., Filipovic A., Bogdanovic A., Zivanovic M. Precision medicine for hepatocellular carcinoma: Clinical perspective. *Journal of Personalized Medicine* 2022, 12:149. DOI: 10.3390/jpm12020149.

81. Gal-Yam E. N., Saito Y., Egger G., and Jones PA. Cancer epigenetics: Modification, screening, and therapy. *Annual Review Medicine* 2008, 59:267-280.

82. Gao W. Kondo Y., Shen L., Shimizu Y., Sano T., Yamao K. et al. Variable DNA methylation patterns associated with the progression of disease in hepatocellular carcinoma. *Carcinogenesis* 2008, 29(10):1901-1910.

83. Ganne-Carrié N., and Nahon P. Hepatocellular carcinoma in the setting of alcohol-related liver disease. *Journal of Hepatology* 2019, 70:284–293.

84. Gasmi M., Peana M., Arshad M., Butnariu M., Menzel A., and Bjørklund G. Krebs cycle: activators, inhibitors and their roles in the modulation of carcinogenesis. *Archives of Toxicology* 2021, 95:1161–1178. DOI: 10.1007/s00204-021-02974-9.

85. Giraud J., Chalopin D., Blanc JF., and Saleh M. Hepatocellular carcinoma immune landscape and the potential of immunotherapies. *Frontiers in Immunology* 2021, 12: 655697. DOI: 10.3389/fimmu.2021.655697.

86. Giri P., and Mohapatra B. Copy number variant (CNV). *Encyclopedia of animal cognition and behavior* 2017. DOI: 10.1007/978-3-319-47829-6_8-1.

87. van Gisbergen MW., Zwilling E., and Dubois LJ. Metabolic rewiring in radiation oncology toward improving the therapeutic ratio. *Frontiers in Oncology* 2021, 11:653621. DOI: 10.3389/fonc.2021.653621.

88. Gordan JD., Kennedy EB., Abou-Alfa GK., Beg MS., Brower ST., et al. Systemic therapy for advanced hepatocellular carcinoma: ASCO guideline. *Journal of Clinical Oncology* 2020, 38:4317-4345. DOI: 10.1200/JCO.20.02672.

89. Grgurevic I., Bozin T., Mikus M., Kukla M., and O'Beirne J. Hepatocellular carcinoma in non-alcholic fatty liver disease: From epidemiology and diagnostic approach. Cancers 2021, 13(22):5844. DOI: 10.3390/cancers13225844.

90. Guo J., Li L., Guo Bin., Liu D., Shi J., et al. Mechanisms of resistance to chemotherapy and radiotherapy in hepatocellular carcinoma. *Translational Cancer Research* 2018, 7(3): 765-781. DOI: 10.21037/tcr.2018.05.20.

91. Gupta GS. LDH- C4: a target with therapeutic potential for cancer and contraception. *Molecular and Cellular Biochemistry* 2012, 371:115–27.

92. Haferlach T., Kohlmann A., Wieczorek L., Basso G., Kronnie GT., et al. Clinical utility of microarray-based gene expression profiling in the diagnosis and subclassification of leukemia: Report from the international microarray innovations in leukemia study group. *Journal of Clinical Oncology* 2010, 28(15):2529-2537.

93. Hatanaka T., Naganuma A., and Kakizaki S. Lenvatinib for hepatocellular carcinoma: A literature review. *Pharmaceuticals* 2021, 14:36. DOI: 10.3390/ph14010036.

94. Hatzimichael E., Lagos K., Sim VR., Briasoulis E., and Crook T. Epigenetics in diagnosis, prognosis assessment and treatment of cancer: An update *EXCLI Journal* 2014, 13:954-976.

95. Héberlé É., and Bardet AF. Sensitivity of transcription factors to DNA methylation. *Essays in Biochemistry* 2019, 63(6):727–741. DOI: 10.1042/EBC20190033.

96. Heimbach JK., Kulik LM., Finn RS., Birlin CB., Abecassis MM., et al. AASLD guidelines for the treatment of hepatocellular carcinoma. *Hepatology* 2018, 67(1):258-380. DOI: 10.1002/ hep.29086.

97. Hewitt DW., Brown ZJ, and Pawlik TM. Current perspectives on the surgical management of perihilar cholangiocarcinoma. *Cancers* 2022, 14:2208. DOI: 10.3390/can cers14092208.

98. Holoch D., and Moazed D. RNA-mediated epigenetic regulation of gene expression. Nature Reviews Genetics 2015, 16(2):71-84. DOI: 10.1038/nrg3863.

99. Hölzen L., Mitschke J., Schönichen C., Hess ME., Ehrenfeld S., et al. RNA interference screens discover proteases as synthetic lethal partners of PI3K inhibition in breast cancer cells. *Theranostics* 2022, 12(9):4348-4373. DOI: 10.7150/thno.68299.

100. Hua Y., Liang C., Zhu J., Miao C., Yu Yi., et al. Expression of lactate dehydrogenase C correlates with poor prognosis in renal cell carcinoma. *Tumor Biology* 2017, 1-10. DOI: 10.1177/1010428317695968.

101. Huang A., Garraway LA., Ashworth A., and Weber B. Synthetic lethality as an engine for cancer drug target discovery. *Nature Reviews Drug Discovery* 2020, 19: 23-38. DOI: 10. 1038/s41573-019-0046-z.

102. Huang J., Ye X., Guan J., Chen B., Li Q., et al. Tiam1 is associated with hepatocellular metastasis. *International Journal of Cancer* 2013, 132:90-100.
103. Huang K., Huang, SF., Chen IH., Liao CT., and Wang HM. Methylation of *RASSF1A*, *RASSF2A* and *HIN-1* is associated with poor outcome after radiotherapy, but not surgery, in oral squamous cell carcinoma. *Clinical Cancer Research* 2009, 15(12):4174-4180.
104. Iden S., and Collard JG. Crosstalk between small GTPases and polarity proteins in cell polarization. *Nature Reviews Molecular Cell Biology* 2008, 9: 846–859. DOI: 10.1038/ nrm2521.
105. Iglehart JD., and Silver DP. Synthetic lethality-A new direction in cancer-drug development. *The New England Journal of Medicine* 2009, 361:189-191. DOI: 10.1056/ NEJMe0903044.
106. Issa JP. Epigenetics. *FEBS Letters* 2011, 585(13):1993.
107. Jansen A., and Verstrepen KJ. Nucleosome positioning in *Saccharomyces cerevisiae*. *Microbiology and Molecular Biology Reviews* 2011, 75(2):301–320.
108. Jeng LB., Liao LY., Shih FY., and Teng CF. Dendritic-cell-vaccine-based immunotherapy for hepatocellular carcinoma: Clinical trials and recent preclinical studies. *Cancers* 2022, 14:4380. DOI: 10.3390/cancers14184380.
109. Jeong SU., and Kang HJ. Recent updates on the classification of hepatoblastoma according to the international pediatric liver tumours consensus. *Journal of Liver Cancer* 2022, 22(1):23-29. DOI: 10.17998/jlc.2022.02.24.
110. Kan Z., Zheng H., Liu X., Li S., Barber TD., et al. Whole-genome sequencing identifies recurrent mutations in hepatocellular carcinoma. *Genome Research* 2013, 23:1422–1433.
111. Kang WH., Tak E., Hwang S., Song GW., Jwa E., et al. Metformin-associated chemopreventive effects on recurrence after hepatic resection of hepatocellular carcinoma: From in vitro to a clinical study. *Anticancer Research* 2018, 38: 2399-2407. DOI: 10.21873/anticanres.12490.
112. Katariya NN., Lizaola-Mayo BC., Chascsa, DM., Giorgakis E., Aqel BA., et al. Immune checkpoint inhibitors as therapy to down-stage hepatocellular carcinoma prior to liver transplantation. *Cancers* 2022, 14:2056. DOI: 10.3390/cancers14092056.
113. Kendall T., Verheij J., Gaudio E., Evert M., Guido M., et al. Anatomical, histomorphological and molecular classification of cholangiocarcinoma. *Liver International* 2019, 39(Suppl.1):7–18. DOI: 10.1111/liv.14093.

114. Khan AA., Allemailem KS., Alhumaydhi FA., Gowder SJT., and Rahmani AH. The biochemical and clinical perspectives of lactate dehydrogenase: An Enzyme of active metabolism. *Endocrine, Metabolic & Immune Disorders - Drug Targets*, 2020, 20(6): 855-868. DOI: 10.2174/1871530320666191230141110.
115. Khong H., and Overwijk WW. Adjuvants for peptide-based cancer vaccines. *Journal for Immuno Therapy of Cancer* 2016, 4:56. DOI: 10.1186/s40425-016-0160-y.
116. Kierans SJ., and Taylor CT. Regulation of glycolysis by the hypoxia-inducible factor (HIF): implications for cellular physiology. *Journal of Physiology* 2021,599:23–37. DOI: 10.1113/JP280572.
117. Kilaru S., and Baffy G. Metformin and hepatocellular carcinoma. *Journal of Symptoms and Signs* 2015, 4(1):15-24.
118. Kim EH., Kim MS., CHO CK., JUNG WG., Kyoung Y., et al. Low and high linear energy transfer radiation sensitization of HCC cells by metformin. *Journal of Radiation Research* 2014, 55:432–442. DOI: 10.1093/jrr/rrt131.
119. Kim EH., Kim MS., Furusawa Y., Uzawa A., Han S., et al. Metformin enhances the radiosensitivity of human liver cancer cells to γ–rays and carbon ion beams. *Oncotarget* 2016, 7(49):80568-80578. DOI: 10.18632/oncotarget.12966.
120. Kim J., Chang JW., and Park JY. Nivolumab for advanced hepatocellular carcinoma with multiple lung metastases after sorafenib failure. *Journal of Liver Cancer* 2020, 20(1):72-77. DOI: 10.17998/jlc.20.1.72.
121. Klustein M., Nejman D., Greenfield R., and Cedar H. DNA methylation in cancer and aging. *Cancer Research* 2016, 76(12):1-5.
122. Kodali S., Shetty A., Shekhar S., Victor DW., Ghobrial RM. Management of intrahepatic cholangiocarcinoma. *Journal of Clinical Medicine* 2021, 10:2368. DOI: 103390/jcm10 112368.
123. Kong L., Du W., Cui Z., Wang L., Yang Z., et al. Expression of lactate dehydrogenase C in MDA-MB-231 cells and its role in tumour invasion and migration. *Molecular Medicine Reports* 2016, 13:3533-3538. DOI: 10.3892/mmr.2016.4963.
124. Kouzarides T. Chromatin modifications and their function. *Cell* 2007, 128:693-705.
125. Kudo M. Pembrolizumab for the treatment of hepatocellular carcinoma. *Liver Cancer* 2019, 8:143-154. DOI: 10.1159/000500143.

126. Kumar M., Zhao X., and Wang XW. Molecular carcinogenesis of hepatocellular carcinoma and intrahepatic cholangiocarcinoma: one step closer to personalized medicine? *Cell and Bioscience* 2011, 1:5.
127. Lazarus JV., Palayew A., Carrieri P., Ekstedt M., and Marchesini G. European 'NAFLD preparedness index'-Is Europe ready to meet the challenge of fatty liver disease? *JHEP Reports* 2021, 3:100234. DOI: 10.1016/j.jhepr.2021.100234.
128. Lee DD., and Seung HB. Learning the parts of objects by non-negative matrix factorization. *Nature* 1999, 401:788-791.
129. Lee IC., Chen YZ., Chao Y., Huo TI., Li CP., et al. Determinants of survival after sorafenib failure in patients with BCLC-C hepatocellular carcinoma in real-world practice. *Medicine*, 2015, 94(14):e688. DOI: 10.1097/MD.0000000000000688. ·
130. Lee JS., Das A., Jerby-Arnon L., Arafeh R., Auslander N., et al. Harnessing synthetic lethality to predict the response to cancer treatment. *Nature Communications* 2018, 9:2546. DOI: 10.1038/s41467-018-04647-1.
131. Lemery S., and Pazdur R. Approvals in 2021: dangling accelerated approvals, drug dosing, new approvals and beyond. *Clinical Oncology* 2022, 19:217-218. DOI: 10.1038/s41571-022-00605-5.
132. Lendvai G., Szekerczés T., Illyés I., Dóra R., Kontsek E., et al. Cholangiocarcinoma: classification, histopathology and molecular carcinogenesis. *Pathology & Oncology Research* 2020, 26:3–15. DOI: 10.1007/s12253-018-0491-8.
133. Levine AJ., and Puzio-Kuter AM. The control of the metabolic switch in cancers by oncogenes and tomor suppressor genes. *Science* 2010, 330(6009):1340-1344. DOI: 10.1126/science.1193494.
134. Li C., Liu X., Wu J., Ji X., and Xu Q. Research progress in toxicological effects and mechanism of aflatoxin B1 toxin. *PeerJ*. 2022, 10:e13850. DOI: 10.7717/peerj.13850.
135. Lim HY., Ho QS., Low J., Choolani M., and Wong KP. Respiratory competent mitochondria in human ovarian and peritoneal cancer. *Mitochondrion* 2011, 11:437–443. DOI: 10.1016/j.mito.2010.12.015.
136. Liu Y., Ding Y., Huang J, Wang S., et al. MiR-141 Suppresses the migration and invasion of HCC cells by targeting Tiam1. *PLoS ONE* 2014, 9(2):e88393. DOI: 10.1371/journal.pone.0088393.

137. Liu Y., Wu M., Liu C., Ki XL., and Zheng J. SL^{2}MF: Predicting synthetic lethality in human cancers via logistic matrix factorization. *IEEE/ACM Transactions on Computational Biology and Bioinformatics* 2020, 17(3):748-757.

138. Llovet JM., Kelley RK., Villanueva A., Singal AG., Pikarysky E., et al. Hepatocellular carcinoma. *Nature Reviews Disease Primers* 2021, 7:6. DOI: 10.1038/s415 72-020-00240-3.

139. Llovet JM., Castet F., Heikenwalder M., Maini MK., Mazzaferro V., et al. Immunotherapies for hepatocellular carcinoma. *Clinical Oncology* 2022, 19:151-172. DOI: 10. 1038/ s41571-021-00573-2.

140. Lo RCL. An update on the histological subtypes of hepatocellular carcinoma. *Hepatoma Research* 2019, 5:41. DOI: 10.20517/2394-5079.2019.021.

141. Lohitesh K., Chowdhury R., and Mukherjee S. Resistance a major hindrance to chemotherapy in hepatocellular carcinoma: an insight carcinoma: an insight. *Cancer Cell International* 2018, 18:44. DOI: 10.1186/s12935-018-0538-7.

142. Lv J., Zhou Z., Wang J., Yu H., Lu H., et al. Prognostic value of lactate dehydrogenase expression in different cancers: A meta-analysis. *Clinical Investigation* 2019, 358(6): 412-421.

143. Ma L., Chua MS., Andrisani O., and So S. Epigenetics in hepatocellular carcinoma: An update and future therapy perspectives. *World Journal of Gastroenterology* 2014, 20(2): 333-345.

144. Manzini G., Henne-Bruns G., Porzsolt F., and Kremer M. Is there a standard for survival therapy of hepatocellular carcinoma in healthy and cirrhotic liver? A comparison of eight guidelines. *BMJ Open Gastroenterology* 2017, 4e000129.

145. Marrero JA., Kulik LM., Sirlin CB., Zhu AZ., Finn RS., et al. Diagnosis, staging, and management of hepatocellular carcinoma: 2018 Practice guidance by the American Association for the Study of Liver Diseases. *Hepatology*, 2018, 68(2):723-750.

146. Matsushita H., and Takaki A. Alcohol and hepatocellular carcinoma. *BMJ Open Gastroenterology* 2019, 6:e000260. DOI: 10.1136/bmjgast-2018-000260.

147. Mazzio E., Mack N., Badisa RB., and Soliman KFA. Triple isozyme lactic acid dehydrogenase inhibition in fully viable MDA-MB-231 cells induces cytostatic effects that are not reversed by exogenous lactic acid. *Biomolecules* 2021, 11:1751. DOI: 10.3390/biom11121751

148. Merkel A., and Esteller M. Experimental and bioinformatics approaches to studying DNA methylation in cancer. *Cancers* 2022, 14:349. DOI: 10.3390/cancers14020349.
149. Mishra D., and Banerjee D. Lactate Dehydrogenases as metabolic links between tumour and stroma in the tumour microenvironment. *Cancers* 2019, 11:750; DOI:10.3390/ cancers110 60750.
150. Moawad AW., Szklaruk J., Lall C., Blair KJ., Kaseb AO., et al. Angiogenesis in hepatocellular carcinoma; pathophysiology, targeted therapy, and role of imaging. *Journal of Hepatocellular Carcinoma* 2020, 7:77–89.
151. Montalvo-Ortiz BL., Castillo-Pichardo L., Hernández E., Humphries-Bickley T., Mota-Peynado ADL., et al. Characterization of EHop-016, novel small molecule inhibitor of Rac GTPase *The Journal of Biological Chemistry* 2012, 287(16):13228–13238.
152. Moore L, Le T., and Fan G. DNA methylation and its basic function. *Neuropsychopharmacology* 2013, 38:23–38.
153. Moribe T., Iizuka N., Minura, T., Kimmura, N., Tamatsukuri, S., et al. Methylation of multiple genes as molecular markers for diagnosis of a small, well-differentiated hepatocellular carcinoma. *International Journal of Cancer* 2009, 125:388-397.
154. Morris K. V. The theory of RNA-mediated gene evolution. *Epigenetics* 2015, 10: 1-5.
155. Mukund A., Srinivasan SV., Rana S., Vijayaraghavan R., Patidar Y., et al. Response evaluation of locoregional therapies in combined hepatocellular-cholangiocarcinoma and intrahepatic cholangiocarcinoma versus hepatocellular carcinoma: a propensity score matched study. *Clinical Radiology* 2022, 77:121e129.
156. Müller-Knapp, S., and Brown, J. Epigenetic probes: Open access drug discovery. *Tocris Scientific Review Series* 2004, 1-12.
157. Mungamuri SK., and Mavuduru VA. Role of epigenetic alterations in aflatoxin-induced hepatocellular carcinoma. *Liver Cancer International* 2020, 1:41–50. DOI: 10.1002/lci2.20.
158. Muntean AG., and Hess JL. Epigenetic dysregulation in cancer. *The American Journal of Pathology* 2009, 175(4):1353-1361. DOI: 10.2353/ajpath.2009.081142.
159. Muscato JD., Morris HG., Mychack A., Rajagopal M., Baidin V. Rapid inhibitor discovery by exploiting synthetic lethality. *Journal of the American Chemistry Society* 2022, 144:3696-3705.

160. Negrini S., Gorgoulis VG., and Halazonetis TD. Genomic instability-an evolving hallmark of cancer. *Nature Reviews Molecular Cell Biology* 2010, 11:220-228. DOI: 10. 1038/nrm2858.
161. Ni L. Advances in human dendritic cell- based immunotherapy against gastrointestinal cancer. *Frontiers in Immunology* 2022, 13:887189. DOI: 10.3389/fimmu.2022.887189.
162. Niamh M., Armelle M., Simon W., Vio B., Laure M., et al. Profiling of a panel of radioresistant prostate cancer cells identifies deregulation of key miRNAs. *Clinical and Translational Radiation Oncology* 2017, 2:63-68.
163. Nile D., Rae C., Walker DJ., Waddington JC., Vincent I., et al. Inhibition of glycolysis and mitochondrial respiration promotes radiosensitisation of neuroblastoma and glioma cells. *Cancer & Metabolism* 2021, 9: 24. DOI: 10.1186/s40170-021-00258-5.
164. Nindrea RD., Harahap WA., Aryandono T., and Lazuardi L. Association of BRCA1 promoter methylation with breast cancer in Asia: A meta-analysis *Asian Pacific. Journal of Cancer Prevention* 2018, 19 (4):885-889.
165. Niu M., Yi M., Li N., Wu K., and Wu K. Advances of targeted therapy for hepatocellular carcinoma. *Frontiers in Oncology* 2021, 11:719896. DOI: 10.3389/fonc.2021.719896.
166. Niu ZS., Niu XJ., and Wang WH. Genetic alterations in hepatocellular carcinoma: An update. *World Journal of Gastroenterology* 2016, 22(41): 9069- 9095. DOI: 10. 3748/ wjg. v22. i41. 9069.
167. Nordlund J, Backlin CL, Wahlberg P, Busche S, Berglund EC, Eloranta ML, et al. Genome-wide signatures of differential DNA methylation in pediatric acute lymphoblastic leukemia. *Genome Biology* 2013, 14:r105.
168. ÓBrien A., Zhou T., Tan C., Alpini G., and Glaser S. Role of Non-Coding RNAs in the progression of liver cancer: Evidence from experimental models. *Cancers* 2019, 11:1652. DOI: 10.3390/cancers11111652.
169. O' Connor K., Walsh JC., and Schaeffer DF. Combined hepatocellular- cholangiocarcinoma (cHCC-CC): a distinct entity. *Annals of Hepatology* 2014, 13(3):317-322.
170. Odet F., Gabel SA., Williams J., London RE., Goldberg E., et al. Lactate dehydrogenase C and energy metabolism in mouse sperm. *Biology of Reproduction* 2011, 85:556–564. DOI: 10.1095/biolreprod. 111.091546.
171. Okoye IS., Houghton M., Tyrrell L., Barakat K., and Elahi S. Coinhibitory receptor

expression and immune checkpoint blockade: Maintaining a balance in CD8+ T Cell responses to chronic viral infections and cancer. *Frontiers in Immunology* 2017, 8: 1215. DOI: 10.3389/fimmu.2017.01215.

172. Olova N., Krueger F., Andrews S., Oxley D., Berrens RV., et al. Comparison of whole-genome bisulfite sequencing library preparation strategies identifies sources of biases affecting DNA methylation data. *Genome Biology* 2018, 19:33. DOI: 10.1186/s13 059-018-1408-2.
173. Ozen C., Yildiz G., Dancan AT., Cevik D., Ors A., et al. Genetics and epigenetics of liver cancer. *New Biotechnology* 2013, 30:381-384.
174. Pajak B., Siwiak E., Sołtyka M., Priebe A., Zieli´nski R., et al. 2-Deoxy-D-Glucose and its analogs: From diagnostic to therapeutic agents. *International Journal of Molecular Sciences* 2020, 21:234. DOI: 10.3390/ijms21010234.
175. Pathak HB., Zhou Y., Sethi G., Hirst F., Schilder RJ., et al. A synthetic lethality screen using a focused siRNA library to identify sensitizers to dasatinib therapy for the treatment of epithelial ovarian cancer. *PLoS ONE* 2015, 10(12) : e0144126. DOI: 10. 1371/ journal. pone .0144126.
176. Peek R., and Reddy KR. Gastroenterology and hepatology news. Gastroenterology 2008, 134:379–380.
177. Pérez-Romasanta LA., González-Del Portillo E., Rodríguez-Gutiérrez A., and Matías-Pérez, Á. Stereotactic radiotherapy for hepatocellular carcinoma, radiosensitization strategies and radiation-immunotherapy combination. *Cancers* 2021, 13:192. DOI: 10.3390cancers 1302 0192.
178. Peters T., and Peters MT. Package DMRcate. 2016. The updated version, accessed on January 7, 2023, is: http://52.71.54.154/packages/devel/bioc/manuals/DMRcate/man/ DMRcate.pdf.
179. Peter TJ., Buckley MJ., Statham AL., Pidsley R., Samaras K., et al. De novo identification of differentially methylated regions in the human genome. *Epigenetics and Chromatin* 2015, 8:6. DOI: 10.1186/1756-8935-8-6.
180. Pino RM., and Singh J. Appropriate clinical use of lactate measurements. *Anesthesiology* 2021, 134:637–44. DOI: 10.1097/ALN.0000000000003655.
181. Pinyopornpanish K., Khoudari G., Saleh MA., Angkurawaranon C., Pinyopornpanish K., et al. Hepatocellular carcinoma in nonalcoholic fatty liver disease with or without cirrhosis: a

population-based study. *BMC Gastroenterology* 2021, 2139. DOI: 10.1186/ s12876-021-01978-0.

182. Pös O., Radvanszky J., Styk J., Pös Z., Buglyó G., et al. Copy number variation: Methods and clinical applications. *Applied Sciences* 2021, 11:819. DOI: 10.3390/app11020819.
183. Qi S., Deng S., Lian Z., and Yu K. Novel drugs with high efficacy against tumour angiogenesis. *International Journal of Molecular Sciences* 2022, 23, 6934. DOI: 10.3390/ ijms23136934.
184. Rae Colin., Sey CH., and Mairs R., Radiosensitization of prostate cancer cells by 2-deoxyglucose. *Madridge Journal of Oncogenesis* 2018, 2(1):30-34. DOI: 10.18689/mjo-1000105.
185. Rani R., and Kumar V. When will small molecule lactate dehydrogenase inhibitor realize their potential in the cancer clinic? *Future Medical Chemistry* 2017, 9(11):1113-1115.
186. Rao M., Gao C., Guo M., Law BYK., and Xu Y. Effects of metformin treatment on radiotherapy efficacy in patients with cancer and diabetes: a systematic review and meta-analysis. *Cancer Management and Research* 2018, 10:4881–4890.
187. Raoul JL., Gilabert M., Adhoute X., and Edeline J. An in-depth review of chemical angiogenesis inhibitors for treating hepatocellular carcinoma. *Expert Opinion on Pharmacotherapy* 2017, 18(14):1467–1476. DOI: 10.1080/14656566.2017.1378346.
188. Rashed WM., Kandeil MAM., Mahmoud MO., and Ezzat S. Hepatocellular carcinoma in Egypt: A comprehensive overview. *Journal of the Egyptian National Cancer Institute* 2020, 32:5. DOI: 10.1186/s43046-020-0016-x.
189. Ratti M., Lampis A., Ghidini M., Salati M., Mirchev MB., et al. MicroRNAs (miRNAs) and long non-coding RNAs (lncRNAs) as new tools for cancer therapy: First steps from bench to beside. *Targeted Oncology* 2020, 15:261-278. DOI: 0.1007/s11523-020-00717-x.
190. Rebouissou S., and Nault JC. Advances in molecular classification and precision oncology in hepatocellular carcinoma. *Journal of Hepatology* 2020,72:215–229.
191. Repáraz D. Aparicio B., Llopiz D., Hervás-Stubbs S., and Sarobe P. Therapeutic vaccines against hepatocellular carcinoma in the immune checkpoint inhibitor era: Time for neoantigens? *International Journal of Molecular Sciences.* 2022, 23, 2022. DOI: 10.3390/ijms23042022.
192. Ruffoni A., Ferri N., Pinto A., Pellegrino S., Contini A., et al. Identification of the first enantiopure Rac1–Tiam1 protein–protein interaction inhibitor and its optimized synthesis *via*

phosphine free remote group directed hydroarylation. *Medicinal Chemistry Communications* 2019,**10**:310-314.

193. Sakakura C., Miyagawa K., Fukuda KI., Nakashima, S., Yoshikawa, T., et al. Frequent silencing of *RUNX3* in esophageal squamous cell carcinomas is associated with radioresistance and poor prognosis. *Oncogene* 2007, 26:5927-5938.
194. Sarcognato S., Sacchi D., Fassan M., Fabris L., Cadamuro M., et al. Cholangiocarcinoma. *Pathologica* 2021, 113:158-169. DOI: 10.32074/1591-951X-252.
195. Sasaki K., Nishina S., Yamauchi A., Fukuda K., Hara Y., et al. Nanoparticle-mediated delivery of 2-deoxy-D-glucose induces antitumor immunity and cytotoxicity in liver tumors in mice. *Cellular and Molecular Gastroenterology and Hepatology* 2021, 11(3):739-762. DOI: 10.1016/j.jcmgh.2020.10.010.
196. Saung MT., Pelosof L., Casak S., Donoghue M., Lemery S., et al. FDA Approval Summary: Nivolumab Plus Ipilimumab for the Treatment of Patients with Hepatocellular Carcinoma Previously Treated with Sorafenib. *The Oncologist* 2021, 26:797–806.
197. Schauer SN., Carreira PE., Shukla R., Gerhardt D., Gerdes, P., et al. L1 retrotransposition is a common feature of mammalian hepatocarcinogenesis. *Genome Research.* 2018, 28:639-653. DOI: 10.1101/gr.226993.117.
198. Schwab M., Thunborg, K., Azimzadeh O., von Toerne C., Werner C., et al. Targeting cancer metabolism breaks radioresistance by impairing the stress response. *Cancers* 2021, 13:3762. DOI: 10.3390/cancers13153762.
199. Schwalbe EC., Nunga L., Lafta F., Barrow TM., and Strathdee G. Integration of genome-level data to allow identification of subtype-specific vulnerability genes as novel therapeutic targets. *Oncogene* 2021, 40:5213-5223. DOI: 10.1038/s41388-021-01923-1.
200. Scott DA., Richardson AD, Filipp FV.,Knutzen CA., Chiang GG., et al. Comparative Metabolic flux profiling of melanoma cell lines: Beyond the Warburg effect. *The Journal of Biological Chemistry* 2011, 286(49):42626–42634.
201. Setton J., Zinda M., Riaz N., Durocher D., Zimmermann M. et al. Synthetic lethality in cancer therapeutics: The next generation. *Cancer Discovery* 2021, 11(7): 1626-1635. DOI: 10.1158/2159-8290.CD-20-1503.
202. Shahrisa A., Tahmasebi-Birgani M., Ansari H., Mohammadi Z., Carloni V., et al. The pattern of gene copy number alteration (CNAs) in hepatocellular carcinoma; an in silico analysis. *Molecular Cytogenetics* 2021, 14:33. DOI: 10.1186/s13039-021-00553-2.

203. Shang N., Figini M., Shangguan J., Wang B., Sun C., et al. Dendritic cells-based immunotherapy. *American Journal of Cancer Research* 2017, 7(10):2091-2102.
204. Sharma A. Singh K., and Almasan A. Histone H2AX phosphorylation: A marker for DNA damage DNA Repair. *Protocols, Methods in Molecular Biology* 2012, 920:613-626.
205. Shibata S., Sogabe S., Miwa M., Fujimoto T., Takakura N., et al. Identification of the first highly selective inhibitor of human lactate dehydrogenase B. *Scientific reports* 2021, 11(1):21353. DOI: 10.1038/s41598-021-00820-7.
206. Shukla R., Upton KR., Mu noz-Lopez M., Gerhardt DJ., Fisher ME., Nguyen T., et al. Endogenous retrotransposition activates oncogenic pathways in hepatocellular carcinoma. *Cell* 2013, 153:101–111. DOI: 10.1016/j.cell.2013.02.032.
207. Sia D., Villanueva A., Friedman SL., and Llovet JM. Liver cancer cell of origin, molecular class, and effects on patient prognosis. *Gastroenterology* 2017, 152:745–761.
208. Singh D., Banerji AK., Dwarakanath BS., Tripathi RP., Gupta JP., et al. Optimizing Cancer Radiotherapy with 2-Deoxy-D-Glucose. *Strahlentherapie und Onkologie* 2005, 181:507-514. DOI: 10.1007/s00066-005-1320-z.
209. Sinicrope FA., Foster NR., Thibodeau SN., Marsoni S., Monges G., et al. DNA mismatch repair status and colon cancer recurrence and survival in clinical trials of 5-fluorouracil-based adjuvant therapy. *Journal of the National Cancer Institute* 2011, 103:863-875.
210. Skehan P, Storeng R, Scudiero D, Monks A, McMahon J, et al. New colorimetric cytotoxicity assay for anticancer-drug screening. *Journal of the National Cancer Institute* 1990, 4;82(13):1107-12. DOI: 10.1093/jnci/82.13. 1107.
211. Song CW., Lee H., Dings RPM., Williams B., Powers J., et al. Metformin kills and radiosensitizes cancer cells and preferentially kills cancer stem cells. *Scientific Reports* 2012, 2:362. DOI: 10.1038/srep00362.
212. Sun X., Dong M., Gao Y., Wang Y., Du L., et al. Metformin increases the radiosensitivity of non-small cell lung cancer cells by destabilizing NRF2. *Biochemical Pharmacology* 2022, 199:114981. DOI: 10.1016/j.bcp.2022.114981.
213. Tan S., Day D., Nicholls SJ., and Segelov E. Immune checkpoint inhibitor therapy in oncology. *Journal of the American College of Cardiology* 2022, 4(5): 579-597. DOI: 10.1016/j.jaccao.2022.09.004.
214. Thompson JM., Nguyen QH., Singh M., and Razo OV. Approaches to identifying synthetic lethal interactions in cancer. *Yale Journal of Biology and Medicine* 2015, 88: 145-155.

215. Tomizawa M., Shinozaki F., Motoyoshi Y., Sugiyama T., Yamamoto s., et al. 2-Deoxyglucose and sorafenib synergistically suppress the proliferation and motility of hepatocellular carcinoma cells. *Oncology Letters* 2017, 13800- 804. DOI: 10. 3892/ol. 2016.5510

216. Topatana W., Juengpanich S., Li S., Cao J., Hu J., et al. Advance in synthetic lethality for cancer therapy: cellular mechanism and clinical translation. *Journal of Hematology & Oncology* 2020, 13:118. DOI: 10.1186/s13045-020-00956-5.

217. Trojan J. Cabozantinib for the treatment of advanced hepatocellular carcinoma: Current data fand future perspectives. *Drugs* 2020, 80(1). DOI: 10.1007/s40265-020-01361-5.

218. Urbańska K., and Orzechowski A. Unappreciated role of LDHA and LDHB to control apoptosis and autophagy in tumour cells. *International Journal of Molecular Science* 2019, 20:2085. DOI: 10.3390/ijms20092085.

219. Vafaei S., Zekiy AO., Khanamir RA., Zaman BA., Ghayourvahdat A., et al. Combination therapy with immune checkpoint inhibitors (ICIs); a new frontier. *Cancer Cell International* 2022, 22:2. DOI: 10.1186/s12935-021-02407-8.

220. Verset G., Borbath V., Karwal M., Verslype C., Vlierberghe HV., et al. Pembrolizumab monotherapy for previously untreated advanced hepatocellular carcinoma: Data from the open- label, phase II KEYNOTE- 224 trial. *Clinical Cancer Research* 2022, 28: 2547–54. DOI: 10.1158/1078-0432.CCR-21-3807.

221. Vial G., Detaille D., and Guigas B. Role of mitochondria in the mechanism(s) of action of metformin. *Frontiers in Endocrinology* 2019,10: 294. DOI: 10.3389/fendo.2019. 00294.

222. Vijig J., and Dong X. Pathogenic mechanisms of somatic mutation and genome mosaicism in aging. *Cell* 2020, 182:12-23.

223. Villanueva A. Hepatocellular carcinoma. *New England Journal of Medicine* 2019, 380(15):1450-1462. DOI: 10.1056/NEJMra1713263.

224. Villanueva A., Portela A., Sayols S., Battiston C., Hoshida Y., et al. DNA methylation-based prognosis and epidrivers in hepatocellular carcinoma. *Hepatology* 2015, 61:1945-1956. DOI: 10.1002/hep.27732.

225. Vogel A., Meyer T., Sapisochin G., Salem R., and Saborowski A. Hepatocellular Carcinoma *Lancet* 2022, 400: 1345–62. DOI: 10.1016/ S0140-6736(22)01200-4.

226. Vogel A., Qin S., Kudo M., Su Y., Hudgens S., et al. Lenvatinib versus sorafenib for first-line treatment of unresectable hepatocellular carcinoma: patient-reported outcomes from a

randomised, open-label, non-inferiority, phase 3 trial. *Lancet Gastroenterology & Hepatology* 2021; 6:649–58. DOI: 10.1016/ S2468-1253(21)00110-2.

227. Vos S., van Diset PJ., and Moelans CB. A systematic review on the frequency of BRCA promoter methylation in breast and ovarian carcinomas of *BRCA* germline mutation carriers: Mutually exclusive, or not? *Clinical Reviews in Oncology* 2018, 127:29-41.
228. Younossi ZM., and Henry L. Epidemiology of non-alcoholic fatty liver disease and hepatocellular carcinoma. *JHEP Reports* 2021, 3:100305.
229. Waddington C. The epigenotype. *Endeavour* 1942, 1:18–20.
230. Wang J., Li E., Yang H., Wu J., Lu HC., et al. Combined hepatocellular-cholangiocarcinoma: a population level analysis of incidence and mortality trends. *World Journal of Surgical Oncology* 2019, 17:43.
231. Wang L., Yang Q., Peng S., and Liu X. The combination of the glycolysis inhibitor 2-DG and sorafenib can be effective against sorafenib-tolerant persister cancer cells. *Onco Targets and Therapy* 2019, 12:5359–5373. DOI: 10.2147/OTT.S212465.
232. Wang T., Yu H., Hughes NW., Liu, B., Kendirli A., et al. Gene essentiality profiling reveals gene networks and synthetic lethal interaction with oncogenic Ras. *Cell* 2017, 168(5): 890-903.
233. Wang Y., Li G., Wan F., Dai B., and Ye D. Prognostic value of D-lactate dehydrogenase in patients with clear renal cell carcinoma. *Oncology Letters* 2018, 16:866-874. DOI: 10.3892/ol.2018.8782.
234. Wang Y., Lu LC., Guan Y., Ho MC., Lu S., et al. Atezolizumab plus bevacizumab combination enables an unresectable hepatocellular carcinoma resectable and links immune exclusion and tumour dedifferentiation to acquired resistance. *Experimental Hematology and Oncology* 2021, 10:45. DOI: 10.1186/s40164-021-00237-y.
235. Warburg, O. On the origin of cancer cells. *Science* 1956, 123:309–314.
236. Warburg O. On the metabolism of cancer cells. *Naturwissenschaften* 1924, 12:1131–1137.
237. Waseem D., and Tushar P. Intrahepatic, Perihilar and distal cholangiocarcinoma: Management and outcomes. *Annals of Hepatology* 2017, 16(1):133-139.
238. Wei X., Yanga J., Adair SJ., Ozturk H., Kuscu C., et al. Targeted CRISPR screening identifies PRMT5 as synthetic lethality combinatorial target with gemcitabine in pancreatic cancer cells. *Proceedings of the National Academy of Sciences of the United States of America*. 2020, 117(45):28068–28079. DOI: 10.1073/pnas.2009899117.

239. Willers H., Azzoli CG., Santivasi WL., and Xia F. Basic mechanisms of therapeutic resistance to radiation and chemotherapy in lung cancer. *The Cancer Journal* 2013, 19(3):200-207. DOI: 10.1097/PPO.0b013e318292e4e3.

240. Williamson, J., Harris, D. A. Benyon, J., and Jenkins, G. Review of the development of DNA methylation as a marker of response to neoadjuvant therapy and outcomes in rectal cancer. *Clinical Epigenetics* 2015, 7:10:1-9.

241. Yang X., Lay F., Han H., and Jones PA. Targeting DNA methylation for epigenetic therapy. *Trends in Pharmacological Sciences* 2010, 31(11):536-546.

242. Yang Y., Ren L., Yang H., Ge B., Li W., et al. Research progress on anti-angiogenesis drugs in Hepatocellular Carcinoma. *Cancer Plus* 2021, 3233–40. DOI: 10.18063/cp.v3i2. 319.

243. Yau T., Park JW., Finn RS.,Mathurin P., Edeline J., et al. CheckMate 459: A randomized, multi-center phase III study of nivolumab (NIVO) vs sorafenib (SOR) as first-line (1L) treatment in patients (pts) with advanced hepatocellular carcinoma (aHCC). *Annals of Oncology* 2019, 1(30):v874–v875. DOI: 10.1093/annonc/mdz394.029.

244. Yoon J., and Mao Y. Dissecting molecular genetic mechanisms of 1q21.1 CNV in neuropsychiatric disorders. *International of Molecular Sciences* 2021, 22:5811. DOI: 10.3390/ijms22115811.

245. Wu Y., Liu Z., and Xu X. Molecular subtyping of hepatocellular carcinoma: A step toward precision medicine. *Cancer Communications* 2020, 40:681–693. DOI: 10.1002/cac2.12115.

246. Xiong Y., Lu QJ., Zhao J., and Wu GY. Metformin inhibits growth of hepatocellular carcinoma cells by inducing apoptosis via mitochondrion-mediated pathway. *Asian Pacific Journal of Cancer Prevention* 2012, 13:3275-3279.

247. Yang F., Deng K., Zheng H., Liu Z., and Heng Y. Progress of targeted and immunotherapy for hepatocellular carcinoma and the application of next-generation sequencing. *Annals of Hepatology* 2022, 27:100677. DOI: 10.1016/j.aohep.2022.100677.

248. Yang X., Lay F., Han H., and Jones PA. Targeting DNA methylation for epigenetic therapy. *Trends in Pharmacological Sciences* 2010, 31(11):536-546.

249. Yang Y., Wu Q., Li N., Che S., Jin T., et al. Upregulation of Tiam1 contributes to cervical cancer disease progression and indicates poor survival outcome. *Human Pathology* 2018, 75:179–188.

250. Younossi ZM., and Henry L. Epidemiology of non-alcoholic fatty liver disease and hepatocellular carcinoma. *JHEP Reports* 2021, 3:100305.

251. Ždralević M., Brand A., Ianni LD., Dettmer K., Reinders J., et al. Double genetic disruption of lactate dehydrogenases A and B is required to ablate the "Warburg effect" restricting tumour growth to oxidative metabolism. *Journal of Biological Chemistry* 2018, 293(41):15947–15961.
252. Zhao W., Shan B., He D., Cheng Y., Li B., et al. Recent progress in characterizing long noncoding RNAs in cancer drug resistance. *Journal of Cancer* 2019, 10(26):6693-6702. DOI: 10.7150/jca.30877.
253. Zhang H., Zhang W., Jiang L., and Chen Y. Recent advances in systemic therapy for hepatocellular carcinoma. *Biomarker Research* 2022, 10: 3. DOI: 10. 1186/ s40364- 021-00350-4.
254. Zhang KF., Wang J., Guo J., Huang YY., and Huang TR. Metformin enhances radiosensitivity in hepatocellular carcinoma by inhibition of specificity protein 1 and epithelial-to-mesenchymal transition. *Journal of Cancer Research and Therapeutics* 2019, 15:1603-1610.
255. Zhang W., and Xu J. DNA methyltransferases and their roles in tumorigenesis. *Biomarker Research* 2017, 5:1-8.
256. Zhang Y., Huang G., Miao H., Song Z., Zhang X., et al. Apatinib treatment may improve survival outcomes of patients with hepatitis B virus-related sorafenib-resistant hepatocellular carcinoma. *Therapeutic Advances in Medical Oncology* 2020, 12:1-13. 10.1177/175883 59209374.
257. Zhang X., Liu P., Shang Y., Kerndl H., Kumstel S., et al. Metformin and LW6 impairs pancreatic cancer cells and reduces nuclear localization of YAP1. *Journal of Cancer* 2020, 11(2):479-487. DOI: 10.7150/jca.33029.
258. Zhang Y., and Reinberg D. Transcription regulation by histone methylation: interplay between different covalent modifications of the core histone tails. *Gene and Development* 2018, 2343-2360.
259. Zhang YJ., Ahsan H., Chen Y., Lunn RM., Wang LY., et al. High frequency of promoter hypermethylation of RASSF1A and *p16* and its relationship to aflatoxin B_1-DNA adduct levels in human hepatocellular carcinoma. *Molecular Carcinogenesis* 2002, 35: 85-92.
260. Zhao B., Luo J., Yu T., Zhou L., Lv H., and Shang P. Anticancer mechanisms of metformin: A review of the current evidence. *Life Sciences* 2020, 254:117717. DOI: 10. 1016 j. lfs. 2020.117717.

261. Zheng C, Wu X, Zeng R, Lin L, Xu L, Li E., et al. Computational prediction of hot spots and binding site of inhibitor NSC23766 on Rac1 binding with Tiam1. *Frontiers in Chemistry* 2021, 8:625437. DOI: 10.3389/fchem.2020.625437.
262. Zheng J. Energy metabolism of cancer: Glycolysis versus oxidative phosphorylation (Review). *Oncology Letters* 2012, 4:1151-1157. DOI: 10.3892/ol.2012.928.
263. Zheng, Y. Dbl family guanine nucleotide exchange factors. *Trends in Biochemical Sciences* 2001, 26(12):724-732.
264. Zheng Z., Liu Z., Zhang H., Guo X., Jia X., et al. Efficacy and safety of apatinib in advanced hepatocellular carcinoma: A multicenter real world retrospective study. *Frontiers in Pharmacology* 2022, 13:894016. DOI: 10.3389/fphar.2022.894016.
265. Zhou C., Zhang W., Chen W., Yin Y., Atyah M., et al. Integrated analysis of copy number variations and gene expression profiling in hepatocellular carcinoma. *Scientific Reports* 2017, 7:10570. DOI: 10.1038/s41598-017-11029-y.
266. Zhou H., Kann MG., Mallory EK., Yang, YH., Bugshan A., et al. Recruitment of Tiam1 semaphorin 4D activates Rac and enhances proliferation, invasion, and metastasis in oral squamous cell carcinoma. *Neoplasia* 2017, 19(2):65-74.
267. Zhu AX, Finn RS, Edeline J., Cattan S., Ogasawara S., et al. Pembrolizumab in patients with advanced hepatocellular carcinoma previously treated with sorafenib (KEYNOTE-224): a non-randomised, open-label phase 2 trial. *Lancet Oncol* 2018, 19: 940–52. DOI: 10.1016/S1470-2045(18)30351-6.
268. Zhu AX., Kang YK., Yen CJ., Finn RS., Galle PR., et al. Ramucirumab after sorafenib in patients with advanced hepatocellular carcinoma and increased α-fetoprotein concentrations (REACH-2): a randomised, double-blind, placebo-controlled, phase 3 trial. *Lancet Oncology* 2019, 20:282–296. DOI: 10.1016/S1470-2045(18)30937-9.
269. Zhu L., Li HD., Xu JJ., Li JJ., Cheng M., et al. Advancements in the alcohol-associated liver disease model. *Biomolecules* 2022, *12*(8):1035. DOI: 10.3390/biom120 81035.
270. Znati S., Carter R., Vasquez M., and Westhorpe A. Radiosensitisation of hepatocellular carcinoma cells by vandetanib. *Cancers* 2020, 12(7):1878. DOI: 10.3390/cancers12071878.
271. http://cshprotocols.cshlp.org /content/2006/1/pdb.rec538.full?text_only=true.
272. https://cytosmart.com/resources/resources/clonogenic-assay-what-why-and-how.
273. https://gco.iarc.fr/today/data/factsheets/cancers/11-Liver-fact-sheet.pdf.
274. https://gco.iarc.fr/today/data/factsheets/cancers/39-All-cancers-fact-sheet.pdf.

275. https://gco.iarc.fr/today/data/factsheets/populations/764-thailand-fact-sheets.pdf.
276. https://gco.iarc.fr/today/data/factsheets/populations/826-united-kingdom-fact-sheets.pdf.
277. https://link.springer.com/content/pdf/10.1007/978-1-61779-080-5_20.pdf.
278. https://proceedings.neurips.cc/paper/2000/file/f9d1152547c0bde01830b7e8bd60024c-Paper.pdf.
279. https://www.angibodies.com/ western-blotting.
280. https://www.cancerresearchuk.org/health-professional/cancer-statistics/mortality#heading-Four.
281. https://www.cancerresearchuk.org/health-professional/cancer-statistics/statistics-by-cancer-type/liver-cancer.
282. https://www.cancerresearchuk.org/health-professional/cancer-statistics/statistics-by-cancer-type/liver-cancer#heading-One.
283. https://www.cancerresearchuk.org/health-professional/cancer-statistics/statistics-by-cancer-type/liver-cancer#heading-Two.
284. https://www.cruk.cam.ac.uk/research-groups/jodrell-group/combenefit.
285. https;//www.illumina.com
286. https://www.macmillan.org.uk/dfsmedia/1a6f23537f7f4519bb0cf4c45b2a629/9468-10061/2022- cancer- statistics-factsheet.
287. https://www.macmillan.org.uk/_images/can cer-statistics-factsheet_tcm9-260514.pdf.
288. https://www.medchemexpress.com/_R__GNE-140.html.
289. https://www.oncomine.com/blog/detecting-copy-number-variants-in-the-cancer-genome.
290. http://www.who.int/cancer/en/.